# The comparative cardiovascular and non-cardiovascular actions of cannabidiol: an important *Cannabis* therapeutic agent

**Amna C. Mazeh**

ORCID iD: 0000-0003-0431-2055

**Doctor of Philosophy**

April 2021

Department of Biochemistry and Pharmacology

School of Biomedical Sciences

Faculty of Medicine, Dentistry and Health Sciences

The University of Melbourne

Submitted in total fulfilment for the degree of Doctor of Philosophy

# Abstract

Cannabidiol is a major non-intoxicating *Cannabis* compound that is prescribed for the treatment of seizures in children with rare treatment-resistant epilepsy, and has been suggested to have extensive therapeutic potential including in the cardiovascular system. However, the mechanisms underlying the cardiovascular effects of cannabidiol remain elusive. Therefore the goal of this project was to further the understanding of the cardiovascular effects of cannabidiol and the interaction of cannabidiol with the cannabinoid receptors. More specifically, the project aimed to examine the local vascular and haemodynamic effects of cannabidiol, and the potential mechanisms involved in cannabidiol-specific cardiovascular effects. This study also aimed to pharmacologically characterise the cannabinoid receptor type 1 ($CB_1$) activity of cannabidiol using the rat vas deferens bioassay. As previous studies using the isolated vas deferens bioassay have been performed in modified physiological salt solution (PSS) without $Mg^{2+}$, this study sought to standardise the assay by examining the effect of varying $Mg^{2+}$ concentrations on neurotransmitter-induced contractions in the vas deferens.

To examine the vascular effects of cannabidiol, wire myography was used to quantify clinically used concentrations of cannabidiol (0.3-3 μM) on the effects of various contractile agents in rat isolated small resistance arteries. The effects of cannabidiol in small resistance arteries were compared with larger conduit arteries, given the morphological and functional differences between different artery types. The potential vascular mechanisms of action of cannabidiol in small resistance arteries were further investigated by pretreating arteries with various inhibitors prior to the treatment with cannabidiol and subsequent contractions. The vascular actions of cannabidiol were further compared with its actions on the contraction of various isolated non-vascular tissues – bronchial, urogenital, cardiac and skeletal muscles, using organ baths. To study the haemodynamic actions of cannabidiol, rats were anaesthetised and intravenously administered with cannabidiol. Evaluation of the acute cardiovascular actions of cannabidiol included measurements of heart rate and mean arterial pressure. Carotid and mesenteric vascular conductance and hindpaw cutaneous blood flow were

measured to assess the effects of cannabidiol on haemodynamics. The potential haemodynamic mechanisms of action of cannabidiol were investigated by intravenously pretreating rats with various inhibitors prior to cannabidiol administration. Experiments on the vas deferens bioassay were performed in organ baths. The vas deferens bioassay was standardised by evaluating the influence of varying $Mg^{2+}$ concentrations (0-3 mM) in the PSS on neurotransmitter-induced contractions. The $CB_1$ receptor activity of cannabidiol was pharmacologically characterised by evaluating the ability of cannabidiol to alter $CB_1$ receptor agonist-induced modulation of electrically evoked contractions in the standardised vas deferens bioassay.

Cannabidiol, at clinically relevant concentrations, potently inhibited the contractions of small resistance arteries to multiple agents while being devoid of activity in large conduit arteries. The sensitivity of the small resistance arteries to cannabidiol involves CGRP and voltage-operated calcium channels. Non-vascular smooth muscles were generally unaffected by cannabidiol even at 10-100 times the therapeutic plasma level. Intravenously administered cannabidiol 10-30 mg/kg caused acute bradycardia and hypotension. Furthermore, cannabidiol modulated vascular tone by increasing vascular conductance and cutaneous blood flow. Electrically-induced contractions of vas deferens tissues were altered under non-physiological conditions ($Mg^{2+}$ 0 mM in PSS). Cannabidiol antagonised $CB_1$ receptor-mediated inhibition of contraction of the rat vas deferens in a manner consistent with simple competitive antagonism. The resulting potency of cannabidiol as a competitive antagonist of $CB_1$ agonists was consistent with its binding affinity at the $CB_1$ receptor.

In conclusion, this project has broadened the understanding of the cardiovascular effects of cannabidiol by demonstrating that cannabidiol has potent vascular effects that are selective for small resistance arteries, which are the main contributors to peripheral vascular resistance and subsequent blood pressure regulation. The sensitivity of the small resistance arteries to cannabidiol involves CGRP and voltage-operated calcium channels. The vascular effects were confirmed *in vivo*, as cannabidiol transiently increased carotid vascular conductance and hindpaw cutaneous blood flow. This project has also contributed to the understanding of the pharmacological interactions of

cannabidiol and $CB_1$ receptors. Given that altering $Mg^{2+}$ concentration in the PSS altered vas deferens responses, the vas deferens should be studied under physiological conditions ($Mg^{2+}$ 1.2 mM). The $CB_1$ antagonist activity of cannabidiol may have implications for neurotransmission modulation when plasma concentrations are raised above 1 μM.

# Declaration

I declare that:

i) the thesis comprises only their original work towards the PhD except where indicated in the preface;

ii) due acknowledgement has been made in the text to all other material used,

iii) the thesis is fewer than 100 000 words in length, exclusive of tables, maps, bibliographies and appendices.

Amna Mazeh

April 2021

# Preface

Content from the following thesis chapters have been published or submitted for publication:

i) Chapter 2: Mazeh *et al.* (2019)

ii) Chapter 3: Submitted for publication

iii) Chapter 4: Mazeh *et al.* (2021)

# Acknowledgements

It is with the deepest sense of gratitude that I acknowledge the support of all those who were instrumental in my PhD journey and oh, what a journey it has been.

I would first like to express my gratitude and appreciation to my supervisors Associate Professor Christine Wright and Professor James Angus. It has been nothing short of amazing to have supervisors with your passion for pharmacology and scientific rigour. Christine, under your supervision I have learnt the value of being disciplined and conscientious. Your unwavering support has been a great source of comfort throughout my candidacy. I have equally enjoyed our discussions about research-related and unrelated matters. Jim, your excitement and curiosity about research have been a strong driving force in my candidacy. Every meeting with you left me excited for the next set of pilot experiments and for that I am grateful.

I would also like to extend my appreciation to the other members of the Cardiovascular Therapeutics Unit. Mark and Linda, thank you for patiently teaching me all the experimental techniques and for your experimental assistance throughout my candidacy. Mark, I have thoroughly enjoyed our everyday debates and long conversations. Linda, it is rare to meet a person who can calmly turn any crisis into a solution. I cherish your optimism, encouragement and our shared love for chemical exfoliants. I would further like to thank Khammy. I admire your work ethic and willingness to always encourage me when I needed it the most. I have specifically appreciated your hit-or-miss puns and your clumsiness around the lab. My PhD experience would not have been the same without the wonderful students in the laboratory. Thank you, Nhi, Ash, Daria and Alex, for the great company which involved much laughter.

I would further like to acknowledge the following members of the Department of Biochemistry and Pharmacology, Dr Rosa McCarty, Dr Graham Mackay and Associate Professor James Ziogas, for providing me with the great opportunity to teach, which has

become a major source of joy for me. I also want to extend my gratitude to professor Norman Saunders for the opportunity to be involved in the Virtual Sailing project and for all the interesting topics you have brought to my attention over the years. To associate professor Kate Dziegielewska, I have cherished our conversations in the corridor, tea room or over a good cup of coffee.

I feel a deep sense of gratitude to all my friends who have not only been supportive but also very patient with me. I want to start by thanking my friends in Sweden, Nina, May and Razan, your love and support kept my spirit up during hard times. I also want to thank Ela and Martin, I am excited to reunite with you as soon as the world allows us to. I am also extremely lucky to have made such wonderful friends here in Australia. Nithya, you have been a great companion during my PhD and I have thoroughly enjoyed your self-deprecating humour. To Kat, our monthly catch-ups have been close to life-changing. Our meetings have left me lighter on days when I have felt burdened. I also want to thank Lauren, Corinne, Fabienne and Bridget. You were my first friends in Australia and spending time with you has been the highlight of my weeks. To Evie, I was lucky to first get to know you during our exchange in the US and was even luckier to end up living in the same city as you in Australia. Thanks for your support and all the distractions. To all my friends, I look forward to never leave another event with the excuse of having PhD-related work to do.

To my partner, Alex. I could not have imagined better support during this time. I am grateful to you for always cheering me on and reminding me that I am capable of more than I know. In your Master's thesis you wrote that I am the TPP to your Coenzyme$Q_{10}$ but as I am not as nerdy as you, I will simply say that you have been and continue to be a major source of my happiness.

Till min familj, ert stöd och villkorslösa kärlek är ovärderligt. Allt jag gjort har varit möjligt på grund av er, och allt jag gör, gör jag för er.

# Table of Contents

# List of tables

# List of figures

# Dedication

This thesis is dedicated to my parents for unconditionally loving and supporting me.
Your strength inspires me every day.

Er dotter för alltid.

# Chapter 1

General introduction

## 1.1 Human medicinal *Cannabis* use — From the 3rd millennium BCE to today

Humans have used the *Cannabis* plant as a source for textiles, clothing, food and medicine for thousands of years (reviewed in Andre *et al.*, 2016; Kendall & Alexander, 2017; Pertwee, 2014; Pisanti & Bifulco, 2017; Pisanti & Bifulco, 2019; Russo, 2007). According to archaeological records, humans first exploited *Cannabis* at the end of the Ice Age, ten thousand years ago. However, *Cannabis* likely originated millions of years ago during the Pleistocene epoch (reviewed in Pisanti & Bifulco, 2019). Written evidence shows that early human use of *Cannabis* for medicinal purposes originated in China (ca 2700 Before the Common Era; BCE) under the rule of the emperor Shen Nung (Figure 1-1). Legend has it that he had the incredible ability of the direct observation of the therapeutic effects of ingested plants, through his transparent abdomen, awarding him the title of the father of Chinese medicine. Two thousand years after the reign of the emperor Shen Nung, *Cannabis* was listed in the Chinese pharmacopeia (Shen Nung Pen Ts'ao Ching). The Pen Ts'ao Ching describes *Cannabis*' ability to stimulate appetite and relieve pain and cramps (Mechoulam, 2005; Pisanti & Bifulco, 2017). The psychotropic effects of *Cannabis* are rarely depicted in ancient Chinese writings, with the exception for a text in the Pen Ts'ao Ching describing that the overuse of *Cannabis* causes the user to "see demons" and "communicate with spirits" (Pisanti & Bifulco, 2019). In the Pen Ts'ao Ching, the female *Cannabis* flower is referred to as MáFěn, Má meaning hemp. According to linguistic analysis, various Chinese compound words that share the properties of *Cannabis* are made up by the word Má, including the compound words for "numb" (mámù) and "anaesthetics and narcotics" (mázuì; reviewed in Li, 1974).

**Figure 1-1.** *Shen Nung* the divine farmer.
A painting by Guo Xu (1503) depicting the Chinese emperor Shen Nung chewing on a branch. Emperor Shen Nung had great influence in teaching the practice of agriculture, acupuncture and the use of plant-based medicine, including Cannabis. Picture source: Shen Yun Performing Arts (2020).

Early human medicinal *Cannabis* use has also been established in Egypt. More specifically, the hieroglyphics word for *Cannabis* has been discovered on pyramid stones (ca 2350 BCE) and subsequent papyrus, e.g. Ebers papyrus (ca 1550 BCE; Pisanti & Bifulco, 2019). The scriptures suggest that the Egyptians used *Cannabis* to treat eye ailments, possibly as an antiglaucoma or anti-inflammatory treatment. They also explored various *Cannabis* routes of administration including vaginal suppositories to cool the uterus and eliminate heat and rectal suppositories for analgesic and anti-inflammatory purposes, also through the mouth, fumigation and skin. The ancient Egyptian word for *Cannabis* is shemshemet which is represented by the hieroglyphic symbols of a basin/pool ('sh' sound) and an owl ('m' sound); repeated twice, a loaf of bread ('t' sound) and two ideographic determinative symbols of a grain and a plant (Figure 1-2). In addition to the scriptures, physical evidence supports the use of medicinal *Cannabis* in ancient Egypt as *Cannabis* pollen was found inside the mummy of Rameses II who died ca 1213 BCE (Russo, 2007). Evidence of human medicinal

*Cannabis* use has also been observed in Japan, India, Europe, Arab countries, North and South Africa and America.

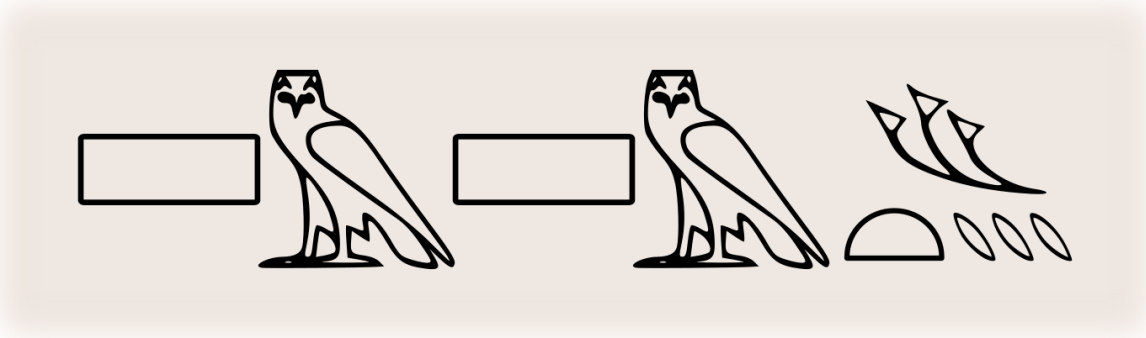

**Figure 1-2.** Hieroglyph symbols for the ancient Egyptian word for *Cannabis*: *Shemshemet*. *Shemshemet* is made up by the hieroglyphs for a basin and an owl; repeated twice, followed by a loaf of bread and two ideographic determinative symbols of a grain and a plant, indicating that the word refers to a plant. Hieroglyphs were reproduced from an image found in Russo (2007).

The Irish scientist and physician William Brooke O'Shaughnessy provided the first modern descriptions of the therapeutic properties of *Cannabis* through pharmacological and toxicological studies (MacGillivray, 2017; Pisanti & Bifulco, 2017). In the early- to mid-19$^{th}$ century, O'Shaughnessy tested the safety of *Cannabis* in mice, rabbits, cats and dogs. He further ascertained the safety and effects of *Cannabis* in patients with epilepsy, cholera, rheumatism and tetanus, concluding that *Cannabis* was analgesic and myorelaxant. He was early to suggest that *Cannabis* could potentially treat epilepsy and consequently treated an infant suffering from convulsions with *Cannabis*. The work of O'Shaughnessy influenced other researchers around Europe to generate reports on *Cannabis*' positive therapeutic effects in migraine, insomnia, hysteria, asthma and neuralgia. The French psychiatrist Jacques-Joseph Moreau experimented with *Cannabis* on himself and his students in 1840 to describe the acute psychoactive effects of *Cannabis*. While treating his patients with mental disorders he observed that *Cannabis* calmed them, improved their sleep quality and increased their appetite. The findings made by O'Shaughnessy and Moreau on *Cannabis*' medicinal potential spread

throughout Europe during the mid-19$^{th}$ century to the early-20$^{th}$ century, which came to be referred to as the Golden Age of *Cannabis* (Pertwee, 2014). In fact, during this period *Cannabis* was increasingly commercialised as a medical product, resulting in the production of various *Cannabis* preparations by pharmaceutical companies including Bristol-Meyers in the United States and Merck in Germany. The pharmaceutical companies manufactured *Cannabis* pills, tinctures and extracts. Nonetheless, the western use of medicinal *Cannabis* declined in the first decades of the 20$^{th}$ century. This was partly due to the highly variable efficacy profile of *Cannabis* between patients and preparations. During this time, drugs with better pharmacological profiles were discovered like aspirin which improved the treatment of pain and inflammation, without inducing psychotropic effects. Legal restrictions further limited the use of *Cannabis*, as a result of anti-*Cannabis* campaigns by the US Federal Bureau of Narcotics. This eventually resulted in *Cannabis* being heavily taxed under the "Marihuana Tax Act" in 1937, limiting its recreational and medicinal use. This marked the start of the *Cannabis* prohibitionist era. While *Cannabis* was still legal, high taxation negatively impacted the progression of medicinal *Cannabis* research. *Cannabis* was eventually also removed from the US Pharmacopoeia in 1941. In the 1960s there was a surge in drug recreational use, including *Cannabis*, which resulted in the classification of *Cannabis* as a substance of abuse under the United Nations' 1961 Single Convention on Narcotic Drugs (section 1.4). The regulation of *Cannabis* did not prevent the new era of *Cannabis* research, which started in 1963 and 1964 when the structure and stereochemistry of the main phytochemicals cannabidiol and $\Delta^9$-tetrahydrocannabinol ($\Delta^9$-THC or THC) were elucidated (Gaoni & Mechoulam, 1964; Mechoulam & Shvo, 1963), 23 years after the first isolation of cannabidiol (Adams *et al.*, 1940). Cannabidiol and THC share the same biosynthetic pathway (section 1.3.2) and therefore have similar chemical structures (Figure 1-3) while generally possessing opposing effects *in vivo*, including in the cardiovascular system (section 1.7). It took 26 years before the first cannabinoid receptor was cloned, followed by the isolation of the first endogenous cannabinoid, marking the beginning of the research into the ever-expanding endocannabinoid system (section 1.6.1). We know today that the *Cannabis* plant is the production site for over 500 different phytochemicals (section 1.3), many of which have rich medicinal benefits. Cannabidiol, the focus of my thesis, is a promising therapeutic candidate for a

wide range of diseases and conditions (section 1.5), including in the cardiovascular system (section 1.7.1)

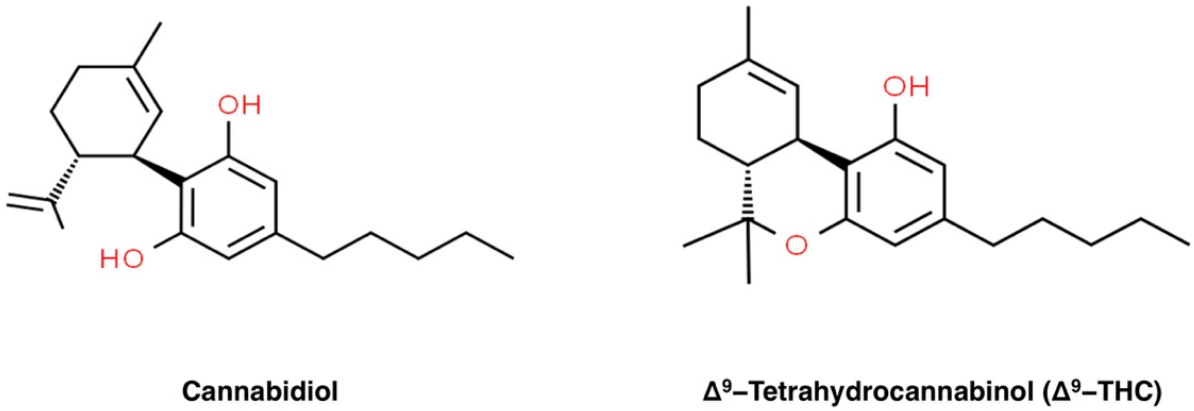


**Figure 1-3.** The chemical structures of the main phytocannabinoids in *Cannabis*: cannabidiol and $\Delta^9$-THC.
Cannabidiol and THC are abundant phytocannabinoids in *Cannabis* with bi-and tricyclic structures, respectively, with the same molecular formula ($C_{21}H_{30}O_2$).

## 1.2 The discovery of the endocannabinoid System

After decades of medicinal research on *Cannabis* and the psychotropic compound THC, the first endogenous cannabinoid receptor was discovered in 1988 (Howlett, 2005). The discovery that the effects of *Cannabis* compounds were mediated by endogenous $G_{i/o}$-protein-coupled cannabinoid receptors were aided by the development of potent THC-like synthetic cannabinoids and the new technique of radiolabelling of ligands. The radiolabelling of Pfizer's synthetic cannabinoid CP 55,940 provided evidence of a high-affinity binding site in rat brain membrane for the ligand. Furthermore, unlabelled cannabinoids, like THC, were capable of displacing [$^3$H]-CP 55,940, providing further evidence that they are competing for the same site (Devane *et al.*, 1988). The cloning of the human and rat cannabinoid type 1 receptor ($CB_1$) provided the final evidence of the existence of an endogenous $G_{i/o}$-protein-coupled ($G_{i/o}$PC) cannabinoid receptor (Gerard *et al.*, 1990; Matsuda *et al.*, 1990). Shortly after, a second $G_{i/o}$PC cannabinoid receptor ($CB_2$) was isolated from a human promyelocytic leukemia cell line HL60, which shared 44% amino acid homology with the $CB_1$ receptor (Munro *et al.*, 1993). The discovery of cannabinoid receptors has been followed by much research on their signalling and physiological roles. $CB_1$ receptors are predominantly found in central and peripheral nerve terminals where they negatively modulate neurotransmitter release (Chapter 3; reviewed in Howlett *et al.*, 2002). $CB_2$ receptors are mainly expressed in immune cells to modulate cytokine release and immune cell migration (Appendix 1).

The discovery of the cannabinoid receptors prompted the search for endogenous cannabinoid receptor agonists. The screening for a potential endogenous candidate focused on lipophilic compounds as THC was known to be a lipophilic cannabinoid receptor ligand. The search was successful and resulted in the discovery of *N*-arachidonoyl-ethanolamine in pig brain membranes (Devane *et al.*, 1992). The endogenous cannabinoid (endocannabinoid) was named anandamide, coined after the Sanskrit word for bliss: *ananda*. Further evidence that anandamide was acting through the $CB_1$ receptor was established by utilising the vas deferens bioassay, in which a $CB_1$ receptor agonist negatively modulates neurotransmitter induced contractions of the tissue (Chapter 3; Devane *et al.*, 1992). Shortly after the discovery of anandamide, it was

reported that several mammalian tissues contained other fatty acid derivatives with similar behaviour and structure to anandamide. The second endocannabinoid, 2-arachidonoyl-glycerol (2-AG), was isolated from canine gut (Mechoulam *et al.*, 1995). The endocannabinoids share similar chemical structures, with an arachidonate acyl chain on one end and a polar alcohol functional group on the other (Figure 1.4; Kendall & Alexander, 2017). The endocannabinoids appear to be synthesised "on-demand" upon neuronal activation and they act as retrograde synaptic messengers throughout the nervous system (reviewed in Fowler *et al.*, 2017). The endocannabinoids are metabolised intracellularly, anandamide by fatty acid amide hydrolase (FAAH) and 2-AG by monoacylglycerol lipase (MAGL; Fowler *et al.*, 2017). According to the IUPHAR Receptor Nomenclature and Drug Classification System, the endocannabinoid system consists of nine endocannabinoids, two cannabinoid receptors and a group of enzymes involved in the synthesis and breakdown of the endocannabinoid system (reviewed in Witkamp, 2016). There is a growing consensus that the endocannabinoid system should be expanded to include a larger group of chemicals, receptors and enzymes referred to as the 'endocannabinoidome' (section 1.6.2; reviewed in Cristino *et al.*, 2020; Di Marzo, 2018; Witkamp, 2016). The endocannabinoid system is an important regulator of various physiological functions and processes. Abnormalities or exogenous modulation of the endocannabinoid system can contribute to the pathogenesis of various diseases. It is therefore important to investigate the extent to which medically important *Cannabis* compounds modulate the endocannabinoid system.

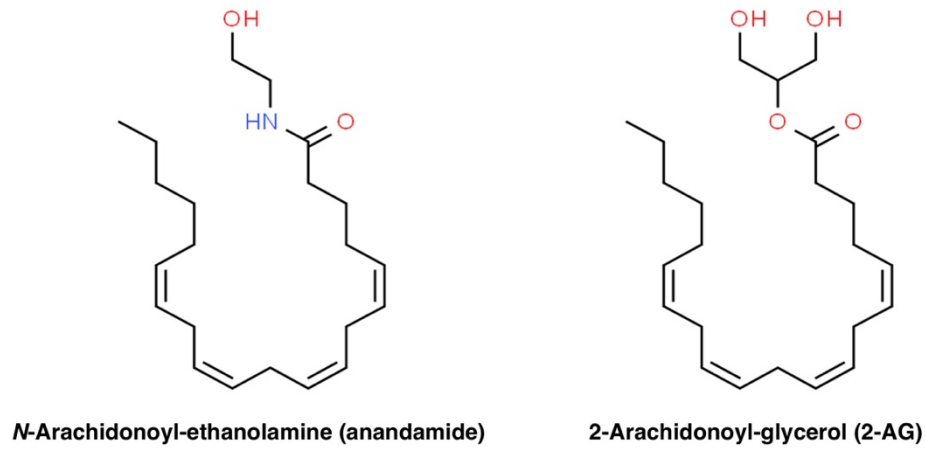


**Figure 1-4.** The chemical structures of the endocannabinoids: anandamide and 2-arachidonoyl-glycerol (2-AG).

## 1.3 The botany and phytochemistry of *Cannabis*

*Cannabis* is a phytochemical-rich plant and synthesises more than 545 phytochemicals representing most chemical classes known (Elsohly & Slade, 2005; Flores-Sanchez & Verpoorte, 2008; Pertwee, 2014). The phytochemical composition depends on the strain and growing conditions of the plant (Di Marzo & Petrocellis, 2006) and the secondary metabolites can be classified into three main chemical groups: phytocannabinoids (section 1.3.2), terpenes (section 1.3.3) and phenolic compounds (section 1.3.4; Figure 1–5; Andre *et al.*, 2016).

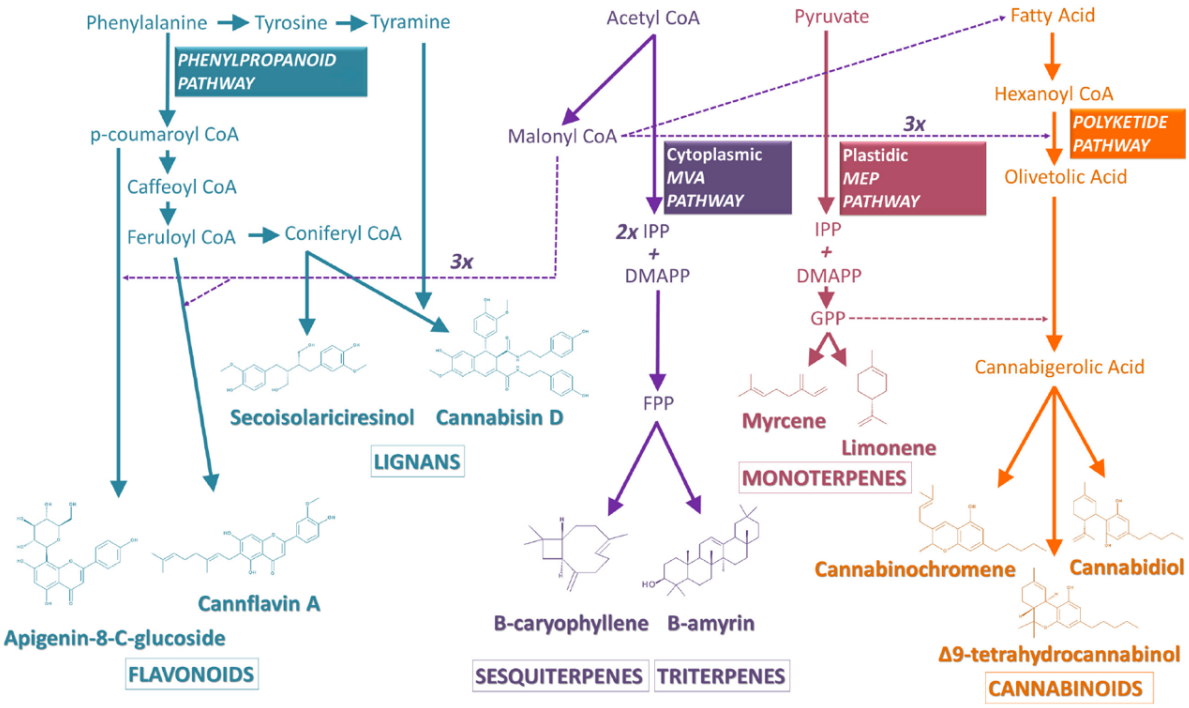


**Figure 1-5.** Schematic presentation of the biosynthetic pathways of *Cannabis*' secondary metabolites.
The figure illustrates the biosynthetic pathways of the main phytochemicals found in *Cannabis*: cannabinoids, terpenes and the phenolic compounds flavonoids. The bold arrows show the catalytic reaction pathways of the secondary metabolites. The dashed arrows show the transportation of precursors. The figure was adapted from Andre *et al.* (2016).

### 1.3.1 *Cannabis* botany

*Cannabis* is one of nine genera in the family *Cannabaceae* (McPartland, 2018). There are taxonomic disagreements concerning the number of species in the genus *Cannabis*; while some studies claim that *Cannabis* is polytypic (containing different species), others suggest that the species *sativa* is monotypic and highly polymorphic (reviewed in Chandra *et al.*, 2017). The disagreement originates from the mid-18$^{th}$ century when the Swedish taxonomist Carl von Linné described *Cannabis sativa L.* as a single species, while the French naturalist Jean-Baptiste Lamarck, 32 years later, classified Indian *Cannabis* (*C. indica*) as a different species from European *Cannabis* (C. sativa; McPartland, 2018). Phytochemical and genetic research support Linné's one-*Cannabis*-species claim with an additional subspecies division of *Cannabis sativa L.* (sativa, indica and possibly ruderalis; McPartland, 2018). There are morphological, phytochemical and origin differences between *sativa* and *indica* (McPartland, 2018). *Sativa* is a tall, well-branched plant with a fibrous stalk and narrow leaflets, high THC to cannabidiol content and originates in Europe, whereas *indica* is a shorter, compact plant with a woody stalk and broad leaflets, high cannabidiol to THC content, and originates in Asia (Figure 1-6; reviewed in Chandra *et al.*, 2017; McPartland, 2018). Often the formal nomenclature of *Cannabis* subspecies is confused with the vernacular nomenclatures of "Sativa", "Indica" and "Ruderalis" (Figure 1-6) which has led to mislabelling of different subspecies and inconsistency in *Cannabis* nomenclature (McPartland, 2018). Today, the widespread hybridisation of different subspecies have rendered cultivation-based distinction of *Cannabis* pointless, thus experts have suggested a modified chemovar-based classification (McPartland, 2018).

*Cannabis* is an annual flowering dioecious plant, where female and male flowers are found in different plants; however, monoecious plants are found in rare cases (Chandra *et al.*, 2017). Male plants are tall and skinny, while female plants are more robust. The *Cannabis* phytochemicals are produced in fine hair structures called trichomes (Figure 1-7) which cover the stems, leaves and bracts and are part of the *Cannabis* defence mechanism (Andre *et al.*, 2016; Chandra *et al.*, 2017). The trichomes are either categorised as glandular or non-glandular, with the main synthesis occurring in glandular trichomes.

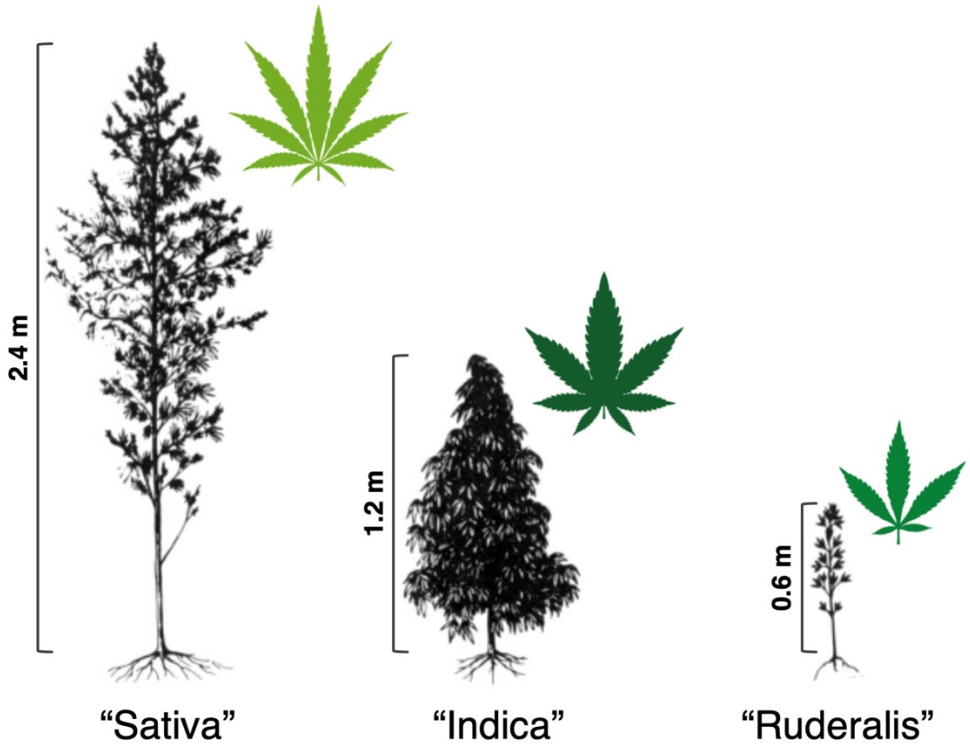


**Figure 1-6.** The vernacular *Cannabis* taxonomy. The figure was adapted from Anderson (1980) and inspired by McPartland (2018).

### 1.3.2 Phytocannabinoids

The medicinal properties of *Cannabis* are generally mediated by C21 skeleton terpenophenolic chemicals called phytocannabinoids, making them the most well-studied phytochemical group (Andre *et al.*, 2016; Flores-Sanchez & Verpoorte, 2008). Currently, 112 phytocannabinoids have been isolated and are classified into 11 subclasses, including $\Delta^9$-THC-, cannabidiol-, cannabinol-, cannabigerol- and cannabichromene-type chemicals (Andre *et al.*, 2016; Chandra *et al.*, 2017; Elsohly & Slade, 2005). Phytocannabinoids are relatively unique to *Cannabis*, with the exception of cannabigerol-like compounds (amorfrutins) which have been identified in plants from the genera *Radula* (Hanus *et al.*, 2016) and *Helichrysum* (Pollastro *et al.*, 2017). The most abundant and well-studied phytocannabinoids are $\Delta^9$-THC, cannabidiol and cannabinol (Chandra *et al.*, 2017; Flores-Sanchez & Verpoorte, 2008). Cannabinoids exist in two

forms either as cannabinoid acids with an attached carboxyl group or as neutral cannabinoids. Cannabinoid acids are non-enzymatically decarboxylated into neutral forms in the plant during storage and heating for smoking (Andre *et al.*, 2016; Chandra *et al.*, 2017; Hanus *et al.*, 2016). Phytocannabinoids are biosynthesised through the polyketide and the plastidal 2-C-methyl-D-erythritol 4-phosphate (MEP) pathways, producing the cannabinoid precursor cannabigerol (Figure 1-5; reviewed in more detail in Andre *et al.*, 2016).

Phytocannabinoids mediate most health benefits and adverse effects associated with the medicinal use of *Cannabis*. The list of pharmacological effects of cannabinoids is long and includes antiepileptic, antinociceptive, appetite stimulation, anti-inflammatory, antioxidant, cardiovascular, antimicrobial and a range of positive effects in psychiatric disorders including anxiety, sleep and depression (reviewed in Flores-Sanchez & Verpoorte, 2008). Phytocannabinoids mediate some of their effects by modulating the endocannabinoid system (section 1.2). THC is the phytocannabinoid responsible for the intoxicating effects of *Cannabis* through the activation of $CB_1$ receptors. Upon the discovery of the medicinal effects of THC, a synthetic THC compound (Marinol®; Solvay Pharmaceuticals, Belgium) was designed to treat nausea and vomiting resulting from chemotherapy, and eventually to stimulate appetite in patients with AIDS (section 1.5; Pertwee, 2008a; Robson, 2005). Due to the adverse effects of THC, it has fewer medicinal uses than cannabidiol (section 1.5.1). Cannabidiol, on the other hand, has gained increased attention for its antiepileptic properties and is currently being trialled for a wide range of diseases (section 1.5).

#### 1.3.2.1 What defines a compound as a cannabinoid?

The adjective "cannabinoid" refers to cannabinoid receptor ligands and chemicals with similar structures to THC, irrespective of whether they target cannabinoid receptors or not (Pertwee *et al.*, 2010), making the terminology confusing. Cannabinoid receptors were defined after the phytocannabinoids with affinity for the receptors, before the discovery of the structurally different endocannabinoids (Figure 1-4). Today, most phytocannabinoids have a poor affinity to the cannabinoid receptors with the exception

of $\Delta^9$-THC, $\Delta^8$-THC and cannabinol (Hanus *et al.*, 2016), which has resulted in suggestions of renaming the receptors after the endogenous ligands (Pertwee *et al.*, 2010). To make the adjective ”cannabinoid” less ambiguous the prefixes “endo”, “phyto” and “synthetic” are used throughout this thesis to emphasise the origins of the cannabinoids.

### 1.3.3 Terpenes

There is great diversity between different *Cannabis* strains, which can be characterised by the plant’s specific terpene fingerprint (Booth & Bohlmann, 2019). Over 200 different terpenes have been identified in *Cannabis*, making it the largest group of phytochemicals (Rice & Koziel, 2015). The composition of terpenes determines the odour and flavour of a *Cannabis* strain. Terpenes are aromatic compounds which are classified by the number of 5-carbon isoprene units, where monoterpenes consist of 2 isoprene units (10 carbons) and sesquiterpenes of 3 isoprene units (15 carbons; Figure 1-5). Terpenes are produced in the secretory glandular trichomes (Figure 1-7) in the *Cannabis* roots, flower and leaves (Andre *et al.*, 2016). Two pathways mediate the synthesis of terpenes, the MEP pathway which is mainly responsible for the synthesis of mono-, di- and tetraterpenes and the mevalonate (MVA) pathway which is responsible for sesquiterpene and triterpene synthesis (Figure 1-5; Andre *et al.*, 2016; Chandra *et al.*, 2017). The two main monoterpenes are conveniently named D-limonene and α-pinene after their lemony and piney odours (Chandra *et al.*, 2017). Other abundant terpenes are β-myrcene, terpinolene (monoterpenes), α-humulene and *β*-Caryophyllene (sesquiterpenes; Andre *et al.*, 2016; Chandra *et al.*, 2017). The terpene content in *Cannabis* flowers is 3.5% or higher and up to 10% in trichomes (reviewed in Russo & Marcu, 2017).

The extent of contribution from terpenes to *Cannabis*’ medicinal benefits is still under debate (Russo & Marcu, 2017). Some of the suggested potential therapeutic effects of terpenes include anti-inflammatory, anxiolytic, analgesic and anticancer (Andre *et al.*, 2016). *β*-Caryophyllene is a bicyclic sesquiterpene with an interesting cyclobutane structure (Figure 1-5). It is found in large amounts in spice and food plants including

black pepper, oregano and cinnamon (Gertsch *et al.*, 2008). *β*-Caryophyllene interacts with the endocannabinoid system to induce anti-inflammatory and analgesic effects mediated by its nanomolar affinity for the $CB_2$ receptor (Gertsch *et al.*, 2008; Klauke *et al.*, 2014). While *β*-Caryophyllene is hydrophobic (Log P 6.7), it has a wide therapeutic index and is considered safe due to its low toxicity (Gertsch *et al.*, 2008).

It has been suggested that terpenes modulate the effects of phytocannabinoids like THC. For instance, it has been reported that the monoterpene limonene enhanced the euphoric effects of THC, while myrcene enhanced the mellowness and sleepiness caused by THC (reviewed in Russo & Marcu, 2017). Furthermore, terpenes alleviate the adverse effects of THC in whole-plant *Cannabis*, compared to the adverse effects of THC alone (Russo, 2013).

**Figure 1-7.** Detailed macro photograph of a *Cannabis* bud with visible hairs and trichomes. Glandular trichomes are the *Cannabis* production site for cannabinoids and terpenes. Source: roxxyphotos/Adobe stock.

### 1.3.4 Phenolic compounds

Phenolic compounds are the most widely distributed secondary metabolites in the plant kingdom, with over 10,000 different structures including phenolic acids, flavonoids, stilbenes and lignans (Andre *et al.*, 2016; Andre *et al.*, 2010). The main role of phenolic compounds is to protect plants from oxidative stress by acting as antioxidants (reviewed in Andre *et al.*, 2016). Phenolic compounds are produced via the phenylpropanoid pathway (Figure 1-5) in the cytoplasm and are then stored in either the vacuole or cell wall. While the flavonoid pathway has been extensively studied in other plants, there have been no *Cannabis*-specific studies of this pathway (Andre *et al.*, 2016; Flores-Sanchez & Verpoorte, 2008).

Phenolic compounds have similar therapeutic benefits to phytocannabinoids and terpenes, including anti-inflammation, anticancer and neuroprotective effects (Andre *et al.*, 2010). About 20 flavonoids have been identified in *Cannabis*, including apigenin, cannflavin A and cannflavin B which are unique to *Cannabis*. Apigenin has demonstrated anxiolytic and oestrogenic properties, while cannflavin has potent anti-inflammatory effects by inhibiting prostaglandin E2 (Flores-Sanchez & Verpoorte, 2008).

## 1.4 Medicinal *Cannabis* regulations

As discussed, humans have used medicinal *Cannabis* for thousands of years until a relatively recent era of prohibition, starting in 1937 (section 1.1), which hampered the research on *Cannabis*' medicinal potential. However, in the last 20 years, medicinal *Cannabis* use has resurged, resulting in a renewed scientific interest of its potential medicinal benefits. Consequently, regulations and policies around *Cannabis* have eased. This section emphasises the current regulations of medicinal *Cannabis* internationally with a focus on high-income countries, including Australia.

### 1.4.1 International regulations

According to the United Nations' Single Convention on Narcotic Drugs in 1961, *Cannabis*, *Cannabis* resins and extracts were listed as schedule-1 illicit drugs (United Nations Office on Drugs and Crime, 1961). The Single Convention prohibits the production, distribution and possession of *Cannabis* among other drugs, with the exception of medical and scientific purposes. Hence there is no international law prohibiting the use of *Cannabis* products for medicinal purposes. The United Nations have recently suggested that cannabidiol products containing 2% or less THC should not be subject to international controls (United Nations, 2020). There are currently four cannabinoid-based medicines available around the world, two synthetic cannabinoid- and two *Cannabis*-based treatments (section 1.5).

Canada was the first G7 country to legalise *Cannabis* for both medical and recreational purposes in 2018 (Pusiak *et al.*, 2021). Other countries have since then followed by easing *Cannabis* restrictions to varying degrees. The main international agencies responsible for the regulation of *Cannabis* products are the European Medicines Agency (EMA) and the US Food and Drug Administration (FDA). European countries can gain marketing access to drugs either through a single authorisation of the product throughout EU countries or through a non-centralised route whereby each country applies for marketing access (Abuhasira *et al.*, 2018). To date, the EMA has not approved market authorisation for any *Cannabis*- or synthetic cannabinoid-based medications. However, the EMA has issued an orphan designation of *Cannabis* products (European

Monitoring Centre for Drugs and Drug Addiction, 2018), which should not be confused with marketing authorisation. For a disease to be considered as an orphan disease it has to fit a strict set of criteria including being a rare disease that only affects 5 out of 10,000 people in the EU. Some countries have also, through a non-centralised route, authorised the use of some *Cannabis* products. No EU country has authorised the smoking of *Cannabis* as a possible route of administration, due to the difficulties of controlling the *Cannabis* content between different plants and the health danger associated with inhaling smoke. Similarly to the EMA, the FDA has not approved any *Cannabis* treatments until recently when a cannabidiol-based oral solution (Epidiolex®; section 1.5.2) was given market authorisation. In contrast to the EMA, the FDA has approved two synthetic THC-like cannabinoids, namely dronabinol (Marinol® and Syndros®) and nabilone (Cesamet®; section 1.5). *Cannabis* is under federal regulations in the US where it is classified as a schedule 1 drug meaning that *Cannabis* use is prohibited for any purpose (Abuhasira *et al.*, 2018). Nonetheless, some US states have issued laws allowing the use of medical *Cannabis*, hence counteracting federal laws. At the time of writing this thesis medicinal *Cannabis* is approved in 33 US states and the district of Colombia (D.C.), nine states have legalised recreational use and 15 states allow restricted use of *Cannabis*.

### 1.4.2 Australian regulations

The Australian Narcotic Drugs Act of 1967 was a response to the Single Convention of 1961 and intended to "prevent the abuse and diversion of controlled narcotics" and to "ensure that controlled narcotics are available for medicinal and research purposes in Australia" (The Office of Drug Control, 2019). Up to 2016, the Narcotic Drug Act regulated narcotic drugs principally by licensing the manufacture of narcotics, mainly applying to morphine obtained from the opium poppy. The regulation of the import, export and manufacture of *Cannabis* and cannabinoids were under other Commonwealth laws. State and Territory laws were responsible for permitting the cultivation of *Cannabis* in Australia mainly for industrial and horticultural purposes. Outside of this, *Cannabis* and cannabinoids were treated as illegal narcotics by Australian laws. In 2016, the Narcotic Drug Act 1967, was amended to permit the

cultivation and production of *Cannabis* and its resin in Australia. The main objective was to enable a sustainable supply of medicinal *Cannabis* products for therapeutic purposes and to allow for the facilitation of scientific research into medicinal *Cannabis*, this while ensuring that Australia remained compliant with the Single Convention. However, patient access to *Cannabis* and cannabinoids is still regulated by commonwealth, state and territory laws.

The Therapeutic Goods Act 1989 was established by the Australian Therapeutic Goods Administration (TGA) to set the regulatory framework for medicines in Australia and to ensure that they are safe and fit for their intended purposes (Therapeutic Goods Administration, 2018). The Act allows for the access of unapproved therapeutic goods including *Cannabis* products. A patient can access *Cannabis* treatments through their prescriber would apply for the Special Access Scheme (SAS). The prescriber must have considered all clinically appropriate treatment options before they apply for the SAS. The TGA is unable to vouch for the quality, safety and effectiveness of unapproved drugs accessed through the SAS, hence the prescriber and patient accept responsibility for any adverse effects, as these drugs remain unregulated by the TGA. To date, the TGA has approved *Cannabis* SAS applications for the treatment of neuropathic pain, cancer pain, palliative care indications, refractory paediatric epilepsy, spasticity from neurological conditions, chemotherapy-induced nausea and vomiting and anorexia and wasting associated with chronic illness such as cancer, among other indications. By January 2020, 3151 SAS applications have been approved compared to 738 in February 2019. Patient access to cannabidiol further improved in May 2017 when cannabidiol was rescheduled from a schedule 8 drug (S8; Controlled Drug) to schedule 4 (S4; Prescription Only Medicine; Therapeutic Goods Administration, 2017). This only applies to *Cannabis* extracts where cannabidiol makes up at least 98% of total cannabinoid content. Certain cannabidiol preparations including oral, oral mucosal and sublingual formulations were recently further down scheduled to schedule 3 (Therapeutic Goods Administration, 2020). For a cannabidiol product to be a schedule 3 drug it needs to fulfil the following criteria: i) cannabidiol must be derived from *Cannabis* or if synthetic only contain the (-)-cannabidiol enantiomer; ii) have a maximum recommended dose of 60 mg or less; iii) have up to a 30 days' supply per

pack; iv) the cannabidiol content must be 98% or more of total cannabinoids in preparation; v) any other cannabinoids have to make up 2% or less of total cannabinoid content, and have to be naturally occurring cannabinoids; vi) must only apply for treatment of adults (>18 years); and vii) the packaging must be child-safe.

Under federal law, *Cannabis* is illegal in all Australian states and territories. However, the Australian Capital Territory (ACT) has added amendments to exempt individuals from criminal punishment in certain circumstances (Australian Federal Police, 2020). An individual adult is allowed to possess up to 50 g of dried *Cannabis*, or up to 150 g of fresh *Cannabis*, grow up to two *Cannabis* plants at their home per person with a maximum of four plants per household. However, it is an offence to use *Cannabis* in public places, expose children to *Cannabis*, artificially cultivate *Cannabis*, or grow it on publicly accessible places. Under the Narcotic Drug Act, it is still illegal for an individual in the ACT to use *Cannabis* as a minor, share *Cannabis* with others or drive with any traces of *Cannabis* in their blood system.

Similarly to the rest of the world, Australians have expressed an increased interest in medicinal *Cannabis* (Therapeutic Goods Administration, 2018). This has put pressure on prescribers to find evidence of *Cannabis'* medicinal potential in treating various conditions. In response, the Commonwealth Department of Health together with the state and territory governments have provided clinical guidance documents. These documents provide prescribers with guidelines on the use of medicinal *Cannabis* in various conditions including nausea and vomiting, epilepsy in paediatric and young adults, multiple sclerosis, palliative care and chronic non-cancer pain (Therapeutic Goods Administration, 2018). The guides are intended to provide support for prescribers and dispensers on current, non-biased evidence on the use of medicinal *Cannabis* for various medical conditions in patients. They also guide health professionals on how to prescribe medicinal *Cannabis* under the current access schemes and to provide patients with an understanding of how *Cannabis* can be used to alleviate symptoms of various conditions.

## 1.5 Current cannabidiol treatments

Cannabidiol was discovered 80 years ago by the American chemist Roger Adams, who stated that "It [cannabidiol] has none of the physiological activity typical of Marihuana" (Adams *et al.*, 1940; section 1.1). Early pharmacological studies of individual cannabinoids demonstrated that THC, but not cannabidiol, induced catalepsy in mice (Loewe, 1946). It is known today that the ability of a cannabinoid to induce catalepsy in rodents correlates with its psychotropic abilities (reviewed in Pertwee, 2006). It was long believed that THC was the only main "active" cannabinoid, as it demonstrated pronounced psychomimetic effects. Thus, cannabidiol was overlooked by researchers for many years (Burstein, 2015). However, in the last decade, there has been a dramatic increase in research on cannabidiol, apparent by the cumulative number of publications on the topic over the years. Publications with "cannabidiol" or "CBD" in the title from the last 5 years (2016-2020) amount to 60% of all publications on the topic from 1963 when the structure of cannabidiol was elucidated. In comparison, while there are substantially more publications on THC (3829 compared to 1829 cannabidiol publications), the last 5 years only account for 17% of total publications. In contrast to THC, cannabidiol is often claimed to be devoid of psychoactivity. This is misleading as cannabidiol has demonstrated therapeutic potential in a wide range of psychiatric disorders including psychosis, depression, anxiety, drug-cravings and cognitive impairment (reviewed in Bonaccorso *et al.*, 2019). The comparison of psychotropic effects between THC and cannabidiol is likely referring to cannabidiol's inability to induce intoxications, unlike THC. Cannabidiol, while not causing intoxication on its own, can alleviate the intoxicating effects of THC and also dampen adverse effects like impaired spatial working memory and cognitive impairment (Di Marzo, 2014). Cannabidiol has been suggested to be medicinally beneficial in treating inflammation, nausea, emesis, epilepsy and as an antioxidant. As of today, there are 110 active, recruiting or to be recruiting clinical trials involving cannabidiol, with the majority of studies investigating its effects on mental/psychotic disorders (U.S. National Library of Medicine, 2020).

Until recently all cannabinoid therapeutics contained THC or THC-mimetic compounds, including Cesamet®, Marinol®, Syndros® and Sativex® (Abuhasira *et al.*, 2018). Cesamet® is an oral capsule that contains nabilone, a synthetic THC-like cannabinoid, indicated for the treatment of nausea and vomiting resulting from chemotherapy treatments. Similarly, Marinol® (oral capsules) and Syndros® (oral solution) contain synthetic $\Delta^9$-THC for the treatment of AIDS-induced anorexia. It is also used to treat nausea and vomiting induced by chemotherapy when other treatments are insufficient. Sativex® is an oromucosal spray that contains equal amounts of THC and cannabidiol and is mainly used in the treatment of spasticity associated with multiple sclerosis (discussed in more detail in section 1.5.1). Today, Epidiolex®, a cannabidiol-only oral solution is showing promising antiseizure effects in children with rare forms of epilepsy (section 1.5.2).

### 1.5.1 Sativex®

Sativex® (oromucosal spray; GW pharmaceuticals, UK) was the first *Cannabis*-based therapeutic to be approved by any country. It is mainly used to treat spasticity in patients with the chronic autoimmune disease multiple sclerosis. Sativex® is currently approved for the treatment of spasticity in over 25 countries, including Australia, New Zealand, Canada, US, Israel, UK and several other European countries (GW Pharmaceuticals, 2019b). Israel and Canada have also approved Sativex® for the treatment of pain resulting from cancer and multiple sclerosis. Sativex® consists of *Cannabis* extracts in a water-ethanol solution with equivalent THC and cannabidiol concentrations of 27 mg/ml and 25 mg/ml, respectively. GW Pharmaceuticals has selectively bred two different chemovars of *Cannabis* which yield high concentrations of either THC (>90% of total cannabinoid content) or cannabidiol (>85% of total cannabinoid content; Barnes, 2006). Sativex® also contains other minor cannabinoids (5-6%) and terpenes (Russo & Guy, 2006).

Current medications for mild to moderate spasticity are not completely effective and their prolonged use is associated with numerous adverse effects. Although the treatments for severe spasticity are effective, they are invasive, expensive and entail a

risk of infection, which has limited their use (reviewed in Giacoppo *et al.*, 2017). This has prompted patients with multiple sclerosis to self-medicate with *Cannabis* to control their symptoms (Baker *et al.*, 2007; Ware *et al.*, 2005). In a questionnaire study on *Cannabis* self-medication in the UK, the majority of subjects reported that they used *Cannabis* to treat chronic pain, multiple sclerosis and/or depression (Ware *et al.*, 2005). The use of unregulated *Cannabis* has several disadvantages involving its illegal status, phytochemical content and route of administration. Self-medication with *Cannabis* cannot ensure safe and consistent dosage of appropriate phytocannabinoids. Sativex® provides a safer route of administration through the oral mucosa and application-based dosage control. Good manufacturing practises used during the production of Sativex® ensures high consistency of phytochemical constituents. Smoking is a common route of administration for individuals suffering from multiple sclerosis and who choose to self-medicate with *Cannabis* (Ware *et al.*, 2005). Smoking is associated with several adverse effects including, chronic coughs dyspnoea, sputum production, chest tightness and hoarse voice (Ribeiro & Ind, 2016). In contrast, oromucosal administration of cannabinoids allows direct and rapid access to the circulation, bypassing first-pass hepatic metabolism (section 1.5.3.1).

There is strong evidence for the use of THC and cannabidiol in treating multiple sclerosis symptoms. Rodent studies support the involvement of $CB_1$ receptors in the pathogenesis of spasticity (Pryce & Baker, 2007). $CB_1$ receptor agonists induce antispastic activity, which is attenuated in $CB_1^{-/-}$ mice (Pryce & Baker, 2007). THC in Sativex® is likely mediating antispasticity by partially activating prejunctional $CB_1$ receptors, hence negatively modulating neurotransmitter release (Chapter 3; Russo & Guy, 2006). In contrast to THC, cannabidiol is a low-affinity ligand at cannabinoid receptors (Chapter 3). The rationale of combining THC with cannabidiol to treat symptoms of multiple sclerosis resides in the ability of cannabidiol to enhance the beneficial effects of THC while alleviating the adverse effects (reviewed in McPartland & Russo, 2001), commonly referred to as the "entourage" effect of cannabinoids. Patients with multiple sclerosis who suffer from both spasticity and neuropathic pain respond better to the combination of THC and cannabidiol than to THC alone (reviewed in Russo & Guy, 2006). THC and cannabidiol treatments have several

advantages to THC only treatments, including less sedation, memory impairment, intoxication, and improved sleep and walking time (Russo & Guy, 2006). Furthermore, the combination of THC and cannabidiol induce acceptable adverse effects without creating tolerance over time (Russo & Guy, 2006).

### 1.5.2 Epidiolex®

Epidiolex® (oral solution; GW pharmaceuticals, UK) is the first cannabidiol-only therapeutic to be approved by the FDA. It is currently used to treat severe refractory epilepsy syndromes in children, including Dravet syndrome, Tuberous Sclerosis Complex, Infantile Spasms and Lennox-Gastaut syndrome (GW Pharmaceuticals, 2019a). About a third of patients with epilepsy suffer from drug-resistant seizures which increases morbidity and mortality, causing some to resort to self-medication with *Cannabis* (Chen *et al.*, 2018; reviewed in Samanta, 2019). The legalisation of *Cannabis* has made over-the-counter phytocannabinoid treatments accessible for patients. Parents of children with epilepsy have successfully decreased the seizure frequency using cannabidiol-rich *Cannabis* preparations (Porter & Jacobson, 2013). However, in an FDA analysis, 33% of over-the-counter claimed cannabidiol preparations contained no cannabidiol (U.S. Food and Drug Administration, 2020). Thus, as a result of the lack of regulation of *Cannabis* products and the numerous clinical trials which support a role for cannabidiol in treating refractory epilepsy, in 2018 the FDA approved Epidiolex® – a 99% pure cannabidiol extract (Sekar & Pack, 2019). The anticonvulsive effects of cannabidiol were assessed in a double-blind clinical study of 120 children and young adults with refractory epilepsy seizures (Devinsky *et al.*, 2017). Patients treated with cannabidiol experienced a 39% median decrease in convulsive seizures while placebo-treated patients experienced a 13% decrease. There was no significant comparable decrease in non-convulsive seizures between the patients who received cannabidiol treatment and placebo. Cannabidiol-treated patients suffered more adverse events, including, vomiting, diarrhoea, somnolence, fatigue, pyrexia and elevated liver aminotransferase enzymes (section 1.5.3.4) which indicates that the liver is undergoing metabolic stress (Devinsky *et al.*, 2017).

The underlying antiepileptic mechanism of cannabidiol is yet to be fully elucidated; it likely involves several pharmacological targets (section 1.6), hence producing cumulative antiepileptic effects (reviewed in Samanta, 2019). Cannabidiol is assumed to attenuate excitatory neurotransmission through γ-aminobutyric acid (GABA)-mediated inhibition (section 1.6.3.7) and by modulating intracellular calcium through transient receptor potential (TRP) channels (section 1.6.2.4), the orphan G-protein coupled receptor GPR55 (section 1.6.2.1) or the voltage-dependent anion channel 1 (reviewed in Samanta, 2019). It has also been postulated that cannabidiol induces antiepileptic effects through anti-inflammatory actions by modulating TNF-α and inhibiting adenosine reuptake (section 1.6.3.2). 5-$HT_{1A}$ and 5-$HT_{2A}$ receptor agonism may also be responsible for some of the anti-epileptic effects of cannabidiol (section 1.6.3.1; Chen *et al.*, 2019).

Despite the availability of Epidiolex®, many families of children with epilepsy still opt to use cannabidiol-rich *Cannabis* preparations due to easier access, lower cost and the widespread perception that whole plant extracts are more efficient than cannabidiol-only products (reviewed in Anderson *et al.*, 2020). These unregulated cannabidiol preparations tend to also contain low doses of THC. Animal studies on the potential medicinal benefits of THC against seizures are conflicting, with reports of both anticonvulsive and pro-convulsive effects. A recent study investigated whether the combination of cannabidiol and THC would produce greater anticonvulsive effects in a $Scn1a^{+/-}$ mouse model of Dravet syndrome than either phytocannabinoid administered alone (Anderson *et al.*, 2020). The study found that acute administration (i.p.) of subthreshold cannabidiol (12 mg/kg) and THC (0.1 mg/kg) decreased hyperthermia-induced seizures to a greater extent than either phytocannabinoid administered on its own. The authors suggest that cooperative pharmacodynamic actions of cannabidiol and THC are inducing anticonvulsive effects through the modulation of neuronal excitability. THC can modulate glutamate release while cannabidiol can induce antiepileptic effects by targeting GPR55, TRPV1 and GABA receptors (section 1.6). Surprisingly, the cotreatment of $Scn1a^{+/-}$ mice with phytocannabinoid-infused chow, not only failed to decrease spontaneous convulsions but also increased the severity of the seizures and mortality. Interestingly, higher THC doses on their own did not increase

spontaneous convulsions. Based on this study the authors concluded that cannabidiol and THC comedication of children with epilepsy should be closely monitored.

### 1.5.3 Pharmacokinetic profile of cannabidiol

While cannabidiol has a wide range of therapeutic potential, the use of cannabidiol as an effective treatment is hampered by its pharmacokinetic limitations (reviewed in Millar *et al.*, 2020). The pharmacokinetic limitations of cannabidiol include poor bioavailability (section 1.5.3.1), low solubility and inter-individual pharmacokinetic variability. As a highly lipophilic molecule, cannabidiol has an alcohol to water partition coefficient (log P) of 6.3 (Odi *et al.*, 2020). Due to the lipophilic nature of cannabidiol, cannabidiol therapeutics are usually formulated in oil or alcohol preparations such as liquid solution (e.g., Epidiolex®), soft-gel capsules, oromucosal spray (e.g., Sativex®), or sublingual sprays. A novel cannabidiol formulation to increase the delivery of cannabidiol has been suggested (section 1.5.3.6), which would increase the bioavailability of cannabidiol while decreasing the efficacy variability between patients (Millar *et al.*, 2020).

#### 1.5.3.1 Absorption

The route of administration of cannabinoids determines their level of absorption to the circulatory system and subsequent bioavailability. Inhaled cannabinoids reach maximum plasma concentrations rapidly ($T_{max}$ 3 to 10 min) due to their quick absorption, resulting in a bioavailability of 31% (Ohlsson *et al.*, 1986). In contrast, the absolute bioavailability of oromucosal administered cannabidiol or THC is unknown, as these compounds have not been intravenously administered (Therapeutic Goods Administration, 2013). Due to the high lipid solubility of cannabidiol and THC, they are absorbed rapidly by the oral mucosa into the circulation, hence bypassing extensive first-pass hepatic metabolism. Oromucosal phytocannabinoids reach maximum plasma concentrations within 1-1.5 h ($T_{max}$) which results in a maximum plasma concentration ($C_{max}$) that is a fraction of what is observed with inhalation. Additionally, the $C_{max}$ of cannabidiol is generally less than half of THC during oromucosal administration (Therapeutic Goods Administration, 2013). The coadministration of Sativex® with high-

fat food increased the absorption of both THC and cannabidiol by 3- and 5-fold, resulting in a subsequent $C_{max}$ increase of 1.6- and 3.3-fold, respectively. Due to the influence of food on the pharmacokinetics of Sativex®, it is evident that significant amounts of cannabinoids are absorbed via the gastrointestinal tract, due to drug being swallowed rather than being absorbed by the mucosa.

Oral administration of cannabidiol (e.g., Epidiolex®) undergoes extensive first-pass hepatic metabolism, resulting in a low bioavailability (between 6-20%; Devinsky *et al.*, 2014; Therapeutic Goods Administration, 2013). As expected, Epidiolex® at the recommended dose for children with refractory epilepsy takes longer to reach a maximum concentration ($T_{max}$ 2.5-5 h) than either inhaled or oromucosal administered cannabidiol (Devinsky *et al.*, 2014). The concentration-time profile of orally administered cannabidiol is useful for patients with a chronic disorder where long-term benefits of cannabidiol are required, e.g., patients with epilepsy. As noted above for Sativex®, several studies have demonstrated that the administration of oral cannabidiol in conjunction with a meal significantly enhances the absorption of cannabidiol and hence the maximum plasma concentration (Millar *et al.*, 2018). This effect is more evident with high-fat food which dissolves the lipophilic cannabidiol, thus, increasing the absorption and bioavailability of cannabidiol.

#### 1.5.3.2 Distribution

The distribution of cannabinoids in the body is governed by their lipophilicity. Cannabinoids therefore generally distribute to well-vascularised tissues like lung, heart, brain and liver and subsequently to less vascularised fatty tissues (reviewed in Lucas *et al.*, 2018). As cannabidiol is highly lipophilic and distributes extensively to fatty tissues, it subsequently has a high volume of distribution (~32 L/kg; calculation based on intravenous administration; Devinsky *et al.*, 2014). Additionally, cannabidiol binds extensively to proteins (~90%), primarily to P-glycoproteins (section 1.5.3.4; Devinsky *et al.*, 2014; Therapeutic Goods Administration, 2013; Zhu *et al.*, 2006).

### 1.5.3.3 Metabolism & elimination

Cannabidiol is predominantly metabolised hepatically by cytochrome P450 (CYP 450) isoenzymes, primarily by CYP2C19 and CYP3A4 (Zendulka *et al.*, 2016). During metabolism, cannabidiol is hydroxylated to its main active metabolite 7-OH-cannabidiol, which is subsequently metabolised to the inactive metabolite 7-COOH-cannabidiol (Devinsky *et al.*, 2018). There is limited knowledge on the pharmacological activity of cannabidiol metabolites. It would therefore be interesting to investigate to what extent they contribute to cannabidiol's therapeutic effects. The metabolites are mainly eliminated via the faecal route and to a lesser extent, the renal route (Devinsky *et al.*, 2014; Therapeutic Goods Administration, 2013). The half-life of cannabidiol is highly dependent on the route of administration, ranging from 1.1 h to 5 days (Millar *et al.*, 2018). More specifically, based on 24 studies which analysed the pharmacokinetic profile of cannabidiol in humans, the half-life was 1-11 h for oromucosal administration, 24 h for intravenous administration, 31 h for smoking and 2-5 days for chronic oral administration (reviewed in Millar *et al.*, 2018). The long half-life probably reflects the storage of cannabidiol in fatty tissues and the subsequent slow redistribution.

### 1.5.3.4 Pharmacokinetic interactions

Little data exist on drug-drug interactions with cannabidiol. Nonetheless, concerns have been raised over cannabidiol's potential pharmacokinetic interactions with other drugs (Chen *et al.*, 2019; Devinsky *et al.*, 2014; Lucas *et al.*, 2018). The metabolism of cannabidiol is highly dependent on the CYP3A4 and CYP2C19 isozymes. This was made evident by the changes in cannabidiol maximum plasma concentration in healthy male subjects during coadministration with the CYP3A4 inducer rifampicin ($C_{max}$ -52%) or with the CYP3A4 inhibitor ketoconazole (Cmax: +89%; Stott *et al.*, 2013). An *in vitro* study has also demonstrated that cannabidiol is a potent CYP2C19 inhibitor (Jiang *et al.*, 2013). Pharmacokinetic interactions are of concern in patients using cannabidiol as an adjunct to their epilepsy medicine, as some of the epilepsy drugs are highly metabolised by the same CYP isozymes as cannabidiol. Clobazam and valproates are the two most common antiepileptic drugs used by children with Dravet syndrome (Devinsky *et al.*, 2017). Clobazam is a benzodiazepine used for short-term treatment of anxiety

symptoms in adults and as an adjunctive agent in children with refractory epilepsy (Devinsky *et al.*, 2017; NPS MedicineWise, 2020; Russell *et al.*, 2018). It is metabolised by CYP3A4 to the active metabolite *N*-desmethylclobazam, which mediates 20% of clobazam's activity (Russell *et al.*, 2018). *N*-desmethylclobazam is subsequently metabolised by CYP2C19 to its inactive metabolite. In a clinical trial, cannabidiol was investigated as a possible adjunct to clobazam in children with refractory epilepsy (Geffrey *et al.*, 2015). The comedication significantly increased clobazam and *N*-desmethylclobazam plasma concentrations by 60 ± 80% and 500 ± 300% (± standard deviation), respectively. The adverse effects reported were similar to those commonly seen in patients treated with high doses of clobazam and were alleviated once the dose had been decreased. The plasma concentration of cannabidiol was not affected by the presence of clobazam. Valproate, a commonly used anticonvulsant, in combination with cannabidiol increases aspartate aminotransferase and alanine aminotransferase, in patients with Dravet syndrome (Devinsky *et al.*, 2017; Devinsky *et al.*, 2018). High aminotransferase concentrations are associated with hepatotoxicity. In a clinical study on the effects of cannabidiol on treatment-resistant Dravet syndrome in children, elevated aminotransferase levels were observed in 12 out of 120 patients, all of which were being co-medicated with valproate (Devinsky *et al.*, 2017). In another clinical study, they assessed the safety and pharmacokinetic interactions with cannabidiol in 34 patients with Dravet syndrome; all patients with aminotransferase abnormalities were taking concomitant valproate (Devinsky *et al.*, 2018). The aminotransferase increase was resolved while patients continued their treatment or upon the trial completion, which indicates that the elevated aminotransferase levels were induced by transient metabolic stress (Devinsky *et al.*, 2017; Devinsky *et al.*, 2018). The mechanism of the pharmacokinetic interaction between valproate and cannabidiol is unknown as the two drugs do not share the same metabolism pathway (Morrison *et al.*, 2019).

Cannabidiol, compared to other cannabinoids, uniquely inhibits P-glycoprotein-mediated drug transport *in vitro* (Zhu *et al.*, 2006). P-glycoproteins are ATP-dependent efflux transporters; hence inhibition of the transporter would increase intracellular concentrations of P-glycoprotein-dependent compounds (Zhu *et al.*, 2006). The

potential role of P-glycoproteins in cannabidiol's pharmacokinetic interactions has not been investigated further.

Coadministration of various cannabinoids enhances the plasma concentration of cannabinoids, as they share similar pharmacokinetic profiles. In both animal and human studies, cannabidiol and THC treatment induced increased plasma and tissue concentrations of phytocannabinoids (Anderson *et al.*, 2020; Arkell *et al.*, 2019). Due to the increased access of unregulated cannabidiol (section 1.4.1), there is widespread unreported self-medication that can cause severe cannabidiol-induced indirect adverse effects of co-administered drugs. This is evident in a case study of a 13-year-old girl suffering from metastasised cancer and pain who was being treated with the opioid methadone (Madden *et al.*, 2020). Unbeknown to her physicians the parents were also treating the daughter with high oral cannabidiol doses with the hope of it having anti-tumour effects. The girl's physicians were contacted by the parents as the girl was experiencing increased fatigue and sleepiness, symptoms that were worsening by the day. Upon the discovery that the patient had been treated with cannabidiol by the parents, methadone plasma concentrations were measured revealing that there was a significant enhancement which could explain the adverse effects experienced by the child.

#### 1.5.3.5 Plasma concentration

The relevance of nonclinical studies highly depends on the experimental conditions used. It is of great importance that experiments are performed under physiological conditions including using clinically relevant concentrations when evaluating the potential medicinal benefits of a drug. Based on both clinical and nonclinical studies, cannabidiol has extensive medicinal benefits. However, many cannabidiol studies use supraphysiological concentrations, which are deemed to be clinically irrelevant as these concentrations are higher than those detected in humans or what is pharmacokinetically possible to achieve, especially with cannabidiol's poor pharmacokinetic profile. It is especially important to use clinically relevant concentrations when studying the potential mechanism(s) of actions of a drug as there

is a loss of target selectivity with increased drug concentration. This is particularly relevant for cannabidiol, as it is a promiscuous drug with many targets over a great range of concentrations (section 1.6; Figure 1-8). Table 1-1 summarises the plasma concentrations of cannabidiol in patients with epilepsy who have been treated with an oral cannabidiol solution and in mice with hyperthermia-induced seizures that were treated with i.p. injections of cannabidiol. The plasma concentrations of cannabidiol in humans have been important in determining what concentrations of cannabidiol to use when exploring its effects on vascular tone *ex vivo* and mechanisms of action in this thesis (Chapter 4).

#### 1.5.3.6 How to improve cannabidiol's pharmacokinetic profile

The main pharmacokinetic challenges with cannabidiol result from its hydrophobic properties which limit its oral bioavailability. Cannabidiol's bioavailability can be increased by changing the route of administration to inhalation of vaporised cannabidiol. In five individuals, vaporised cannabidiol resulted in a bioavailability of 31% compared to 6% during oral administration (Ohlsson *et al.*, 1986). A more recent study confirmed a substantial higher bioavailability of cannabidiol when vaporised compared to orally dosed (Spindle *et al.*, 2020). In 12 healthy females and males, vaporised cannabidiol-induced a 10-fold higher whole-blood cannabidiol concentration (104.6 ± 76.5 ng/ml) than oral cannabidiol (11.1 ± 14.7 ng/ml) administration. The advantage of the inhaled route compared to oral administration is the quick delivery of cannabidiol which results in a faster (shorter $T_{max}$) maximum plasma concentration ($C_{max}$) and therefore an increased overall bioavailability. However as discussed in Millar *et al.* (2020), the large standard deviations indicate that there is great inter-subject pharmacokinetic variability. In addition, the solubiliser used to create the cannabidiol vaporiser solution may be a cause of irritation for some patients.

A recent publication explored different methods of improving the water solubility of cannabidiol which could lead to higher absorption and therefore also a greater bioavailability (Koch *et al.*, 2020). This is promising, as aqueous solubility-enhanced cannabidiol preparations would increase the therapeutic benefits of cannabidiol.

**Table 1-1.** Cannabidiol plasma concentrations in animals and humans

| Subjects | Drug treatment | Blood sample collection | Dose (mg/kg/d) | Plasma concentration (ng/ml)* | Mean converted concentration (μM)† | Reference |
|---|---|---|---|---|---|---|
| Scn1a$^{+/-}$ mice<br>Dravet syndrome model | Acute i.p. injections<br>3 study groups | After the end of hyperthermia-induced seizures experiment | 12 | 402 ± 59 | 1.28 | Anderson *et al.* (2020) |
| | | | 25 | 771 ± 82 | 2.45 | |
| | | | 100 | 2826 ± 242 | 8.99 | |
| Children (4-10 y/o)<br>Dravet syndrome | Oral solution<br>3-week treatment including dose titration<br>3 study groups | 3 weeks of treatment<br>2.5 h post-dose time point | 5 | 130 ± 170 | 0.41 | Devinsky *et al.* (2018) |
| | | | 10 | 242 ± 159 | 0.77 | |
| | | | 20 | 380 ± 370 | 1.21 | |
| Children and teenagers (4-19 y/o)<br>Refractory epilepsy | Oral solution<br>8-week treatment including dose titration<br>1 study group | Measurement within the same study group at 4 (20 mg/kg/d) weeks and 8 weeks (25 mg/kg/d) | 20 | 82-1000 ($\bar{x}$=388) | 1.23 | Geffrey *et al.* (2015) |
| | | | 25 | 100-800 ($\bar{x}$=450) | 1.43 | |

*Plasma concentrations are expressed as mean ± S.E.M. Anderson *et al.* (2020) and mean ± S.D. Devinsky *et al.* (2018). †Calculations are made on the basis of cannabidiol's molecular weight ($M_w$) of 314.5 g/mol.

## 1.6 The diverse pharmacological targets for cannabidiol

Cannabidiol is a promiscuous drug as it has multiple targets over a wide range of concentrations. Despite extensive preclinical evidence on the medicinal benefits of cannabidiol, the specific pharmacological targets remain unknown. Over 65 unique pharmacological targets have been reported in the literature for cannabidiol (reviewed in Ibeas Bih *et al.*, 2015) across the endocannabinoid system (section 1.6.1), endocannabinoidome (section 1.6.2) and other targets (section 1.6.3). Some of the targets are unlikely to be relevant as the effects of cannabidiol have only been observed at supraphysiological concentrations (≥10 μM), which cannot realistically be achieved *in vivo* (Ibeas Bih *et al.*, 2015).

This section summarises the main pharmacological targets for cannabidiol in different conditions with the exception of the cardiovascular system which is discussed in more detail in Chapter 4 and Chapter 5.

### 1.6.1 Endocannabinoid system

#### 1.6.1.1 $CB_1$ receptors

There is a clear structural overlap between cannabidiol and THC (Figure 1-3). Whereas THC is a planar molecule, cannabidiol has an angled configuration resulting in its poor affinity at the $CB_1$ orthosteric site ($K_i$: 3.3 μM) (Burstein, 2015; reviewed in McPartland *et al.*, 2015). Unlike THC, cannabidiol does not induce the classic $CB_1$ receptor agonist-like tetrad of hypolocomotion, analgesia, catalepsy and hypothermia (Long *et al.*, 2010). Several studies have demonstrated that cannabidiol displaces exogenous $CB_1$ agonists in various *in vitro* assays (pooled $K_B$: 88.5 nM; $n$=6) (reviewed in McPartland *et al.*, 2015), including the vas deferens bioassay (reviewed in Chapter 3). Interestingly, cannabidiol inhibits $CB_1$ agonists with a 37-fold greater potency than its affinity at the orthosteric site, suggesting that it has indirect $CB_1$ activity. Recent studies have confirmed this by demonstrating that cannabidiol negatively modulates the $CB_1$ receptor by acting at an allosteric site (Laprairie *et al.*, 2015; Tham *et al.*, 2018). To further complicate matters, cannabidiol has $CB_1$ agonistic *in vivo* effects at higher concentrations (>10 μM) which are antagonised by $CB_1$-selective inverse agonists or are absent in $CB_1$ knockout mice

(reviewed in McPartland *et al.*, 2015), most likely due to augmented endocannabinoid tone (section 1.6.1.3).

### 1.6.1.2 $CB_2$ receptors

There are limited data on the involvement of $CB_2$ receptors in the *in vivo* effects of cannabidiol. Cannabidiol has a low affinity at $CB_2$ receptors (pooled $K_i$: 3.6 μM, *n*=6) (reviewed in McPartland *et al.*, 2015). Cannabidiol acts at the orthosteric $CB_2$ receptor site, unlike its activity at $CB_1$ receptors (Tham *et al.*, 2018). At high concentration, cannabidiol (10 μM) displays inverse agonism by inhibiting [$^{35}$S]GTPγS binding in human $CB_2$-CHO cells ($E_{max}$: -15% below basal response, $EC_{50}$: 503 nM) (Thomas *et al.*, 2007). Similar to the activity of cannabidiol at the $CB_1$ receptors, cannabidiol antagonises the $CB_2$-active agonist with higher potency ($K_B$) than its affinity ($K_i$) at the $CB_2$ orthosteric sites in human CHO ($K_B$: 65 nM) (Thomas *et al.*, 2007) and HEK293A ($K_B$: 641 nM) (Tham *et al.*, 2018) cells. The discrepancy in potency is likely a result of the differences in the cell lines used including the species origins of cells.

Cannabidiol induces $CB_2$-dependent anti-inflammatory effects in animal models of hypoxic-ischaemic brain injury. More specifically, in hypoxic-ischaemic immature brain forebrain slices from newborn mice, cannabidiol (100 μM) significantly decreased release of several proinflammatory cytokines (Castillo *et al.*, 2010). These effects were reversed by $CB_2$ or adenosine receptor antagonists. Given the high concentrations of cannabidiol used, this finding may be deemed clinically irrelevant. In a hypoxic-ischaemic brain injury model in newborn piglets cannabidiol (1 mg i.v.) decreased pro-inflammatory IL-1 levels (Pazos *et al.*, 2013). The effects of cannabidiol were reversed by $CB_2$ or 5-$HT_{1A}$ antagonists.

### 1.6.1.3 Indirect $CB_1$ receptor activation

As various studies have demonstrated that the effects of cannabidiol can be reversed by $CB_1$ antagonists, cannabidiol has been claimed to exert indirect $CB_1$ agonism by augmenting endocannabinoid tone (reviewed in McPartland *et al.*, 2015). The $CB_1$ antagonists rimonabant or AM251 reverse a range of cannabidiol-mediated *in vivo*

effects including cannabidiol-exacerbated (10 mg/kg i.p.) sepsis-induced gastric hypomobility in mice (De Filippis *et al.*, 2008), cannabidiol-facilitated (2 µg i.c.v. injections) extinction of fear in rats (Bitencourt *et al.*, 2008), cannabidiol-induced (15-60 mg/kg i.p.) decrease in obsessive-compulsive behaviour in mice (Casarotto *et al.*, 2010) and cannabidiol-attenuated (5-60 mg/kg i.p.) aggressive behaviour in mice (Hartmann *et al.*, 2019). Furthermore, cannabidiol-rich plant extract (p.o.) induced neurogenesis in wild type mice, but not in $CB_1$ knockout mice (Wolf *et al.*, 2010).

Cannabidiol can augment endocannabinoid tone through various mechanisms including inhibition of the hydrolysis of the endocannabinoid anandamide by blocking of FAAH enzymes, inhibition of the uptake of anandamide through a putative transporter or by activation of phospholipase $A_2$ and therefore mobilisation of arachidonic acid – a precursor of endocannabinoids (Bisogno *et al.*, 2001; De Petrocellis *et al.*, 2011; reviewed in McPartland *et al.*, 2015). Cannabidiol inhibits the hydrolysis of anandamide and the putative anandamide transporter with a pooled potency ($IC_{50}$) of 19.8 µM and 20.2 µM, respectively (reviewed in McPartland *et al.*, 2015). Furthermore, cannabidiol mobilises arachidonic acid with a potency of 6.4 µM ($EC_{50}$; Burstein & Hunter, 1978; Evans *et al.*, 1987; White & Tansik, 1980). The indirect $CB_1$ agonism of cannabidiol could explain the synergistic effects observed between cannabidiol and THC, which is also ascribed to the ability of cannabidiol to modulate the metabolism of THC during co-administration, hence increasing the $CB_1$ partial agonism effects of THC (reviewed in McPartland *et al.*, 2015).

### 1.6.2 Endocannabinoidome

Since the discovery of the endocannabinoid system, various other long-chain fatty-acid amides have been identified. These mediators share similar properties to the endocannabinoids, including the biosynthetic pathway, receptor targets and/or degradation enzymes. Therefore, an expanded endocannabinoid system has been suggested, namely the "endocannabinoidome" (reviewed in Cristino *et al.*, 2020; Di Marzo, 2018; Witkamp, 2016). The endocannabinoidome includes mediators biochemically related to endocannabinoids, and their receptor and degradation

enzymes. Some of the pharmacological targets in the endocannabinoidome involve the well-studied receptors TRPV1, PPARγ, PPARα and the orphan GPCRs GPR55 and GPR18, which are yet to be fully characterised.

### 1.6.2.1 The orphan GPCR GPR55

GPR55, an orphan GPCR, was initially described as a novel cannabinoid receptor (Ryberg *et al.*, 2007). However, GPR55 appears to have low sequence identity with cannabinoid receptors (McPartland *et al.*, 2006). The receptor is expressed in rat intestines including the ileum, duodenum and colon (Lin *et al.*, 2011), in various regions of the mouse brain including the frontal cortex and striatum (Ryberg *et al.*, 2007), and human osteoclasts and osteoblasts (Whyte *et al.*, 2009). While the physiological function of GPR55 is not well understood, it appears to have a potential role in inflammation and to be involved in energy homeostasis by regulating food intake, gut motility, fuel storage in adipocytes and insulin secretion (reviewed in Liu *et al.*, 2015).

The direct affinity and efficacy of cannabidiol at GPR55 have not been measured. However, cannabidiol antagonises GPR55 agonists in three cell assay studies with a pooled mean $IC_{50}$ of 433 nM (reviewed in McPartland *et al.*, 2015; Ryberg *et al.*, 2007; Whyte *et al.*, 2009). In human monocytes and NK cells, cannabidiol antagonised the release of proinflammatory cytokines IL-12 and TNF-α resulting from GPR55 activation by O-1602, a cannabidiol analogue (Chiurchiù *et al.*, 2015).

### 1.6.2.2 The orphan GPCR GPR18

GPR18 is another orphan GPCR in the endocannabinoidome. The receptor is expressed in many different cell types. It is found at highest levels in spleen and bone marrow followed by the lungs, thymus and cerebellar mouse tissues (Regard *et al.*, 2008). Interestingly, GPR18 is one of the most highly expressed GPCR in melanoma metastases from different individuals (Qin *et al.*, 2011). GPR18 sustains human tumour cell survival, hence inhibition of the receptor increases apoptosis of tumour cells (Qin *et al.*, 2011). Similar to GPR55, the physiological functions of GPR18 are not well understood. However, modulation of the receptor appears to be associated with a range of

physiological processes including cardiac physiology, sperm physiology, cellular migration, immunomodulation, intraocular pressure, obesity, pain and cancer (Sotudeh *et al.*, 2019). It has been proposed that GPR18 is endogenously targeted by the fatty acid metabolite resolvin D2 - an immunoresolvent that stimulates resolution of acute inflammation (Chiang *et al.*, 2015). Another suggested endogenous ligand is the lipid derivative N-arachidonoyl glycine (NAGly; McHugh *et al.*, 2010; McHugh *et al.*, 2012). However, data confirming endogenous ligands for the receptor are conflicting hence the orphan status of GPR18.

Cannabidiol is a weak partial agonist or antagonist at GPR18 ($EC_{50}$ 51.1 μM) (McHugh *et al.*, 2012). However, cannabidiol potently antagonises THC at GPR18 with a calculated $K_B$ of 57.1 nM (McHugh *et al.*, 2012).

#### 1.6.2.3 Other orphan GPCRs

Except for GPR55 and GPR18, cannabidiol also modulates the activity of three other orphan GPCRs, including GPR3, GPR6 and GPR12 (Brown *et al.*, 2017; Laun & Song, 2017). These receptors share approximately 60% amino acid identity and are phylogenetically related to cannabinoid receptors (reviewed in Laun *et al.*, 2019). GPR3, GPR6 and GPR12 were cloned in the early- to mid-1990s and are expressed in various brain regions. Similar to other GPCRs, these orphan receptors regulate various physiological processes. GPR3 may be involved in the pathology of Alzheimer's disease as it is overly expressed in brain tissue collected post-mortem from patients with this disease (Laun & Song, 2017). GPR6 has been suggested as a possible target for both Alzheimer's and Parkinson's diseases and plays an important role in instrumental learning. Besides the brain, GPR12 is also expressed in oocytes where it mediates meiotic arrest (Brown *et al.*, 2017). All three orphan GPRs are coupled to both $G_s$- and $G_i$-proteins. Few molecular targets for these GPRs have been identified, hence their orphan status. Both endocannabinoids and a range of different phytocannabinoids were tested as potential targets (Brown *et al.*, 2017; Laun & Song, 2017). Neither the endocannabinoids anandamide and 2-AG nor the phytocannabinoids $\Delta^9$-THC, cannabinol, cannabigerol and cannabichromene had any effect at these GPRs.

Cannabidiol was the only cannabinoid that interacted with the GPRs. It inhibited the recruitment of β-arrestin2 at both GPR6 and GPR3, acting as an inverse agonist with $EC_{50}$ values of 1.22 μM and 0.18 μM, respectively. Cannabidiol is also an inverse agonist at GPR12 where it inhibited cAMP accumulation with an approximate $EC_{50}$ of 1 μM (Brown *et al.*, 2017).

#### 1.6.2.4 TRPV1 channels

TRPV1 is a cation channel that is activated by ligands, heat and protons (Tominaga *et al.*, 1998). The channels are mainly involved in nociception. Some of cannabidiol's anti-inflammatory, analgesic and antiseizure effects are likely mediated by TRPV1 channels. Cannabidiol interacts with the channels by firstly activating them followed by the subsequent desensitisation (De Petrocellis *et al.*, 2011; Iannotti *et al.*, 2014). This has been demonstrated in three separate fluorescence-based calcium HEK 293 cell assays overexpressing human TRPV1 channels (Bisogno *et al.*, 2001; De Petrocellis *et al.*, 2011; Ligresti *et al.*, 2006). Cannabidiol elevated intracellular calcium with an $EC_{50}$ of 3.6 μM (Bisogno *et al.*, 2001), 1 μM and 1.2 μM (cannabidiol botanical extract; pooled $EC_{50}$: 1.9 μM) (De Petrocellis *et al.*, 2011). The ability of cannabidiol to desensitise TRPV1 channels has also been evaluated against capsaicin-induced TRPV1 activation (0.1 μM), resulting in an $IC_{50}$ of 0.6 μM (cannabidiol botanical extract; De Petrocellis *et al.*, 2011). Furthermore, in a patch-clamp electrophysiology study of HEK 293 cells expressing different rat TRPV channels, cannabidiol (3-30 μM) concentration-dependently activated and rapidly desensitised TRPV1 (Iannotti *et al.*, 2014).

In a mouse model of hepatitis, cannabidiol decreased several pro-inflammatory cytokines including IL-2 and TNF-α (Hegde *et al.*, 2011). These effects were not observed in TRPV1 knockout mice. Cannabidiol (10 mg/kg p.o.) also attenuated peripheral hyperalgesia in carrageenan intraplantar injected rats which was reversed by the TRPV1 antagonist capsazepine (2 mg/kg i.p.; Costa *et al.*, 2004). Interestingly, the analgesic effects of cannabidiol and THC were greater than the effect of THC-only treatment, which is believed to result from cannabidiol's interaction with TRPV1 channels (Comelli *et al.*, 2008). Cannabidiol's antiseizure effects are likely mediated by multiple effector

targets (section 1.5.2), including TRPV1 channels, since they are involved in both the onset and progression of epilepsy (Iannotti *et al.*, 2014; Nazıroğlu, 2015). TRPV1 channels are expressed in the hippocampus, the main brain region that mediates epilepsy symptoms. Desensitisation of TRPV1 channels would likely decrease neuronal excitability and neuronal transmission (Nazıroğlu, 2015). Cannabidiol's TRPV1-mediated anti-epileptic effects have recently been demonstrated in an animal study where cannabidiol attenuated seizure and EEG activity in a pentylenetetrazole mouse model of epilepsy; the effects were reversed by TRPV1, $CB_1$ or $CB_2$ antagonists (Vilela *et al.*, 2017).

#### 1.6.2.5 PPARγ

PPARγ, which is also known as the glitazone receptor, is a nuclear receptor that is mainly responsible for glucose metabolism and lipid storage. Some of cannabidiol's reported anticancer effects are believed to be mediated by PPARγ. In lung cancer cell lines (A549 and H460) and human primary cells from patients with lung cancer, cannabidiol (1-3 μM)-induced apoptosis of cancer cells was paralleled by the upregulation of PPARγ and COX-2 mRNA (Ramer *et al.*, 2013). Furthermore, cannabidiol has demonstrated promising neuroprotective effects in models of Alzheimer's disease (Karl *et al.*, 2012; Vallée *et al.*, 2017). The mechanism of action has been suggested to involve the upregulation of PPARγ (de la Monte & Wands, 2006). Cannabidiol also decreases reactive gliosis and the consequent neurodegeneration resulting from β-amyloid-induced neurotoxicity of rat hippocampal sections (Esposito *et al.*, 2011). More specifically, cannabidiol treatment (10 mg/kg i.p.) of rats for 15 consecutive days induced neuroprotection mediated by PPARγ as the protective effects of cannabidiol were reversed by the PPARγ antagonist GW9662 (1 mg/kg i.p.). The potency of cannabidiol at PPARγ receptors has been assessed in two binding studies in HEK 293 cells, resulting in an $IC_{50}$ of 5 μM (O'Sullivan *et al.*, 2009) and $EC_{50}$ of 20.1 μM (Granja *et al.*, 2012).

### 1.6.3 Endocannabinoidome-independent targets

#### 1.6.3.1 5-$HT_{1A}$ receptors

5-$HT_{1A}$ receptors negatively modulate neurotransmission and are involved in autonomic control. Cannabidiol has a relatively low affinity at the orthosteric site of serotonin receptors (reviewed in McPartland *et al.*, 2015). The approximate pooled affinity ($K_i$) of cannabidiol for 5-$HT_{1A}$ receptors is 16 μM. While cannabidiol is not a potent orthosteric 5-$HT_{1A}$ receptor agonist, it can indirectly potentiate the activation of the receptors at lower concentrations (reviewed in Pertwee, 2014). This is evident by the ability of cannabidiol to enhance the stimulation of [$^{35}$S]GTPγS binding in rat brainstem, induced by a 5-$HT_{1A}$ receptor agonist (Rock *et al.*, 2012). Interestingly, this enhancement was apparent with a cannabidiol concentration of 100 nM, but not with 1, 10, 32 and 1000 nM, indicative of a bell-shaped 5-$HT_{1A}$ function. This is supported by *in vivo* data where cannabidiol's 5-$HT_{1A}$ receptor-mediated effects are either biphasic or bell-shaped (reviewed in Pertwee, 2014). Several beneficial *in vivo* effects of cannabidiol can be blocked by 5-$HT_{1A}$ receptors antagonists. Cannabidiol induces 5-$HT_{1A}$-mediated attenuation of nausea and vomiting in several animal studies. Cannabidiol (5 mg/kg i.p.) decreased lithium chloride-induced conditioned gaping (a measure of nausea) in rats by acting on 5-$HT_{1A}$ receptors in the dorsal raphe nucleus (Rock *et al.*, 2012). Similarly, cannabidiol attenuated both cisplatin- (Parker *et al.*, 2006) and lithium chloride-induced (Parker *et al.*, 2004) vomiting and anticipatory retching in house musk shrews. The antinausea and anti-vomiting effects in rats and shrews are most likely due to indirect activation of 5-$HT_{1A}$ receptors in the brainstem as local injections of cannabidiol into the dorsal raphe nucleus caused antinausea effects in rats (Rock *et al.*, 2012).

Cannabidiol also induces 5-$HT_{1A}$-mediated anxiolytic effects (Crippa *et al.*, 2018; reviewed in McPartland *et al.*, 2015; Pertwee, 2014). Cannabidiol injected into the dorsolateral periaqueductal gray in rats caused bell-shaped dose-response curved anxiolytic-like effects in the elevated plus-maze test (Campos & Guimarães, 2008). Cannabidiol also has 5-$HT_{1A}$-mediated anxiolytic-like effects when injected in other brain structures involved in anxiety-like behaviours, including the bed nucleus of the

stria terminalis (Gomes *et al.*, 2012) and the prelimbic prefrontal cortex (Fogaça *et al.*, 2014). Bell-shaped dose-response curves for the anxiolytic effects of cannabidiol have also been confirmed recently in humans. This was firstly shown through a simulated public speaking test, where an oral dose of 300 mg significantly decreased anxiety in subjects while speaking, but not 150 and 600 mg (Linares *et al.*, 2019). Similarly in a previous study, subjects underwent public speaking in a real situation test, where anxiety measures were decreased with cannabidiol 300 mg, but not 100 and 900 mg (Zuardi *et al.*, 2017).

In mice, 5-$HT_{1A}$ receptors also mediate cannabidiol-induced anti-catalepsy (Gomes *et al.*, 2013b) and antidepressant effects (Zanelati *et al.*, 2010). While in rats, cannabidiol causes antinociception (Maione *et al.*, 2011) and improvement in locomotion and cognition in mouse models of hepatic encephalopathy induced by bile duct-ligation, a model (Magen *et al.*, 2010).

#### 1.6.3.2 Adenosine $A_{2A}$ receptors

Adenosine is involved in immunosuppression and is released in response to cellular stress and inflammation (Carrier *et al.*, 2006). Termination of adenosine signalling is highly dependent on cellular reuptake. Cannabidiol indirectly activates adenosine receptors by inhibiting adenosine reuptake (reviewed in McPartland *et al.*, 2015; Pertwee, 2014). More specifically, cannabidiol inhibits the reuptake of adenosine into murine microglia and RAW264.7 macrophages (Carrier *et al.*, 2006) with a pooled $IC_{50}$ of 122 nM (McPartland *et al.*, 2015). The adenosine $A_{2A}$ receptor is likely involved in some of cannabidiol's anti-inflammatory properties (reviewed in Burstein, 2015). Cannabidiol's adenosine $A_{2A}$ receptor-mediated anti-inflammatory effects have been demonstrated in different mice models with induced inflammation including lipopolysaccharide (LPS)-treated mice (cannabidiol 1 mg/kg i.p. treatment; Carrier *et al.*, 2006), Theiler's murine encephalomyelitis virus-induced demyelinating disease (TMEV), an MS model (cannabidiol 5 mg/kg i.p. treatment; Mecha *et al.*, 2013) and LPS-induced acute lung injury in mice (cannabidiol 20 mg/kg i.p. treatment; Ribeiro *et al.*, 2012). In all these studies adenosine $A_{2A}$ antagonists attenuated the anti-inflammatory

effects of cannabidiol. Cannabidiol also attenuated the incidence and duration of ventricular tachycardia in rats (cannabidiol 50 μg/kg i.v. treatment; Gonca & Darıcı, 2015). However, cannabidiol's antiarrhythmic effects were mediated by the adenosine $A_1$ receptor rather than the adenosine $A_{2A}$ receptor.

#### 1.6.3.3 Glycine receptors

Glycine receptors are ionotropic receptors widely distributed in the central nervous system where they modulate physiological processes by inhibiting neurotransmission, mainly in the spinal cord and brain stem (Lynch, 2004). As glycine receptors are expressed in spinal cord sensory pathways, compounds that activate glycine receptors may function as potential lead analgesic agent. Cannabidiol is a positive allosteric modulator of glycine receptors with a pooled $EC_{50}$ of 11 μM (Ahrens *et al.*, 2009; reviewed in McPartland *et al.*, 2015; Xiong *et al.*, 2011). Chronic pain that results from inflammation or nerve injury is due to loss of inhibitory synaptic transmission within the spinal cord dorsal horns, hence activation of glycine receptors to potentiate inhibition of neurotransmission may induce effective analgesia.

#### 1.6.3.4 μ- and δ-Opioid receptors

Cannabidiol also targets opioid receptors, mainly μ- and δ-opioid receptors (McPartland *et al.*, 2015). In kinetic binding studies in rat cerebral cortex membrane homogenates, cannabidiol allosterically modulates μ- and δ-opioid receptors (Kathmann *et al.*, 2006). At the μ-opioid receptor, cannabidiol accelerated the naloxone-induced dissociation of the agonist $^3$H-DAMGO, resulting in a $pEC_{50}$ of 4.38. Cannabidiol 100 μM accelerated the dissociation of $^3$H-DAMGO by 12-fold, indicative of negative allosteric modulation. This may explain the ability of cannabidiol 10 μM to dextrally shift DAMGO concentration-response inhibitory curves in electrically induced mouse vas deferens contractions (Pertwee *et al.*, 2002). Furthermore, cannabidiol accelerated the dissociation of the antagonist radioligand $^3$H-naltrindole from the δ-opioid receptor by a factor of 2. While cannabidiol allosterically modulates the activity of μ- and δ-opioid receptors, it does this at high concentrations and thus, this cannot be expected to

contribute to any clinically relevant effects (Kathmann *et al.*, 2006; reviewed in McPartland *et al.*, 2015)

#### 1.6.3.5 $\alpha_1$-Adrenoceptors

Cannabidiol has poor efficacy at $\alpha_1$-adrenoceptors. In mouse vas deferens, cannabidiol 10 μM insurmountably antagonised noradrenaline, phenylephrine, and methoxamine-induced contractions (Pertwee *et al.*, 2002). In rat isolated vas deferens experiments performed in our laboratory (Chapter 4), cannabidiol 30 μM did not affect contractions of tissues to noradrenaline compared to the vehicle, while cannabidiol 100 μM decreased maximum contractions by 45% without affecting the potency of noradrenaline (Figure 4-16B).

#### 1.6.3.6 Dopamine $D_2$ receptors

Cannabidiol moderates the effects of dopamine through negative allosteric modulation of dopamine $D_2$ receptors and by indirectly affecting dopamine levels (reviewed in McPartland *et al.*, 2015). Psychosis is mainly treated with dopamine antagonists. Inhibition of dopamine receptors when treating psychosis has several disadvantages, including the devoid of effects on negative and cognitive symptoms (reviewed in Davies & Bhattacharyya, 2019). Direct dopamine receptor antagonism also causes extrapyramidal adverse effects. Cannabidiol treatment of psychosis may avoid extrapyramidal adverse effects by indirectly modulating dopamine levels rather than directly antagonising dopamine receptors. Various preclinical studies support a role for cannabidiol as an antipsychotic medication. For instance, cannabidiol decreases hyperlocomotion in mice induced by amphetamine (dopamine agonist) or ketamine (NMDA glutamate receptor antagonist) without inducing extrapyramidal effects (Moreira & Guimarães, 2005). Hyperlocomotion is used as a model of positive psychotic symptoms (Jones *et al.*, 2011). Antipsychotic effects of cannabidiol have also been confirmed in two double-blind randomised trials where cannabidiol 800 mg (Leweke *et al.*, 2012) and 1000 mg (McGuire *et al.*, 2018) per day as a monotherapy or in conjunction with other antipsychotic drugs, respectively, alleviated signs and symptoms of schizophrenia.

While various animal and human studies have suggested that the antipsychotic effects of cannabidiol are independent of direct dopamine receptor antagonism, a relatively recent study in rat brain striatal cells demonstrated the contrary (Seeman, 2016). Cannabidiol interacted with dopamine $D_2$ receptors in a similar fashion to known dopamine $D_2$ partial agonist aripiprazole, by inhibiting the binding of [$^3$H]-domperidone (dopamine $D_2$ antagonist) at the high- and low-affinity sites of the dopamine $D_2$ receptor with an $IC_{50}$ of 66 nM and 2800 nM, respectively.

#### 1.6.3.7 $GABA_A$ receptors

Cannabidiol increases GABA levels and may positively allosterically modulate the $GABA_A$ receptor (reviewed in McPartland *et al.*, 2015). As described (section 1.5.2), cannabidiol is being used to treat epilepsies like Dravet syndrome in children. One of the mutations involved in the pathogenesis of Dravet syndrome is a mutation in the $\alpha_1$ subunits of voltage-gated sodium channels which are predominantly expressed on inhibitory GABAergic interneurons (Brunklaus & Zuberi, 2014; Steel *et al.*, 2017). This mutation consequently impairs the firing of GABAergic hippocampal interneurons which lowers the seizure threshold. As GABA inhibits neurotransmission in the mammalian CNS by activating $GABA_A$ receptors, an impairment results in the over-excitability of neurons and hence seizures. A recent study demonstrated that both cannabidiol and anandamide were positive allosteric modulators at various $GABA_A$ receptor subtypes at low micromolar concentrations (Bakas *et al.*, 2017). This study also concluded that cannabidiol does not act at the benzodiazepine allosteric site. The potency of cannabidiol ($EC_{50}$) at the α1β2 and α2β2 $GABA_A$ subunits was 3.7 μM and 2.0 μM (Bakas *et al.*, 2017).

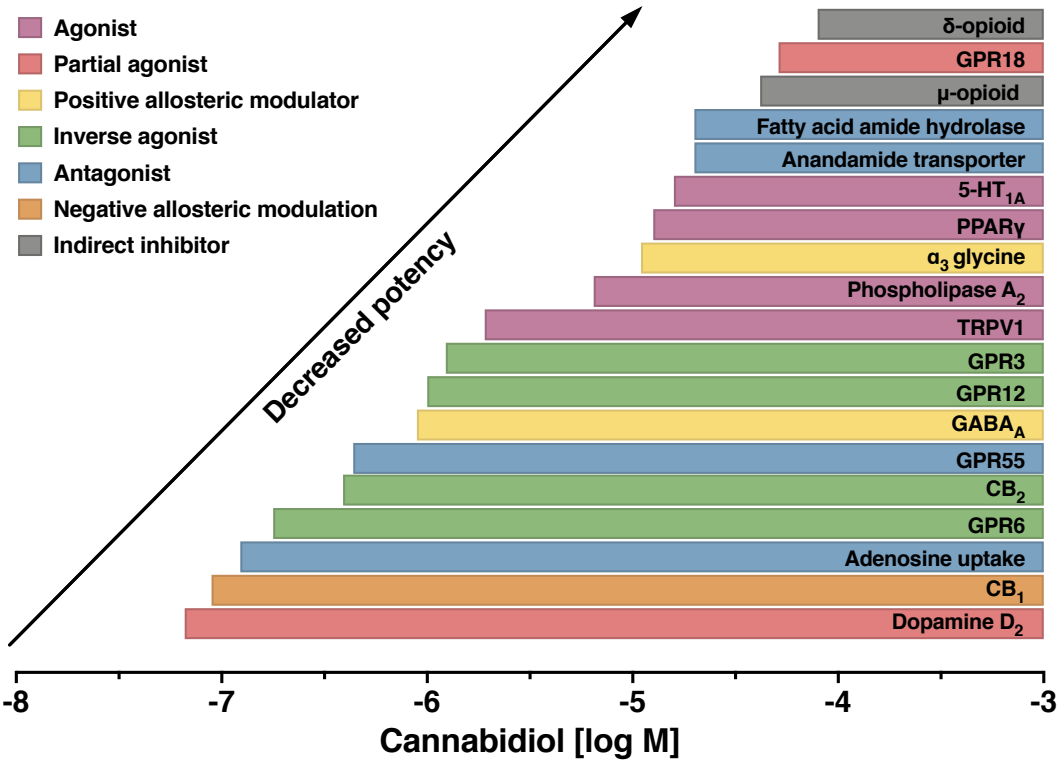


**Figure 1-8.** This graph demonstrates the pharmacological targets for cannabidiol over a wide concentration span.

The bars show the potencies ($EC_{50}$, $IC_{50}$ or $K_B$ values; section 1.6.) and the nature of the interaction between cannabidiol and its targets as indicated by the colour of the bars.

## 1.7 The effects of *Cannabis* in the cardiovascular system

Both exogenous and endogenous cannabinoids induce cardiovascular changes in humans through interactions with the endocannabinoidome. Phytocannabinoids have demonstrated both positive and severe adverse cardiovascular effects.

As of today, 4% of the world's adult population have used *Cannabis* at least once in their lifetime (United Nations Office on Drugs and Crime, 2015). There are increased positive attitudes of the public towards *Cannabis* which may have contributed to its widespread legalisation (Felson *et al.*, 2019). While the adverse effects of *Cannabis* are not well-established, the commonly reported adverse effects include psychiatric conditions such as anxiety and panic attacks in naïve users, an increased risk of psychotic disorders, mood disturbances, mania, depression and *Cannabis* addiction and dependence with repeated and chronic *Cannabis* consumption (Cohen *et al.*, 2019). Cannabinoid use has also been associated with cognitive, structural and functional alterations of the central nervous system. Furthermore, acute and chronic cannabinoid use is associated with respiratory and cardiovascular adverse effects including decreased airway resistance, increased risk of developing airway diseases and lung cancer while also causing increased blood pressure and heart rate, myocardial infarction, cardiomyopathy and sudden cardiac death. While epidemiological studies on the cardiovascular effects of *Cannabis* and its separate components are lacking, they show that patients with previous myocardial infarction/s ran a 4-time higher risk to have another incident within 1 h after smoking *Cannabis* compared to patients who have never had myocardial infarctions (Mittleman *et al.*, 2001). In patients hospitalised for myocardial infarction in the United States, the cardiovascular mortality rate was 2.5 times higher in those who used *Cannabis* less than weekly, and 4.2 times higher amongst those who used *Cannabis* once weekly or more (Mukamal *et al.*, 2008). Recent case reports suggest that *Cannabis* use is associated with an increased risk of cardiovascular disease in younger users who are otherwise considered low-risk (reviewed in World Health Organization, 2016). In a study on *Cannabis*-related hospitalisations in Toulouse in France, one-third of the hospitalisations were attributed to cardiovascular disorders including myocardial infarction, cerebral stroke and thromboarteritis (Jouanjus *et al.*, 2011). The increased

reports of *Cannabis* adverse cardiovascular effects are confounded by increased THC content (World Health Organization, 2016). The THC potency of *Cannabis* has increased over the years as a result of the breeding of THC-dominant *Cannabis* strains (World Health Organization, 2016). The THC content in *Cannabis* has increased from ≤2% in the 1980s to ≥20% in some strains.

The cardiovascular effects of phytocannabinoids are mediated through their interaction with cannabinoid receptors. The adverse effects of phytocannabinoids are primarily mediated by THC through the activation of $CB_1$ receptors (Pacher *et al.*, 2018). While $CB_1$ and $CB_2$ receptors are primarily expressed in the CNS and immune cells (Appendix 1), respectively, functional cannabinoid receptors are also expressed in the cardiovascular system including in the myocardium, vascular endothelium and smooth muscle (Chapter 4) and circulating blood cells (Pacher *et al.*, 2018). $CB_1$ receptors are also expressed in the peripheral nervous system and modulate the release of various neurotransmitter agents (Chapter 3). $CB_1$ receptor activation is associated with various cardiovascular adverse effects. In cultured primary cardiomyocytes and human coronary artery and umbilical endothelial cells, $CB_1$ receptor activation mediates apoptosis *in vitro* (Pacher *et al.*, 2018). The involvement of $CB_1$ receptors in *Cannabis*-induced cardiovascular adverse effects has been demonstrated by the ability of $CB_1$ inhibitors such as rimonabant to reverse the adverse cardiovascular effects in animal studies (reviewed in Pacher *et al.*, 2018). In contrast, $CB_2$ receptor activation induces cardioprotection in animal models of both myocardial infarction, stroke and restenosis by attenuating inflammation.

### 1.7.1 A potential role for cannabidiol in the cardiovascular system

Unlike THC, cannabidiol has demonstrated cardiovascular benefits in animal models of myocardial infarction, stroke, cardiomyopathy and myocarditis, and in cells of human primary cardiomyocytes (Pacher *et al.*, 2018; Stanley *et al.*, 2013a). The vasodilatory effects have been suggested to have potential in treating diseases in the peripheral and cerebral vasculature (Chapter 4). Furthermore, the cardiovascular risks associated with THC are dependent on the THC to cannabidiol ratio of the *Cannabis* in use, whereby

high cannabidiol to THC *Cannabis* strains seem to be cardioprotective (reviewed in Pacher *et al.*, 2018).

## 1.8 Thesis aims

Extensive therapeutic claims have been made for cannabidiol including in the cardiovascular system. Cannabidiol is likely to have a plethora of effects considering the diversity of its pharmacological targets. However, research to date to support the cardiovascular claims and the clinically relevant pharmacological targets are limited. Hence, this study aimed to pharmacologically characterise the $CB_1$ activity of cannabidiol using the rat vas deferens bioassay (Chapter 3). Prior to this, the vas deferens bioassay was standardised as previous studies using the assay have been performed in modified physiological salt solution without $Mg^{2+}$. We therefore examined the effect of varying $Mg^{2+}$ concentrations on neurotransmitter-induced contractions in the vas deferens (Chapter 2). This study also aimed to investigate the local vascular (Chapter 4) and haemodynamic effects of cannabidiol (Chapter 5), and the potential mechanisms involved in cannabidiol-specific cardiovascular effects.

# Chapter 2

Standardisation of the vas deferens bioassay: a cannabinoid receptor pharmacological tool

## 2.1 Introduction

The electrically stimulated vas deferens has been used as a bioassay in studies of a range of pharmacological and physiological processes, ever since its introduction by Hukovic in 1961 (section 2.1.1). It was the first bioassay to confirm the cannabinoid receptor activity of the newly discovered endocannabinoid anandamide (Chapter 3; Devane *et al.*, 1992). Various studies since then support a role for prejunctional $CB_1$ receptors in modulating neurotransmitter release and hence the contraction of vasa deferentia (Chapter 3; Howlett *et al.*, 2002; Pertwee, 1997; Schlicker & Kathmann, 2001). Prior to commencing a pharmacological analysis of cannabidiol's $CB_1$ receptor activity in the vas deferens bioassay (Chapter 3), an attempt to standardise the assay was made to understand why most studies using the bioassay excluded magnesium from the normal composition of Krebs-Henseleit physiological salt solution (PSS; Berzetei-Gurske *et al.*, 1996; Christopoulos *et al.*, 2001; Corbett *et al.*, 1984; Hourani *et al.*, 1993; Lay *et al.*, 2000; North & Surprenant, 2000; Pertwee *et al.*, 2002; Pertwee *et al.*, 1992; Wiley *et al.*, 2011).

### 2.1.1 The vas deferens bioassay

Animal vas deferens tissues have been used extensively in pharmacological studies since their introduction by Seid Huković in 1961. It has been particularly important for the development of autonomic neuropharmacology (Huković, 1997). As with many scientific findings, the usefulness of the vas deferens tissues in biomedical research came about as an accident (Huković, 1997). In 1959, Huković intended to use an experimental animal uterus to repeat studies on the effects of physostigmine by electrically stimulating the uterus-attached hypogastric nerve. Upon euthanising a guinea-pig in the laboratory, he discovered he had been given a male guinea-pig. This led him to isolate and set up a vas deferens in an organ bath instead. He noticed that electrical stimulation of the hypogastric nerve resulted in strong and regular longitudinal contractions of the muscle. Later, Michael Rand, a University of Melbourne Professor of Pharmacology, introduced the assay to Geoff Burnstock and Mollie Holman who demonstrated that sympathetic activation of the vas deferens preparation induced excitatory junction potentials (Burnstock & Holman, 1961). Ten years later in 1971, the Swedish scientist Göran Swedin demonstrated that a 30 s field stimulation of guinea-

pig and rat vas deferens caused biphasic contractions, a fast and slow twitch response (Figure 2-1; Swedin, 1971). He observed that the second phase was sensitive to α-adrenoceptor blockade, while the first phase remained resistant to the blockade. It took more than 20 years after the discovery of the vas deferens bioassay before the first phase was attributed to the cotransmitter ATP (Sneddon & Westfall, 1984).

### 2.1.2 Sympathetic cotransmission of vas deferens

Physiologically, the vas deferens is a duct that conveys spermatozoa from the epididymis on each testis to the urethra. The emission of spermatozoa relies on the activation of adrenergic nerves that causes the smooth muscle layers of the vas deferens to contract (Koslov & Andersson, 2013). Upon nerve stimulation of the vas deferens, there is a release of ATP which elicits a fast contraction (phase 1) by acting on postjunctional $P2X_1$ ion channel receptors, and noradrenaline, which causes slower contraction (phase 2) by acting on postjunctional $\alpha_{1A}$-adrenoceptors (Figure 2-1; Burnstock, 1972; Mallard *et al.*, 1992; McGrath, 1978; Westfall *et al.*, 1978). While the contraction of nerve-stimulated vas deferens is biphasic due to the release of ATP and noradrenaline, a third neurotransmitter is likely implicated in the sympathetic neurotransmission of the vas deferens, namely neuropeptide Y (NPY; Kasakov *et al.*, 1988). Kasakov demonstrated that ATP, noradrenaline and NPY are cotransmitted in the guinea-pig vas deferens. The definite role and actions of NPY in the vas deferens varicosities are still not clearly defined. NPY has been described as having a neuromodulatory role by potentiating the actions of noradrenaline and ATP while not inducing a contraction on its own (Figure 2-1; Ellis & Burnstock, 1990). It is believed that NPY modulates ATP and noradrenaline cotransmission through both pre- and postjunctional actions (Ellis & Burnstock, 1990). NPY is suggested to enhance the effects of ATP and noradrenaline postjunctionally (Figure 2-1) and negatively modulate the release of neurotransmitter prejunctionally. The negative modulation of NPY appears to predominate over its enhancing effects since vasa deferentia simultaneously exposed to a train of electrical stimuli and exogenous NPY (0.3 nM-0.3 μM) resulted in an NPY concentration-dependent inhibition of contraction. However, it can be expected that

during the single electrical stimulation conditions used in this study, NPY would only enhance the contractions of tissues as there is no feedback mechanism to consider.

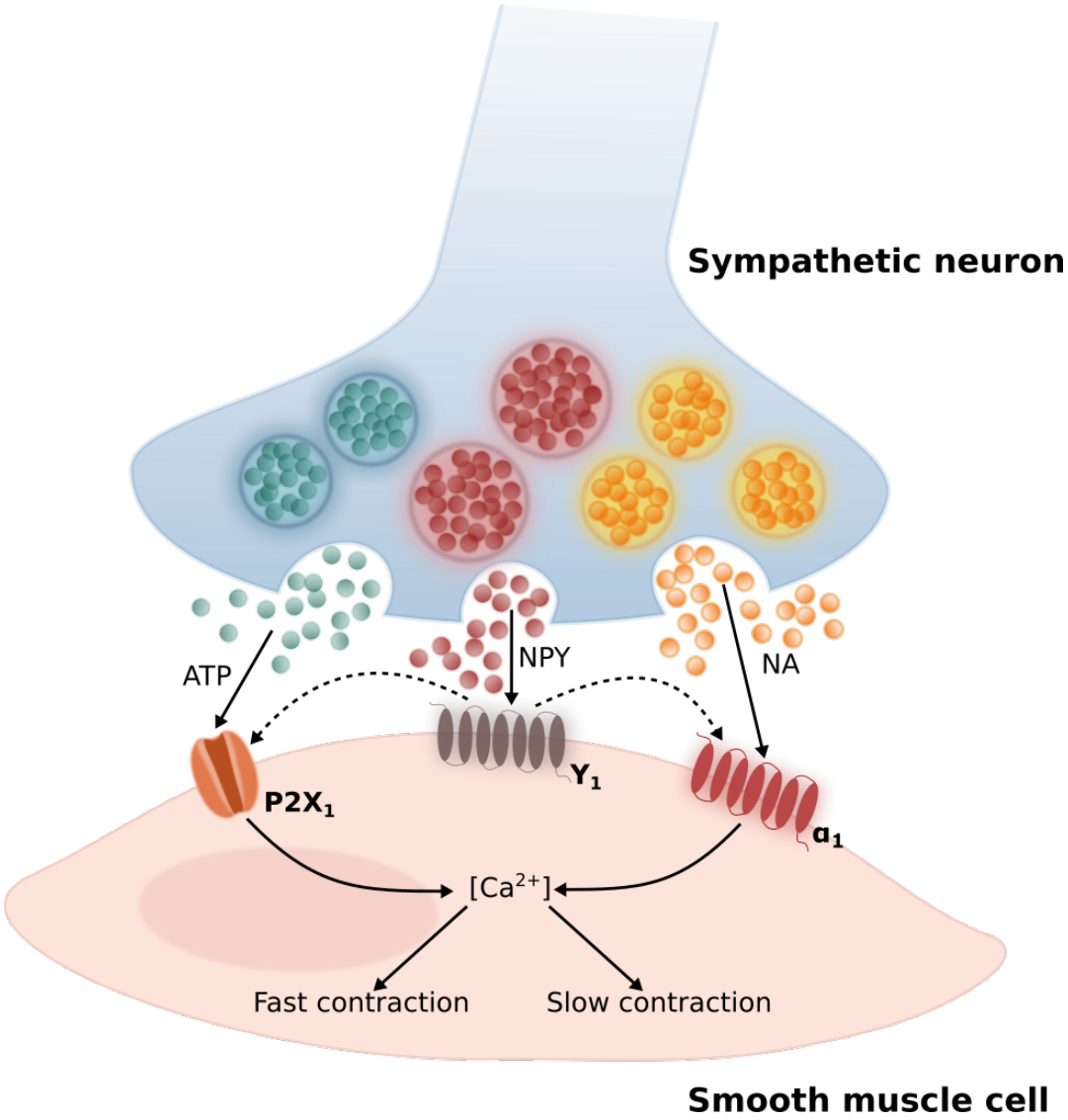


**Figure 2-1.** Simplified schema of the excitatory cotransmission in the vas deferens.
Upon a single sympathetic nerve stimulation, there is a release of ATP, noradrenaline and NPY from the vas deferens nerve varicosities. ATP elicits smooth muscle contraction in the vas deferens by binding to postjunctional $P2X_1$ ion channel receptors, resulting in the opening of non-selective cation channels, causing an influx of $Ca^{2+}$ and excitatory junction potentials. Noradrenaline elicits smooth muscle contraction by binding to postjunctional $\alpha_1$-adrenoceptors, causing an increase in inositol triphosphate which mobilises $Ca^{2+}$ from the endoplasmic reticulum. NPY is believed to potentiate the effects of both ATP and noradrenaline through their respective postjunctional receptors.

#### 2.1.2.1 Neurotransmitter release from nerve varicosities

The neurotransmitters in the vas deferens are stored in prejunctional vesicles (Figure 2-1). There is no conclusive evidence to confirm whether they are co-stored in the same vesicles or in separate vesicles. (Burnstock & Verkhratsky, 2010; Koslov & Andersson, 2013). It is believed that NPY is released from large granular vesicles while ATP and noradrenaline are released from separate small granular vesicles (Burnstock & Verkhratsky, 2010). ATP and noradrenaline are most likely stored in separate vesicles in sympathetic nerve terminals as their release from vesicles is modulated differently by various agents (Burnstock & Verkhratsky, 2010).

#### 2.1.2.2 The role of $P2X_1$-receptors in ATP-induced contractions

The $P2X_1$ receptor is one of seven purinergic P2X receptors found in mammals and is distributed in smooth muscle cells and platelets (Burnstock & Verkhratsky, 2010; Khakh & North, 2006). Upon nerve stimulation of the vas deferens, ATP is released from prejunctional terminals and binds to $P2X_1$ receptors on the smooth muscle. This will activate the opening of nonselective cation channels and a subsequent $Ca^{2+}$ influx which will cause the tissue to contract.

$P2X_1$ receptors clearly mediate ATP-induced contractions as contractions of vasa deferentia isolated from $P2X_1^{(-/-)}$ mice were attenuated by 60% while also not responding to $P2X_1$ agonism (Mulryan *et al.*, 2000). This finding has generated the idea of using $P2X_1$ antagonists as novel male non-hormonal contraceptives, which would likely be a safer alternative to other suggested male contraceptives which cause dysfunction of sperm (Burnstock & Verkhratsky, 2010; Mulryan *et al.*, 2000; White *et al.*, 2013).

ATP is a nucleotide with significant importance in the extracellular signalling between cells. ATP binds to cell-surface P2-purinoceptors, including P2Y (metabotropic) and P2X (ionotropic) receptors. P2X receptors consist of pores which upon the binding of ATP will allow the inflow of ions into the intracellular space which results in a change

in the transmembrane potential. Following signalling, ATP will be rapidly degraded to ADP, AMP and adenosine (Khakh & North, 2006).

#### 2.1.2.3 The role of $\alpha_1$-adrenoceptors in noradrenaline-induced contractions

Noradrenaline-induced contractions in the vas deferens are predominantly a result of binding to $\alpha_1$-adrenoceptors. Interestingly, a study of the rat vas deferens found that while the contractions induced by exogenous noradrenaline were mediated by $\alpha_{1A}$-adrenoceptors, endogenous noradrenaline mediated contractions through $\alpha_{1D}$-adrenoceptors (Honner & Docherty, 1999). When noradrenaline binds to $\alpha_1$-adrenoceptors inositol triphosphate is generated which triggers the release of $Ca^{2+}$ from the endoplasmic reticulum.

### 2.1.3 $Mg^{2+}$, or not $Mg^{2+}$, that is the question

Many studies using the isolated vas deferens bioassay have been performed in modified Krebs-Henseleit solution without $Mg^{2+}$ (Berzetei-Gurske *et al.*, 1996; Christopoulos *et al.*, 2001; Corbett *et al.*, 1984; Hourani *et al.*, 1993; Lay *et al.*, 2000; North & Surprenant, 2000; Pertwee *et al.*, 2002; Pertwee *et al.*, 1992; Wiley *et al.*, 2011). Some reports have indicated that the reason for the use of $Mg^{2+}$-free Krebs' PSS was to enhance the response to nerve stimulation (Hourani *et al.*, 1993). The idea of excluding $Mg^{2+}$ in the Krebs' solution when setting up vasa deferentia may have originated from 1975 (Hughes *et al.*, 1975). This study investigated the effect of morphine on adrenergic transmission in the mouse vas deferens (Hughes *et al.*, 1975). It was observed that the inhibitory effects of morphine on contractions in the mouse vas deferens were more obvious in $Mg^{2+}$-free Krebs', where 1.4 mM of $Mg^{2+}$ caused a 40-60% decrease in contractions compared to $Mg^{2+}$-free Krebs' solution. Other studies have shared the observation of $Mg^{2+}$-free PSS enhancing vas deferens contractions. Hourani *et al.* (1993) briefly stated that the reason for using $Mg^{2+}$-free Krebs' solution in their set up of neonatal rat isolated vasa deferentia was to enhance neurotransmitter release, and the presence of $Mg^{2+}$ would likely make it difficult to detect any nerve stimulation-induced responses. In another study, it was reported that the removal of $Mg^{2+}$ from the PSS induced a 6-8 fold increase in the stimulus amplitude evoked by ATP (North & Surprenant, 2000).

In an *ex vivo* bioassay, the conditions used in a laboratory should attempt to mimic that of the conditions of the tissue *in vivo*. Hence, if non-physiological conditions are used, the investigator should ensure minimal interference with the natural function of the tissue. $Mg^{2+}$, being the second most abundant intracellular cation after $K^{+}$, plays an important role in many physiological functions by regulating both cell and tissue functions (Jahnen-Dechent & Ketteler, 2012; Laires *et al.*, 2004). The composition of normal Krebs' PSS includes $Mg^{2+}$ 1.2 mM while human serum $Mg^{2+}$ concentrations are between 0.65 and 1.05 mM (Jahnen-Dechent & Ketteler, 2012). Excluding a component from the PSS which has the purpose to mimic the *in vivo* environment and conditions of the isolated tissue, could alter the function of the tissue and subsequently skew the outcome of a study.

### 2.1.4 Study aims

This study aimed to standardise the vas deferens bioassay by elucidating the effect of varying $Mg^{2+}$ concentrations on neurotransmitter-induced contractions. We used just a single electrical field pulse, repeated every 30 min, rather than dual field pulses (Ellis & Burnstock, 1990) or trains of stimuli to prevent modulation of the release of the cotransmitter agents (prejunctional) by other neuromodulators or actions at the postsynaptic receptors (Driessen *et al.*, 1994; French & Scott, 1983). We also compared the results from the single field pulse with the contractions of single high concentrations of exogenous ATP, noradrenaline and methoxamine in the presence of $Mg^{2+}$ 0, 1.2 and 3 mM, in an attempt to compare the involvement of pre- and postjunctional sites in the effects of $Mg^{2+}$. To test whether $Mg^{2+}$ concentrations were directly affecting the release of neurotransmitters ATP and noradrenaline, we determined the $IC_{50}$ for the highly selective prejunctional N-type calcium channel ($Ca_v2.2$) inhibitor ω-conotoxin GVIA on the contraction to a single pulse.

## 2.2 Materials and methods

The Ethics Committee of the University of Melbourne approved experiments in accordance with The Australian Code for the care and use of animals for scientific purposes (8th edition, 2013, National Health and Medical Research Council, Canberra).

### 2.2.1 Tissue collection and set up

Male Sprague-Dawley rats (250-350 g) were deeply anaesthetised by inhalation of 5% isoflurane in oxygen and killed by a rapid cut through the spinal cord. The whole vasa deferentia were excised and placed in modified Krebs-Henseleit PSS with the following composition (mM): NaCl 119, KCl 4.7, $KH_2PO_4$ 1.2, $NaHCO_3$ 25, $CaCl_2$ 2.5, glucose 11, EDTA 0.026, $MgSO_4$ 0, 1.2 or 3 ($MgSO_4$ content was dependent on the protocol), oxygenated with 95% $O_2$ and 5% $CO_2$ at pH 7.4.

The tissues were pinned down and tied at either side with a silk thread and trimmed to an approximate length of 2 cm. The prostatic end was tied to a stainless-steel hook on a fixed acrylic organ bath leg between two parallel platinum field electrodes, while the epididymal end was tied uppermost to a stainless-steel hook attached to a Grass FTO3C isometric force transducer (Grass Instruments, Quincy, MA, USA) connected to a bridge amplifier and a data acquisition system, Powerlab 8/35 (ADInstruments, Sydney, Australia). The organ bath leg was adjusted vertically with an attached micrometer (Mitutoyo Manufacturing Co., Kawasaki, Japan). The responses were measured on a computer running LabChart 7 Pro software (ADInstruments) with the sampling rate: 100 Hz, range: 2 mV and low pass filter set at 20 Hz. Tissues were suspended in 5 ml organ baths containing either $Mg^{2+}$-free or 3 mM $Mg^{2+}$ PSS, oxygenated with 95% $O_2$ and 5% $CO_2$ at 37°C. The tissues were stretched to 2 g force, followed by a re-stretch to 2 g after 10 min. The bath solutions were changed twice before incubating the tissues with the appropriate PSS for 30 min.

### 2.2.2 Electrically stimulated vasa deferentia

#### 2.2.2.1 Effects of $Mg^{2+}$ on the biphasic contraction to a single electrical pulse

Following incubation of the tissues in either $Mg^{2+}$-free or 3 mM $Mg^{2+}$ PSS, a single square wave nerve stimulation pulse (150 V, 0.5 ms duration) was delivered by a Grass S88 stimulator via a Grass stimulus isolation unit (SIU5), which induced a biphasic contraction. This response was completely inhibited by pretreatment with tetrodotoxin (0.1 μM) indicating that the electrical field pulse only depolarised the nerves and not the muscle. The tissues were incubated in PSS with 3 different concentrations of $Mg^{2+}$ (0, 1.2 and 3 mM), whereby single-pulse stimulations were induced at 30 min intervals, followed by 4 changes of the bath solution, then the composition of the PSS was changed from low to high $Mg^{2+}$ content, or high to low $Mg^{2+}$ content.

Experiments in $Mg^{2+}$-free PSS were also performed in the presence of the $P2X_1$-purinoceptor antagonist NF449 (10 μM), the $\alpha_1$-adrenoceptor antagonist prazosin (100 nM) or vehicle (MilliQ water, 5 μl). In separate experiments, the effects of varying the $Mg^{2+}$ concentration on the sensitivity to ω-conotoxin GVIA, a potent and highly selective inhibitor of the prejunctional N-type (Cav2.2) calcium channel, were tested by constructing ω-conotoxin GVIA concentration-response curves in each of the 3 $Mg^{2+}$ concentrations. The vasa deferentia were incubated with an antagonist or vehicle before inducing single pulse stimulations at 30 min intervals. Tissues were randomised into treatment groups.

#### 2.2.2.2 Time-dependent effects of $Mg^{2+}$

Time-dependent effects under different $Mg^{2+}$ conditions were performed by incubating separate tissues with one of three different concentrations of $Mg^{2+}$ (0, 1.2 and 3 mM) followed by single-pulse stimulations at 30 min intervals for 240 min.

### 2.2.3 Exogenous agonist stimulation of vasa deferentia with ATP and noradrenaline

The vasa deferentia tissues were contracted with either exogenous ATP 100 μM or noradrenaline 10 μM following the same protocol as for the electrically stimulated tissues, with 4 changes of bath solution once the tissues had reached a maximum contraction (~10 s for ATP and ~30 s for noradrenaline).

### 2.2.4 Data and statistical analysis

All data are expressed as the mean ± S.E.M. from *n* experiments. *n* is the number of tissues from separate rats. The responses to the different concentrations of $Mg^{2+}$ in the graphs are given either as the absolute increase from baseline tone or in percentage in relation to the contraction (100%) in normal PSS ($Mg^{2+}$ 1.2 mM). Data were plotted and analysed using Prism 8 (Graphpad Software, La Jolla, CA, USA). Each individual ω-conotoxin GVIA concentration-response curve was fitted to a logistic sigmoidal 4 parameter model using Prism 8 to determine the $E_{max}$ (initial force) and $IC_{50}$ (concentration required to inhibit the contractions by 50%); these values were then averaged for each of the three $Mg^{2+}$-PSS conditions. For the comparison of the change in the mean contraction between the three different PSS conditions, repeated measures one-way ANOVA with Dunnett *post hoc* test for multiple comparisons was performed. For the comparison of the mean contractions between vasa deferentia in the presence of either NF449, prazosin or vehicle, one-way ANOVA with Dunnett *post hoc* test was performed. For comparison of time-dependent effects from baseline stimulation, repeated measures one-way ANOVA with Dunnett *post hoc* test for multiple comparisons was performed. *P* values < 0.05 were considered significant

### 2.2.5 Drugs

Drugs used were: Adenosine 5'triphosphate (ATP) magnesium salt; methoxamine hydrochloride; noradrenaline bitartrate salt; prazosin hydrochloride; tetrodotoxin (all from Sigma-Aldrich, St Louis, MO, USA); and NF449 octasodium salt (4,4',4'',4'''-[carbonylbis[imino-5,1,3-benzenetriylbis(carbonylimino)]]tetrakis-1,3-benzenedisulfonic acid, octasodium salt; Cayman Chemical, Ann Arbor, MI, USA); and

ω-conotoxin GVIA (Tocris Bioscience, Bio-Techne Ltd., Abingdon, United Kingdom) All drugs were dissolved in MilliQ water. Single-use aliquots of ATP ($10^{-2}$ M), methoxamine ($10^{-1}$ M), NF449 ($10^{-2}$ M), noradrenaline ($10^{-1}$ M), prazosin ($10^{-3}$ M), tetrodotoxin ($10^{-4}$ M) or ω-conotoxin GVIA ($10^{-3}$ M) were stored at –20°C.

## 2.3 Results

### 2.3.1 Do peak contractions to cotransmitters ATP and noradrenaline, phase 1 and 2, respectively, interact?

The high-speed digital recording of the contractile response to a single electrical field pulse clearly indicates two peaks or phases (Figure 2-2). The first peak is considered to be the fast contraction to cotransmitter ATP and the second is the response to cotransmitter noradrenaline. As the $Mg^{2+}$ was decreased to 0 mM, the first peak is enhanced, but in high $Mg^{2+}$ 3 mM, both peaks were attenuated compared with control $Mg^{2+}$ 1.2 mM.

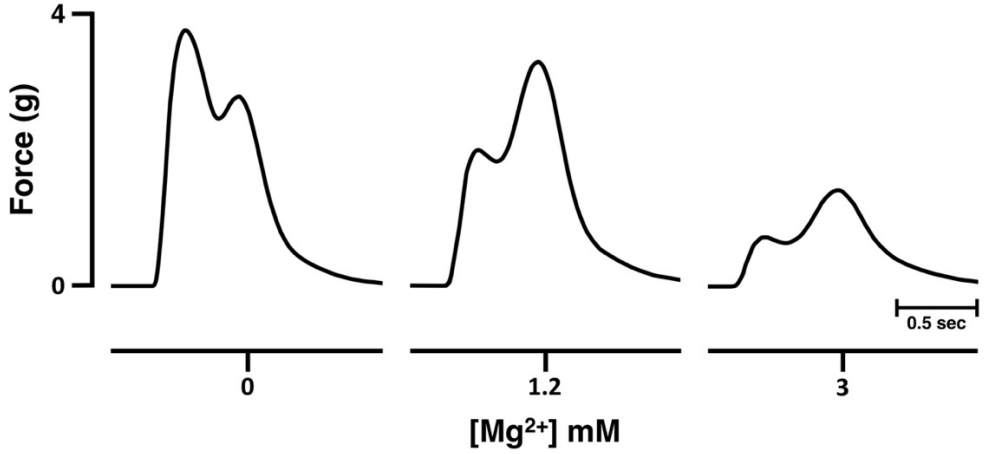


**Figure 2-2.** Representative Labchart® traces of biphasic contractile responses of rat isolated vas deferens following a single electrical field pulse in the presence of PSS with different $Mg^{2+}$ concentrations (0, 1.2 or 3 mM).
In each case, the initial fast peak contraction is the ATP-mediated contraction while the second slow peak is the noradrenaline-mediated contraction.

To confirm that the first and second peaks were mediated by ATP and noradrenaline, respectively, and whether there is any interaction between the cotransmitters, the contraction profile to a single field pulse was recorded in the absence of $Mg^{2+}$ (0 mM), in drug-free PSS, or with prazosin 100 nM or NF449 10 μM to inhibit the post-junctional $\alpha_1$-adrenoceptors or $P2X_1$ purinoceptors, respectively. The competitive antagonism of either receptor type did not significantly alter the peak contraction response to the

remaining cotransmitter compared to respective controls ($P$>0.2; Figure 2-3). The concentrations of prazosin and NF449 chosen to antagonise noradrenaline and ATP were sufficient to completely block the contraction peak to that cotransmitter (Figure 2-3).

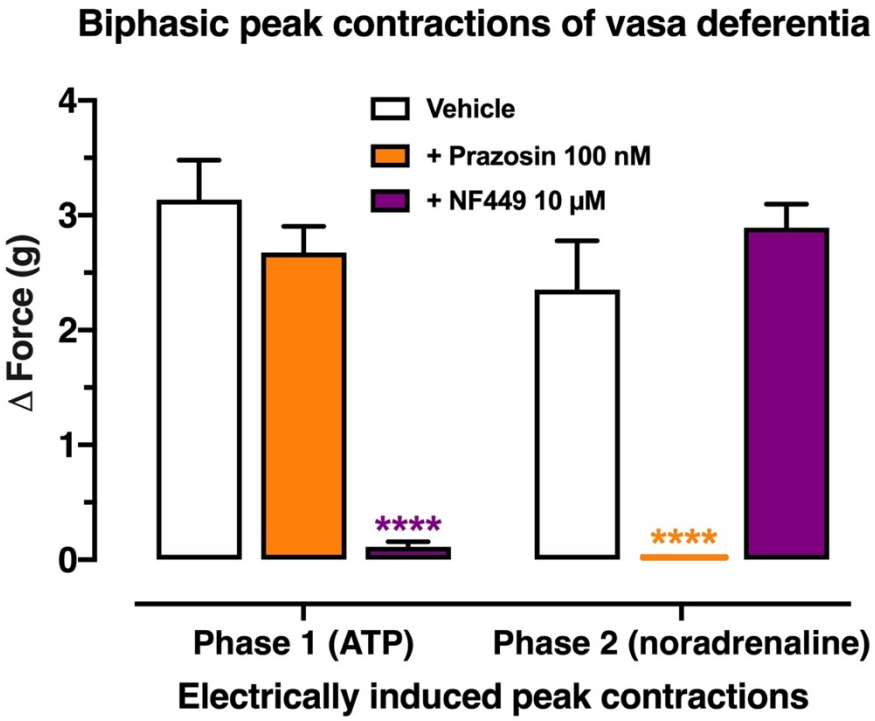


**Figure 2-3.** Cotransmitter biphasic peak contractions of vasa deferentia in response to a single field pulse in $Mg^{2+}$-free PSS under 3 conditions: (i) control (vehicle), open bars, $n$=5; (ii) prazosin 100 nM pretreatment, orange bars, $n$=6; or (iii) NF449 10 µM pretreatment, magenta bars, $n$=5. Phase 1 peak was mediated by ATP acting on P2X1-receptors as it was sensitive to NF449 and the phase 2 peak was mediated by noradrenaline as it was abolished by prazosin. The error bars are ± S.E.M. $n$, number of tissues from separate rats. One-way ANOVA with Dunnett post hoc test was performed; ****$P$≤0.0001 compared to the respective vehicle control group

### 2.3.2 Effects of $Mg^{2+}$ on the biphasic contraction to a single electrical pulse

Since the distinct peaks in the contractile response to a single electrical pulse were separated in time and appeared to be independent of the other in magnitude, the time to reach peak 1 and peak 2 and the peak force were determined in the rising $Mg^{2+}$ concentration protocol of 0, 1.2 and 3 mM and falling $Mg^{2+}$ concentration protocol of 3, 1.2 and 0 mM. Time from the electrical stimulus to the first (ATP) peak was 279 ± 7 ms

(*n*=6), 261 ± 5 ms (*n*=6) and 248 ± 3 ms (*n*=6) for the average of both the rising and falling $Mg^{2+}$ concentration protocols of 0, 1.2 and 3 mM (Figure 2-4A). For the second (noradrenaline) peak, the average time from electrical stimulus to the peak for the two protocols was 636 ± 6 ms (*n*=7), 627 ± 5 ms (*n*=7) and 649 ± 5 ms (*n*=7), corresponding to 0, 1.2 and 3 mM $Mg^{2+}$, respectively.

The rising and falling $Mg^{2+}$ concentration protocol data were combined to show the overall effect of $Mg^{2+}$ concentration on change in force of contraction (Δ force; Figure 2-4B). While the peak Δ force was similar for ATP and noradrenaline, peaks in 0 mM $Mg^{2+}$, normal (1.2 mM) and high (3 mM) $Mg^{2+}$ concentrations markedly attenuated the ATP peak, but only high $Mg^{2+}$ concentrations decreased the noradrenaline peak (Figure 2-4B).

To exploit the benefits of within tissue responses we normalised the force of contraction and time to peak contraction to 100% in each tissue in the presence of normal PSS ($Mg^{2+}$ 1.2 mM). For the combined protocols, the time to peak contraction was generally unaltered by changing $Mg^{2+}$ concentration except for the ATP peak where there was an increase in time of 107 ± 2% when the $Mg^{2+}$ was lowered from 1.2 to 0 mM (*P*=0.03) and for the noradrenaline contraction where there was a small but significant increase in time to peak of 104 ± 0.7% when the $Mg^{2+}$ was raised from 1.2 to 3 mM (*P*=0.005; Figure 2-4C).

The phase 1 ATP contraction was 170 ± 8% (*n*=10) in 0 mM $Mg^{2+}$ compared with normal $Mg^{2+}$ (1.2 mM) and only 39 ± 3% (*n*=10) in high $Mg^{2+}$ (3 mM;
Figure **2-5**A). In contrast, the noradrenaline peak contraction (phase 2) was not affected by 0 mM $Mg^{2+}$ at 97 ± 3% (*n*=10) of responses in normal $Mg^{2+}$, but was decreased significantly in high $Mg^{2+}$ 3 mM to 63 ± 4% (*n*=10); however, this was only half the attenuation observed in the ATP contraction (Figure 2-4D).

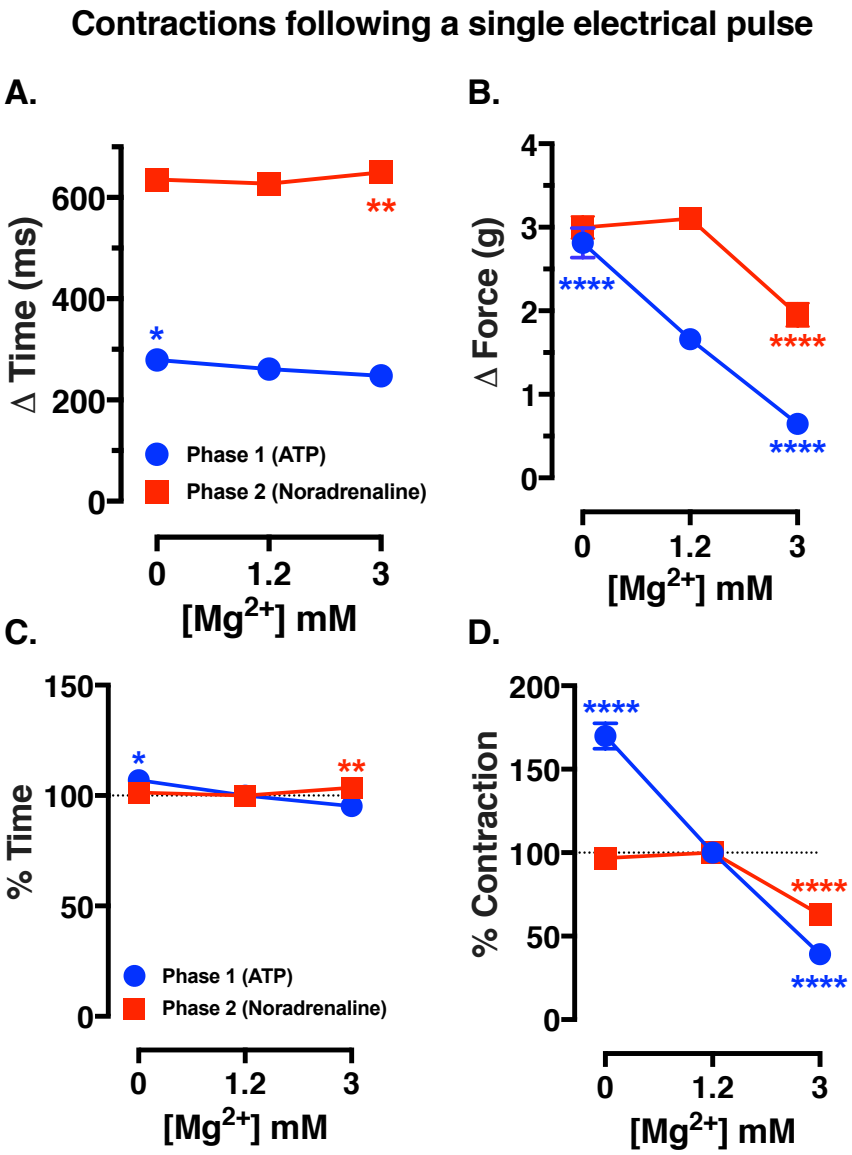


**Figure 2-4.** Contractions of rat isolated vasa deferentia following a single electrical field pulse in the presence of low, normal or high $Mg^{2+}$ concentrations.

Responses shown are the combined data from the rising and falling $Mg^{2+}$ concentration protocols of 0, 1.2 and 3 mM. A. Time from electrical stimulus to the peak contraction (Δ time, ms) for the phase 1 ATP-mediated contraction (*n*=6) or the phase 2 noradrenaline-mediated contraction (*n*=7). B. Peak increase in force (Δ force, g) for the phase 1 ATP- mediated contraction (*n*=10) or the phase 2 noradrenaline-mediated contraction (*n*=10). C. Time from electrical stimulus to the peak contraction expressed as a percentage of the respective responses taken as 100% in PSS containing a normal $Mg^{2+}$ concentration (1.2 mM) for the phase 1 ATP-mediated contraction (*n*=6) or the phase 2 noradrenaline-mediated contraction (*n*=7). D. Peak increase in force expressed as a percentage of the respective responses taken as 100% in PSS containing a normal $Mg^{2+}$ concentration (1.2 mM) for the phase 1 ATP-mediated contraction (*n*=10) or the phase 2 noradrenaline-mediated contraction (*n*=10). Values are mean ± S.E.M. (error bars not shown are contained within the symbol). *n*, number of tissues from separate rats. Repeated measures one-way ANOVA with Dunnett post hoc test was performed; **P*<0.05, ***P*<0.01 or *****P*<0.0001 compared to respective $Mg^{2+}$ 1.2 mM (normal) group.

### 2.3.3 Effects of $Mg^{2+}$ concentration on the prejunctional sensitivity to ω-conotoxin GVIA

ω-Conotoxin GVIA is a potent and highly selective, concentration-dependent inhibitor of the prejunctional N-type ($Ca_V2.2$) calcium channel. In $Mg^{2+}$ 0 mM and the presence of prazosin 100 nM, the ATP-mediated contraction to a single field pulse was decreased to zero by increasing the concentrations of ω-conotoxin GVIA ($10^{-10}$ to $10^{-7}$ M; Figure 2-5A). The $pIC_{50}$ was 8.13 ± 0.04. As the $Mg^{2+}$ concentration was elevated to 1.2 or 3 mM, the contractions in the absence of ω-conotoxin GVIA (baseline) were decreased as observed before (see Figure 2-4B) and the ω-conotoxin GVIA $IC_{50}$ shifted left. The small left shift in ω-conotoxin GVIA $IC_{50}$ with $Mg^{2+}$ 0–3 mM was 1.7-fold ($P$=0.018; Figure 2-5A).

In the presence of NF449 (10 μM), the noradrenaline-mediated control contraction to a single electrical pulse was unaffected by the rise in $Mg^{2+}$ from 0 to 1.2 mM, but significantly decreased in $Mg^{2+}$ 3 mM (baseline, Figure 2-5B), as observed in Figure 2-4B. The $pIC_{50}$ for ω-conotoxin GVIA (8.26 ± 0.06 in $Mg^{2+}$ 0 mM) was slightly left-shifted as the $Mg^{2+}$ concentration increased to 3 mM, but the shift of 1.4-fold was not significant ($P$=0.28; Figure 2-5B).

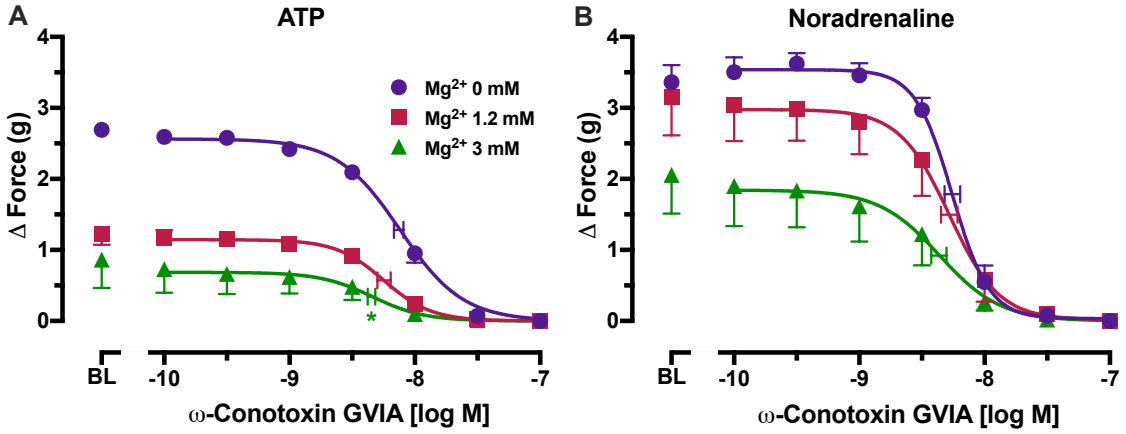


**Figure 2-5.** Contractions of rat isolated vasa deferentia following a single electrical field pulse in the presence of low (0 mM), normal (1.2 mM) and high (3 mM) $Mg^{2+}$ and increasing concentrations of the N-type $Ca^{2+}$ channel antagonist ω-conotoxin GVIA.
Peak increases in force (Δ force in g; mean ± SEM, *n*=3) are shown (A) for the phase 1 ATP-mediated contraction in the presence of prazosin 100 nM and (B) for the phase 2 noradrenaline-mediated contraction in the presence of NF449 10 μM. Every 30 min the single pulse was repeated in the presence of ω-conotoxin GVIA (10–10 to 10–7 M). BL, baseline contraction to a single electrical field pulse, in each respective $Mg^{2+}$ concentration, before the addition of ω-conotoxin GVIA. Horizontal bars are ± 1 S.E.M. of the individual fitted $IC_{50}$ values placed at the mean for each line. The left shift of the ω-conotoxin GVIA $IC_{50}$ of the ATP-mediated contraction for 0 to 3 mM $Mg^{2+}$ was significant (*$P$=0.018).

### 2.3.4 Effects of $Mg^{2+}$ concentration on exogenous agonist-induced contractions

To study the effects of $Mg^{2+}$ concentration on the contraction response to exogenous ATP (100 μM) and separately noradrenaline (10 μM), the rising concentration ($Mg^{2+}$ 0, 1.2 and 3 mM) and falling concentration ($Mg^{2+}$ 3, 1.2 and 0 mM) protocols were followed. It was evident that ATP 100 μM caused a small, transient peak contraction in normal $Mg^{2+}$ (1.2 mM) PSS of 0.22 ± 0.03 g (*n*=15) compared with the peak contraction to a single field pulse of 1.66 ± 0.09 g (*n*=10). This very weak response to exogenous ATP compared with a single electrical field pulse contrasts starkly with the contraction to 10 μM noradrenaline. Here the peak contraction was 1.1 ± 0.08 g (*n*=16) in normal $Mg^{2+}$ 1.2 mM compared with the contraction response to a single electrical pulse of 3.1 ± 0.1 g (*n*=10).

Evidently, the contraction to the high exogenous ATP concentration (100 μM) could not come close (only 5%) to mimicking the contraction to the ATP released from the single pulse. For exogenous noradrenaline, the maximum contraction was 41% of that induced by the single electrical field pulse. Noting these important differences in the scale of contraction to ATP and noradrenaline from the nerve-released transmitters compared with the contraction to exogenous ATP and noradrenaline, we again observed that exogenous ATP was far more affected by $Mg^{2+}$ than exogenous noradrenaline especially moving from normal to 0 $Mg^{2+}$ or from normal to high $Mg^{2+}$ (3 mM; Figure 2-6).

For the combined protocols in the $Mg^{2+}$-free PSS, the ATP contraction was 147 ± 11% ($n$=15; $P$=0.002) of the contraction in normal $Mg^{2+}$ PSS and was significantly less in $Mg^{2+}$ 3 mM (55 ± 6%, $n$=15; $P$<0.0001; Figure 2-6). Noradrenaline was again not significantly affected by $Mg^{2+}$ 0 mM (118 ± 8%, $n$=16; $P$=0.08) compared with normal (1.2 mM) $Mg^{2+}$, but was significantly attenuated in $Mg^{2+}$ 3 mM to 83 ± 3% ($n$=16; $P$=0.0005; Figure 2-6).

Similarly, the contraction to methoxamine was unaffected by $Mg^{2+}$ 0 mM (112 ± 10%, $n$=6, $P$=0.56) compared with normal $Mg^{2+}$ (1.2 mM) and tended to be attenuated in $Mg^{2+}$ 3 mM to 74 ± 12% ($P$=0.11; Figure 2-6).

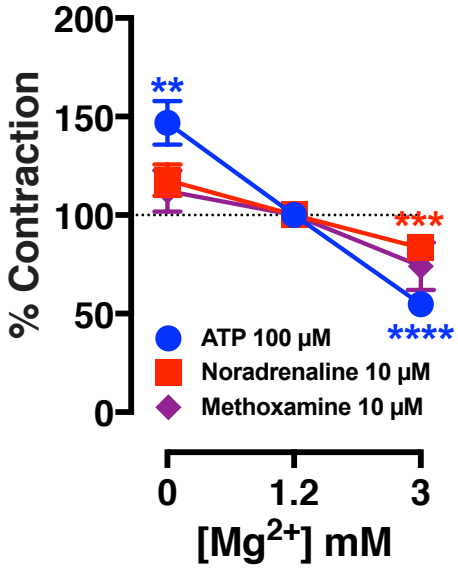


**Figure 2-6.** Contractions of rat isolated vasa deferentia following administration of exogenous ATP, noradrenaline or methoxamine in the presence of low, normal or high $Mg^{2+}$ concentrations.

Data from the rising and falling $Mg^{2+}$ concentration protocols of 0, 1.2 and 3 mM have been combined. Responses are peak increases in force expressed as a percentage of the respective contraction taken as 100% in PSS containing a normal $Mg^{2+}$ concentration (1.2 mM) for ATP 100 µM ($n$=15), noradrenaline 10 µM ($n$=16) or methoxamine 10 µM ($n$=6). Values are mean ± S.E.M. (error bars not shown are contained within the symbol). $n$, number of tissues from separate rats. Repeated measures one-way ANOVA with Dunnett *post hoc* test was performed; $^{**}P<0.01$, $^{***}P<0.001$ or $^{****}P<0.0001$ compared to respective $Mg^{2+}$ 1.2 mM (normal) group.

### 2.3.5 Estimations of the effects of $Mg^{2+}$ on transmitter release

If it is assumed that the effect of changing $Mg^{2+}$ concentration on exogenous ATP and noradrenaline contractions mimicked the postjunctional effects of these cotransmitters, then by subtracting the response to exogenous neurotransmitters from the phase 1/phase 2 responses to the electrical pulse, an estimate of the effect of changing $Mg^{2+}$ on the release of the cotransmitters may be possible. These estimates with the two protocols on the effects of increasing or decreasing $Mg^{2+}$ on the 1$^{st}$ phase (ATP) and 2$^{nd}$ phase (noradrenaline) contractions are shown (Figure 2-7A, B). The postjunctional responses to ATP or noradrenaline (Figure 2-7C, D) are shown for data from Figure 2-6. By subtracting data from Figure 2-7C & D from Figure 2-7A & B, the estimate of the effect of low to high or high to low $Mg^{2+}$ is inducible for the release component of the

phase 1 (ATP) and phase 2 (noradrenaline) peak contractions (Figure 2-7E, F). There appears to be a small enhancement (23%) of the ATP release at $Mg^{2+}$ 0 mM and small inhibition of ATP release (-15%) as $Mg^{2+}$ increases from 1.2 to 3 mM (Figure 2-7E, F). For phase 2, the release of noradrenaline appears to be decreased by 21% when the $Mg^{2+}$ either falls or rises from normal PSS ($Mg^{2+}$ 1.2 mM; Figure 2-7E, F).

### 2.3.6 Time-dependent effects of $Mg^{2+}$

$Mg^{2+}$ 1.2 and 3 mM had no time-dependent effects on ATP induced contractions over a 240 min period (Figure 2-8A). $Mg^{2+}$-free PSS decreased contractions at 210 and 240 min time points by 25 ± 12 and 37 ± 10% ($P$<0.05), respectively. $Mg^{2+}$ 3 mM had no time-dependent effects on noradrenaline induced contractions (Figure 2-8B). In normal PSS, the contractions of tissues increased from first electrical stimulation at 30 to 180 min by 27 to 46% ($P$<0.05) before returning to baseline levels at 210 min ($P$=0.057). Contrarily, $Mg^{2+}$-free PSS decreased contractions in a time-dependent manner by 15 to 53% (at 120-240 min; $P$<0.05).

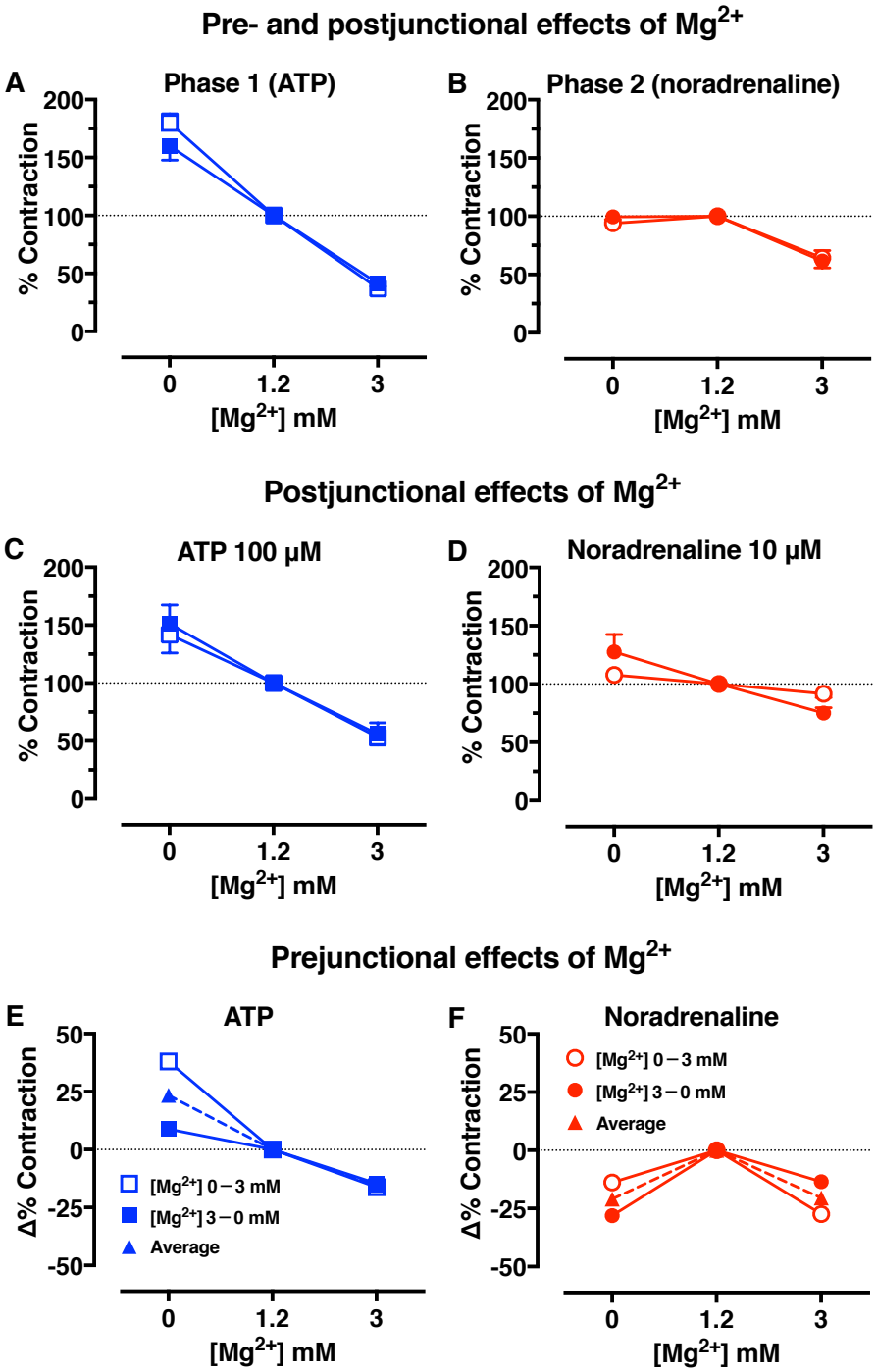


**Figure 2-7.** Average contraction data from 2 sets of experiments (A, B) and (C, D), and the derived data from subtracting (C, D) from (A, B) to arrive at an estimate of the effect of $Mg^{2+}$ on the release of the cotransmitters (E, F).

Set A, B shows the peak contractions to phase 1 (ATP) and to phase 2 (noradrenaline) in the two protocols of increasing $Mg^{2+}$ concentration (open symbols) and decreasing $Mg^{2+}$ concentration (closed symbols). Set C, D shows the peak contractions to exogenous ATP (100 µM) and noradrenaline (10 µM), again under the two protocols of changing $Mg^{2+}$ concentration. Set E, F shows the calculated responses of the $Mg^{2+}$ effects on the release of cotransmitters by subtracting set C, D from set A, B. The responses are compared within the tissue to the response in $Mg^{2+}$ 1.2 mM taken as 100% ±S.E.M. The data are derived from Figure 2-4 and Figure 2-6.

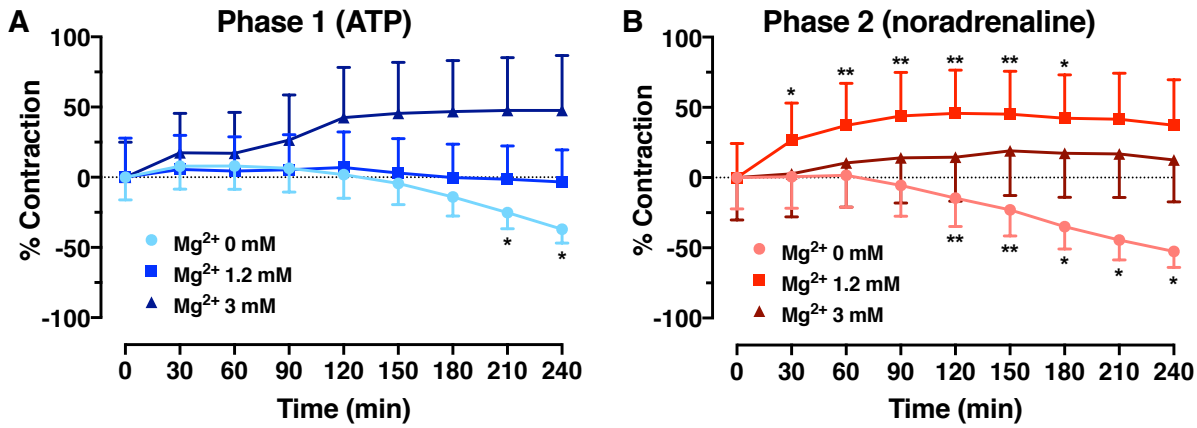


**Figure 2-8.** The time-dependent effects of different $Mg^{2+}$ conditions on ATP- and noradrenaline-mediated contractions to single electrical field pulses at 30 min intervals for 240 min.

Values are mean ± S.E.M. expressed as % contraction compared to time point 0 min. *n*, number of tissues from separate rats is *n*=5. Repeated measures one-way ANOVA with Dunnett *post hoc* test was performed; **P*<0.05 or ***P*<0.01 compared to respective 0 min response.

## 2.4 Discussion

### 2.4.1 Endogenous ATP and noradrenaline

We found that lowering the $Mg^{2+}$ concentration from 1.2 mM to 0 markedly enhanced the first peak of contraction of the rat isolated vas deferens but had no effect on the second peak of the contraction in response to a single electrical pulse. We have confirmed that the first peak of the contraction is solely due to ATP as it was abolished by the $P2X_1$ receptor antagonist NF449 and that the second peak was entirely due to noradrenaline acting at prazosin-sensitive $\alpha_1$-adrenoceptors.

The concentration of NF449, 10 μM, was shown to be selective for ATP $P2X_1$ receptors ($pK_B$ 6.4) with no activity at $\alpha_1$-adrenoceptors (Angus & Wright, 2015). Prazosin, a competitive $\alpha_1$-adrenoceptor antagonist, inhibits nerve-mediated or phenylephrine-mediated contractions in rat or mouse small resistance arteries with a $pK_B$ 9.1 (Angus & Wright, 2015).

The time from the application of the electrical stimulus to the first and second peak indicates the relative time to activation of intracellular $Ca^{2+}$ through the ionotropic $P2X_1$ receptor for ATP at 260 ms compared with the slower metabotropic $\alpha_1$-adrenoceptor coupled through inositol triphosphate at 627 ms for noradrenaline. Our results show that changing the $Mg^{2+}$ concentration made some small but significant increases or decreases in the time to peak contraction. However, the underlying result suggests that the peak ATP-mediated contraction occurs some 2.4 times faster than the noradrenaline peak. Noting the difference in the ATP ionotropic $P2X_1$ receptor and the noradrenaline G-protein-coupled metabotropic $\alpha_1$-adrenoceptor, it is not surprising that lowering $Mg^{2+}$ to zero would remove the competition between $Mg^{2+}$ and $Ca^{2+}$ at the nonselective cation ionotropic $P2X_1$ receptor allowing more $Ca^{2+}$ to flow and enhance the contraction. At the high $Mg^{2+}$ 3 mM concentration, $Ca^{2+}$ would be less available through the $P2X_1$ receptor and to a lesser degree in association with the $\alpha_1$-adrenoceptor activation mechanism.

$Mg^{2+}$-free conditions significantly decreased contraction of vas deferens tissues over time, especially the noradrenaline-induced peak contractions (Figure 2-8). This is of particular importance in studies under $Mg^{2+}$-free conditions that extend for 2 h or more. While the mechanism behind the decreased response over time has not been investigated, it can be hypothesised that since $Mg^{2+}$ plays an important role in regulating both cell and tissue functions (Jahnen-Dechent & Ketteler, 2012; Laires *et al.*, 2004) its absence may result in decreased function of the vas deferens tissue.

### 2.4.2 Exogenous ATP, noradrenaline and methoxamine

We tested a high concentration of ATP (100 μM), noradrenaline (10 μM) and methoxamine (10 μM) as a comparison with the twin peak contractions to single nerve stimulation. However, bath-applied agonists cannot mimic the transient high local concentration of ATP and noradrenaline released in a tight synaptic cleft estimated at 20 nm (Burnstock, 1990). ATP 100 μM caused a weak contraction compared with the first phase contraction in response to the single field pulse. Equally, noradrenaline 10 μM was a poor agonist compared to the phase 2 contraction. These poor contractions will be the result of slow diffusion through thick tissue, metabolism and possibly desensitisation. Nevertheless, the exogenous agonist contractions were similarly affected by the presence of 0, 1.2 or 3 mM $Mg^{2+}$ (Figure 2-6).

In pilot experiments, we tested the more stable αβ-methylene ATP in an attempt to mimic the contraction to ATP. However, the rapid desensitisation of the $P2X_1$ receptors and lack of subsequent responses to the ligand caused this approach to be abandoned. Methoxamine, on the other hand, is a useful tool as it is a selective $\alpha_1$-adrenoceptor agonist devoid of β-adrenoceptor and $\alpha_2$-adrenoceptor activity; it is not subject to neuronal uptake and metabolism that could have affected the contractions to exogenous noradrenaline. We show here that the contraction to methoxamine was affected by high $Mg^{2+}$ similarly to that for exogenous noradrenaline.

### 2.4.3 Cotransmission

With modern technology, we can separate the cotransmitter-dependent contractions following a single electrical pulse into the 2 components of ATP and noradrenaline. This work cannot shed any light on the 3 hypotheses that 1) ATP and noradrenaline are co-stored in the one vesicle; 2) ATP and noradrenaline are stored in separate vesicles; or 3) that they are located in separate varicosities (Burnstock, 1990).

### 2.4.4 Sites of action of $Mg^{2+}$

The contraction to a single field pulse could be affected by $Mg^{2+}$ acting at the release site on sympathetic varicosity or the postjunctional receptor and its smooth muscle effector machinery, or both sites. We have used two approaches to shed some light as to the mechanism of the effect of $Mg^{2+}$ on the single pulse contraction. First, ω-conotoxin GVIA is a highly selective N-type $Ca_v2.2$ calcium channel antagonist. In rat mesenteric small resistance arteries ω-conotoxin GVIA 3 nM completely inhibited excitatory junction potentials and contractions to trains of perivascular nerve stimulation with no effect on the concentration-response curve to KCl (10–70 mM) or noradrenaline (0.1–30 μM; Pruneau & Angus, 1990). Even as high as 10 μM, ω-conotoxin GVIA did not affect contractions to exogenous noradrenaline (0.1–30 μM) in rat small mesenteric arteries (Whorlow *et al.*, 1996). Thus, the sole site of action of ω-conotoxin GVIA would be to inhibit the release of neurotransmitters. We show here that the $IC_{50}$ for ω-conotoxin GVIA was similar for the ATP- and noradrenaline-mediated contractions in $Mg^{2+}$ 0 mM and that raising $Mg^{2+}$ to 3 mM caused only a small increase in sensitivity of <2-fold, which was just significant for ATP. Importantly, there was no difference in the ω-conotoxin GVIA $IC_{50}$ between $Mg^{2+}$ 0 and 1.2 mM where there is a large fall in the contraction to ATP. If $Mg^{2+}$ modified the release of neurotransmitters, we would have expected the addition of $Mg^{2+}$ to alter the potency and therefore the $IC_{50}$ of ω-conotoxin GVIA. The results of this experiment would therefore suggest that the main sites of action of $Mg^{2+}$ are at the postjunctional effector receptors for ATP and noradrenaline. Given the limitations of trying to mimic neural-released ATP and noradrenaline with exogenous ATP, noradrenaline and methoxamine, our study strongly suggests that $Mg^{2+}$ directly competes with $Ca^{2+}$ involved in the ATP $P2X_1$

receptor-mediated contraction, but only at the high (3 mM) concentration does it inhibit the $\alpha_1$-adrenoceptor-mediated contraction.

### 2.4.5 Conclusions

Our work demonstrates that the contractions to each of the cotransmitters ATP and noradrenaline in the rat vas deferens can be determined and are differently altered by low $Mg^{2+}$ concentration, but both are inhibited by high $Mg^{2+}$ concentration. The sites of action of $Mg^{2+}$ are most probably at the postjunctional $P2X_1$ receptor and the $\alpha_1$-adrenoceptor. The ATP-mediated contraction is more sensitive to changing $Mg^{2+}$ concentrations than noradrenaline-mediated contraction consistent with the $P2X_1$ receptor coupled to an ionotropic channel. Our results suggest that this assay with a single electrical field pulse is ideal to test various pre- or postjunctional modulators of cotransmitter release. We suggest that any future publications should carefully justify why the magnesium concentration in PSS should be other than normal 1.2 mM.

# Chapter 3

Pharmacological characterisation of the $CB_1$ receptor antagonist activity of cannabidiol in the rat vas deferens bioassay

## 3.1 Introduction

The advancement of cannabinoid research in the 1990s included the cloning of the first cannabinoid receptor ($CB_1$) (Gerard *et al.*, 1991; Matsuda *et al.*, 1990). Shortly after, Pertwee and colleagues (1992) sought to identify isolated tissues that could serve as bioassays to elucidate the mechanism of action of phytocannabinoids. They established that the mouse isolated vas deferens was an appropriate cannabinoid bioassay as it fulfilled the criteria of being stereoselective in its responses to different homologues of THC, while also producing an effect to THC at concentrations that matched the *in vivo* submaximal psychotropic doses (<1 μM; Pertwee *et al.*, 1992). The same year, the endocannabinoid anandamide was discovered in the porcine brain during the screening of endogenous ligands for the isolated $CB_1$ receptor (section 1.2; Devane *et al.*, 1992). By utilising the newly described mouse isolated vas deferens assay, anandamide was confirmed to have "THC-like" (cannabimimetic) activities in the tissues, indicating that it activated $CB_1$ receptors. Since then, the mouse isolated vas deferens has been utilised to investigate the $CB_1$ receptor activity of various endo-, synthetic- and phytocannabinoids, including cannabidiol.

### 3.1.1 Evidence that prejunctional $CB_1$ receptors modulate neurotransmission

The electrical stimulation of the vas deferens bioassay induces biphasic contractions which are mediated by the neurotransmitters ATP and noradrenaline (Chapter 2; Figure 2-1). Various studies support a role for prejunctional $CB_1$ receptors in modulating neurotransmitter release and hence the contraction of vasa deferentia (Figure 3-1; Howlett *et al.*, 2002; Pertwee, 1997; Schlicker & Kathmann, 2001). The compelling evidence includes that:

i) $CB_1$ receptor agonists like WIN 55,212-2, CP 55,940, THC and anandamide mediate concentration-dependent inhibitions of electrically induced contractions of vasa deferentia (Christopoulos *et al.*, 2001; Lay *et al.*, 2000; Pertwee & Fernando, 1996; Pertwee *et al.*, 2002) and these contractions were inhibited by the sodium channel blocker tetrodotoxin (0.1-0.2 μM), which indicates that the contractions of the tissues were nerve-mediated and not evoked through direct stimulation of the smooth muscle.

ii) $CB_1$ receptor agonists express high potency, stereoselectivity and structure-dependence in their inhibition of electrically induced contractions and their potency at inhibiting contractions correlates with the order of their binding affinity (reviewed in Pertwee, 1997).

iii) $CB_1$ selective antagonists (e.g. rimonabant) attenuate the inhibition of electrically evoked contractions induced by $CB_1$ agonists (Christopoulos *et al.*, 2001; Lay *et al.*, 2000; Pertwee & Fernando, 1996; Pertwee *et al.*, 1995b; Rinaldi-Carmona *et al.*, 1994; Thomas *et al.*, 2007).

iv) The cannabinoid agonist CP 55,940 inhibits the production of cAMP in the mouse vas deferens, an effect that was competitively reversed by the $CB_1$ antagonist rimonabant (Pertwee *et al.*, 1996b). This is relevant as $CB_1$ receptors are coupled to $G_i$ proteins which upon activation would inhibit adenylate cyclase and hence the production of cAMP.

v) THC induced cannabinoid tolerance in mouse vas deferens which did not affect the ability of non-cannabinoid receptors (e.g. $\alpha_2$-adrenoceptors and opioid receptors) to induce twitch responses (Pertwee & Griffin, 1995).

vi) $CB_1$ receptor mRNA has been detected in both mouse and rat vas deferens (Ishac *et al.*, 1996).

vii) While $CB_1$ agonists potently inhibit the contraction of electrically stimulated vas deferens, they do not potently prevent the contraction of exogenous P2X1 and $\alpha_1$-adrenoceptor agonists, indicative of a prejunctional site for $CB_1$ receptors (Lay *et al.*, 2000; Pertwee & Griffin, 1995).

viii) In rat vas deferens preloaded with [$^3$H]-noradrenaline, the cannabinoids THC and anandamide caused a tetrodotoxin (0.5 μM)-sensitive inhibition of electrically induced release of [$^3$H]-noradrenaline, this effect was attenuated by the $CB_1$ antagonist rimonabant (Ishac *et al.*, 1996). Similarly, in $CB_1^{+/+}$ mice, the $CB_1$ receptor agonist WIN 55,212-2 (1 μM) decreased [$^3$H]-noradrenaline release by 64%, while not affecting neurotransmitter release in $CB_1^{-/-}$ mice (Schlicker *et al.*, 2003). Furthermore, rimonabant (0.32 μM) reversed the effects of WIN 55,2121-2 in $CB_1^{+/+}$ tissues.

This evidence supports a role for the vas deferens bioassay in determining the potency of $CB_1$ agonists and antagonists.

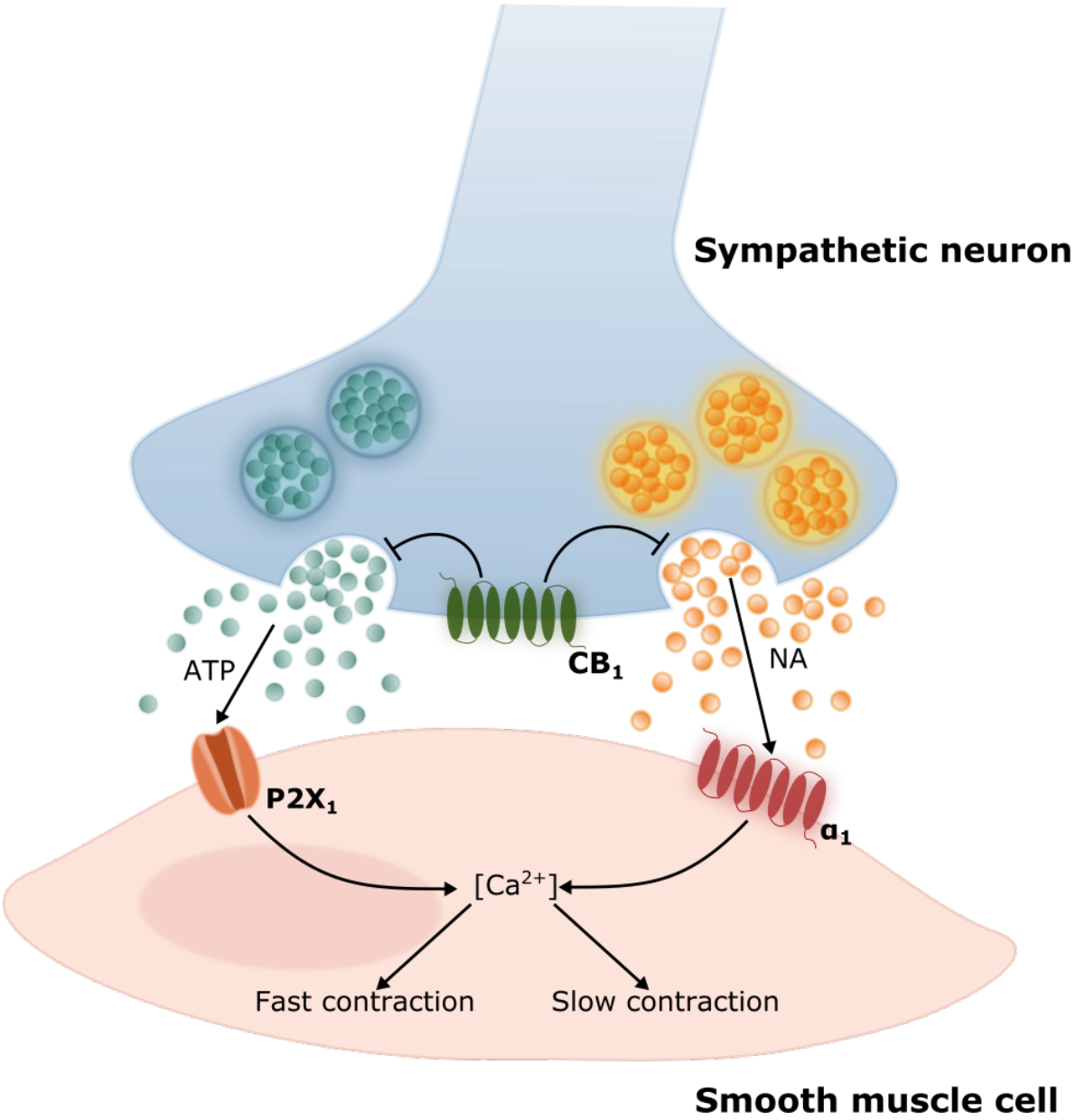


**Figure 3-1.** Simplified schema based on Figure 2-1 of $CB_1$ receptor modulation of excitatory cotransmission in the vas deferens.
Prejunctional $CB_1$ receptor activation negatively modulates the release of the neurotransmitters ATP and noradrenaline and hence neurotransmitter-mediated smooth muscle contraction.

### 3.1.2 Endogenous $CB_1$ receptor tone

It has been suggested that presynaptic $CB_1$ receptors are under endogenous tone (reviewed in Schlicker & Kathmann, 2001). This is based on the ability of the antagonist

rimonabant to cause a significant increase in the amplitude of electrically induced contractions in various tissue preparations including rat vas deferens, mouse urinary bladder and guinea-pig myenteric plexus longitudinal muscle (Christopoulos *et al.*, 2001; Coutts & Pertwee, 1997; Pertwee, 2014; Pertwee & Fernando, 1996; Pertwee *et al.*, 1996a). Additionally, [$^3$H]-noradrenaline release was 37% higher in vasa deferentia from $CB_1^{-/-}$ mice compared to $CB_1^{+/+}$ mice as a result of basal electrical stimulation (Schlicker *et al.*, 2003). In rat vas deferens, the incubation with the amidase inhibitor phenylmethylsulfonyl fluoride (PMSF) mimicked the effects of $CB_1$ agonists by decreasing electrically evoked contractions, indicative of endogenous anandamide tone (Christopoulos *et al.*, 2001). However, PMSF did not modulate exogenous anandamide responses in mouse vas deferens, suggesting that in mouse tissues anandamide is not metabolised by enzymes targeted by PMSF (Pertwee *et al.*, 1995a).

### 3.1.3 $CB_1$ receptor antagonism by cannabidiol and rimonabant

$CB_1$ receptors are the most abundant GPCRs in the central nervous system and are mainly expressed prejunctionally in neurons (reviewed in Howlett *et al.*, 2002; Pertwee, 2008b). $CB_1$ receptors are also found in peripheral tissues including urogenital tissues: the uterus, ovary, testis and vas deferens (Galiegue *et al.*, 1995), albeit to a much lower level (Howlett *et al.*, 2002). The receptors play an important role in modulating neurotransmitter release which is believed to maintain homeostasis in the body by preventing excessive neurotransmitter release and thus maintaining health and preventing disease. $CB_1$ receptors are also expressed in the heart, vasculature and circulating blood cells where the overactivation of the receptors can result in the pathology of various cardiovascular diseases. Hence, $CB_1$-active phytocannabinoids can mediate cardiovascular adverse or beneficial effects by activating or inhibiting $CB_1$ receptors, respectively (section 1.7; Pacher *et al.*, 2018). The increased use of *Cannabis* compounds together with the widespread role of $CB_1$ receptors in human physiology and disease offers a strong incentive to study the $CB_1$ receptor pharmacology of phytocannabinoids.

#### 3.1.3.1 Cannabidiol

The affinity of cannabidiol has been investigated in various human, mouse and rat cell-based binding assays resulting in a pooled mean affinity, $pK_i$, of 5.5 ($K_i$ 3.3 ± 0.8 μM, $n$=15) with no species-specific differences reported (Table 3-1; reviewed in McPartland *et al.*, 2015). It has been suggested that cannabidiol negatively modulates $CB_1$ receptors by acting at an allosteric site (Laprairie *et al.*, 2015; Tham *et al.*, 2018). Recent research has also modelled the potential allosteric sites of cannabidiol at the $CB_1$ receptors (Chung *et al.*, 2019; Jakowiecki *et al.*, 2021). While cannabidiol does not appear to act as a direct $CB_1$ receptor antagonist, it inhibits the effects of $CB_1$ agonists CP 55,940 and WIN 55,212-2 with a pooled potency, $pK_B$, of 7.1 ($K_B$ 88.5 ± 18.5 nM, $n$=5) (reviewed in McPartland *et al.*, 2015). Efficacy studies to date have only been performed in mouse vasa deferentia (Table 3-1; Pertwee *et al.*, 2002; Thomas *et al.*, 2004). However, there are intra- and interspecies differences in the anatomical location and density of $CB_1$ receptors (Silver, 2019) which prompts expanding the efficacy studies of cannabidiol to non-mouse assays. Furthermore, there are differences in rat, mouse and human $CB_1$ mRNA, with slightly higher conservation between rat and human mRNA compared to mouse and human (Chakrabarti *et al.*, 1995; Shire *et al.*, 1996).

.

**Table 3-1.** Current work and literature reported potencies of cannabidiol and rimonabant in modulating the activity of $CB_1$ receptor agonists in electrically stimulated vas deferens

| Antagonist | Agonist | Neurotransmitter | $pK_B$ | Slope | $K_i/K_B$ | Species |
|---|---|---|---|---|---|---|
| **Cannabidiol** $pK_i$: 5.49; $n$=15[a] | WIN 55,212-2 | ATP | 5.90 ± 0.15 | 1.02 (0.84—1.19) | 2.6 | Rat |
| | WIN 55,212-2 | Noradrenaline | 5.29 ± 0.13 | 1.05 (0.66—1.44) | 0.6 | Rat |
| | WIN 55,212-2 | ATP + noradrenaline | 7.2 (6.7—7.5) | — | 51.3 | Mouse[d] |
| | WIN 55,212-2 | ATP + noradrenaline | 6.9 (6.9—7.0) | 1.2 (0.8—1.6) | 25.7 | Mouse[e] |
| | CP 55,940 | ATP + noradrenaline | 7.5 (7.1—7.9) | — | 102.3 | Mouse[e] |
| **Rimonabant** $pK_i$: 8.42; $n$=2[b, c] | WIN 55,212-2 | ATP | 8.39 ± 0.32 | 0.88 (-4.88-6.52) | 0.9 | Rat |
| | WIN 55,212-2 | Noradrenaline | 7.67 ± 0.12 | 0.97 (0.70–1.25) | 0.2 | Rat |
| | WIN 55,212-2 | Noradrenaline | 7.51 ± 0.27 | 1.12 ± 0.30 | 0.1 | Rat[f] |
| | CP 55,940 | Noradrenaline | 7.49 ± 0.25 | 0.85 ± 0.17 | 0.1 | Rat[f] |
| | CP 55,940 | ATP + noradrenaline | 8.6 ± 0.2 | — | 1.5 | Mouse[g] |
| | WIN 55,212-2 | ATP + noradrenaline | 8.85 ± 0.05 | — | 2.7 | Mouse[b] |
| | CP 55,940 | ATP + noradrenaline | 7.98 ± 0.03 | — | 0.4 | Mouse[c] |

$pK_B$ and slope estimates for cannabidiol and rimonabant were derived from this current study (grey highlight) and previous studies in rat and mouse vas deferens tissues. The $pK_B$ values were derived from the global fit where the n was constrained to 1. Values are expressed with ± S.E.M. or 95% confidence limits (shown in parenthesis). Studies referenced: [a]reviewed in McPartland *et al.* (2015); [b]Rinaldi-Carmona *et al.* (1995); [c]Rinaldi-Carmona *et al.* (1994); [d]Thomas *et al.* (2004); [e]Pertwee *et al.* (2002); [f]Christopoulos *et al.* (2001); and [g]Lay *et al.* (2000). Note that all experiments were performed in magnesium-free Krebs' physiological solution with the exception for the experiments in this study (grey highlight) which were performed in normal Krebs' physiological salt solution.

### 3.1.3.2 Rimonabant

Rimonabant, also known as SR141716, is a synthetic selective $CB_1$ receptor inhibitor. The $CB_1$ receptor inhibition by rimonabant decreases appetite which results in weight loss. These effects led to the medical approval of Acomplia®, an anti-obesity treatment, in more than 50 countries (European Medicines Agency, 2007). The rationale behind treating obesity with a $CB_1$ inhibitor is that patients with obesity have a heightened endogenous cannabinoid tone which causes excessive appetite and metabolic alterations (reviewed in Xie *et al.*, 2007). Despite the promising effects on obesity, rimonabant was soon withdrawn from the market due to several adverse psychiatric events including depression, anxiety and an increase in suicide attempts (Sam *et al.*, 2011).

In publications, rimonabant is interchangeably referred to as an antagonist or inverse agonist as several studies indicate that rather than acting as a neutral antagonist at the $CB_1$ receptor, rimonabant may be acting as an inverse agonist, i.e. have intrinsic activity opposite to that of an agonist (Kenakin, 2014). I have decided to refer to rimonabant as an antagonist using the rationale of Kenakin (2014) who states that the term inverse agonist is a misnomer as "these ligands really are simply antagonists with an added feature that allows them to reduce elevated basal activity". In contrast to cannabidiol, rimonabant has high binding affinity at the orthosteric site of the $CB_1$ receptor with a $pK_i$ value of 8.3 ($K_i$: 5.6 ± 0.5 nM) at human $CB_1$ receptors expressed in Chinese hamster ovary cells and $pK_i$ 8.7 ($K_i$: 2.0 ± 0.4 nM) in rat brain synaptosomal membranes (Rinaldi-Carmona *et al.*, 1995; Rinaldi-Carmona *et al.*, 1994). Furthermore, the potency of rimonabant as an inhibitor of $CB_1$ receptor agonists in the vas deferens bioassay matches its affinity at the receptor ($pK_B$: 7.5-8.9; Table 3.1).

## 3.1.4 Lew and Angus method of nonlinear regression analysis

One of the main purposes of utilising the vas deferens bioassay in cannabinoid research has been to confirm $CB_1$ receptor activity and to quantify the efficacy of cannabinoids at the $CB_1$ receptor. $K_B$, the equilibrium dissociation constant of an antagonist-receptor complex is usually determined using functional assays (Kenakin, 2014), in this case, the

electrically stimulated vas deferens bioassay. $K_B$ is further defined as the concentration of antagonist that occupies 50% of the receptors at equilibrium. When determining $K_B$ usually the Schild regression analysis method is used (Arunlakshana & Schild, 1959). The use of Schild analysis is contradicted by the experimental design of this study as one of the requirements is for the concentration-response curves to be performed within one tissue, to allow for the calculation of concentration ratios. Repeating concentration-response curves within one tissue would most likely induce time-dependent effects by altering tissue sensitivity to the cannabinoids. Furthermore, due to the hydrophobic nature of cannabinoids, they require longer incubation times to ensure equilibration of tissue with drug, hence establishing several concentration-response curves in one tissue would be laborious. Stone and Angus (1978) recognised the limitations with Schild analysis and developed a new analytical approach that was further simplified by Lew and Angus (1995). Similar to Schild analysis, the relative placement of the concentration-response curves are predicted, with the difference that instead of using the relative shifts of curves from control to calculate concentration ratios, $pK_B$ estimation is based on the global fitting of individual curve placements, including the control curve (global regression analysis). The Schild analysis emphasizes the control $pEC_{50}$ values to determine the concentration-ratio, which can be a problem when control curves are poorly defined. Conversely, global regression analysis includes the control $pEC_{50}$, thus increasing the degrees of freedom. Another disadvantage with the Schild analysis is that it does not allow for leftward shifts of concentration-response curves from the control, which can sometimes result from the presence of lower concentrations of an antagonist.

By fitting agonist $pEC_{50}$ values in the presence and absence of antagonist, the $pK_B$ is estimated from the following global nonlinear regression analysis equation:

$$pEC_{50} = -\text{Log}\,([B] + 10^{-pK_B}) - \text{Log}\,c \qquad (1)$$

where [B] denotes antagonist concentration. $pK_B$ and c are fitting constants, c is the difference between control $pEC_{50}$ and $pK_B$. The results of the analysis can be plotted in a "Clark plot" (Stone & Angus, 1978), named after A. J. Clark because of the similarities

with his graph displaying log[agonist] vs log[antagonist] that produced 50% of the response ($EC_{50}$; Clark, 1926). The Clark plot merely displays the relationship between the experimental curve placements in the absence and presence of antagonist (agonist $pEC_{50}$) and the corresponding antagonist concentrations together with the calculated $pK_B$ value (-log([B]+$K_B$)) and is not used to calculate $pK_B$ or $pK_A$ values, unlike the Schild plot. There are two methods to confirm whether the dextral shifts of concentration-response curves are competitive. Firstly, by including a "power departure" value, which is equivalent to allowing the slope in the Schild plot to vary from unity (Lew & Angus, 1995). This is obtained by allowing the exponent of [B] (equation 1) to vary from unity, creating the following equation:

$$pEC_{50} = -\text{Log}\,([B]^n + 10^{-pK_B}) - \text{Log}\,c \qquad (2)$$

If the 95% confidence interval for n includes 1, equation 2 can be fitted to include n=1 (equation 1), which indicate that the concentration-response curves are displaced according to simple competitive antagonism. Secondly, plotting ± 2 times the standard error of the difference between the experimentally observed $pEC_{50}$ values and the predicted $pEC_{50}$ values from equation 1 into the Clark plot provides an estimation of the confidence line constrained to 1. If the points of the average experimentally observed $pEC_{50}$s in the absence and presence of antagonist fall within the error bars, it is an indication of simple competitive antagonism. In other words, the confidence line in the Clark plot denotes the behaviour expected by a competitive antagonist and deviation from the line is indicative of deviation from competitive antagonism.

### 3.1.5 Study aims

This study aimed to pharmacologically characterise the $CB_1$ receptor activity of cannabidiol by utilising electrically evoked contractions of the rat vas deferens. To our knowledge, this is the first study to investigate the prejunctional $CB_1$ receptor antagonism by cannabidiol using a rat bioassay. The effects of the antagonist rimonabant were also examined to calibrate the robustness of the assay. We assessed

whether the $K_B$ estimates of cannabidiol and rimonabant were influenced by which neurotransmitter mediated the contraction of the vas deferens.

## 3.2 Methods

### 3.2.1 Animals

The Animal Ethics Committee of the University of Melbourne approved experiments (approval #10246) in accordance with *The Australian Code for the care and use of animals for scientific purposes* (8th edition, 2013, National Health and Medical Research Council, Canberra). Male Sprague-Dawley rats (10-12 weeks old, Biomedical Animal Facility, Melbourne, Australia) were used in this study and housed in groups of 3-4 in standard cages under constant climatic conditions (21°C, 12 h light/dark cycle), with food and water *ad libitum*.

Rats (250-350 g) were deeply anaesthetised by inhalation of 5% isoflurane in 100% oxygen and killed by a rapid cut through the spinal cord. The whole vasa deferentia were excised and placed in Krebs-Henseleit physiological salt solution (PSS; Mazeh *et al.*, 2019) with the following composition (mM): NaCl 119, KCl 4.7, $KH_2PO_4$ 1.2, $NaHCO_3$ 25, $CaCl_2$ 2.5, EDTA 0.026, $MgSO_4$ 1.2 and glucose 11. The PSS was oxygenated with carbogen (95% $O_2$ and 5% $CO_2$) at pH 7.4.

### 3.2.2 Dissection and set up of vasa deferentia

The tissues were pinned down and tied at either side with a silk thread and trimmed to an approximate length of 2 cm. The prostatic end was tied to a stainless-steel hook on a fixed acrylic organ bath leg between two parallel platinum field electrodes, while the epididymal end was tied uppermost to a stainless-steel hook attached to a Grass FTO3C isometric force transducer (Grass Instruments, Quincy, MA, USA) connected to a bridge amplifier and a data acquisition system (Powerlab 8/35, ADInstruments, Sydney, Australia). The organ bath leg was adjusted vertically with an attached micrometer (Mitutoyo Manufacturing Co., Kawasaki, Japan). The responses were measured on a computer running LabChart 7 Pro software (ADInstruments) with sampling rate: 100 Hz, range: 2 mV and low pass filter set at 20 Hz. Tissues were suspended in 5 ml organ baths containing PSS, oxygenated with 95% $O_2$ and 5% $CO_2$ at 37°C. The tissues were stretched to 2 g force, followed by a re-stretch to 2 g after 10 min. The bath solutions were changed twice-before starting the experiments.

### 3.2.3 Electrical stimulation

Tissues were randomly allocated to a drug treatment group prior to the viability test which involved a single electrical square wave nerve stimulation pulse (150 V, 0.5 ms duration). The bath solution was changed twice before incubating the tissues with either the P2X1 receptor inhibitor NF449 (10 μM) or $\alpha_1$-adrenoceptor inhibitor prazosin (100 nM) for 30 min to inhibit the ATP- or noradrenaline-mediated contractions, respectively, leaving a monophasic twitch contraction. This was followed by a single electrical stimulation (150 V, 0.5 ms duration). Tissues were subsequently incubated with either vehicle (DMSO 1%), cannabidiol (10-100 μM) or rimonabant (0.003-10 μM) for 1 h, followed by a single electrical stimulation. Single electrical stimulations were repeated every 30 min prior to half-log cumulative additions of WIN 55,212-2 (0.001-30 μM).

To investigate the potential influence of endogenous anandamide on the contractions of vasa deferentia to electrical stimulation, some tissues were incubated with half-log cumulative additions of the fatty acid amide hydrolase (FAAH) inhibitor URB937 (0.0001-1 μM) or corresponding concentrations of the vehicle (DMSO 0.1-1.24%), prior to single electrical stimulations every 30 min. Time controls were also completed (no addition of URB937 or vehicle) with single electrical stimulations every 30 min to 240 min.

### 3.2.4 Data and statistical analyses

All data are expressed as the mean ± S.E.M. of *n* experiments (each tissue from a separate rat). WIN 55,212-2 concentration-response curves were expressed as % contraction compared to maximum vehicle-, cannabidiol- or rimonabant-only responses (control responses; C) within each vas deferens tissue. Individual sigmoidal concentration-response curves were fitted using Prism 8 (Graphpad Software, La Jolla, CA, USA). $pEC_{50}$, $R_{max}$ and WIN 55,212-2 (0.001 μM) responses for cannabidiol- and rimonabant-treated tissues were compared with corresponding vehicle responses using repeated measures one-way ANOVA with Dunnett post hoc test for multiple comparisons. This test was also performed to compare the effects of URB937 (0.0001-1 μM), DMSO concentrations (0.1-1.24%) or time (0-240 min; time controls) with their respective

baseline contractile responses. Effects of URB937 or DMSO at each cumulative concentration were compared with corresponding time control values by repeated measures two-way ANOVA with Dunnett post hoc test for multiple comparisons. For all repeated measures one-way or two-way ANOVAs, the Greenhouse-Geisser correction for correlation was applied. The basal responses for noradrenaline- or ATP-mediated contractions in the absence of cannabinoid antagonists and agonist were compared using Student's unpaired t test. *P* values < 0.05 were considered significant.

#### 3.2.4.1 Non-Linear regression analysis and Clark plot display

The $CB_1$ receptor antagonist potency of cannabidiol or rimonabant was determined through global non-linear regression analysis (Lew & Angus, 1995) which provided the antagonist dissociation constants, $pK_B$ (–log $K_B$). The $pK_B$ values for cannabidiol or rimonabant were solved by iterative approximations of WIN 55,212-2 $pEC_{50}$ values in the absence or presence of the antagonists cannabidiol or rimonabant using the following equation:

$$pEC_{50} = -\text{Log}\left([B]^n + 10^{-pK_B}\right) - \text{Log } c \qquad (3)$$

where n is a 'power departure' equivalent to allowing the slope of a Schild plot to vary from unity (Lew & Angus, 1995).

Clark plot displays were used to verify if the $CB_1$ activity of cannabidiol or rimonabant conformed to simple competitive antagonism. The points on the Clark plot are the average WIN 55,212-2 $pEC_{50}$ values in the absence and presence of the different antagonist concentrations plotted against the corresponding antagonist –log(B + $K_B$) values. The line in the Clark plot has a gradient of 1 and represents the theoretical WIN 55,212-2 $pEC_{50}$ values (equation 1) that would be obtained if cannabidiol or rimonabant conformed to simple competitive antagonism. The error bars on the line are the standard error of differences (±2 S.E.M.) between the observed WIN 55,212-2 $pEC_{50}$ values and the theoretical $pEC_{50}$ values from equation 1. There are two methods of verifying if cannabidiol or rimonabant displacement of WIN 55,212-2 concentration-

response curves conform to simple competitive antagonism. Firstly, if the 95% confidence interval for n includes 1 (equation 1). Secondly, if the points of WIN 55,212-2 $pEC_{50}$ values in the absence or presence of cannabidiol, or rimonabant, fall within the error bars. Hence, the line in the Clark plot denotes the behaviour expected by a competitive antagonist and deviation from the line is indicative of deviation from competitive antagonism.

### 3.2.5 Drugs

Drugs used were: (-)-cannabidiol (Cayman Chemical, Ann Arbor, MI, USA); NF449 octasodium salt (4,4',4'',4'''-[carbonylbis[imino-5,1,3-benzenetriylbis(carbonylimino)]]tetrakis-1,3-benzenedisulfonic acid, octasodium salt; Cayman Chemical); noradrenaline bitartrate salt (Sigma-Aldrich, St Louis, MO, USA); prazosin hydrochloride (Sigma); rimonabant (rimonabant; Cayman Chemical); URB937 (3'-carbamoyl-6-hydroxybiphenyl-3-yl cyclohexylcarbamate; Cayman Chemical); WIN 55,212-2 mesylate (Tocris Bioscience, Bristol, UK). Cannabidiol, rimonabant, URB937 and WIN 55,212-2 stock solutions and subsequent dilutions were performed in DMSO. NF449, noradrenaline and prazosin were dissolved in MilliQ water. All aliquots were stored at -20°C. Fresh drug dilutions were made daily.

## 3.3 Results

### 3.3.1 The effects of cannabidiol on WIN 55,212-2-mediated inhibition of electrically evoked contractions of the rat vas deferens

The cannabinoid receptor agonist WIN 55,212-2 inhibited electrically induced contractions of NF449 (10 μM) pretreated vasa deferentia in a concentration-dependent manner (Figure 3-2A). Compared to the vehicle (DMSO 1%), cannabidiol (30 μM) attenuated the effects of WIN 55,212-2, in addition to causing a greater increase in control contractions in the absence of WIN 55,212-2 (Figure 3-2B). In tissues with noradrenaline-mediated contractions, cannabidiol 30 and 100 μM induced 6.8- and 21.9-fold dextral shifts, respectively, of WIN 55,212-2 concentration-response curves (Figure 3-3A; $P<0.0001$). In the prazosin pretreated tissues, the dextral shifts of ATP-mediated contraction-response curves were more pronounced, where cannabidiol 10, 30 and 100 μM induced 9.0-, 21.8- and 85.3-fold rightward shifts, respectively (Figure 3-3B; $P<0.01$).

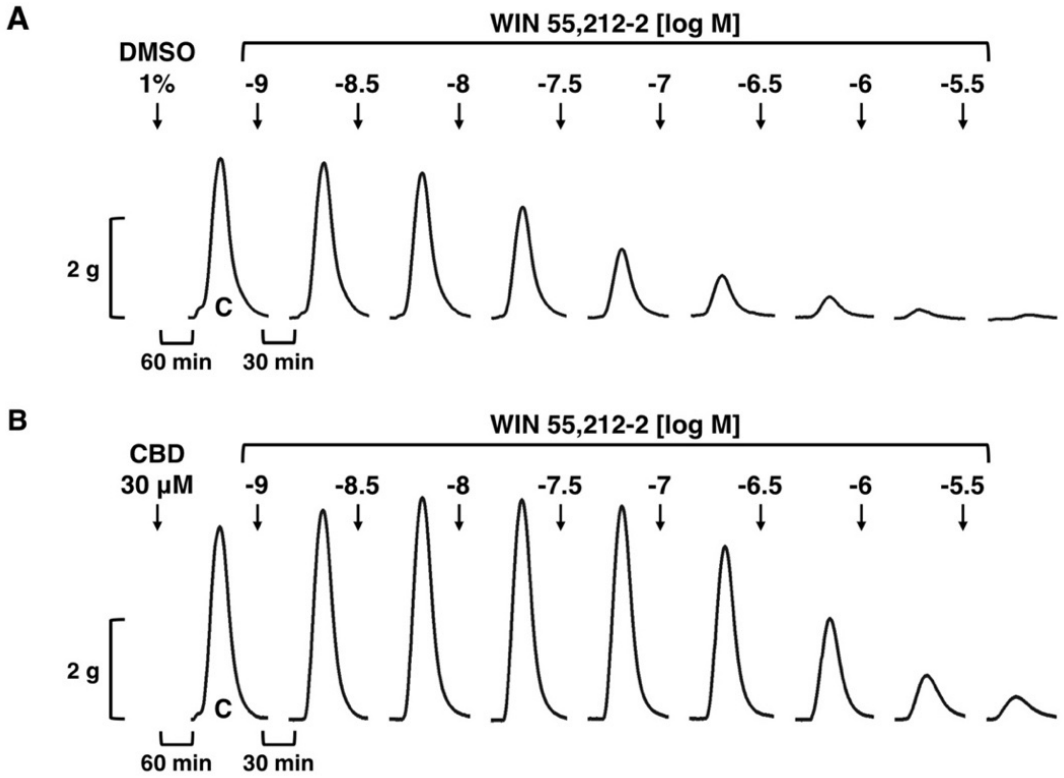


**Figure 3-2.** Representative LabChart® traces of single electrical nerve stimulation pulses of rat vas deferens.

The traces show the influence of 60 min incubation with A. vehicle (DMSO 1%) or B. cannabidiol (CBD; 30 µM) on WIN 55,212-2-induced inhibitions of vasa deferentia contractions mediated by single electrical nerve stimulations (150 V, 0.5 ms duration). ATP-mediated contractions were inhibited by pretreatment with NF449 (10 µM) leaving single noradrenaline-mediated contractions. Nerve stimulations were introduced at 30 min intervals following half-log increment incubations with WIN 55,212-2. C denotes the respective (within tissue) control contraction that all subsequent contractions were normalised against in the following graphs.

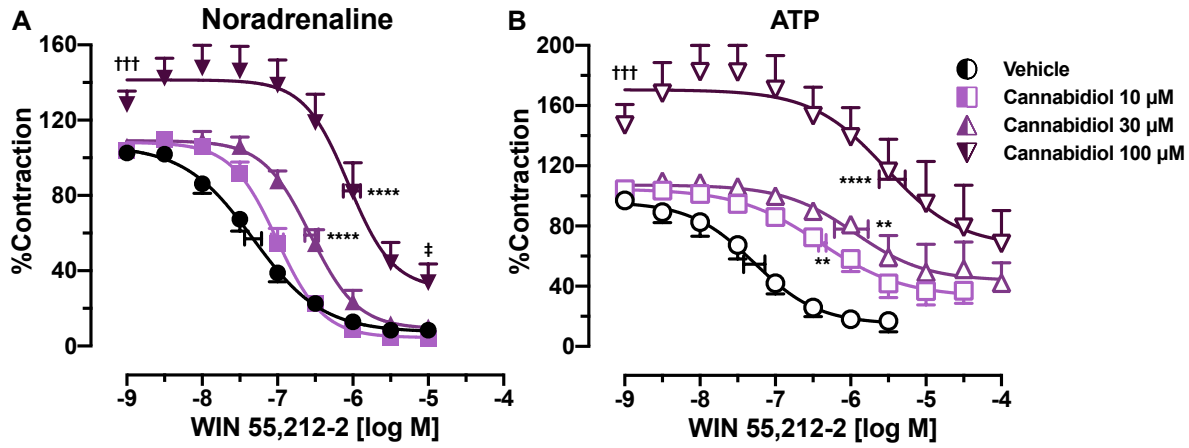


**Figure 3-3.** The effects of cannabidiol (10-100 µM) or vehicle (DMSO 1%) on WIN 55,212-2-induced inhibition of electrically evoked contractions of rat vasa deferentia pretreated with either NF449 (10 µM; A) or prazosin (100 nM; B), favouring noradrenaline- or ATP-mediated contractions, respectively.

Responses are presented as a percentage (%) of the respective control contraction (in the absence of WIN 55,212-2, shown as C in Figure 3-2) in the presence of cannabidiol (10-100 µM) or vehicle (DMSO 1%). Vertical error bars are ± S.E.M. (those not shown are contained within the symbol) and horizontal error bars represent the $EC_{50}$ ± S.E.M. $^{**}P \leq 0.01$ or $^{****}P \leq 0.0001$, $EC_{50}$ compared with respective vehicle group $EC_{50}$. $^{††}P \leq 0.01$ or $^{†††}P \leq 0.001$ compared with respective vehicle group WIN 55,212-2 concentration-response curve. $^{‡}P \leq 0.05$ compared with the corresponding vehicle group maximal inhibition of contraction ($R_{max}$); repeated measures one-way ANOVA with Dunnett *post hoc* test. $n$=7-9 (panel A) and $n$=4-7 (panel B), from separate rats, per treatment group.

### 3.3.1.1 Determination of cannabidiol $CB_1$ receptor potency

To investigate if cannabidiol-induced dextral shifts in WIN 55,212-2 curves conformed to simple competitive antagonism, global regression analysis was performed, and the result was displayed in a Clark plot (Figure 3-4). In the Clark plot, -log([cannabidiol]+$K_B$) points for the cannabidiol concentrations 0-100 µM were all placed within the error bars, indicating that the shifts of $pEC_{50}$ values were in agreement with competitive antagonism. The global regression analysis gave $pK_B$ estimations of 5.29 ± 0.13 ($n$=32) or 5.90 ± 0.15 ($n$=18) in tissues contracted with noradrenaline or ATP, respectively. Hence cannabidiol was 4.1 times more potent in displacing WIN 55,212-2 concentration-response curves in ATP-contracted tissues ($P$=0.0049; Figure 3-4).

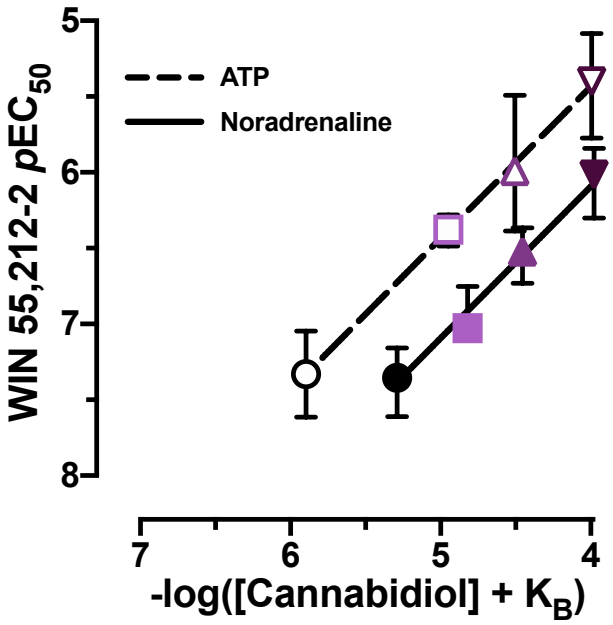


**Figure 3-4.** The Clark plot displays the interaction between increasing concentrations of cannabidiol and WIN 55,212-2 $p$EC$_{50}$ values (from Figure 3-3A, noradrenaline, filled symbols and solid line, and Figure 3-3B, ATP, empty symbols and dashed line).
Symbols reflect the cannabidiol concentrations shown in Figure 3-3. Cannabidiol $p$K$_B$ estimates can be derived from the control point (when [cannabidiol]=0; circle symbol) resulting in $p$K$_B$ values of 5.29 ± 0.13 ($n$=32) and 5.90 ± 0.15 ($n$=18) for noradrenaline- or ATP-mediated contractions, respectively. Vertical error bars are ± 2 S.E.M. of the difference between nonlinear regression-fitted $p$EC$_{50}$ values for cannabidiol and the $p$EC$_{50}$ values fitted for the individual vas deferens tissues at each concentration of cannabidiol (0-100 µM).

### 3.3.2 The effects of rimonabant on WIN 55,212-2-mediated inhibition of electrically evoked contractions of the rat vas deferens

The CB$_1$ antagonist rimonabant induced concentration-dependent dextral shifts of WIN 55,212-2 concentration-response curves mediated by both noradrenaline and ATP (Figure 3-5). In tissues contracted by noradrenaline, rimonabant 0.3, 3 and 10 µM caused a 20.1-, 118.6- and 179.1-fold dextral shift, respectively (Figure 3-5A; $P$<0.0001). Rimonabant 3 and 10 µM attenuated the ability of WIN 55,212-2 to induce near-complete inhibition of noradrenaline contractions, with R$_{max}$ values of 31 and 64%, respectively (Figure 3-5A, $P$≤0.005). Similar to cannabidiol, tissues contracted by ATP were more sensitive to the influence of rimonabant, where all concentrations of rimonabant (0.003-3 µM) inhibited WIN 55,212-2 concentration-response curves

(Figure 3-5B). Rimonabant at 0.3 and 3 µM caused a near-complete attenuation of WIN 55,212-2-induced inhibition of ATP contractile responses ($P$<0.05) and could therefore not be analysed in regard to curve shifts. Rimonabant 0.003 and 0.03 µM, however, induced 4.4- and 7.7-fold dextral shifts, respectively (Figure 3-5B; $P$<0.05).

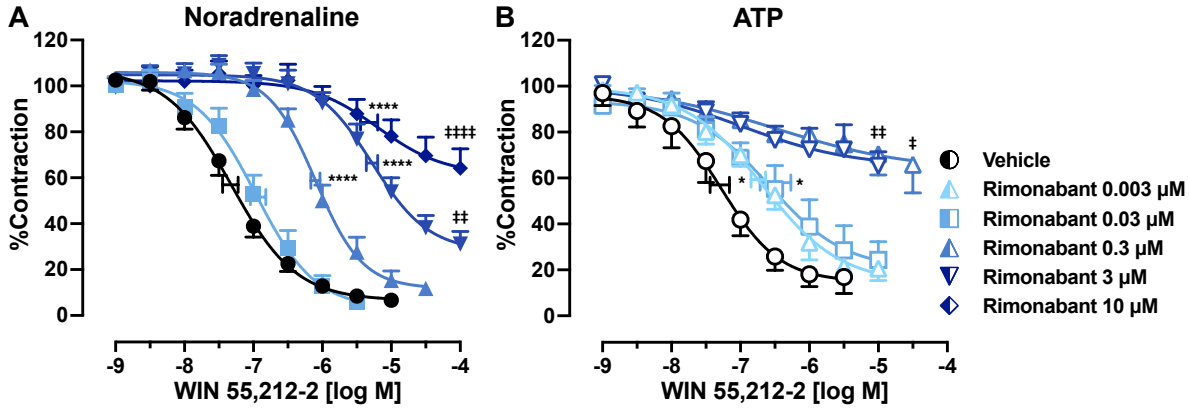


**Figure 3-5.** The effects of rimonabant (0.003-10 µM) or vehicle (DMSO 1%) on WIN 55,212-2-induced inhibition of electrically evoked contractions of rat vasa deferentia pretreated with either NF449 (10 µM; A) or prazosin (100 nM; B), favouring noradrenaline- or ATP-mediated contractions, respectively.
Responses are presented as a percentage (%) of the respective control contraction (in the absence of WIN 55,212-2, shown as C in Figure 3-2) in the presence of rimonabant (0.003-10 µM) or vehicle (DMSO 1%). Vertical error bars are ± S.E.M. (those not shown are contained within the symbol) and horizontal error bars represent the $EC_{50}$ ± S.E.M. *$P$≤0.05 or ****$P$≤0.0001 $EC_{50}$ compared with respective vehicle group $EC_{50}$. ‡$P$≤0.05, ‡‡$P$≤0.01 or ‡‡‡‡$P$≤0.0001 compared with the corresponding vehicle group maximal inhibition of contraction ($R_{max}$); repeated measures one-way ANOVA with Dunnett *post hoc* test. $n$=5-9 (panel A) and $n$=4-5 (panel B), from separate rats, per treatment group.

### 3.3.2.1 Determination of rimonabant $CB_1$ receptor potency

Global regression analysis of rimonabant $pEC_{50}$ values resulted in $pK_B$ estimates of 7.67 ± 0.12 ($n$=25) and 8.39 ± 0.32 ($n$=13), in tissues contracted with noradrenaline and ATP, respectively (Figure 3-6). Similar to cannabidiol, rimonabant was 5.3 times more potent at inhibiting ATP-mediated contractions than contractions mediated by noradrenaline ($P$=0.015).

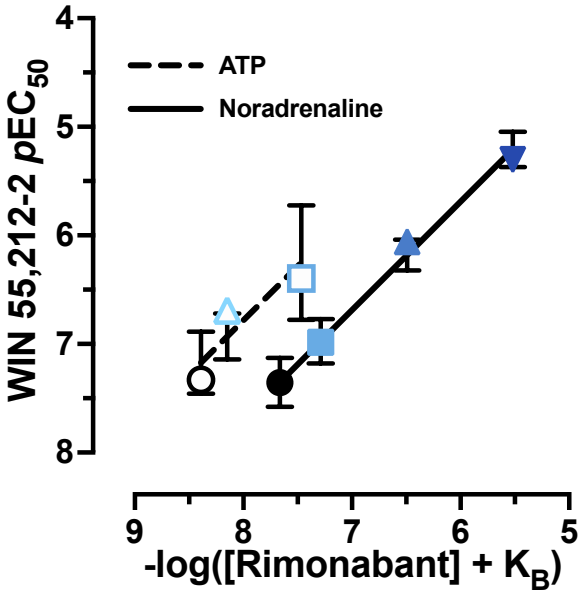


**Figure 3-6.** The Clark plot displays the interaction between increasing concentrations of rimonabant and WIN 55,212-2 $pEC_{50}$ values (from Figure 3-5A, noradrenaline, filled symbols and solid line, and Figure 3-5B, ATP, empty symbols and dashed line).
Symbols reflect the rimonabant concentrations shown in Figure 3-5. Cannabidiol $pK_B$ estimates can be derived from the control point (when [cannabidiol]=0; circle symbol) resulting in $pK_B$ values of 7.67 ± 0.12 ($n$=25) and 8.39 ± 0.32 ($n$=13) for noradrenaline- or ATP-mediated contractions, respectively. Vertical error bars are ± 2 S.E.M. of the difference between nonlinear regression-fitted $pEC_{50}$ values for rimonabant and the $pEC_{50}$ values fitted for the individual vas deferens tissues at each concentration of rimonabant (0-3 μM). WIN 55,212-2 concentration-response curves became very shallow with rimonabant >3 μM for noradrenaline-mediated contractions (Figure 3-5A), and >0.03 μM for ATP-mediated contractions (Figure 3-5B), and $pEC_{50}$ values were not able to be calculated for all tissues, so values were not used in the Clark plot and $pK_B$ analyses.

### 3.3.3 A comparison of cannabinoid responses between tissues with noradrenaline- and ATP-mediated contractions

There was no difference between the responses in the vehicle-treated group to WIN 55,212-2 for tissues contracted with either noradrenaline or ATP (Figure 3-3; $pEC_{50}$ noradrenaline 7.36 ± 0.11 and ATP 7.33 ± 0.14, $P$=0.90; $R_{max}$ noradrenaline 0.1 ±0.0% and ATP 0.2 ± 0.1%, $P$=0.29, Figure 3-7A, B; control (C) noradrenaline 2.0 ± 0.3 g and ATP 1.2 ± 0.1 g, $P$=0.10). There were also no differences in control contractions before

addition of the various cannabinoid antagonist concentrations ($P$>0.05), with the exception of the group of noradrenaline-contracted tissues that were subsequently treated with cannabidiol 30 μM (Figure 3-8A, C; $P$=0.026). The pooled contractions of tissues pretreated with NF449 (10 μM; Figure 3-8A), favouring noradrenaline-mediated contractions, were 39% bigger than ATP-mediated contractions of tissues pre-incubated with prazosin (100 nM; Figure 3-8B; mean contraction noradrenaline 1.90 ± 0.15 g and ATP 1.37 ± 0.11 g; $P$=0.013).

The dextral shifts of WIN 55,212-2 concentration-response curves were accompanied by cannabidiol concentration-independent increases in electrically induced contractions, which were more pronounced in tissues where noradrenaline contractile responses were favoured (Figure 3-7A). In noradrenaline contracted tissues cannabidiol 10, 30 and 100 μM increased basal contractile responses by 56, 114 and 81%, respectively (Figure 3-8C), and in ATP contracted tissues cannabidiol 10 μM increased basal contractions by 56% (Figure 3-7B; $P$<0.05). The higher concentrations of cannabidiol 30 and 100 μM caused insignificant increases in basal ATP contractions of 48 and 29%, respectively (Figure 3-7B; $P$>0.05). Rimonabant 0.3 μM, but not the higher or lower concentrations ($P$>0.05), significantly increased control noradrenaline-mediated contractions by 75% compared to vehicle contractions (Figure 3-7C, $P$=0.014), while rimonabant (0.003-0.3 μM) had no effects on control ATP-mediated contractions (Figure 3-7D; $P$>0.05).

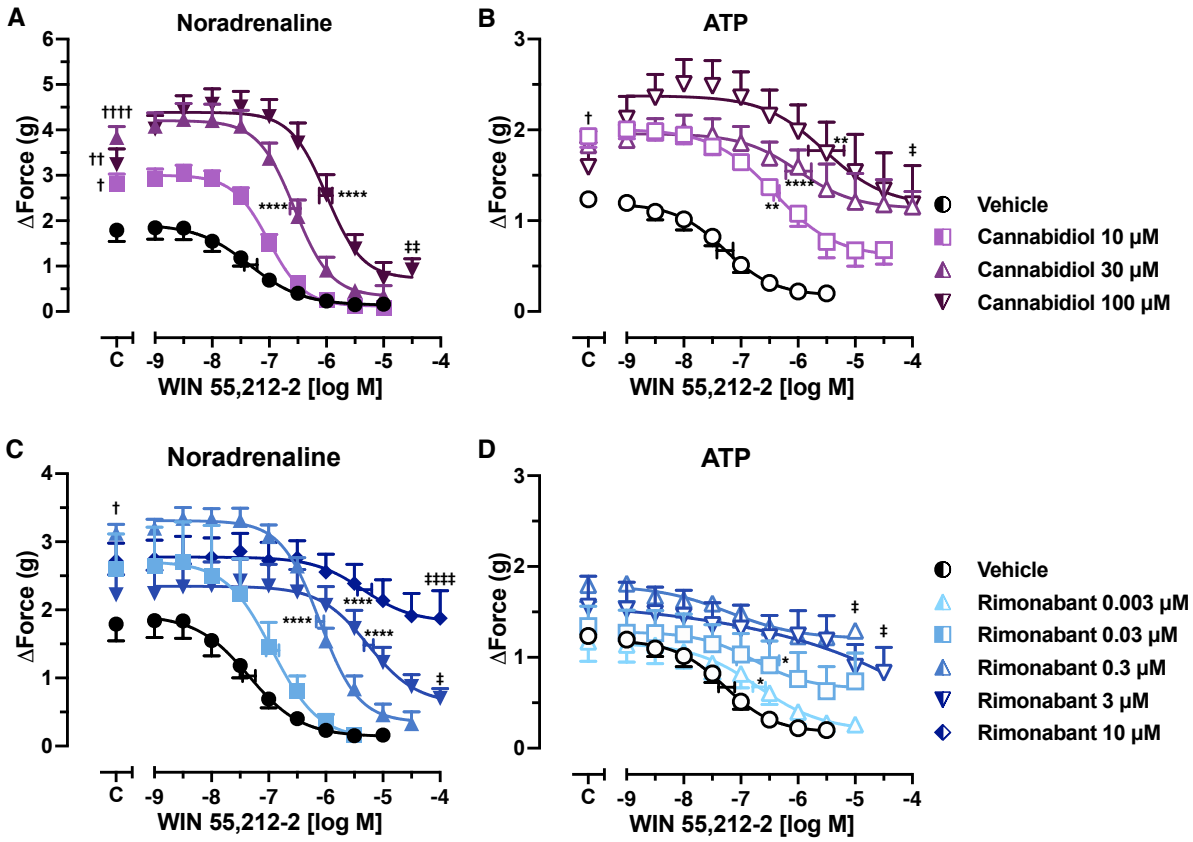


**Figure 3-7.** The absolute effects of cannabidiol (10-100 μM), rimonabant (0.003-10 μM) or vehicle (DMSO 1%) on WIN 55,212-2-induced inhibition of electrically evoked contractions of rat vasa deferentia pretreated with either NF449 (10 μM; A; C) or prazosin (100 nM; B, D), favouring noradrenaline- or ATP-mediated contractions, respectively.

Responses are the absolute force of contraction in grams (g) of the Figure 3-3 and Figure 3-5 data. Vertical error bars are ± S.E.M. (those not shown are contained within the symbol) and horizontal error bars represent the $EC_{50}$ ± S.E.M. *$P$≤0.05, **$P$≤0.01 or ****$P$≤0.0001, $EC_{50}$ compared with respective vehicle group $EC_{50}$. $^{\dagger}P$≤0.05, $^{\dagger\dagger}P$≤0.01 or $^{\dagger\dagger\dagger\dagger}P$≤0.0001 compared with respective vehicle group WIN 55,212-2 concentration-response curve. $^{\ddagger}P$≤0.05, $^{\ddagger\ddagger}P$≤0.01 or $^{\ddagger\ddagger\ddagger\ddagger}P$≤0.0001 compared with the corresponding vehicle group maximal inhibition of contraction ($R_{max}$); repeated measures one-way ANOVA with Dunnett *post hoc* test. $n$=7-9 (panel A), $n$=4-7 (panel B), $n$=5-9 (panel C) and $n$=4-5 (panel D), from separate rats, per treatment group.

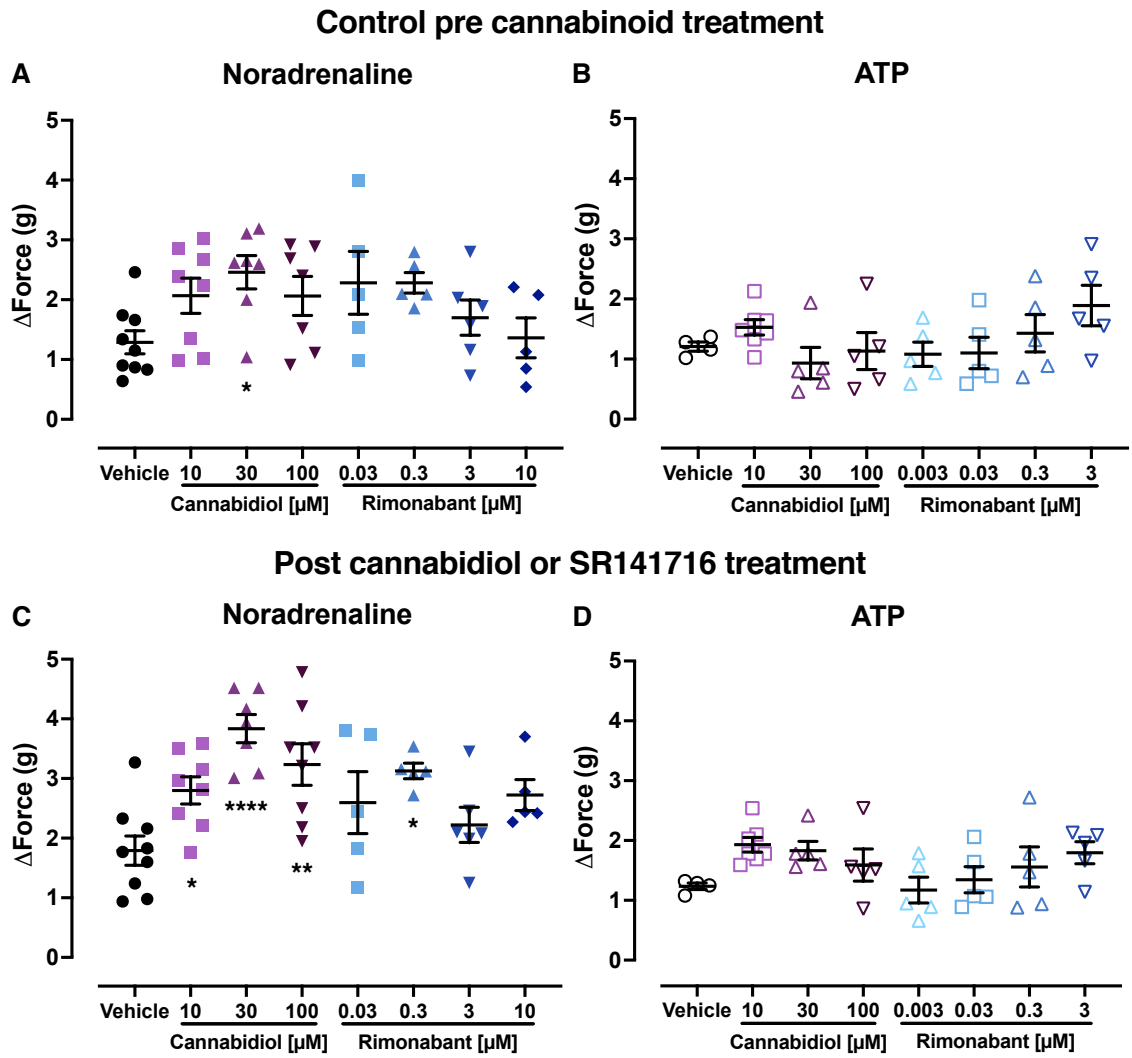


**Figure 3-8.** Individual electrically induced noradrenaline- or ATP-mediated contractions of vas deferens tissues in the presence of NF449 (10 μM; panels A and C) or prazosin (100 nM; panels B and D) prior to cannabinoid treatment (top panels) and after treatment with vehicle, cannabidiol (10-100 μM) or rimonabant (0.003-10 μM) (bottom panels; denoted with C in Figure 3-7).

Contractions are shown as change (Δ) in force (g). Lines with vertical error bars are mean ± S.E.M. **P*≤0.05, ***P*≤0.01 or *****P*≤0.0001 compared with respective vehicle group contractions; repeated measures one-way ANOVA with Dunnett *post hoc* test. *n*=4-9, from separate rats, per treatment group.

### 3.3.4 Lack of influence of endogenous anandamide tone on CB1 receptors in the vas deferens

Treatment of tissues with the FAAH inhibitor URB937 (0.0001-1 μM) did not affect the contraction of vasa deferentia compared to corresponding vehicle concentrations for

either noradrenaline- or ATP-mediated contractions, indicating the absence of endogenous anandamide tone (Figure 3-9; $P>0.05$). For noradrenaline-mediated contractions in the time control group, there were significant increases in force over the 240 min experimental time period ($P=0.004$; Figure 3-9), while this was not observed in the ATP time control group ($P=0.52$). In the noradrenaline groups treated with either vehicle (DMSO) or URB937, there were also increases in contractile force with increasing concentrations ($P<0.0005$ each; Figure 3-9). However, the latter increases were only significantly greater than corresponding values in the noradrenaline time control group for the tissues treated with URB937 0.3 and 1 μM ($P=0.035$). This is unlikely to be a true effect of URB937 as these data completely overlapped those in the DMSO-treated tissues (Figure 3-9).

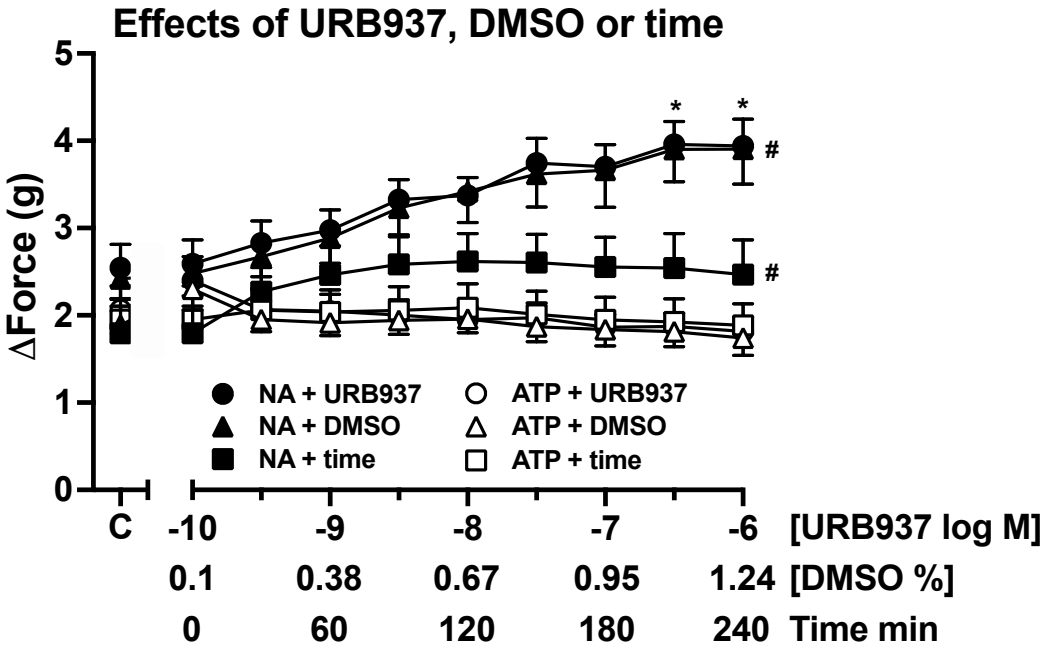


**Figure 3-9.** The effects of URB937 (0.0001-1 μM), corresponding vehicle concentrations (DMSO 0.1-1.24%) or equivalent time controls (no drug or vehicle addition, 0-240 min) on noradrenaline- (NA; closed symbols) or ATP-mediated (open symbols) contractions of electrically stimulated vasa deferentia.
C, contractions before addition of either URB937 or DMSO, or further time. Error bars are ± S.E.M. $^{*}P\leq0.05$, noradrenaline + URB937 values compared with respective noradrenaline time control values; repeated measures two-way ANOVA with Dunnett *post hoc* test. $^{\#}P\leq0.005$, noradrenaline + URB937, noradrenaline + DMSO or noradrenaline + time over treatment protocol within group; repeated measures one-way ANOVA. $n=5$, from separate rats, per treatment group.

## 3.4 Discussion

Most studies to date have assessed the $CB_1$ receptor affinity of cannabidiol using membrane binding preparations from human, rat or mouse brain. Cannabidiol competitive antagonism of $CB_1$ agonists in intact tissue bioassays is limited to two studies utilising the mouse vas deferens (Table 1; Pertwee *et al.*, 2002; Thomas *et al.*, 2004).To our knowledge, this is the first study to use a rat bioassay to examine the $CB_1$ receptor antagonist potency of cannabidiol. Furthermore, we assessed whether the antagonist potency estimations of cannabidiol and rimonabant were dependent on the neurotransmitter mediating the contractions of the rat vas deferens.

### 3.4.1 $CB_1$ receptor potencies of cannabidiol and rimonabant in the rat vas deferens

The current study confirmed that both cannabidiol and rimonabant concentration-dependently attenuated WIN 55,212-2-mediated inhibition of a single pulse electrically induced contraction of rat vasa deferentia, in conditions selecting only noradrenaline- or ATP-mediated contractions. The effects of the lower concentrations of cannabidiol (3-30 μM) are most likely mediated through prejunctional sites, given that contractions of rat vasa deferentia to exogenous noradrenaline were only suppressed in the presence of cannabidiol 100 μM, but not 30 μM (Mazeh *et al.*, 2021). In contrast, in mouse vas deferens tissues cannabidiol 10 μM attenuated contractions to both methoxamine and phenylephrine (Pertwee *et al.*, 2002). Due to previous observation of cannabidiol's effects on exogenous noradrenaline (Mazeh *et al.*, 2021), we assume that the inhibitory effects of a high cannabidiol concentration of 100 μM against WIN 55,212-2-mediated attenuation of contraction were underestimated. In preliminary experiments we found it difficult to investigate the effects of cannabidiol on exogenous ATP–mediated contractions as the contraction faded rapidly. However, we theorise that the effects of cannabidiol would mirror that of exogenous noradrenaline. Hence, very high concentrations of cannabidiol (≥100 μM) are likely to act on other sites than those mediating the contractions to the neurotransmitter noradrenaline.

Lower concentrations of cannabidiol and rimonabant caused parallel and surmountable dextral shifts of WIN 55,212-2 concentration-response curves which are in agreement with competitive antagonism (Kenakin, 2014). The nature of the antagonism was investigated in global regression analysis (Lew & Angus, 1995). According to the analysis, cannabidiol behaved as a competitive surmountable antagonist of WIN 55,212-2, with a $pK_B$ value of 5.29 ± 0.13 and 5.90 ± 0.15 for noradrenaline- (cannabidiol 10-100 μM) and ATP- (cannabidiol 10-30 μM) contracted tissues, respectively (Table 3-1). We found that the antagonist potency ($p$K$_B$) of cannabidiol matched its literature reported binding affinity at the CB$_1$ receptor (Rosenthaler *et al.*, 2014). This is in contrast to earlier findings where the reported potency of cannabidiol, with WIN 55,212-2 as the agonist, in the vas deferens bioassay was well above its affinity - 25.7-51.3-fold greater (Table 3-1; Pertwee *et al.*, 2002; Thomas *et al.*, 2004). Cannabidiol 10-100 μM increased control noradrenaline-mediated contractions. In contrast, only the lower concentration of cannabidiol (10 μM) increased control ATP-mediated contractions, which may have been biased by the lower initial contractions (Figure 3-8B).

Rimonabant, unlike cannabidiol, had little effect on control contractions. Only rimonabant at 0.3 μM caused an increase of basal noradrenaline-mediated contractions (Figure 3-8C), neither higher nor lower concentrations of rimonabant had any effect on contractions (Figure 3-8). This is unlike previous reports, where rimonabant 0.03-3 μM induced significant increases in basal noradrenaline-mediated contractions of rat vas deferens (Christopoulos *et al.*, 2001). In the current study, rimonabant dextrally shifted concentration-response curves in a simple competitive manner, resulting in $p$K$_B$ values of 7.67 ±0.12 and 8.39 ± 0.32 in noradrenaline- and ATP-contracted tissues, respectively (Table 3-1; Figure 3-6). As with cannabidiol, the higher concentrations of rimonabant significantly inhibited the maximal response to WIN 55,212-2, an effect that was more pronounced when contractions were mediated by ATP (Figure 3-5). In contrast to cannabidiol, rimonabant potency estimations were in agreement with those previously reported in mouse and rat vas deferens (Table 3-1, $p$K$_B$ 7.5-8.9), matching the affinity of rimonabant at the CB$_1$ receptor ($p$K$_i$ 8.3-8.7) (Rinaldi-Carmona *et al.*, 1995; Rinaldi-Carmona *et al.*, 1994).

### 3.4.2 Characterisation of the rat vas deferens bioassay for $CB_1$ receptor efficacy studies

Cannabidiol and rimonabant were 4.1- and 5.3-fold, respectively, more potent as competitive inhibitors of WIN 55,212-2 in ATP-contracted compared to noradrenaline-contracted vas deferens. Previous studies have shown that rimonabant inhibits ATP-mediated contractions of mouse vas deferens with a 13-fold greater potency than corresponding noradrenaline-mediated contractions in rat tissues (Christopoulos *et al.*, 2001; Lay *et al.*, 2000). These studies also reported that the potencies of $CB_1$ agonists WIN 55,212-2 and CP 55,940 were lower in rat tissues. The discrepancy in potency between the two studies has been ascribed to the difference in species, where rat tissues may have decreased ligand penetration into the thicker tissues, lower ligand affinity and possibly decreased stimulus-response coupling (Christopoulos *et al.*, 2001). Similarly, the potency estimates of cannabidiol in the current study were 10- to 162-fold lower than what has been previously reported in mouse vas deferens where contractions of tissues were likely predominantly mediated by ATP as the $P_2$ receptor antagonist PPADS almost completely abolished the electrically induced contractions (Table 3-1; Pertwee *et al.*, 2002; Thomas *et al.*, 2004). While it appears that potency estimates of cannabinoids in the vas deferens are highly species-dependent, our study has demonstrated that the responses to the $CB_1$ agonist WIN 55,212-2 were largely unaffected by the neurotransmitter mediating the contractions with similar potency values in each group ($pEC_{50}$ noradrenaline 7.36 and ATP 7.33).

The inhibition of noradrenaline-mediated contractions over time is likely to be underestimated due to the slow increase in contractions in vehicle-treated tissues (Figure 3-9). As mentioned, in tissues with ATP-mediated contractions both cannabidiol and rimonabant inhibited maximum responses to WIN 55,212-2 causing non-parallel dextral shifts of normalised concentration-response curves. While our study demonstrated that cannabidiol and rimonabant potencies are somewhat dependent on the neurotransmitter mediating the contractions of the vas deferens, the species from which the tissues were obtained seems to have a greater influence. Observations from the literature suggest that mouse tissues are more sensitive to the

influence of $CB_1$-active cannabinoids compared to rat tissues. However, it is important to emphasise that different stimulus protocols add further complexity.

The critical issue is whether the $pK_B$ for both cannabidiol and rimonabant is neurotransmitter-sensitive. Receptor theory would suggest that the $pK_B$ for these antagonists acting at the prejunctional $CB_1$ receptor should be independent of the downstream tissue mechanism. However, this assay is acutely dependent on non-equilibrium dynamics of transmitter release and peak tissue response.

Conservatively, as discussed above, we suggest there are several issues that could explain the small 4-5-fold increased potency of cannabidiol and rimonabant as $CB_1$ antagonists in ATP-mediated compared with noradrenaline-mediated contractions. That said, it is still possible that *in vivo* the prejunctional $CB_1$ receptor mediating inhibition of ATP release is significantly more affected by cannabidiol than for noradrenaline-mediated responses.

### 3.4.3 Are $CB_1$ receptors in the vas deferens under endogenous anandamide tone?

Cannabidiol- and rimonabant-induced potentiation of basal contractions in the absence of exogenous cannabinoid agonists can be explained either by inverse agonism, the influence of endogenous cannabinoid agonist tone or off-target potentiation of neurotransmitter release. It has been suggested that presynaptic $CB_1$ receptors are under endogenous tone (reviewed in Schlicker & Kathmann, 2001). This is based on the ability of the antagonist rimonabant to cause a significant increase in the amplitude of electrically induced contractions in various tissue preparations including rat vas deferens, mouse urinary bladder and guinea-pig myenteric plexus longitudinal muscle (Christopoulos *et al.*, 2001; Coutts & Pertwee, 1997; Pertwee, 2014; Pertwee & Fernando, 1996; Pertwee *et al.*, 1996a). Additionally, [$^3$H]-noradrenaline release as a result of basal electrical stimulation was 37% higher in vasa deferentia from $CB_1^{-/-}$ mice compared to $CB_1^{+/+}$ mice (Schlicker *et al.*, 2003). This finding indicates that $CB_1$ receptors are under endogenous tone. However, the current study was unable to support a role for

endogenous anandamide, as increasing concentrations of the FAAH inhibitor URB937 (0.0001-1 μM) had no additional effects to those of vehicle (Figure 3-9). Cannabidiol is likely to enhance the contractions of the vas deferens by acting at a $CB_1$ receptor-independent site to enhance electrically evoked release of both neurotransmitters noradrenaline and ATP. In contrast, a previous study in rat vas deferens found that incubation with the FAAH inhibitor phenylmethylsulphonyl fluoride (PMSF; 200 μM) significantly decreased the amplitude of basal contractions in rat vas deferens, indicating that anandamide is present (Christopoulos *et al.*, 2001). It is important to take into consideration that PMSF is a nonspecific inhibitor of a range of enzymes including proteases, esterases such as acetylcholinesterase, trypsins and the anandamide degrading enzyme FAAH (Deutsch & Chin, 1993; James, 1978; Moss & Fahrney, 1978). Since then, more specific FAAH inhibitors have been developed, including the peripherally acting URB937 (Clapper *et al.*, 2010). In contrast to the multi-target of PMSF, URB937 is selective to FAAH and has limited or no monoacylglycerol lipase activity, as it does not alter the tissue concentrations of the endocannabinoid 2-AG *in vivo* (IC50>100 μM; Clapper *et al.*, 2010). We have yet to investigate the involvement of the endocannabinoid 2-AG in the vas deferens responses.

The ability of rimonabant to induce an effect opposite to that of a $CB_1$ receptor agonist have been ascribed as further evidence for its inverse agonist properties (Christopoulos *et al.*, 2001). However, it would be an oversimplification to regard the cannabidiol- and rimonabant-induced increase of control contractions in the vas deferens as inverse agonism. Cannabidiol, which caused a greater increase in the amplitude of contractions, has generally not demonstrated inverse agonism in cell-based assays (reviewed in McPartland *et al.*, 2015). In contrast, rimonabant which has been proposed to be a $CB_1$ inverse agonist caused a mean decrease of $[^{35}S]GTP\gamma S$ activity of 36% (Breivogel *et al.*, 2001; reviewed in McPartland *et al.*, 2015; Thomas *et al.*, 2007). Hence, we suggest that the ability of cannabinoids to affect basal contractions in the vas deferens should not be used as a measure of inverse agonism. Cannabidiol is likely to enhance the contractions of the vas deferens by acting at a $CB_1$ receptor-independent site to enhance electrically evoked release of both neurotransmitters noradrenaline and ATP.

While a shift in either the $E_{max}$ or $E_{min}$ asymptote is not in agreement with competitive antagonism, in this study it is only observed at high cannabidiol concentrations which is likely due to loss of selectivity to the $CB_1$ receptors.

### 3.4.4 Conclusions

In conclusion, we have demonstrated that cannabidiol antagonises $CB_1$ receptor-mediated inhibition of contraction of the rat vas deferens in a manner consistent with simple competitive antagonism. The resulting potency of cannabidiol as a competitive antagonist of $CB_1$ agonists is consistent with its binding affinity at the $CB_1$ receptor. We have also established that cannabidiol-induced enhancements of basal contractions cannot be ascribed to endogenous anandamide tone on the $CB_1$ receptors. Rimonabant also behaved in a manner consistent with simple competitive antagonism with a potency that matched previous reports in both rat and mouse vas deferens. Furthermore, the estimated potencies of both cannabinoids were influenced to some degree by the neurotransmitter mediating the contractions of the vas deferens. ATP-mediated contractions were more sensitive to the influence of the cannabinoids. While we have not been able to explain this discrepancy, it is unlikely to involve postjunctional sites or any feedback mechanism as the difference is observed during a single electrical stimulation. A limitation of this study is that only one orthosteric $CB_1$ agonist was used when studying the effects of cannabidiol in the vas deferens assay. However, we theorise that the choice of orthosteric $CB_1$ agonist would not have affected the overall outcome of our global regression analysis.

The implications of this work suggest that when cannabidiol's plasma concentrations are raised above 1 μM consideration should be given to its $CB_1$ receptor antagonism especially at prejunctional neuronal sites that would lead to disinhibition of endogenous $CB_1$ modulation of neurotransmission in the central and peripheral nervous systems. Further, our findings suggest that this disinhibition by cannabidiol may be more sensitive when ATP is the transmitter compared to adrenergic noradrenaline.

# Chapter 4

## The vascular effects of cannabidiol in rat isolated tissues

## 4.1 Introduction

To date, most studies investigating the vascular effects of cannabidiol have been performed in large conduit arteries using a high cannabidiol concentration of 10 μM (section 4.1.3, Table 4-1, Table 4-2). We sought to characterise the effects of cannabidiol in small resistance arteries at clinically relevant concentrations (0.3-3 μM; section 1.5.3.5; Table 1-1) as it is well-established that smaller arteries (<300 μm internal diameter, i.d.) are the main contributors to peripheral vascular resistance and subsequent blood pressure regulation (section 4.1.1.1). We posed the question: does the size of arteries influence the effects of cannabidiol?

### 4.1.1 Sometimes size does matter

The vascular circulation is categorised into the systemic and pulmonary circulation (reviewed in Gao, 2017). In the systemic circulation, arteries flow blood from the heart to peripheral tissues while veins return blood from the peripheral tissues back to the heart. Arteries and veins are connected by capillaries whose main role is to enable the delivery of oxygen, nutrients and signal molecules to peripheral tissue cells, while the veins carry cell-produced carbon dioxide, metabolic wastes and signal molecules. The vessels in the different circuits range greatly in size and function. In rats, arteries range from the internal diameter of 3 mm (e.g. aorta) to 7 μm (e.g. capillaries; Mulvany & Halpern, 1977). The different arteries have structures to support their different roles in the cardiovascular system. Arteries generally consist of three layers: the tunica intima, the tunica media and the tunica adventitia (Gao, 2017). The innermost layer, tunica intima, is mainly made of one layer of endothelial cells. The middle layer, tunica media, is made of a combination of smooth muscle cells, elastin and collagen filaments. The outermost layer, tunica adventitia, is generally made of dense fibroelastic tissue which provides arteries with structural stability. The composition and thickness of each layer vary between vessel types (Gao, 2017).

#### 4.1.1.1 Vascular structural differences: small resistance versus large conduit arteries

Arteries can be classified based on the composition of the tunica media. Large conduit arteries, e.g. aorta and carotid arteries, have dense elastic lamella and are therefore also referred to as elastic arteries, while smaller resistance arteries closer to the periphery have a tunica media that is instead dominated by smooth muscle cells.

##### 4.1.1.1.1 Small resistance arteries

The main role of resistance arteries is to provide the connected capillaries with the correct amount of blood at the right pressure (Mulvany & Aalkjaer, 1990). The smooth muscle-rich media tunica of smaller arteries makes them well-equipped for this purpose, by allowing arteries to dilate and contract to modulate the flow and pressure of blood entering the capillaries. Resistance arteries are made up of arterioles (<30-60 μm i.d.) which are arteries closest to capillaries and the small arteries proximal to arterioles. Due to the difficulties associated with performing experiments on very small arteries, usually, the small arteries proximal to the arterioles are used to model the influence of resistance arteries. Small arteries (~100 μm i.d.) contribute significantly to the overall peripheral resistance in vascular beds from various species (reviewed in Mulvany & Aalkjaer, 1990). More specifically, small arteries and arterioles share the peripheral resistance almost equally.

The adventitial layer of small arteries is made up of connective tissues which consist of a combination of elastin and collagen, fibroblasts, mast cells, macrophages and sometimes some Schwann cells with nerve axons (Mulvany & Aalkjaer, 1990). It appears that most nerves in the small arteries are found in the adventitial layer without penetrating the media. In rat mesenteric and renal vascular beds, the nerve volume fraction increases with decreased vessel diameter (ranging from 1 to 3%). In comparison, larger arteries have a smaller volume ratio taken up by smooth muscle cells. The tunica media is bound to the luminal side of the artery by an internal elastic lamina (Mulvany & Aalkjaer, 1990). The number of smooth muscle cell layers in small arteries is proportional to the small artery diameter. There are approximately 6 layers of smooth

muscle cells in arteries with an inner diameter of 300 μm, and a monolayer of smooth muscle cells in arteries with inner diameter of 30-50 μm. Smooth muscle cells subsequently make up 70-85% of small artery wall volume. The innermost layer of the small artery cell wall, the tunica intima, is composed of a squamous structure of endothelial cells that continuously covers the lumen of arteries.

The ability of arteries to resist blood flow (R) is directly correlated to the viscosity of blood (η) and length (L) of the artery, while negatively correlated to the artery radius (r) as demonstrated by Poiseulle's law:

$$R \propto \frac{\eta L}{r^4} \qquad (2)$$

As the length of an artery and the viscosity of blood stays relatively constant, the diameter of a vessel is the main determinant of a vessel's ability to resist the blood flow.

#### 4.1.1.1.2 Large conduit arteries

Large conduit arteries are characterised by large lumens and a tunica media containing multiple layers of elastic laminae which facilitate their elastic properties where they can accept larger volumes of blood at high pressure. The aorta is the main conduit artery, and it consists of two segments: the thoracic and abdominal aorta. The thoracic aorta branches to the carotid artery which is another large conduit artery, while the abdominal aorta branches to the superior mesenteric artery (Liu, 2020). The elastic properties of conduit arteries allow them to buffer the pulsatile flow of blood pumped out of the heart, creating a near-continuous peripheral blood flow (Belz, 1995). The buffering property of large arteries is explained through the Windkessel effect. Windkessel translates in German to "air chamber" and they were originally used in old-fashioned fire hoses where fluid was collected in a reservoir before filling the hose which resulted in a continuous fluid flow from the hose which more efficiently could fight fires. Similarly, large arteries dilate in response to increased pressure during systole creating net storage of blood and will recoil as blood pressure falls during diastole and therefore discharging the remaining blood, hence creating a continuous flow.

### 4.1.2 Wire myography – a means of examining the vascular functions of arteries to drugs

Myography deals with the contractility of muscles (Danish Myo Technology A/S, 2020). Wire myography is the most common technique of studying the vascular functions of vessels. Up until the late 70s, vascular work was mainly performed on large conduit arteries or smaller arteries with internal diameters greater than 300 µm. The techniques at that time were limited and did not allow for studies in smaller arteries (<300 µm i.d.). This prompted Michael J. Mulvany and William Halpern to develop the wire myograph which allowed for the functional measurements of smaller arteries (Mulvany & Halpern, 1977). In their first study with the wire myograph, they successfully investigated the contractile properties of small arteries collected from spontaneously hypertensive rats (SHR) and the normotensive control Wistar Kyoto (WKY) rats. They showed that 3$^{rd}$ and 4$^{th}$ order mesenteric arteries (Figure 4-1) collected from SHR had a 34% greater contractility than arteries from WKY rats.

The *ex vivo* pharmacodynamics of isolated arteries is best studied under physiological conditions to better emulate their *in vivo* environment (Wright & Angus, 2000). Vessels are therefore incubated in Kreb's physiological salt solution (PSS) which has a similar composition to blood (Chapter 2). The PSS temperature is maintained at 37°C and kept carbogenated with 95% $O_2$ and 5% $CO_2$. Small resistance arteries are commonly dissected from the rat mesentery where they are identified as the 3$^{rd}$ and sometimes 4$^{th}$ order branches from the superior mesentery (Figure 4-1). To allow for the control and measurement of internal vessel diameters, vessels are mounted in the myograph between two stainless steel wires (40 µm i.d.) with are carefully fed through the lumen to limit damage to the endothelium. One of the wires is fixed to a force transducer that measures the changes in wall force while the other wire is attached to a micropositioner which allows the manual distancing of wires from each other and therefore also the passive stretching of a vessel. Once a vessel has been mounted on wires it is equilibrated in the PSS at 37°C for 30 min.

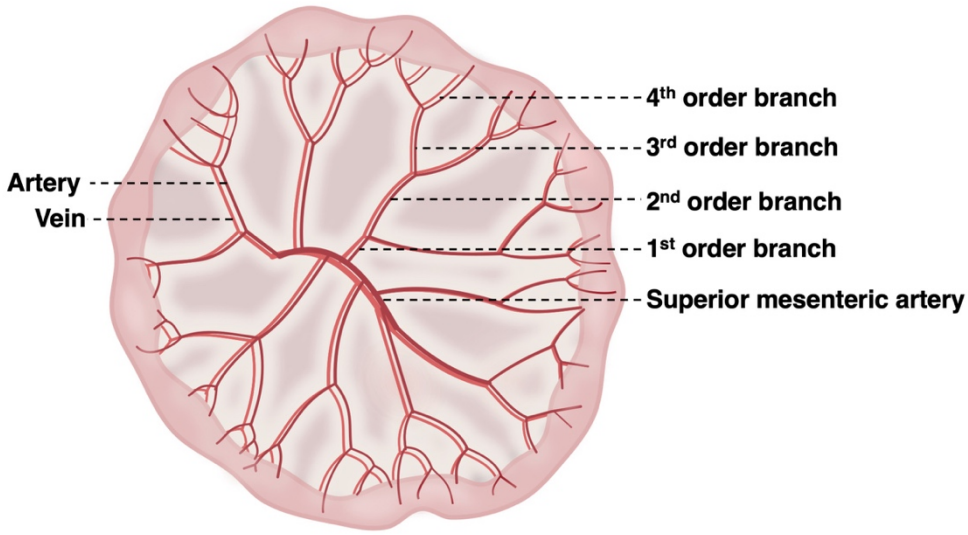


**Figure 4-1.** A schematic drawing of the isolated rat mesentery including the different vascular branch orders.

#### 4.1.2.1 Normalisation of vessels

Arteries are thereafter normalised to ensure standardised baseline experimental conditions for all vessels assessed in the wire myograph. By setting arteries to the same initial resting tension i) it increases reproducibility of data; ii) optimises vessel responses; iii) enables the calculation of vessel diameter; and iv) vessel viability can be evaluated (Danish Myo Technology A/S, 2020). There are various techniques for normalising an artery (Wright & Angus, 2000). Some laboratories will stretch vessels to a predetermined force that is readjusted to the same force if the vessel has lost its tone after a certain amount of time. However, to emulate *in vivo* conditions, vessels should be stretched in accordance with vessels' specific smooth muscle composition and function. Based on wire myograph studies performed in small mesenteric arteries, the optimal transmural wall pressure for small resistance arteries has been determined to be 100 mmHg (Mulvany & Halpern, 1977). The internal circumference of a vessel under a transmural pressure of 100 mmHg is referred to as the $IC_{100}$. The $IC_{100}$ is individually calculated for each vessel by measuring the increased wall tension generated by a vessel

at various internal circumferences which allows for the calculation of the corresponding transmural pressure by using Laplace's law:

$$\text{Transmural pressure} = \frac{\text{Wall tension}}{\text{Internal circumference}/(2 \times \pi)} \quad (3)$$

From Laplace's law, it is apparent that as the vessel internal circumference (in mm) increases the transmural pressure will decrease. Hence, under isometric conditions when the internal circumference is kept constant (as during myography experiments) an increase in wall tension (in mN) would increase the transmural pressure (in mN/mm). During the normalisation process, the internal circumference of a vessel is calculated by constructing a passive length/tension graph (Figure 4-2). As the internal circumference of the vessel is passively increased by adjusting the micropositioner attached to one of the wires in the vessel, a recording of the resulting wall tension is made. The stepwise increment of vessel internal circumference creates an exponential relationship with the resulting wall tension. An isobar (straight line) is added to the length/tension graph which correlates the internal circumference and wall tension of an artery at a specific transmural pressure according to Laplace's law (3). The internal circumference of an artery at a fixed transmural pressure, e.g. 100 mmHg for small resistance arteries, is indicated by the intersection of the isobar with the exponential length/tension curve. Conveniently, we can make $IC_{100}$ calculations through sophisticated data acquisition software (e.g. LabChart®) by manually inserting the micrometre changes that correlate to the passive artery stretches made. From the $IC_{100}$ values, the diameter of a vessel ($D_{100}$) is calculated by dividing the $IC_{100}$ value with the value of $\pi$. In our laboratory, arteries are relaxed to a circumference that equals $0.9IC_{100}$ as previous studies have shown that vessels slightly relaxed to 0.9 of $IC_{100}$ produce the greatest active tension (Mulvany & Halpern, 1977).

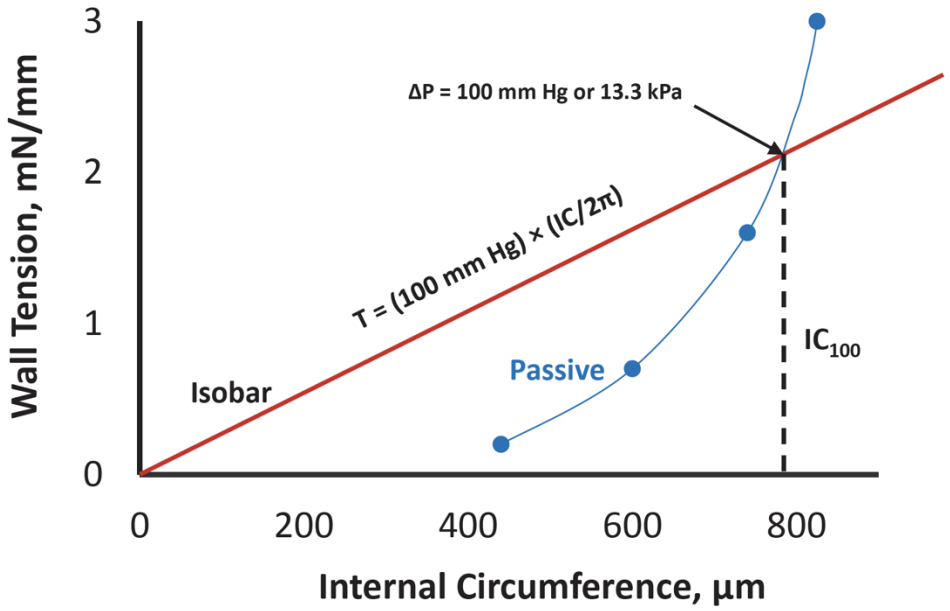


**Figure 4-2.** An example of an arbitrary passive-tension graph generated by Danish Myo Technology A/S (2020).
The blue symbols represent the resulting wall tension of a vessel being passively stretched by using the myograph micrometer. If it is assumed that the transmural pressure (ΔT) chosen is 100 mmHg, the LabChart® software will use the artery data to calculate the isobar formula (T=100 mmHg x (IC)/2π). The intersection of the isobar with the curved line connecting the blue symbols of the measured wall tension at each increased internal circumeference (IC) represents the calculated internal circumference of an artery with a transmural pressure of 100 mmHg ($IC_{100}$).

#### 4.1.2.2 Viability of vessels

Before commencing the experiment, the viability of a vessel is evaluated (Figure 4-3). Firstly the maximum active force is evaluated by exposing vessels to high noradrenaline concentration (10 µM) and depolarising solution termed KPSS (where $NA^+$ in PSS has been replaced by $K^+$, creating a 124 mM potassium solution). Prior to experimental protocols, arteries are also exposed to KPSS only to achieve a reference maximum contraction as all subsequent responses are expressed as %KPSS. To test the integrity of the endothelium, vessels are precontracted with noradrenaline to 80% of maximum KPSS contraction followed by the addition of the endothelium-dependent vasodilator agonist acetylcholine 1 µM. The extent of the relaxation is a strong indicator of a vessel's

nitric oxide-dependent vasorelaxant effects. In this study, arteries relaxed to >70% of precontraction are considered to have an intact endothelium.

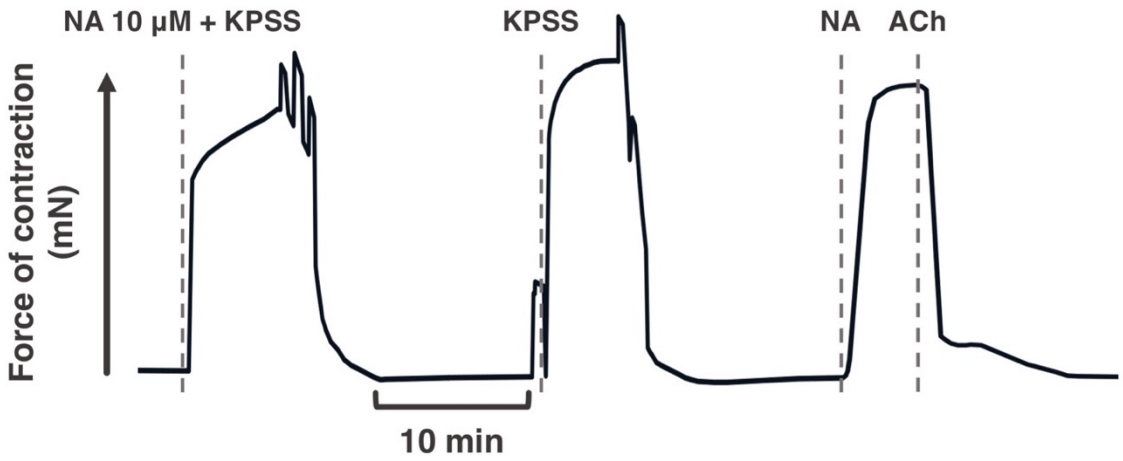


**Figure 4-3.** A LabChart® trace of a small mesenteric artery undergoing viability testing. The artery was first exposed to noradrenaline (NA) and high-potassium PSS (KPSS) followed by KPSS-only exposure 10 min later which will act as the reference maximal contraction for the subsequent experimental responses (expressed as %KPSS). To examine the integrity of the endothelium, the artery was sub-maximally contracted with noradrenaline and then exposed to acetylcholine (Ach 1 µM). The force of contraction is measured in mN.

### 4.1.3 Vascular effects of cannabidiol

In isolated arteries, cannabidiol either acutely relaxed precontracted arteries or potentiated the relaxation to acetylcholine and sodium nitroprusside (Table 4-1, Table 4-2). In aortae from healthy rats, cannabidiol 10 µM incubation for 2 h significantly enhanced vasorelaxation to acetylcholine (Stanley *et al.*, 2013b). In another study, cannabidiol 10 µM administration to precontracted aortae caused time-dependent relaxation (O'Sullivan *et al.*, 2009). While studies in small resistance arteries are limited, the vasorelaxation effects of cannabidiol appear to be more pronounced in smaller arteries compared to large conduit arteries. In rat isolated small mesenteric arteries precontracted with phenylephrine, acute cannabidiol administration caused maximum relaxation with a $pIC_{50}$ of 5.66 ± 0.06 (Baranowska-Kuczko *et al.*, 2020;

Offertaler *et al.*, 2003). This full relaxation of small mesenteric resistance arteries has also been reported for anandamide, while the larger superior mesenteric artery only relaxed by 40% (Randall *et al.*, 2004). In human isolated large pulmonary arteries precontracted with U46619, acute cannabidiol 10 μM did not cause relaxation. Further, in the same paper, in rat small mesenteric arteries (250 μm i.d.) pretreatment with cannabidiol 1 μM had no effect on phenylephrine concentration-response curves (Baranowska-Kuczko *et al.*, 2020).

Cannabidiol has a broad spectrum of actions at multiple targets over a wide range of concentrations (reviewed in McPartland *et al.*, 2015; section 1.6 ) which may explain the heterogeneity in the reports of the vascular targets of cannabidiol (Table 4-1, Table 4-2).

**Table 4-1.** Literature-reported *ex vivo* rat vascular effects and targets of cannabidiol under physiological conditions

| Rats | Vascular bed | [Cannabidiol] | Protocol | Effect | $CB_1$ | $CB_2$ | $G_{i/o}PCR$ | PPARγ | TRPV1 | NOS | SOD | De-endothelisation | Calcium | Reference |
|---|---|---|---|---|---|---|---|---|---|---|---|---|---|---|
| WKY | sMA | 0.1-30 µM | Precontracted with PE | $pEC_{50}$: 6.0 | ↔ | ↔ | | | ↔ | | | ↔ | | Baranowska-Kuczko *et al.* (2020) |
| DOCA-salt sham | sMA | 0.1-30 µM | Precontracted with PE | $pEC_{50}$: 5.5 | ↔ | ↔ | | | ↔ | | | ↔ | | Baranowska-Kuczko *et al.* (2020) |
| ZL | sMA | 10 mg/kg i.p.; for 7 days | Precontracted with MeOx Relax with ACh/nuding | ↔ | | | | | | | | | | Wheal *et al.* (2017) |
| ZL | sMA | 1 µM incubation for 2 h prior to exp | Precontracted with MeOx Relax with ACh | ↑$R_{max}$: +28% | | | | | | | | | | Stanley *et al.* (2013b) |
| SD | sMA | Not specified | Not specified | $R_{max}$: ~100% $pA_2$: 5.66 | | | | | | | | | | Offertaler *et al.* (2003) |
| – | perfused MVB | 10 µM | Precontracted with PE | ↔ | | | | | | | | | | Jarai *et al.* (1999) |
| ZL | FA | 10 mg/kg i.p.; for 7 days | Precontracted with MeOx Relaxation with ACh/SNP | ↔ | | | | | | | | | | Wheal *et al.* (2017) |
| ZL | FA | 10 µM incubation for 2 h prior to exp | Precontracted with MeOx ± U46619 Relaxation with ACh | ↑$R_{max}$: +15% ↔$pEC_{50}$ | ↔ | | | | | | | | | Wheal *et al.* (2014) |
| ZL | FA | 10 µM incubation for 2 h prior to exp | Precontracted with MeOx ± U46619 Relaxation with SNP | ↑$R_{max}$: +17% | | | | | | | | | | Wheal *et al.* (2014) |
| ZL | FA | 10 µM incubation for 2 h prior to exp | Precontracted with MeOx Relax with ACh | ↔ | | | | | | | | | | Stanley *et al.* (2013b) |
| ZL | Aorta | 10 mg/kg i.p.; for 7 days | Precontracted with MeOx | ↔ | | | | | | | | | | Wheal *et al.* (2017) |

| | | | | | | | | | | | | | |
|---|---|---|---|---|---|---|---|---|---|---|---|---|---|
| | | | Relax with ACh/SNP | | | | | | | | | | |
| ZL | Aorta | 1 μM incubation for 2 h prior to exp | Precontracted with U46619 Relax with ACh | ↔ | | | | | | | | | Stanley *et al.* (2013b) |
| ZL | Aorta | 10 μM incubation for 2 h prior to exp | Precontracted with U46619 Relax with ACh | ↔ | | | | | | | | | Stanley *et al.* (2013b) |
| Wistar | Aorta | 10 μM | Precontracted with MeOx + U46619 | ↑$R_{max}$: +43% (1 h) ↑$R_{max}$: +52% (2 h) | ↔ | ↔ | ↔ | ↑$R_{max}$: +27% (1 h) ↑$R_{max}$: +33% (2 h) | ↔ | ↔ | ⊣/↔ ↑$R_{max}$: +26% (1 h) | ↔ | ⊣ ↑$R_{max}$: +15% (1 h) ↑$R_{max}$: +9% (2 h) | O'Sullivan *et al.* (2009) |

**ACh**, acetylcholine; **$CB_1$**, cannabinoid receptor type 1; **$CB_2$**, cannabinoid receptor type 2; **$CB_e$**, endothelial cannabinoid receptor; **De-endothelisation**, rubbing off the endothelium of a vessel; **DOCA-salt**, deoxycorticosterone acetate and sodium chloride hypertensive rats; **CGRP**, calcitonin gene-related peptide; **COX**, cyclooxygenase; **FA**, femoral arteries; **$G_{i/o}$PCR**, $G_{i/o}$-protein-coupled receptor; **i.p.**, intraperitoneal; **MeOx**, methoxamine; **MVB**, mesenteric vascular bed; **NOS**, nitric oxide synthase; **PE**, phenylephrine; **PPARγ**, peroxisome proliferator-activated receptor-gamma; **PE**, phenylephrine; **SD**, Sprague-Dawley; **sMA**, small mesenteric arteries; **SNP**, sodium nitroprusside; **SOD**, superoxide dismutase; **TRPV1**, transient receptor potential vanilloid receptor 1; **U46619**, Thromboxane $A_2$ agonist; **ZL**, Zucker lean rats that are non-diabetic controls for Zucker diabetic fatty rats (ZDF); **WKY**, Wistar Kyoto rats; **↔**, no change; **↑**, increase compared to vehicle; **⊣**, attenuation of cannabidiol effect

**Table 4-2.** Literature-reported *ex vivo* rat vascular effects and targets of cannabidiol under non-physiological conditions

| Rats | Vascular bed | [Cannabidiol] | Protocol | Effect | $CB_1$ | $CB_2$ | $CB_e$ | FAAH | PPAR-γ | TRPV1 | COX | NOS | SOD | De-endothelisation | Reference |
|---|---|---|---|---|---|---|---|---|---|---|---|---|---|---|---|
| SHR | sMA | 0.1-30 μM | Precontracted with PE | $pEC_{50}$: 5.6 | ⊣ $pEC_{50}$: 5.1 | ↔ | | | | ↔ | | | | ↔ | Baranowska-Kuczko *et al.* (2020) |
| DOCA-salt | sMA | 0.1-30 μM | Precontracted with PE | $pEC_{50}$: 5.9 | ⊣ $pEC_{50}$: 5.3 | ⊣ $pEC_{50}$: 5.2 | | | | ↔ | | | | ⊣ $pEC_{50}$: 4.6 | Baranowska-Kuczko *et al.* (2020) |
| ZDF | sMA | 10 mg/kg i.p.; for 7 days | Precontracted with MeOx Relax with ACh | ↑$R_{max}$ ↑$pEC_{50}$ | | | | | | | ⊣ | ⊣ | | | Wheal *et al.* (2017) |
| ZDF | sMA | 10 mg/kg i.p.; for 7 days | Precontracted with MeOx Relax with SNP | ↔ | | | | | | | | | | | Wheal *et al.* (2017) |
| ZDF | sMA | 1 μM incubation for 2 h prior to exp | Precontracted with MeOx Relax with ACh | ↔ | | | | | | | | | | | Stanley *et al.* (2013b) |
| ZDF | FA | 10 mg/kg i.p.; for 7 days | Precontracted with MeOx Relax with ACh/SNP | ↔ | | | | | | | | | | | Wheal *et al.* (2017) |
| ZDF | FA | 10 μM incubation for 2 h prior to exp | Precontracted with MeOx ± U46619 Relax with ACh | ↑$R_{max}$: +19% ↔$pEC_{50}$ | ↔ | ⊣ | ↔ | ↔ | ↔ | | ⊣ | ↔ | ⊣ | ↔ | Wheal *et al.* (2014) |
| ZDF | FA | 10 μM incubation for 2 h prior to exp | Precontracted with MeOx ± U46619 Relax with SNP | ↔ | | | | | | | | | | | Wheal *et al.* (2014) |
| ZDF | FA | 10 μM incubation for 2 h prior to exp | Precontracted with MeOx ± U46619 Relax with HU308 | ↑$R_{max}$: +35% | | | | | | | | | | | Wheal *et al.* (2014) |
| ZDF | FA | 10 μM incubation for 2 h prior to exp | Precontracted with MeOx Relax with ACh | ↔ | | | | | | | | | | | Stanley *et al.* (2013b) |

| | | | | | |
|---|---|---|---|---|---|
| ZDF | Aorta | 10 mg/kg i.p.; for 7 days | Precontracted with MeOx Relax with ACh/SNP | ↔ | Wheal *et al.* (2017) |
| ZDF | Aorta | 1 μM incubation for 2 h prior to exp | Precontracted with U46619 Relax with ACh | ↑$R_{max}$: +26% | Stanley *et al.* (2013b) |
| ZDF | Aorta | 10 μM incubation for 2 h prior to exp | Precontracted with U46619 Relax with ACh | ↑$R_{max}$: +36% | Stanley *et al.* (2013b) |

**ACh**, acetylcholine; **$CB_1$**, cannabinoid receptor type 1; **$CB_2$**, cannabinoid receptor type 2; **$CB_e$**, endothelial cannabinoid receptor; **De-endothelisation**, rubbing off the endothelium of a vessel; **DOCA-salt sham**, normotensive control of deoxycorticosterone acetate and sodium chloride rats; **CGRP**, calcitonin gene-related peptide; **COX**, cyclooxygenase; **FA**, femoral arteries; **$G_{i/o}$PCR**, $G_{i/o}$-protein-coupled receptor; **i.p.**, intraperitoneal; **MeOx**, methoxamine; **NOS**, nitric oxide synthase; **PE**, phenylephrine; **PPARγ**, peroxisome proliferator-activated receptor-gamma; **PE**, phenylephrine; **SHR**, Spontaneously Hypertensive Rats; **sMA**, small mesenteric arteries; **SNP**, sodium nitroprusside; **SOD**, superoxide dismutase; **TRPV1**, transient receptor potential vanilloid receptor 1; **U46619**, Thromboxane $A_2$ agonist; **ZDF**, Zucker diabetic fatty rats; **↔**, no change; **↑**, increase compared to vehicle; **⊣**, attenuation of cannabidiol effect

### 4.1.4 Study aims

In the present work, we set out to quantify the actions of clinically used concentrations of cannabidiol (0.3-3 μM) on the effects of a wide range of contractile agents in rat isolated small resistance arteries and compare these with larger conduit arteries. We have also explored the mechanism of action of cannabidiol in small resistance arteries. Finally, we compared the vascular actions of cannabidiol with its actions on the contraction of various non-vascular tissues – bronchial, urogenital, cardiac and skeletal muscles.

## 4.2 Methods

### 4.2.1 Animals

The Animal Ethics Committee of the University of Melbourne approved experiments (approval #10246) in accordance with *The Australian Code for the care and use of animals for scientific purposes* (8th edition, 2013, National Health and Medical Research Council, Canberra). Male Sprague-Dawley rats (10-12 weeks old, Biomedical Animal Facility, Melbourne, Australia) were used in this study and housed in groups of 3-4 in standard cages under constant climatic conditions (21°C, 12 h light/dark cycle), with food and water *ad libitum*.

Rats (250-350 g) were deeply anaesthetised by inhalation of 5% isoflurane in 100% oxygen and killed by a rapid cut through the spinal cord. All experiments were performed in Krebs-Henseleit physiological salt solution (PSS) with the following composition (mM): NaCl 119, KCl 4.7, $KH_2PO_4$ 1.2, $NaHCO_3$ 25, $CaCl_2$ 2.5, EDTA 0.026, $MgSO_4$ 1.2 and glucose 5.5 for bronchi, mesenteric, saphenous and tail arteries and 11 for vasa deferentia, atria and hemidiaphragm. The PSS was oxygenated with carbogen (95% $O_2$ and 5% $CO_2$) at pH 7.4.

### 4.2.2 Isolated arteries

*Mesenteric arteries*: The abdomen was opened, the jejunum removed, and its attached vascular fan was pinned out on a Silastic-bottomed petri dish filled with oxygenated PSS. The superior mesenteric artery (i.d. 888 ± 95 µm) and third- or fourth-order mesenteric artery branches (i.d. 200-350 µm) were trimmed from attached tissue. *Saphenous arteries*: The muscle over the right hindlimb was exposed and fresh PSS was added while dissecting out large and small saphenous arteries. The saphenous arteries were isolated by dissecting out the left first-order large saphenous artery (i.d. 623 ± 18 µm) and the right second-order small saphenous artery (i.d. 288 ± 12 µm). *Tail arteries*: The tail was pinned dorsal side up on a Silastic-covered petri dish filled with PSS, the skin opened to expose the midventral artery (i.d. 923 ± 30 µm) which was carefully lifted and dissected out.

Small segments (2 mm long) of each artery type were mounted on 40 µm diameter stainless-steel wires connected to force transducers in myograph chambers (Model 610M and 620M; Danish Myo Technology, Aarhus Denmark). Responses were captured by a Powerlab (4/30 or 8/35) A/D converter (ADInstruments, Bella Vista, NSW, Australia) and measured on a Mac computer running LabChart 7 Pro data acquisition software (ADInstruments). After an equilibration period in PSS at 37°C, arteries were normalised by stepwise stretching, allowing for the calculation of the artery i.d. under an equivalent transmural pressure of 100 mmHg ($D_{100}$). The artery diameter was then partially decreased to $0.9D_{100}$, i.e. a transmural pressure equivalent to about 60 mmHg to allow for maximum contraction to develop when a contractile agent is applied (described in more detail by Angus & Wright, 2000). This passive force remained for the rest of the experiment. After a 30 min equilibration, artery viability was tested. Arteries were exposed to a potassium-rich depolarising solution (KCl replacing NaCl, termed KPSS) and noradrenaline 10 µM for 2 min before being washed with PSS. After 10 min (or until the contractile force was back to baseline), arteries were re-exposed to KPSS for 2 min to obtain the maximal contraction and then washed with PSS. All responses were expressed as a percentage of the KPSS response in each artery. After 10 min equilibration, the arteries were precontracted with noradrenaline to ~80% KPSS contraction, followed by the addition of acetylcholine 1 µM to test the integrity of the endothelium (only arteries that relaxed by >70% were used in experiments). The arteries were then washed with PSS and exposed to one of the following protocols.

### 4.2.3 Isolated artery protocols

#### 4.2.3.1 Concentration-response curves to different contractile agents

Cannabidiol (0.3, 1 and 3 µM; each dissolved in DMSO 0.1%) or vehicle (DMSO 0.1%) were added to the baths and equilibrated for 30 min, followed by cumulative additions of half-log increments of a contractile agent. We chose this cannabidiol pretreatment protocol rather than applying cannabidiol to a precontracted artery to allow 30 min incubation of a single concentration of cannabidiol. We also found that the lack of stability of precontracted small mesenteric arteries made this alternate latter protocol difficult to use. Large saphenous, mesenteric and tail arteries were exposed to the

contractile agonist methoxamine (0.01-100 μM), while small saphenous arteries were exposed to either methoxamine (0.01-300 μM) or 5-HT (0.01-10 μM). In small mesenteric arteries cumulative concentration-contraction responses to endothelin-1 (0.1-100 nM), arginine vasopressin (0.01-30 nM), U46619 (0.001-3 μM), methoxamine (0.01-100 μM), 5-HT (0.01-10 μM) or α-methyl-5-HT (0.01-10 μM) were constructed. Only a single concentration-response curve to an agent was constructed in each artery preparation. Separate arteries were incubated with CGRP (small mesenteric arteries 0.1-100 nM or superior mesenteric arteries 100 nM) or vehicle (MilliQ water) for 30 min, followed by cumulative additions of methoxamine (0.01-100 μM).

#### 4.2.3.2 Potential mechanism of action of cannabidiol

To explore the mechanism of action of cannabidiol, small mesenteric arteries were equilibrated with one of the following treatments for 30 min (except B) (literature supporting the chosen treatment concentrations shown): (A) olcegepant 1 μM (CGRP receptor antagonist); (B) capsaicin 1 μM (transient receptor potential cation channel 1 (TRPV1) receptor desensitiser; arteries incubated for 1 h followed by a wash out of capsaicin); (C) L-NAME 100 μM (nitric oxide synthase (NOS) inhibitor); (D) indomethacin 3 μM (cyclooxygenase inhibitor); (E) combination of olcegepant 1 μM, L-NAME 100 μM and indomethacin 3 μM; (F) GW9662 1 μM (peroxisome proliferator-activated receptor γ (PPARγ) antagonist); (G) rimonabant 300 nM (cannabinoid receptor type 1 ($CB_1$) antagonist); (H) SR144528 30 nM ($CB_2$ receptor antagonist) (Abood *et al.*, 2019); or (I) O-1918 3 μM (inhibitor of endothelium-mediated vasorelaxation of cannabinoids). After treatment incubation, arteries were incubated with cannabidiol (1 or 3 μM) or vehicle (DMSO 0.1%) for 30 min and then a concentration-contraction curve was constructed with cumulative additions of either methoxamine or 5-HT (0.01-100 μM). Small saphenous arteries were equilibrated with olcegepant (1 μM) followed by the incubation of cannabidiol (3 μM) or vehicle (DMSO 0.1%) for 30 min and cumulative additions of 5-HT (0.01-30 μM). We chose to examine the mechanism of action of cannabidiol in detail against methoxamine as it is a selective $\alpha_1$-adrenoceptor agonist that mimics sympathetic vasomotor contraction and 5-HT as a

different vasoactive amine acting at mainly 5-$HT_{1A}$ receptors as a contractile agonist of small arteries.

The general involvement of the endothelium was tested by denuding the endothelium of small mesenteric arteries with a hair. The integrity of the smooth muscle contractions and the lack of acetylcholine-mediated vasorelaxation was tested after the denudation. Only arteries that maintained >80% of the previous KPSS contraction and <5% of acetylcholine-mediated relaxation were used.

#### 4.2.3.3 Potential role of calcium

To study the role of extracellular calcium, mesenteric arteries were washed with calcium-free PSS and allowed to equilibrate for 10 min. The intracellular calcium storage was depleted by repeatedly exposing the arteries to KCl (80 mM) or methoxamine (10 µM) for 5 min before washing the arteries with calcium-free PSS. This was followed by the incubation of arteries with cannabidiol (0.3, 1 and 3 µM), CGRP (100 nM) or vehicle (DMSO 0.1%) for 30 min. Arteries treated with cannabidiol or vehicle were thereafter incubated with either KCl (80 mM) or methoxamine (10 µM) for 5 min to induce the opening of calcium channels, and CGRP-treated arteries were incubated with methoxamine (10 µM) for 5 min, prior to construction of a $CaCl_2$ concentration-contraction curve (cumulative additions, 0.01-10 mM). One set of arteries were pretreated with olcegepant (1 µM) 30 min before cannabidiol (3 µM) or vehicle (DMSO 0.1%) incubation for additional 30 min and were then incubated with methoxamine (10 µM) for 5 min, prior to construction of a $CaCl_2$ concentration-contraction curve (cumulative additions, 0.01-10 mM).

To assess the involvement of L-type voltage-operated calcium channels, arteries were incubated in normal PSS with cannabidiol (0.3, 1 and 3 µM) or vehicle (DMSO 0.1%) for 30 min prior to the addition of KCl 20 mM and cumulative additions of the L-type voltage-operated calcium channel agonist Bay K8644 (0.1-300 nM).

### 4.2.4 Isolated non-vascular smooth muscle: bronchi and vasa deferentia

*Bronchi*: The left lung lobe was isolated and pinned on a Silastic-bottomed petri dish with oxygenated PSS, dorsal side up. The main bronchus was cut, exposing the opening of secondary bronchi; tissue surrounding the bronchi was removed and the ends of bronchi were lifted and separated from attached pulmonary arteries. Small segments of bronchi (2 mm in length) were mounted in myographs, as described above. After an equilibration period in PSS at 37°C, the bronchi were stretched to 1.5 mN, followed by a re-stretch 10 min later. After a 10 min equilibration of stretched bronchi, tissue viability was tested. The bronchi were exposed to KPSS and carbachol (100 µM) for 2 min, before being washed with PSS. All responses were expressed as % KPSS + carbachol (100 µM) maximum contraction in each tissue. Following the viability test, cannabidiol (10, 30 and 100 µM) or vehicle (DMSO 1%) was added to the baths and equilibrated for 1 h, followed by cumulative additions of half-log increments of carbachol (0.01-300 µM).

*Vasa deferentia*: The whole vasa deferentia were excised by pushing the testis up towards the abdomen and then cutting it loose from the epididymis towards the prostate end. It was pinned down to a Silastic-bottomed petri dish with oxygenated PSS, tied at either side with a silk thread and trimmed to an approximate length of 2 cm. The prostatic end was tied to a stainless-steel hook on a fixed acrylic organ bath leg, while the epididymal end was tied uppermost to a stainless-steel hook attached to a Grass FT03C isometric force transducer (Grass Instruments, Quincy, MA, USA) connected to a Powerlab 8/35 data acquisition system (ADInstruments). The organ bath leg was adjusted vertically with an attached micrometer (Mitutoyo Manufacturing Co., Kawasaki, Japan). The responses were measured on a computer running LabChart 7 Pro data acquisition software (ADInstruments). Tissues were suspended in 5 ml organ baths containing PSS oxygenated with 95% $O_2$ and 5% $CO_2$ at 37°C, stretched to 2 g force, washed and equilibrated for 30 min. The viability of the tissues was tested by exposing the tissues to noradrenaline (10 µM) for 2 min and then washed. After 10 min of equilibration, the tissues were incubated with either cannabidiol (30 and 100 µM) or vehicle (DMSO 1%) for 1 h, followed by cumulative additions of half-log increments of noradrenaline (0.01-300 µM).

### 4.2.5 Isolated cardiac muscle: left and right atria

The heart was isolated and placed in a Silastic-bottomed petri dish filled with oxygenated PSS. The atria were isolated, connective tissue removed and left and right atria separated. Metal hooks were placed on each side of the atrium. One side of the tissue was pierced with a stainless-steel hook attached to a Grass FT03C isometric force transducer connected to a bridge amplifier and a Powerlab 8/35data acquisition system (ADInstruments) while the other side was hooked to a fixed acrylic organ bath leg between two parallel platinum field electrodes. Atria were suspended in 25 ml organ baths containing PSS oxygenated with 95% $O_2$ and 5% $CO_2$ at 37°C. The tissues were stretched to 1 g force, followed by a re-stretch to 1 g after 10 min, followed by a wash. The left atrium rested between two punctate platinum electrodes to enable the delivery of a train of field pulses (0.5 Hz, 0.2 ms duration) by a Grass S88 stimulator via a Grass stimulus isolation unit (SIU5). This stimulus frequency was chosen to conserve cardiac tissue viability as it is a >1 mm thick muscle, requiring oxygenation by diffusion from the bathing solution. The voltage of the stimulation was gradually increased until the threshold voltage was reached, followed by a 150% increase in the threshold voltage. Both atria were equilibrated for 30 min before their viability was tested by exposing the tissues to isoprenaline (1 and 0.1 μM, left and right atria, respectively) for 2 min and then washed. All responses were expressed as % of the maximum isoprenaline response. Once responses returned to baseline, atria were incubated with either cannabidiol (10-100 μM) or vehicle (DMSO 1%) for 1 h, followed by cumulative additions of half-log increments of isoprenaline (0.01-1000 nM).

### 4.2.6 Isolated skeletal muscle: phrenic nerve-hemidiaphragm

The upper ribcage was removed caudally to the thymus exposing the phrenic nerves and their attachments to the diaphragm. The thymus ends of the nerves were tied with a silk thread and then cut free from attached connective tissues, ensuring remaining attachments to the diaphragm. The diaphragm with attached phrenic nerves was isolated from connective tissue and transferred to a Silastic-bottomed petri dish filled with oxygenated PSS. The diaphragm was bisected along the midline, creating two

separate hemidiaphragms with a centrally attached phrenic nerve. The proximal end of the tissue was tied to a stainless-steel hook attached to a Grass FT03C isometric force transducer connected to a Powerlab 8/35 data acquisition system, while the distal end was tied to a stainless-steel hook on a fixed acrylic organ bath leg. The phrenic nerve was threaded through a platinum electrode. The responses were measured on a computer running LabChart 7 Pro data acquisition software. Tissues were suspended in 15 ml organ baths containing PSS oxygenated with 95% $O_2$ and 5% $CO_2$ at 32°C. The tissues were stretched to 2 g force, followed by a re-stretch to 2 g after 10 min and equilibrated for 20 min. Trains of field pulses (4 V, 0.1 Hz, 0.2 ms duration) were delivered by a Grass S88 stimulator via a Grass stimulus isolation unit (SIU5) and increased to 150% of the voltage threshold (100%) of the individual tissue for 30 min before the tissues were incubated with a single addition of either cannabidiol 30 μM or DMSO (0.3%) for 2 h.

### 4.2.7 Data and statistical analysis

All data are expressed as the mean ± S.E.M. of *n* experiments (each tissue from a separate rat). Contractile responses in arteries are expressed as the percentage of the maximum reference contraction to KPSS (%KPSS) within each artery. The individual data points showing the correlation between artery internal diameter and the inhibition of contraction induced by cannabidiol (3 μM) are expressed as the % decrease in contraction compared to maximum contraction to KPSS, in each artery. Responses in bronchi and left atria are expressed as the % of the maximum response to KPSS + carbachol (100 μM) or isoprenaline (1 μM), respectively, within each tissue. Responses in the right atria are given as the % of the maximum tachycardia to isoprenaline (0.1 μM). Contractions of vasa deferentia or hemidiaphragms are given as the absolute increase in force from baseline tone.

Data were plotted and analysed using Prism 8 (GraphPad Software, La Jolla, CA, USA). Individual sigmoidal agonist concentration-response curves were fitted and the $pEC_{50}$ (–log of the concentration (M) of agonist required to elicit the half-maximal response, $EC_{50}$) and $R_{max}$ (maximum response) determined for each tissue. For comparison of

$pEC_{50}$ or $R_{max}$ values between >2 treatment groups, repeated measures one-way ANOVA with Dunnett's *post hoc* test for multiple pairwise comparisons was performed. Two groups were compared using a Student's unpaired *t*-test. Statistical significance was taken as $P<0.05$.

### 4.2.8 Drugs

Drugs used were: Acetylcholine bromide; 8-methyl-N-vanillyl-6-nonenamide (capsaicin); carbamoylcholine chloride (carbachol); GW9662 (2-chloro-5-nitro-N-phenylbenzamide); indomethacin; 5-hydroxytryptamine (5-HT) creatinine sulfate; (-)-isoproterenol (+)-bitartrate (isoprenaline); L-nitro arginine methyl ester (L-NAME); methoxamine hydrochloride; α-methyl-5-hydroxytryptamine maleate; (-)-noradrenaline bitartrate (all from Sigma-Aldrich, St Louis, MO, USA); (-)-cannabidiol; O-1918; rimonabant; SR144528; U46619 (all from Cayman Chemical, Ann Arbor, MI, USA); Arg8-vasopressin (AVP; Aviva Systems Biology, San Diego, CA, USA); calcitonin gene-related peptide (CGRP); endothelin-1 (Auspep, Melbourne, VIC, Australia); Bay K8644 (Bayer, Leverkusen, Germany); and BIBN 4096 (olcegepant; Tocris Bioscience, Bristol, UK). Cannabidiol, capsaicin, GW9662, O-1918, olcegepant, rimonabant, SR144528 and U46619 were dissolved in DMSO. The other drugs were dissolved in MilliQ water apart from indomethacin that was dissolved in 0.1 M $Na_2CO_3$ in addition to water. All aliquots were stored at -20°C as single-use $10^{-4}$-$10^{-1}$ M aliquots.

## 4.3 Results

### 4.3.1 Effects of cannabidiol on the contraction of small mesenteric arteries

Cannabidiol 3 μM inhibited the contraction of rat isolated small mesenteric arteries to each of the contractile agents tested (endothelin-1, arginine vasopressin, U46619, methoxamine, 5-HT and α-methyl-5-HT) with marked attenuation of the maximum response ($R_{max}$) to each agent (Figure 4-4 and Figure 4-5; Table 4-3). With endothelin-1, cannabidiol 3 μM caused a small 2.6-fold rightward shift in the agonist $pEC_{50}$ ($P$<0.05; Figure 4-4A) with a 55% decrease in $R_{max}$ ($P$<0.0001); lower cannabidiol concentrations of 0.3-1 μM had no effect. Qualitatively similar findings were observed with arginine vasopressin and U46619 (Figure 4-4B-C and Figure 4-5) where the agonist contraction curves were near flattened ($R_{max}$ -69% and -82% compared with the vehicle group, respectively; $P$<0.0001, Table 4-3) by incubation with cannabidiol 3 μM; $pEC_{50}$ values could not be determined in most tissues. Concentration-contraction response curves to 5-HT (Figure 4-5E and Figure 4-5) were already completely abolished by cannabidiol at 1 μM. In methoxamine- or α-methyl-5-HT-contracted arteries, cannabidiol 0.3, 1 and 3 μM caused a concentration-dependent rightward shift and collapse of the response curves (Figure 4-4D and F). Cannabidiol 0.3 μM pretreatment resulted in small 3.7-fold and 2.2-fold increases in methoxamine and α-methyl-5-HT $pEC_{50}$ values, respectively ($P$<0.05, Table 4-3), while cannabidiol 1 μM shifted methoxamine curves by 9.1-fold, all with no significant decrease in $R_{max}$; contraction curves to both agents were virtually abolished with cannabidiol 3 μM, similar to the other tested agents, except for endothelin-1 (Figure 4-4, Figure 4-5 and Table 4-3).

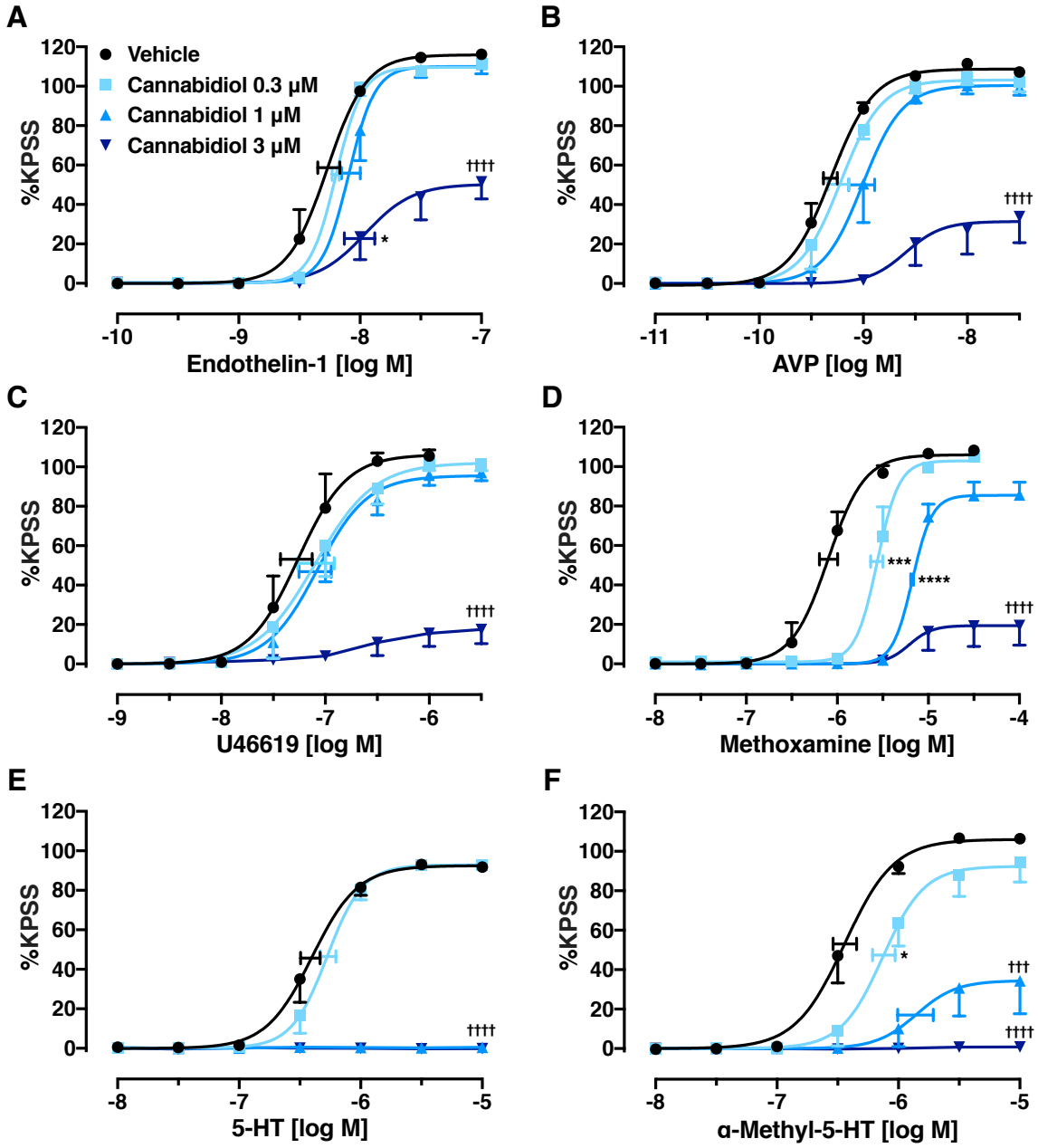


**Figure 4-4.** Effects of cannabidiol (0.3-3 µM) or vehicle (DMSO 0.1%) on concentration-contraction curves to different contractile agents in rat isolated mesenteric arteries.
A. endothelin-1; B. AVP (arginine vasopressin); C. U46619 (thromboxane mimetic); D. methoxamine; E. 5-HT (5-hydroxytryptamine); and F. α-methyl-5-HT. The responses are shown as % of the maximum contraction to KPSS within each artery ($n$=5-10, from separate rats, per treatment group). Vertical error bars are ± S.E.M.; horizontal error bars represent the $EC_{50}$ ± S.E.M. *$P$<0.05, ***$P$≤0.001 or ****$P$<0.0001 compared with respective vehicle-treated group $EC_{50}$. $^{\dagger\dagger\dagger}P$≤0.001 or $^{\dagger\dagger\dagger\dagger}P$<0.0001 compared with respective vehicle group $R_{max}$ (maximal contraction). Repeated measures one-way ANOVA with Dunnett *post hoc* test was performed, with the exception for 5-HT or α-methyl-5-HT $EC_{50}$ analysis, where Student's unpaired $t$-test was performed.

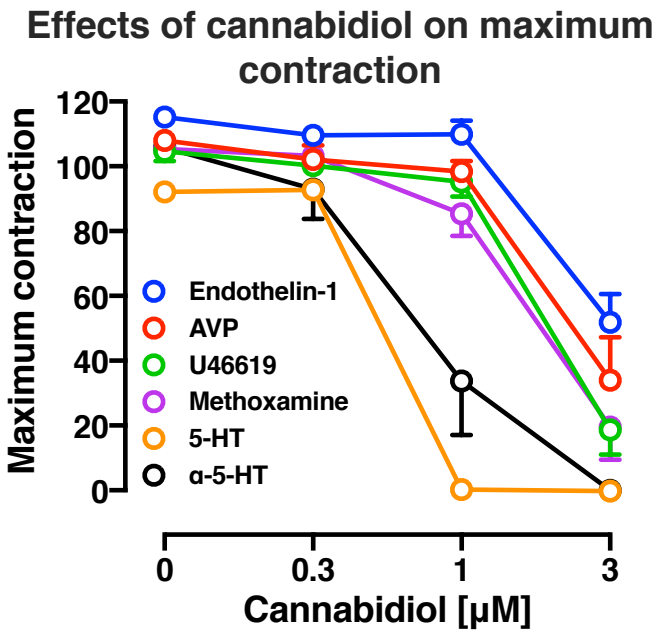


**Figure 4-5.** Reproduced maximum %KPSS from Figure 4-4 to different contractile agents in the presence of vehicle (DMSO 0.1%; 0 in the graph) and cannabidiol (0.3-3 μM).
The responses are shown as % of the maximum contraction to KPSS within each artery (*n*=5-10, from separate rats, per treatment group). Error bars are ± S.E.M.

**Table 4-3.** Effects of cannabidiol on sensitivity ($pEC_{50}$) and maximum response ($R_{max}$) to vascular contractile agents in mesenteric arteries

| | Cannabidiol pretreatment | | | |
|---|---|---|---|---|
| **Contractile agent** | **Vehicle** | **0.3 µM** | **1 µM** | **3 µM** |
| **Endothelin-1** | *n* = 5 | *n* = 5 | *n* = 6 | *n* = 6 |
| $pEC_{50}$ | 8.26 ± 0.09 | 8.20 ± 0.03 | 8.10 ± 0.08 | 7.84 ± 0.13[a] |
| $R_{max}$ (%) | 115 ± 3 | 110 ± 2 | 110 ± 4 | 52 ± 9[a] |
| **Vasopressin** | *n* = 5 | *n* = 5 | *n* = 5 | *n* = 5 |
| $pEC_{50}$ | 9.32 ± 0.07 | 9.24 ± 0.10 | 9.02 ± 0.13 | n.d. |
| $R_{max}$ (%) | 108 ± 1 | 102 ± 4 | 98 ± 3 | 34 ± 13[a] |
| **U46619** | *n* = 5 | *n* = 5 | *n* = 5 | *n* = 5 |
| $pEC_{50}$ | 7.27 ± 0.15 | 7.09 ± 0.18 | 7.08 ± 0.16 | n.d. |
| $R_{max}$ (%) | 105 ± 3 | 100 ± 3 | 95 ± 5 | 19 ± 8[a] |
| **Methoxamine** | *n* = 5 | *n* = 5 | *n* = 5 | *n* = 10 |
| $pEC_{50}$ | 6.13 ± 0.10 | 5.56 ± 0.07[a] | 5.17 ± 0.02[a] | n.d. |
| $R_{max}$ (%) | 105 ± 2 | 103 ± 1 | 85 ± 7 | 20 ± 10[a] |
| **5-HT** | *n* = 5 | *n* = 5 | *n* = 5 | *n* = 5 |
| $pEC_{50}$ | 6.39 ± 0.08 | 6.27 ± 0.06 | n.d. | n.d. |
| $R_{max}$ (%) | 92 ± 2 | 93 ± 2 | 0 ± 0[a] | 0 ± 0[a] |
| **α-Methyl-5-HT** | *n* = 5 | *n* = 7 | *n* = 7 | *n* = 5 |
| $pEC_{50}$ | 6.43 ± 0.10 | 6.08 ± 0.09[b] | n.d. | n.d. |
| $R_{max}$ (%) | 106 ± 2 | 93 ± 9 | 34 ± 17[a] | 0 ± 0[a] |

Values are mean ± S.E.M. of $pEC_{50}$ and Rmax from concentration-contraction response curves shown in Fig. 1. 5-HT, 5-hydroxytryptamine. [a]$P<0.05$ compared with respective values in the vehicle-treated group; repeated measures one-way ANOVA with Dunnett *post hoc* test. $P<0.05$ compared with the respective vehicle-treated group; Student's unpaired *t*-test. *n*, number of arteries, each from separate rats. n.d., not determined.

### 4.3.2 Potential mechanisms of action of cannabidiol in small mesenteric arteries

To investigate the potential mechanisms of action of cannabidiol, arteries were co-incubated with receptor and/or enzyme antagonists (Figure 4-6) prior to incubation with vehicle or cannabidiol followed by the construction of concentration-contraction

curves to methoxamine (Figure 4-7) or 5-HT (Figure 4-8). In the presence of any of the antagonists tested, the methoxamine or 5-HT $pEC_{50}$ and $R_{max}$ values of vehicle-treated arteries were comparable to the Control (no co-incubation with antagonist) vehicle group (Table 4-4; $P$>0.1, one-way ANOVA with Dunnett's *post hoc* test).

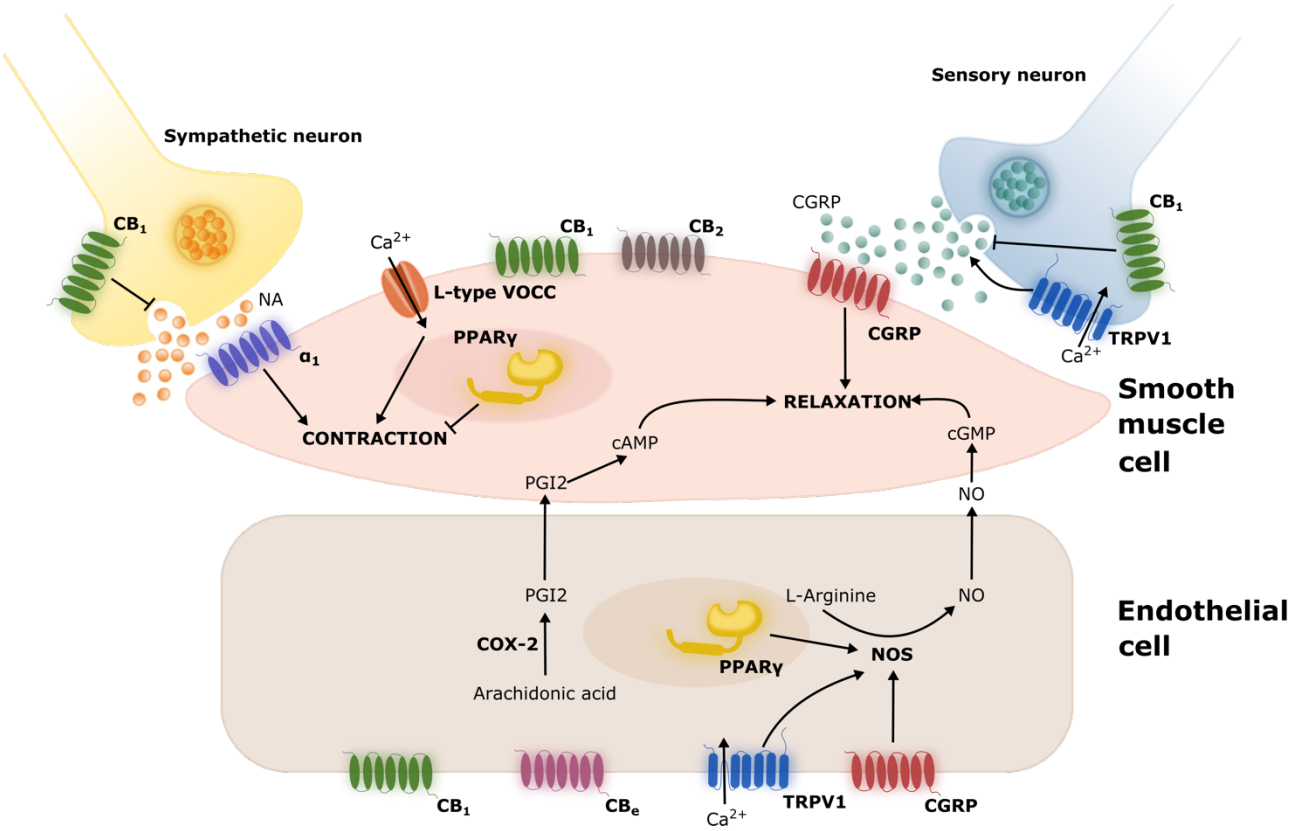


**Figure 4-6.** Schematic drawing of various potential vascular drug targets investigated in this project.
To study the mechanisms of action of cannabidiol in small resistance arteries the following receptors and enzymer were blocked: CGRP receptors, TRPV1 receptor, NOS, COX, PPARγ receptors, $CB_1$ receptors, $CB_2$ receptors and $CB_e$ receptors.

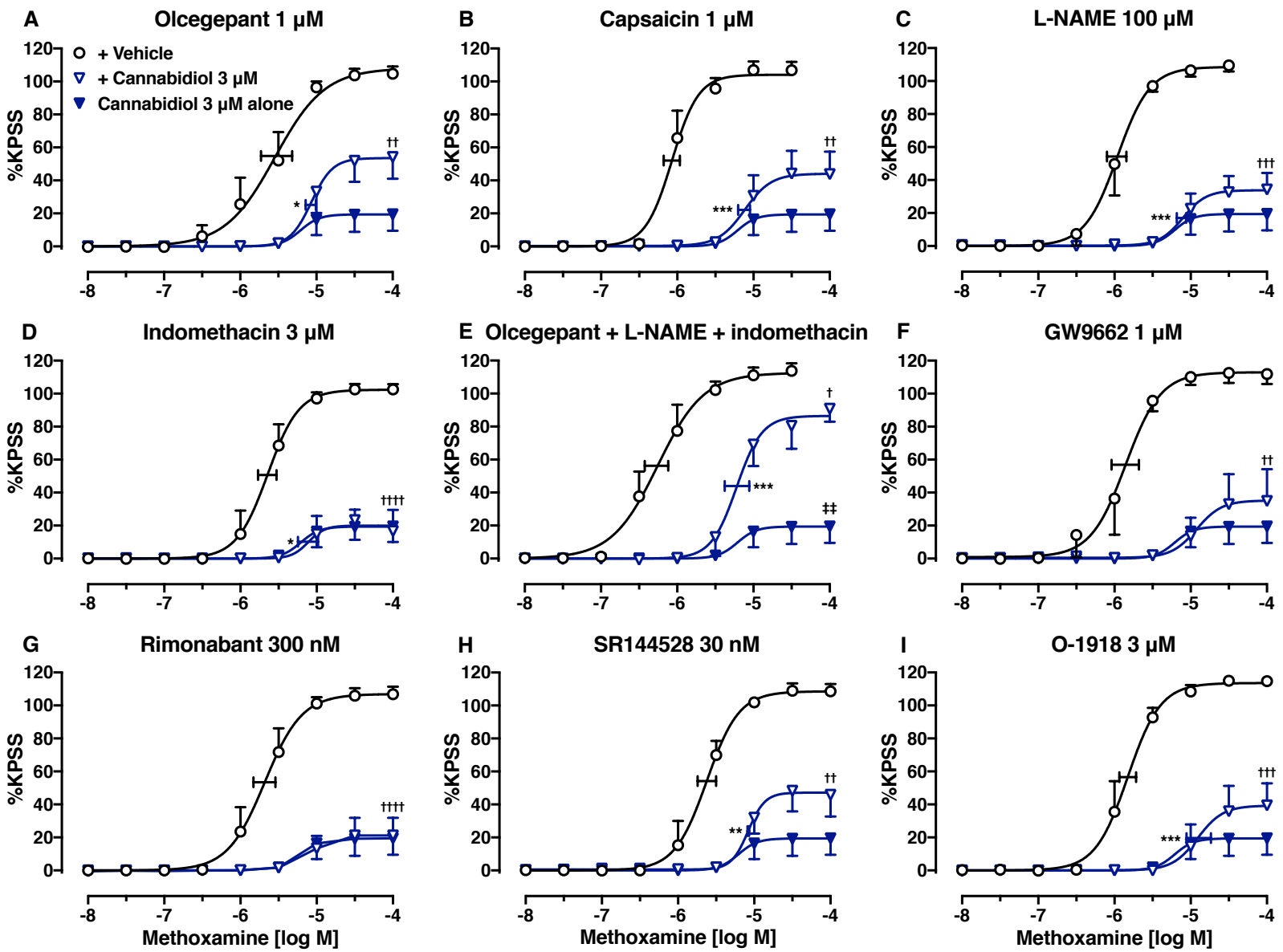
A
Olcegepant 1 μM
+ Vehicle
+ Cannabidiol 3 μM
Cannabidiol 3 μM alone
B
Capsaicin 1 μM
C
L-NAME 100 μM
D
Indomethacin 3 μM
E
Olcegepant + L-NAME + indomethacin
F
GW9662 1 μM
G
Rimonabant 300 nM
H
SR144528 30 nM
I
O-1918 3 μM
%KPSS
Methoxamine [log M]

**Figure 4-7.** Effects of cannabidiol (3 μM) or vehicle (DMSO 0.1%) on methoxamine concentration-contraction curves in rat isolated mesenteric arteries pretreated with various antagonists: A. olcegepant 1 μM; B. capsaicin 1 μM; C. L-NAME 100 μM; D. indomethacin 3 μM; E. a combination of olcegepant 1 μM, L-NAME 100 μM and indomethacin 3 μM; F. GW9662 1 μM; G. Rimonabant 300 nM; H. SR144528 30 nM; and I. O-1918 3 μM. Each antagonist, or combination (E), was added followed by a co-incubation with vehicle (DMSO 0.1%) or cannabidiol (3 μM) (open symbols). As a reference, the methoxamine contraction-response curve in the presence of cannabidiol alone (3 μM) from Figure 4-4D is plotted in each panel (filled symbols). The responses are shown as % of the maximum contraction to KPSS within each artery ($n$=5-7, from separate rats, per treatment group). Vertical error bars are ± S.E.M.; horizontal error bars represent the $EC_{50}$ ± S.E.M. *$P$<0.05, **$P$≤0.01 or ***$P$<0.001 compared with respective vehicle-treated group $EC_{50}$ and $^{\dagger\dagger}P$≤0.01, $^{\dagger\dagger\dagger}P$≤0.001 or $^{\dagger\dagger\dagger\dagger}P$<0.0001 compared with respective vehicle group $R_{max}$ (maximal contraction); Student's unpaired $t$-test (cannabidiol alone treatment group from Figure 4-4D was not included in this analysis). $^{\ddagger\ddagger}P$≤0.01 $R_{max}$ between cannabidiol-treated arteries in the presence and absence of combined antagonist pretreatment (E).

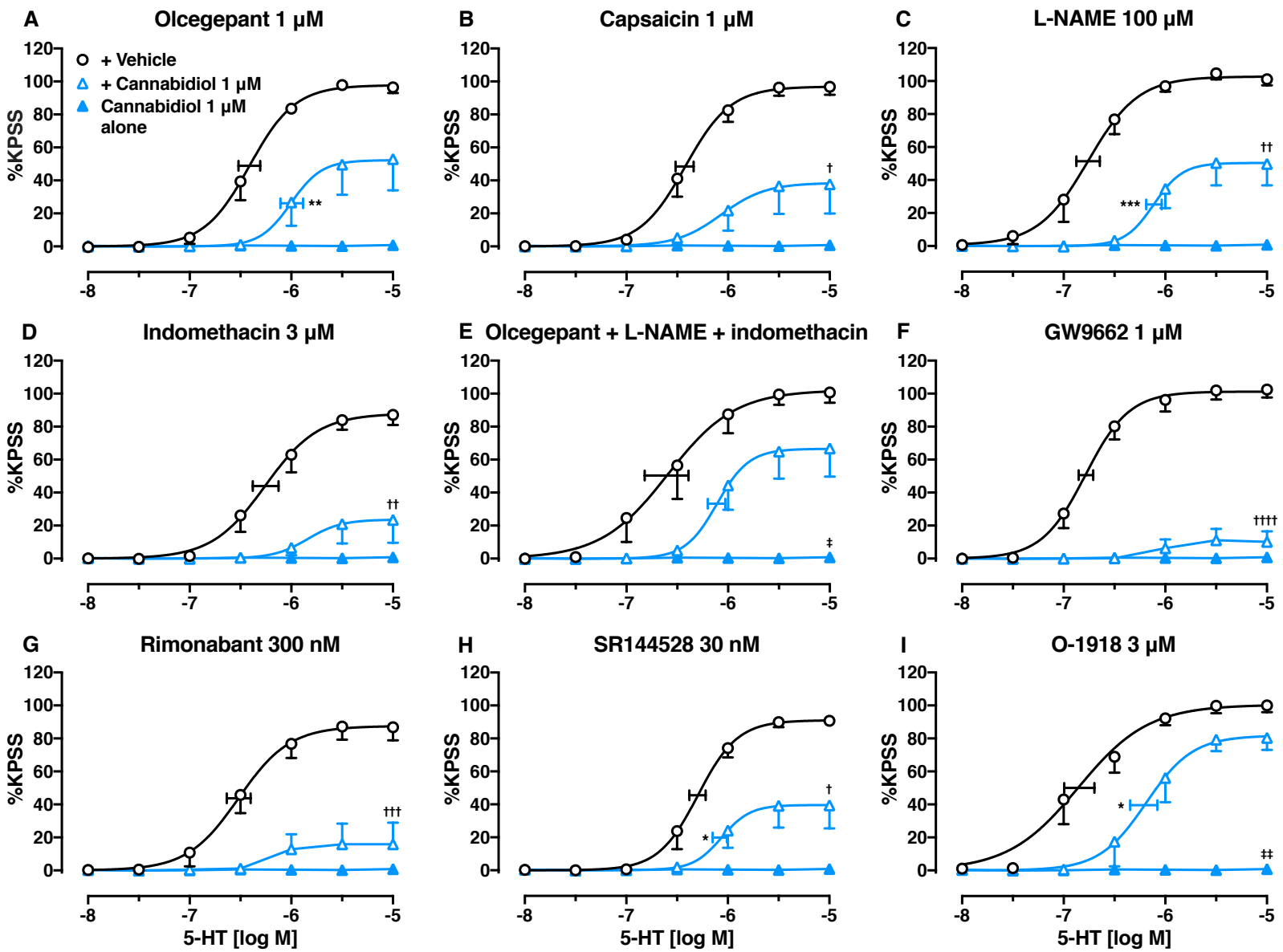
A
Olcegepant 1 μM
+ Vehicle
+ Cannabidiol 1 μM
Cannabidiol 1 μM alone
B
Capsaicin 1 μM
C
L-NAME 100 μM
D
Indomethacin 3 μM
E
Olcegepant + L-NAME + indomethacin
F
GW9662 1 μM
G
Rimonabant 300 nM
H
SR144528 30 nM
I
O-1918 3 μM
%KPSS
5-HT [log M]

**Figure 4-8.** Effects of cannabidiol (3 μM) or vehicle (DMSO 0.1%) on 5-HT concentration-contraction curves in rat isolated mesenteric arteries pretreated with various antagonists: A. olcegepant 1 μM; B. capsaicin 1 μM; C. L-NAME 100 μM; D. indomethacin 3 μM; E. a combination of olcegepant 1 μM, L-NAME 100 μM and indomethacin 3 μM; F. GW9662 1 μM; G. Rimonabant 300 nM; H. SR144528 30 nM; and I. O-1918 3 μM. Each antagonist, or combination (E), was added followed by a co-incubation with vehicle (DMSO 0.1%) or cannabidiol (1 μM) (open symbols). As a reference, the 5-HT contraction-response curve in the presence of cannabidiol alone (1 μM) from Figure 4-4E is plotted in each panel (filled symbols). The responses are shown as % of the maximum contraction to KPSS within each artery ($n$=4-7, from separate rats, per treatment group). Vertical error bars are ±S.E.M.; horizontal error bars represent the $EC_{50}$ ± S.E.M. *$P$<0.05, **$P$≤0.01 or ***$P$<0.001 compared with respective vehicle-treated group $EC_{50}$ and $^{\dagger}P$<0.05, $^{\dagger\dagger}P$≤0.01, $^{\dagger\dagger\dagger}P$≤0.001 or $^{\dagger\dagger\dagger\dagger}P$<0.0001 compared with respective vehicle group $R_{max}$ (maximal contraction); Student's unpaired $t$-test (cannabidiol alone treatment group from Figure 4-4E was not included in this analysis). $^{\ddagger}P$<0.05 $R_{max}$ between cannabidiol-treated arteries in the presence and absence of combined antagonist pretreatment (E).

**Table 4-4.** Effects of various antagonists on contractions to methoxamine or 5-hydroxytryptamine in mesenteric arteries pretreated with cannabidiol or vehicle

| | Methoxamine | | 5-Hydroxytryptamine | |
|---|---|---|---|---|
| **Antagonist** | **Vehicle** | **CBD 3 μM** | **Vehicle** | **CBD 1 μM** |
| **Control** | *n* = 5 | *n* = 10 | *n* = 5 | *n* = 5 |
| $pEC_{50}$ | 6.13 ± 0.10 | n.d. | 6.39 ± 0.08 | n.d. |
| $R_{max}$ (%) | 105 ± 2 | 20 ± 10[a] | 92 ± 2 | 0 ± 0[a] |
| **Olcegepant 1 μM** | *n* = 6 | *n* = 5 | *n* = 5 | *n* = 6 (4[b]) |
| $pEC_{50}$ | 5.65 ± 0.20 | 5.08 ± 0.07[a] | 6.45 ± 0.11 | 5.90 ± 0.11[a] |
| $R_{max}$ (%) | 103 ± 4 | 54 ± 13[a] | 96 ± 3 | 53 ± 19 |
| **Capsaicin 1 μM** | *n* = 5 | *n* = 6 | *n* = 6 | *n* = 7 |
| $pEC_{50}$ | 6.02 ± 0.11 | 5.10 ± 0.08[a] | 6.40 ± 0.09 | n.d. |
| $R_{max}$ (%) | 105 ± 5 | 44 ± 14[a] | 97 ± 5 | 38 ± 18[a] |
| **L-NAME 100 μM** | *n* = 5 | *n* = 5 | *n* = 6 | *n* = 6 |
| $pEC_{50}$ | 5.97 ± 0.13 | 5.04 ± 0.06[a] | 6.78 ± 0.12 | 6.06 ± 0.08[a] |
| $R_{max}$ (%) | 107 ± 4 | 34 ± 10[a] | 103 ± 4 | 50 ± 13[a] |
| **Indomethacin 3 μM** | *n* = 5 | *n* = 5 | *n* = 5 | *n* = 7 |
| $pEC_{50}$ | 5.65 ± 0.12 | 5.08 ± 0.13[a] | 6.27 ± 0.13 | n.d. |
| $R_{max}$ (%) | 101 ± 3 | 20 ± 9[a] | 87 ± 6 | 24 ± 14[a] |
| **Olc + L-NAME + Ind[c]** | *n* = 6 | *n* = 6 | *n* = 5 | *n* = 7 (5[b]) |
| $pEC_{50}$ | 6.27 ± 0.15 | 5.11 ± 0.16[a] | 6.59 ± 0.22 | 6.09 ± 0.09 |
| $R_{max}$ (%) | 110 ± 5 | 89 ± 7[a] | 99 ± 6 | 66 ± 17 |
| **GW9662 1 μM** | *n* = 5 | *n* = 5 | *n* = 5 | *n* = 6 |
| $pEC_{50}$ | 5.91 ± 0.18 | n.d. | 6.78 ± 0.07 | n.d. |
| $R_{max}$ (%) | 110 ± 5 | 34 ± 19[a] | 102 ± 5 | 10 ± 6[a] |
| **Rimonabant 300 nM** | *n* = 6 | *n* = 5 | *n* = 7 | *n* = 7 |
| $pEC_{50}$ | 5.71 ± 0.14 | n.d. | 6.52 ± 0.12 | n.d. |
| $R_{max}$ (%) | 105 ± 5 | 23 ± 10[a] | 86 ± 8 | 16 ± 13[a] |
| **SR144528 30 nM** | *n* = 5 | *n* = 5 | *n* = 5 | *n* = 7 |
| $pEC_{50}$ | 5.65 ± 0.12 | 5.08 ± 0.01[a] | 6.28 ± 0.08 | 6.02 ± 0.07[a] |
| $R_{max}$ (%) | 107 ± 5 | 47 ± 13[a] | 91 ± 2 | 39 ± 14[a] |
| **O-1918 3 μM** | *n* = 5 | *n* = 5 | *n* = 4 | *n* = 5 |
| $pEC_{50}$ | 5.83 ± 0.11 | 4.77 ± 0.16[a] | 6.85 ± 0.15 | 6.17 ± 0.13[a] |
| $R_{max}$ (%) | 111 ± 2 | 39 ± 14[a] | 98 ± 5 | 79 ± 7 |

Values are mean ± S.E.M. of $pEC_{50}$ and $R_{max}$ from concentration-contraction response curves shown in Figure 4-7 and Figure 4-8. CBD, cannabidiol. [a]$P<0.05$ compared with respective values in vehicle-treated group; Student's unpaired *t*-test. *n*, number of arteries, each from separate rats; [b]in brackets, *n* for $pEC_{50}$ values, *n* outside brackets for $R_{max}$. [c]Combined antagonist treatment with olcegepant 1 μM, L-NAME 100 μM and indomethacin 3 μM. n.d., not determined.

#### 4.3.2.1 Involvement of CGRP and endothelial factors

The CGRP inhibitor olcegepant (1 μM) partly reversed the effects of cannabidiol on methoxamine- and 5-HT-contracted arteries (Figure 4-7A and Figure 4-8A; Table 4-4). With olcegepant co-incubation, the methoxamine concentration-contraction curve in the presence of cannabidiol 3 μM was shifted 3.7-fold to the right of the vehicle control curve, which was like the effects observed with cannabidiol alone (Figure 4-7A and Table 4-4). However, the methoxamine $R_{max}$ was greater with olcegepant and cannabidiol co-incubation (52% of the respective vehicle control group; *P*=0.004) compared with cannabidiol alone (19% of control). In 5-HT-contracted arteries, olcegepant substantially recovered responses with a 3.5-fold rightward shift in the presence of cannabidiol 1 μM (*P*=0.0098) and $R_{max}$ values tending to be decreased but not significantly different from the vehicle control group (*P*=0.072; Figure 4-8A and Table 4-4).

The effects of cannabidiol 3 μM on the contractions to methoxamine persisted in the presence of the capsaicin (1 μM; TRPV1 desensitiser), L-NAME (100 μM; NOS inhibitor) and indomethacin (3 μM; cyclooxygenase inhibitor) (Figure 4-7B-D and Table 4-4). In contrast, contractions to 5-HT in the presence of cannabidiol 1 μM were partly reversed (in a similar manner to the effects of olcegepant) when coincubated with capsaicin, L-NAME or indomethacin (Figure 4-8B-D). The coincubation of olcegepant, L-NAME and indomethacin in combination recovered the agonist contraction curves to a greater extent than either antagonist alone for the methoxamine or 5-HT contraction curves with significant increases in $R_{max}$ compared with cannabidiol alone (Figure 4-7E and Figure 4-8E; *P*<0.05, Table 4-4). Interestingly denuding the endothelium did not reverse the effects of cannabidiol on either methoxamine or 5-HT contractions (Figure 4-9).

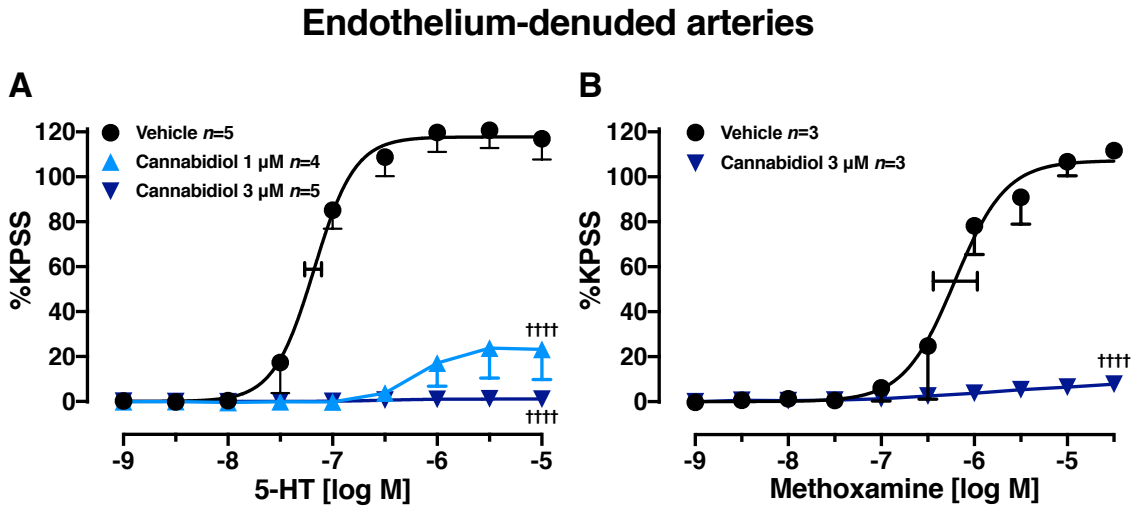


**Figure 4-9.** Effects of cannabidiol (1 or 3 µM) or vehicle (DMSO 0.1%) on concentration-contraction curves to A. 5-hydroxytryptamine (5-HT) or B. methoxamine in endothelium-denuded arteries.

Denudation of arteries was confirmed by precontraction to 80% KPSS maximum with noradrenaline and then testing relaxation to acetylcholine 1 µM – only those with <5% relaxation responses were used. The responses are shown as % of the maximum contraction to KPSS within each artery. *n*, arteries from separate rats, per treatment group. Vertical error bars are ±S.E.M. (those not shown are contained within the symbol); the horizontal error bars represent the $EC_{50}$ ± S.E.M. $^{††††}P<0.0001$ compared with respective vehicle group $R_{max}$ (maximal contraction); one-way ANOVA with Dunnett's *post hoc* test (panel A) or Student's unpaired *t*-test (panel B).

To further elucidate a potential role for endogenous CGRP in the effects of cannabidiol we studied the interaction of exogenous CGRP with methoxamine (Figure 4-10). CGRP 1-100 nM caused concentration-dependent rightward shifts of 4.3-19.9-fold of methoxamine concentration-contraction response curves ($P<0.05$) and decrease in the $R_{max}$ (to 52% of the vehicle group with CGRP 100 nM; $P=0.0005$, Figure 4-10).

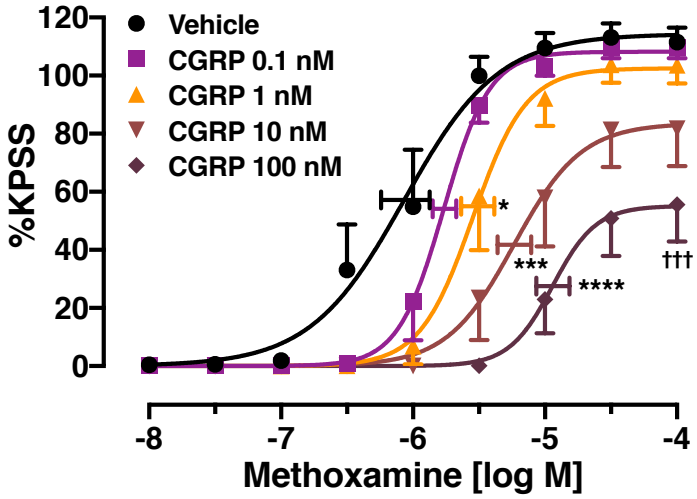


**Figure 4-10.** Effects of CGRP (0.1-100 nM) on methoxamine concentration-contraction curves in rat isolated mesenteric arteries.
The responses are shown as % of the maximum contraction to KPSS within each artery (*n*=6-7, from separate rats, per treatment group). Vertical error bars are ± S.E.M.; horizontal error bars represent the $EC_{50}$ ± S.E.M. **P*<0.05, ****P*≤0.001 or *****P*<0.0001 compared with vehicle group $EC_{50}$ and $^{\dagger\dagger\dagger}P$≤0.001 compared with vehicle $R_{max}$ (maximal contraction); repeated measures one-way ANOVA with Dunnett *post hoc* test.

### 4.3.2.2 Involvement of PPARγ and cannabinoid receptors

The cannabidiol-induced inhibition of contraction to methoxamine or 5-HT was unaffected by the presence of the PPARγ antagonist GW9662 1 μM (Figure 4-7F and Figure 4-7F; Table 4-4) or the $CB_1$ receptor antagonist rimonabant (300 nM) (Figure 4-7G and Figure 4-8G). The $CB_2$ receptor antagonist SR144528 (30 nM) was without significant effect on the inhibition of methoxamine contractions caused by cannabidiol (3 μM) (Figure 4-7H), however, SR144528 pretreatment did partially restore contractions to 5-HT in the presence of cannabidiol 1 μM (Figure 4-8H and Table 4-4). O-1918 (3 μM), an inhibitor of endothelium-dependent vasodilation to cannabinoids, had no effect on the cannabidiol-induced inhibition of contraction to methoxamine (Figure 4-7I), but interestingly, it restored the maximum contraction ($R_{max}$) to 5-HT in the presence of cannabidiol to a level not different from the vehicle control (Figure 4-8I and Table 4-4), with a 4.8-fold rightward shift of the 5-HT contraction-response curve.

#### 4.3.2.3 Involvement of methoxamine- and potassium-induced calcium entry

Cannabidiol 1 and 3 μM inhibited calcium-dependent contractions in small mesenteric arteries Figure 4-11. Cannabidiol caused a concentration-dependent inhibition of contraction to $CaCl_2$ in both KCl (80 mM) or methoxamine (10 μM) pretreated arteries. In KCl pretreated arteries, cannabidiol 1 μM caused a 2.6-fold dextral shift of the $CaCl_2$ concentration-contraction response curve with a decrease in $R_{max}$ of 44% compared with the vehicle group ($CaCl_2$ $pEC_{50}$, vehicle 3.19 ± 0.09 and cannabidiol 1 μM 2.77 ± 0.05, $P$=0.0007; $R_{max}$, vehicle 71 ± 6% and cannabidiol 1 μM 40 ± 8%, $P$=0.0011; Figure 4-11A). In methoxamine 10 μM pretreated arteries, cannabidiol 1 μM caused a small 1.5-fold rightward shift in the $CaCl_2$ curve without a significant decrease in $R_{max}$ ($CaCl_2$ $pEC_{50}$, vehicle 3.79 ± 0.04 and cannabidiol 1 μM 3.60 ± 0.04, $P$=0.03; Figure 4-11B). In KCl- or methoxamine-pretreated arteries, the higher concentration of cannabidiol (3 μM) caused a near-complete inhibition of contraction to $CaCl_2$ (Figure 4-11A-B). Cannabidiol 1-3 μM concentration-dependently attenuated the maximum contractions to Bay K8644, an L-type voltage-operated calcium channel agonist (cannabidiol 1 μM -59% ($P$=0.0004) and cannabidiol 3 μM -90% ($P$<0.0001) compared with vehicle group $R_{max}$; Figure 4-11C). The Bay K8644 $pEC_{50}$ tended to be 2.5-fold right-shifted in the presence of cannabidiol 1 μM, but this did not reach significance ($P$=0.28); $pEC_{50}$ values could not be determined with cannabidiol 3 μM (Figure 4-11C).

Similarly to cannabidiol, CGRP (100 nM) inhibited contractions to $CaCl_2$ in methoxamine (10 μM) pretreated arteries, causing a 2.1-fold dextral shift of contraction responses to $CaCl_2$, while also attenuating the $R_{max}$ ($CaCl_2$ $pEC_{50}$, vehicle 3.95 ± 0.07 and CGRP 100 nM 3.62 ± 0.09, $P$=0.03; $R_{max}$ in CGRP group -69% of vehicle group, $P$=0.0004; Figure 4-11D). However, olcegepant did not attenuate cannabidiol 3 μM-induced inhibition of contractions to $CaCl_2$ (Figure 4-12).

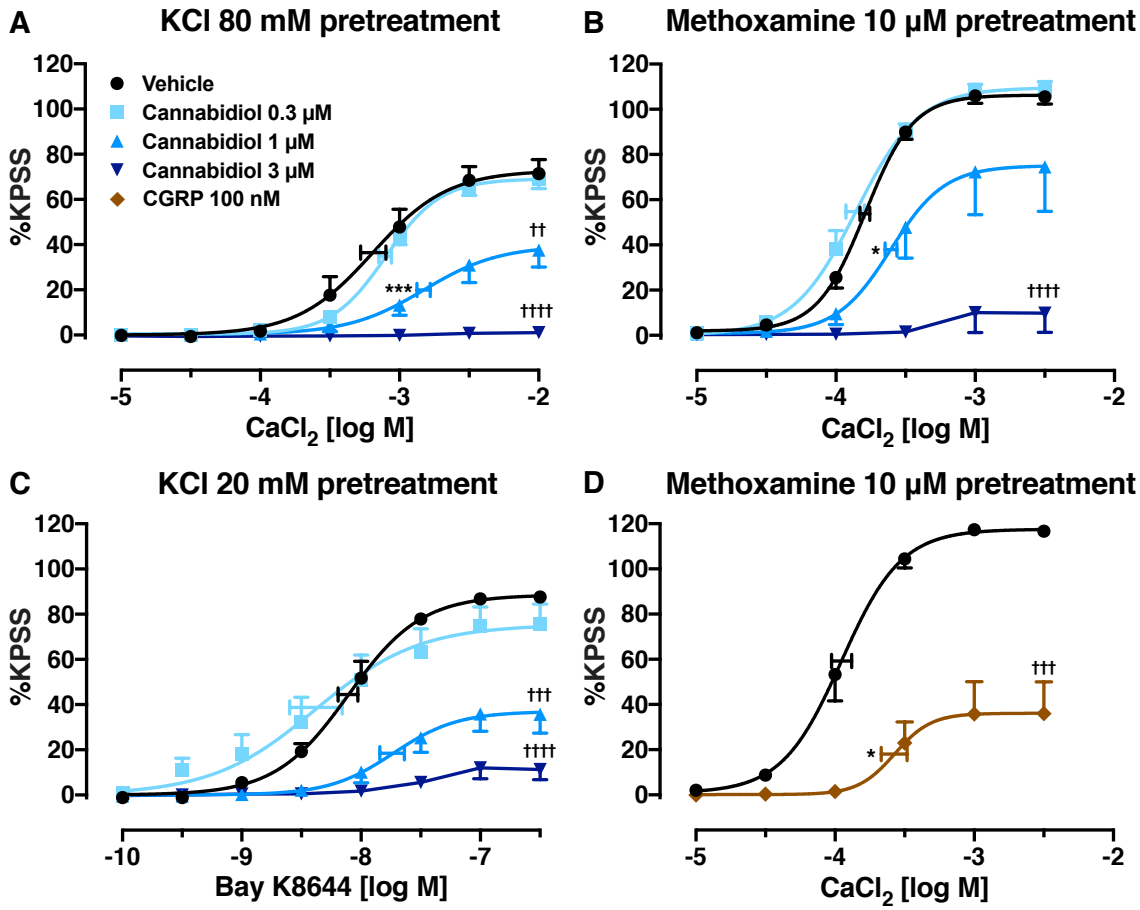


**Figure 4-11.** Effects of cannabidiol (0.3-3 µM) or CGRP (100 nM) on $CaCl_2$ or Bay K8644 concentration-contraction curves in rat isolated mesenteric arteries.

Concentration-contraction curves to $CaCl_2$ were in calcium-free PSS (A, B, D) and to Bay K8644 (C) were in normal PSS. Arteries were pre-incubated with either KCl 80 mM (A), methoxamine 10 µM (B, D) or KCl 20 mM (C). The responses are shown as % of the maximum contraction to KPSS within each artery ($n$=5-6, from separate rats, per treatment group). Vertical error bars are ± S.E.M.; horizontal error bars represent the $EC_{50}$ ± S.E.M. *$P$<0.05 or ***$P$≤0.001 compared with respective vehicle-treated group $EC_{50}$ and $^{\dagger\dagger}P$≤0.01, $^{\dagger\dagger\dagger}P$≤0.001 or $^{\dagger\dagger\dagger\dagger}P$<0.0001 compared with respective vehicle group $R_{max}$ (maximal contraction). Repeated measures one-way ANOVA with Dunnett *post hoc* test was performed, except for panel D where Student's unpaired $t$-test was performed.

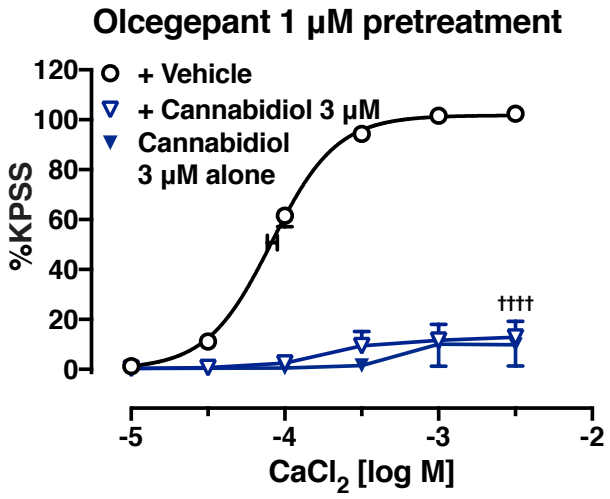


**Figure 4-12.** Effects of cannabidiol or vehicle (DMSO 0.1%) on $CaCl_2$ concentration-contraction curves in rat isolated mesenteric arteries pretreated with olcegepant 1 µM (open symbols). As a reference, the $CaCl_2$ contraction-response curve in the presence of cannabidiol alone (3 µM) from Figure 4-11B is plotted (filled symbols). Arteries were in calcium-free PSS and preincubated with methoxamine 10 µM before beginning the $CaCl_2$ curve. Responses are shown as % of the maximum contraction to KPSS within each artery ($n$=5-6, from separate rats, per treatment group). Vertical error bars are ± S.E.M. (those not shown are contained within the symbol); the horizontal error bar represents the $EC_{50}$ ± S.E.M. $^{††††}P$<0.0001 compared with vehicle group $R_{max}$ (maximal contraction); Student's unpaired $t$-test.

### 4.3.3 A comparison of the effects of cannabidiol in small and large arteries

#### 4.3.3.1 Cannabidiol effects on methoxamine and 5-HT responses in small and large arteries

The contractions to methoxamine or 5-HT of small saphenous arteries were inhibited by cannabidiol 3 µM (Figure 4-12A, B) in the same manner as observed in small mesenteric arteries (Figure 4-4). In small saphenous arteries cannabidiol 3 µM caused a 5.3-fold rightward shift and attenuation of $R_{max}$ (-66% of vehicle $R_{max}$, $P$<0.0001) in methoxamine concentration-contraction curves (methoxamine $pEC_{50}$, vehicle 5.11 ± 0.15 and cannabidiol 3 µM 4.39 ± 0.01, $P$=0.004; Figure 4-13A). Compared to the small mesenteric arteries (Figure 4-4D), the saphenous arteries were less sensitive to cannabidiol <3 µM, while also being relatively insensitive to methoxamine. Methoxamine was 10.5 times more potent in small mesenteric arteries compared to saphenous arteries. In small saphenous arteries, like in small mesenteric arteries,

cannabidiol inhibited contractions to 5-HT to a greater degree than to methoxamine (Figure 4-13B). Cannabidiol 3 μM caused a decrease in $R_{max}$ of -87% of that in the vehicle group ($P$<0.0001). In contrast to methoxamine, 5-HT showed similar potency in small mesenteric and small saphenous arteries.

In large saphenous arteries, only cannabidiol 3 μM had a significant effect on methoxamine contraction curves with a 5.2-fold rightward shift and small 10% decrease in $R_{max}$ (Figure 4-13C; methoxamine $p$EC$_{50}$, vehicle 6.23 ± 0.03 and cannabidiol 3 μM 5.51 ± 0.09, $P$<0.0001; $R_{max}$, vehicle 102 ± 2% and cannabidiol 3 μM 91 ± 3%, $P$=0.039). In large superior mesenteric and tail arteries, cannabidiol 0.3-3 μM was without effect on methoxamine contraction responses (Figure 4-13D-E).

In general, there was a negative correlation between artery internal diameter and the maximum inhibition of contraction to methoxamine by cannabidiol 3 μM (Figure 4-14; $r^2$ = 0.7), where the smaller resistance arteries were more sensitive to cannabidiol. In addition, methoxamine was 2 times more potent in small mesenteric arteries compared to the superior mesenteric arteries.

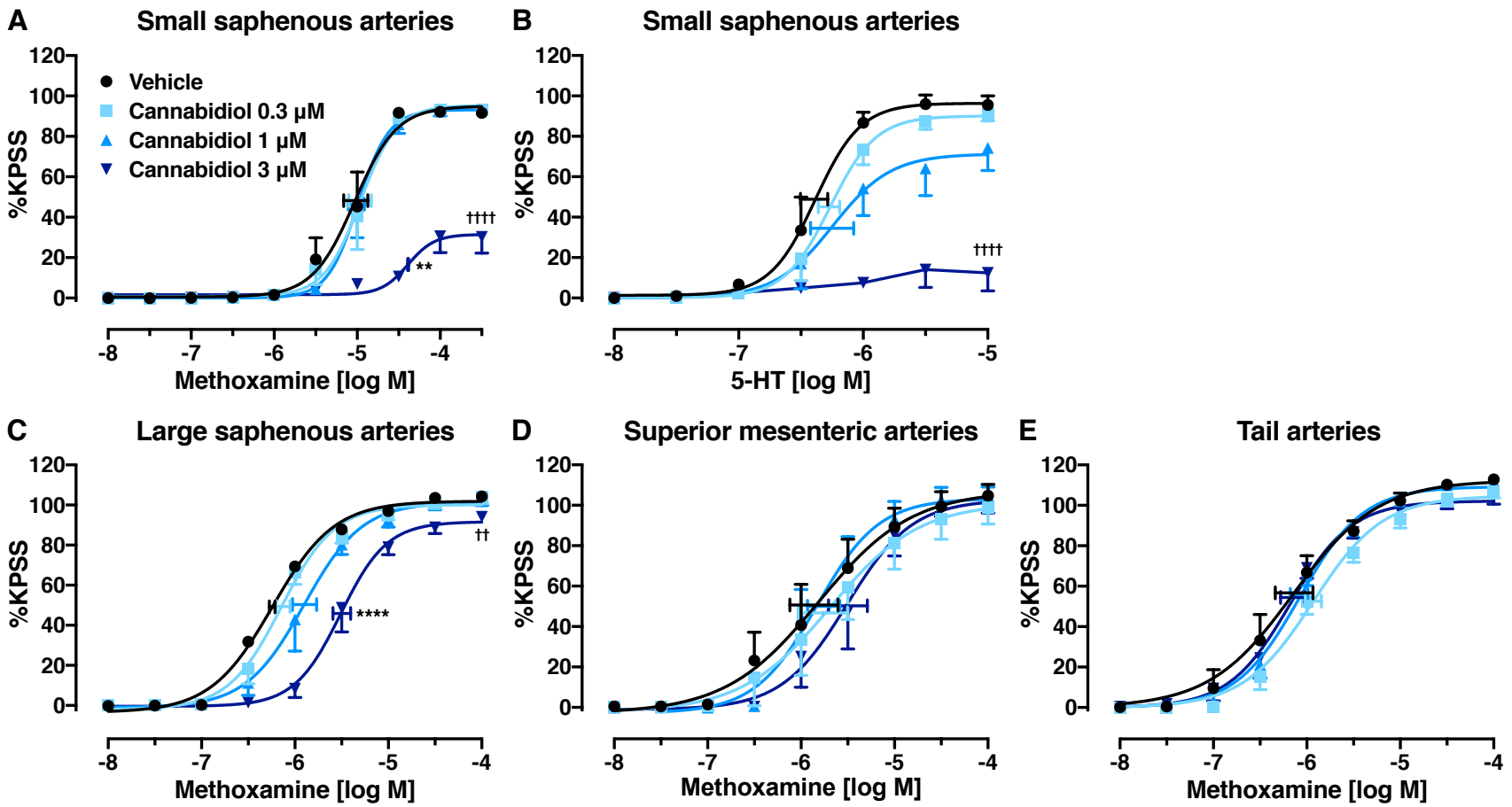


**Figure 4-13.** Effects of cannabidiol (0.3-3 µM) on methoxamine or 5-HT concentration-contraction curves in rat isolated small or large arteries. A, B. Small saphenous arteries (internal diameter, i.d., 288 ± 12 µm); C. large saphenous arteries (i.d. 623 ± 18 µm); D. superior mesenteric arteries (i.d. 888 ± 95 µm); and E. tail arteries (i.d. 923 ± 30 µm). The responses are shown as % of the maximum contraction to KPSS within each artery (*n*=5-7, from separate rats, per treatment group). Vertical error bars are ± S.E.M. (those not shown are contained within the symbol); horizontal error bars represent the $EC_{50}$ ± S.E.M. $^{**}P \leq 0.01$ or $^{****}P < 0.0001$ compared with respective vehicle-treated group $EC_{50}$ and $^{\dagger\dagger}P \leq 0.01$ or $^{\dagger\dagger\dagger\dagger}P < 0.0001$ compared with respective vehicle group $R_{max}$ (maximal contraction); repeated measures one-way ANOVA with Dunnett *post hoc* test.

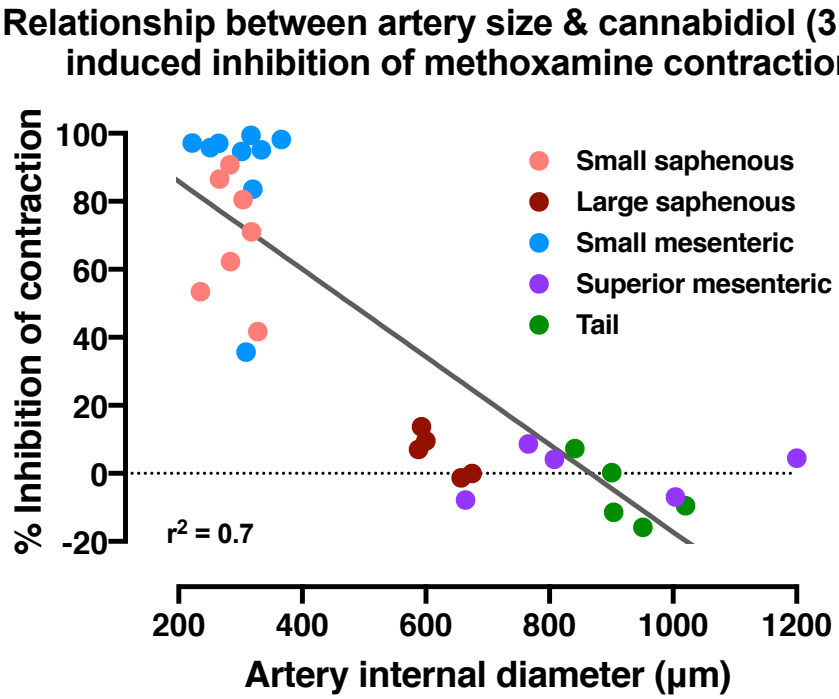


**Figure 4-14.** The relationship between artery size (internal diameter) and cannabidiol (3 µM)-induced inhibition of contraction to methoxamine in rat isolated small (saphenous and mesenteric) and large (saphenous, superior mesenteric and tail) arteries ($n$=5-10, from separate rats, per artery group).

Each data point represents the internal diameter of an individual artery and % inhibition of contraction is from the maximum KPSS response (based on data from Figure 4-13). The linear regression line shows a negative relationship between artery internal diameter and inhibition of contraction with a slope of -0.13 and $r^2$ of 0.7 ($n$ = 32; $P$<0.0001).

#### 4.3.3.2 Involvement of CGRP in the effects of cannabidiol in small saphenous and superior mesenteric arteries

To investigate the role of CGRP in the effects of cannabidiol in small saphenous arteries, tissues were incubated with the CGRP antagonist olcegepant (1 μM; Figure 4-15A). Olcegepant partly reversed the inhibitory effects of cannabidiol 3 μM, allowing 4 out of 6 arteries to concentration-dependently contract to 5-HT ($p$EC$_{50}$, vehicle 6.31 ± 0.20 and cannabidiol 6.06 ± 0.08, $P$=0.37), with attenuation in $R_{max}$ of -45% compared to the vehicle group ($P$=0.03), in marked contrast to the almost complete lack of response to 5-HT when vessels were treated with cannabidiol 3 μM alone. Olcegepant pretreatment did not change the sensitivity or $R_{max}$ of 5-HT contractions in the presence of vehicle (Figure 4-15A and Figure 4-4B; $p$EC$_{50}$ $P$=0.74 and $R_{max}$ $P$=0.65).

Like cannabidiol 3 μM (Figure 4-13D), CGRP 100 nM had no effect on methoxamine concentration-contraction response curves in superior mesenteric arteries (methoxamine $p$EC$_{50}$, vehicle 5.52 ± 0.13 and CGRP 5.20 ± 0.09, $P$=0.09; $R_{max}$, vehicle 102 ± 5% and CGRP 86 ± 6%, $P$=0.06; Figure 4-15B).

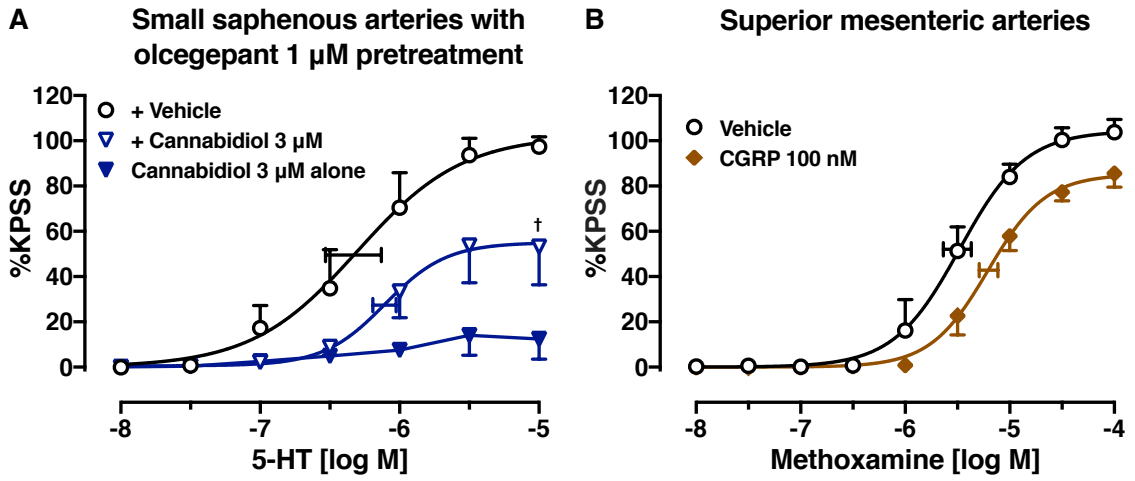


**Figure 4-15.** Influence of CGRP in rat isolated small saphenous and superior mesenteric arteries. A. Concentration-contraction curves to 5-HT in the presence of olcegepant 1 µM with vehicle (DMSO 0.1%) or with cannabidiol (3 µM), or cannabidiol (3 µM) alone (no olcegepant, filled symbol; reproduced from Figure 4-13. B) in small saphenous arteries. B. Concentration-contraction curves to methoxamine in the presence of vehicle (Milli-Q water) or CGRP (100 nM) in superior mesenteric arteries. The responses are shown as % of the maximum contraction to KPSS within each artery ($n$=5-7, from separate rats, per treatment group). Vertical error bars are ± S.E.M. (those not shown are contained within the symbol); horizontal error bars represent the $EC_{50}$ ± S.E.M. $^{\dagger}P$<0.05 compared with respective vehicle group $R_{max}$ (maximal contraction); Student's unpaired $t$-test

### 4.3.4 Effects of cannabidiol on non-vascular muscle

To test whether the effects of cannabidiol are limited to vascular smooth muscle, we investigated the effects of cannabidiol (10-100 µM) on various non-vascular tissues, including bronchial, urogenital, cardiac and skeletal muscle (Figure 4-16). The contractions of bronchial smooth muscle and vasa deferentia to carbachol and noradrenaline, respectively, were unaffected by lower concentrations of cannabidiol (10 and/or 30 µM; Figure 4-16A-B). Cannabidiol 100 µM decreased the maximum contraction of bronchi by 20% and vasa deferentia by 45% ($P$<0.05), without shifting the agonist concentration-contraction curves.

In contrast to the non-vascular smooth muscle tissues, the contraction of left atria to isoprenaline was sensitive to the lower concentrations of cannabidiol 10 and 30 µM but resistant to cannabidiol 100 µM (isoprenaline $pEC_{50}$, vehicle 8.60 ± 0.07, cannabidiol

10 μM 7.94 ± 0.12 ($P$<0.0001), cannabidiol 30 μM 8.24 ± 0.05 ($P$=0.004) and cannabidiol 100 μM 8.45 ± 0.05 ($P$=0.35); Figure 4-16C); $R_{max}$ was unaffected by cannabidiol. Isoprenaline-induced increases in right atrial rate were not affected by cannabidiol 10-100 μM (Figure 4-16D; $pEC_{50}$ $P$>0.11). In ~30% of experiments, incubation of cannabidiol 100 μM completely stopped the passive beating of the right atria before the cumulative additions of isoprenaline. The skeletal muscle preparation of the hemidiaphragm demonstrated similar insensitivity to cannabidiol as the other non-vascular muscle tissues. Cannabidiol 30 μM had no effect on the electrically induced contractions of the hemidiaphragm (Figure 4-16E).

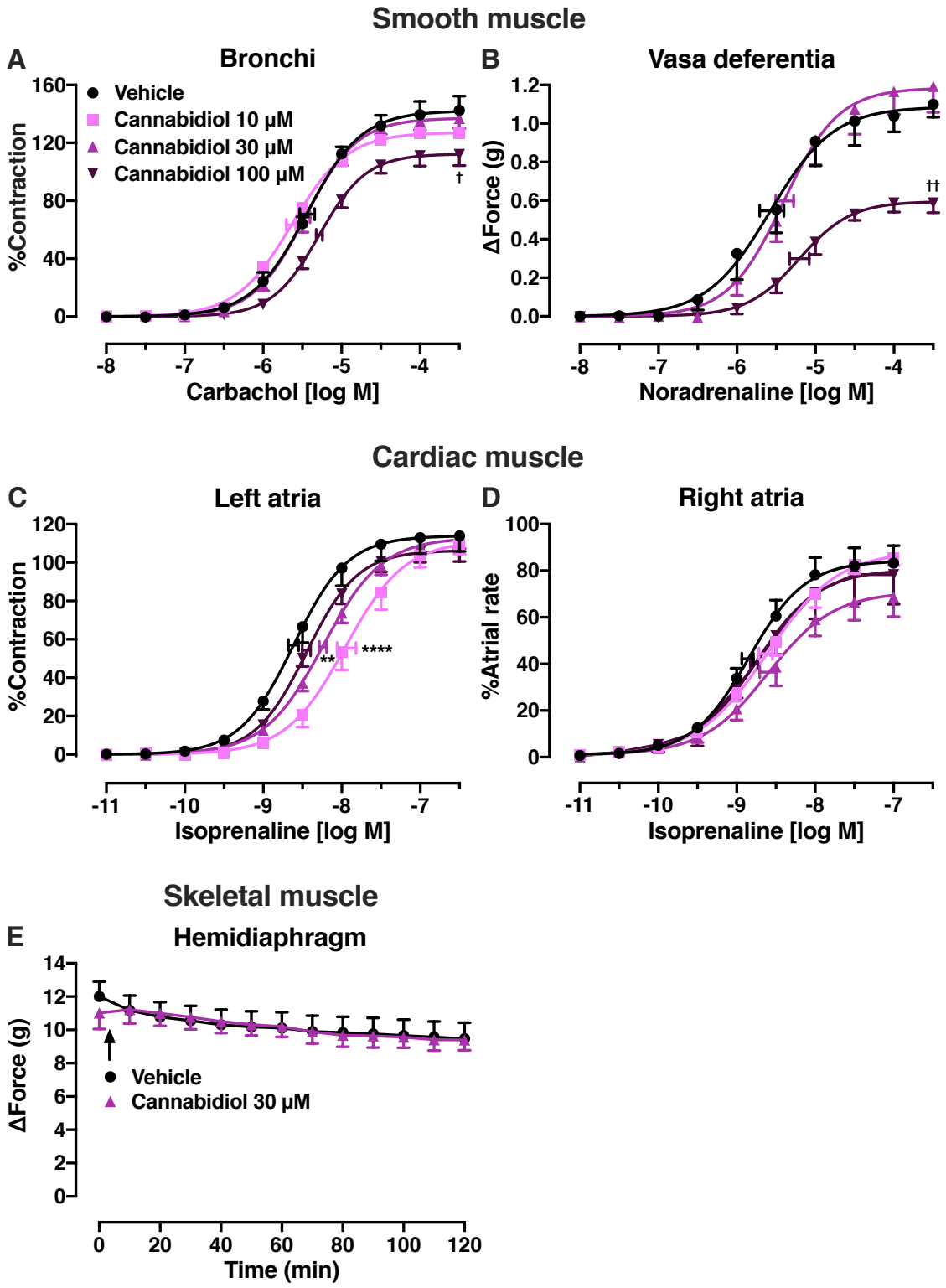
Smooth muscle
A
Bronchi
Vehicle
Cannabidiol 10 µM
Cannabidiol 30 µM
Cannabidiol 100 µM
%Contraction
Carbachol [log M]
B
Vasa deferentia
ΔForce (g)
Noradrenaline [log M]
Cardiac muscle
C
Left atria
%Contraction
Isoprenaline [log M]
D
Right atria
%Atrial rate
Isoprenaline [log M]
Skeletal muscle
E
Hemidiaphragm
ΔForce (g)
Vehicle
Cannabidiol 30 µM
Time (min)

**Figure 4-16.** The effects of cannabidiol on rat isolated non-vascular muscle contraction responses in: A. bronchi to carbachol (cannabidiol 10-100 μM; *n*=5-6); B. vasa deferentia to noradrenaline (cannabidiol 10-30 μM; *n*=5 each); C. left atria to isoprenaline (force of contraction; cannabidiol 10-100 μM; *n*=6-8); D. right atria to isoprenaline (atrial rate; cannabidiol 10-100 μM; *n*=3-6); and E. hemidiaphragm to electrical phrenic nerve stimulation (cannabidiol 30 μM; *n*=5).
Vehicle treatment groups were *n*=5-6 each. A, C and D: Responses are shown as % of the maximum response within each tissue to different agents (see methods). B and E: Responses are shown as the absolute increase (change Δ) from baseline force (g). Vertical error bars are ± S.E.M. (those not shown are contained within the symbol); horizontal error bars represent the $EC_{50}$ ± S.E.M. $^{**}P \leq 0.01$ or $^{****}P < 0.0001$ compared with respective vehicle-treated group $EC_{50}$ and $^{\dagger}P < 0.05$ or $^{\dagger\dagger}P \leq 0.01$ compared with respective vehicle group $R_{max}$ (maximal contraction); repeated measures one-way ANOVA with Dunnett *post hoc* test.

## 4.4 Discussion

### 4.4.1 Small resistance arteries

We decided to assess the effects of cannabidiol on the contractions rather than the relaxation of tissues as we observed that cannabidiol-induced maximum relaxation was delayed (Figure 4-17). Ideally, concentration-response curves should be performed with drugs that reach maximum responses quickly to limit the interference of time-dependent changes in vascular tone.

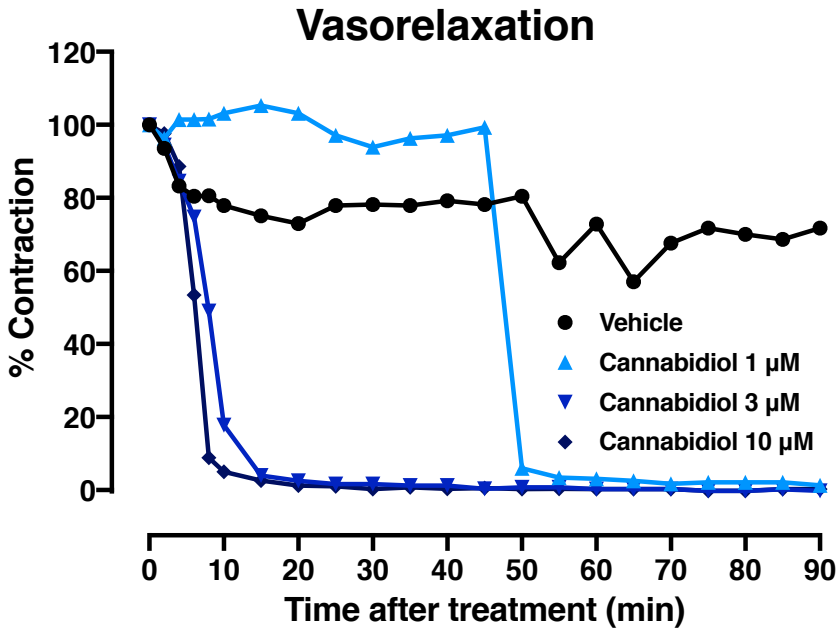


**Figure 4-17.** Vasorelaxant effects of cannabidiol (1-10 µM) or vehicle (DMSO 0.1%) from time of administration at 0 min to 90 min after administration.
The responses are shown as % of the contraction prior to cannabidiol administration (0 min). *n*=1; *n*, arteries from separate rats, per treatment.

In the rat small mesenteric artery mounted and stretched to a passive tension that reflects its diameter at a transmural pressure of about 60 mmHg, there is generally no active tension present. Thus, any pretreatment, such as cannabidiol, or other agents we used here that may induce relaxation cannot be observed on this passive tension. However, when the artery is contracted with the concentration-response curve to methoxamine or 5-HT the interaction with the pretreatment becomes obvious as a

right-shift of the contraction curve or depression of the $R_{max}$ depending upon the interactions between the constrictor stimulus and the opposing relaxation stimulus from the pretreatment. In small arteries, preincubated with cannabidiol, the sensitivity of contraction-response curves to a rightward shift and/or depression of the maximum contraction to a range of agents is probably dependent on the efficiency of receptor-transduction coupling. For example, the concentration-contraction curve for methoxamine was right-shifted 10-fold with a near-normal maximum in the presence of cannabidiol 0.3-1 μM suggesting $\alpha_1$-adrenoceptor reserve before the maximum response collapsed in the presence of cannabidiol 3 μM. In contrast, for most other contractile agents, the concentration-response curves were generally markedly depressed at 1 or 3 μM cannabidiol. It is important to acknowledge that our 30 min incubation of the small arteries with cannabidiol 0.1-3 μM allows a longer equilibration time than applying cumulative concentrations of cannabidiol to a precontracted artery (see Baranowska-Kuczko *et al.*, 2020). The rationale of using a 30 min drug incubation is to ensure proper drug-receptor equilibration. Our results clearly show that cannabidiol pretreated for 30 min does significantly right-shift and/or attenuate the concentration-response curves to a range of contractile agents. At cannabidiol 1 μM, the subsequent concentration-response curves to endothelin-1 and U46619 were hardly affected but at cannabidiol 3 μM these concentration-response curves were significantly depressed. In comparison, the concentration-response curve to methoxamine and 5-HT were very sensitive to cannabidiol at just 1 μM. However, in the study of Baranowska-Kuczko *et al.* (2020), also in rat small mesenteric arteries, they found that 1 μM cannabidiol pretreatment had no effect on subsequent concentration-response curves to phenylephrine in WKY, SHR, or DOCA salt-treated rats. They did not report the effect of any higher concentration of cannabidiol in this protocol. Further, they reported that cannabidiol added from 0.1-30 μM on submaximally contracted arteries with phenylephrine could completely inhibit the contraction. We contend that in our present cannabidiol pretreatment protocol, there is the distinct advantage of a 30 min equilibration before completing the contractile agent concentration-response curve. It is important to note the rat mesenteric small artery is very sensitive to just a 3-fold increase in cannabidiol. For example, the concentration-response curve to U46619 was unaffected by pretreatment with 1 μM cannabidiol but completely inhibited with 3 μM

cannabidiol. Similarly, the 5-HT concentration-response curve was unaffected by 0.3 μM cannabidiol but completely inhibited by just 1 μM cannabidiol pretreatment (Figure 4-4C and E).

In the vasculature the effects of cannabidiol have been suggested to be mediated by the endothelium, superoxide dismutase, cyclooxygenase, prostanoid $EP_4$, NOS, calcium-activated potassium channels ($K_{Ca}$), $CB_1$-, $CB_2$-, TRPV1- and PPARγ receptors (Baranowska-Kuczko *et al.*, 2020; O'Sullivan *et al.*, 2009; Stanley *et al.*, 2015; Wheal *et al.*, 2014; Wheal *et al.*, 2017). In Zucker diabetic fatty (ZDF) rats, chronic *in vivo* treatment with cannabidiol enhanced vasorelaxation to acetylcholine of isolated small mesenteric arteries (Wheal *et al.*, 2017). The effects of cannabidiol were mediated by cyclooxygenase and NOS. Cannabidiol had no effect on arteries from corresponding non-diabetic rats. Another study suggested that the effects of acute administration of cannabidiol in small mesenteric arteries isolated from spontaneously hypertensive rats, DOCA-salt hypertensive rats or normotensive controls were mediated by $CB_1$ receptors, in addition to the involvement of $CB_2$ receptors and the endothelium to a varying degree (Baranowska-Kuczko *et al.*, 2020). In our study, neither denuding the endothelium (Figure 4-9) nor inhibition of cyclooxygenase, NOS, $CB_1$-, $CB_2$-receptors or PPARγ completely reversed the effects of cannabidiol on methoxamine and 5-HT contractions. Cannabidiol-induced inhibition of contractions was partly reversed by the CGRP receptor inhibitor olcegepant in the small mesenteric and saphenous arteries. Arteries were cotreated with L-NAME, indomethacin and olcegepant as all three compounds target pathways involved in vasorelaxation. The co-incubation of arteries with L-NAME, indomethacin and olcegepant significantly reversed most of the effects of cannabidiol on methoxamine and 5-HT contractions. While CGRP may play a role in mediating the effects of cannabidiol, we cannot be sure that cannabidiol is targeting the release of CGRP from perivascular sensory neurons, as the inhibition of prejunctional TRPV1 receptors had no effect on the contractions. The reversal of most of the effects of cannabidiol in the presence of both L-NAME and olcegepant may be explained by the involvement of both NO-dependent- and independent-pathways in the effects of CGRP (Kumar *et al.*, 2019). The dependence on NO varies between different vascular beds, whereas in rat mesenteric artery smooth muscle cells, CGRP-induced relaxation was

independent of the endothelium (McNeish *et al.*, 2012), which may explain the inability of L-NAME and endothelial denudation alone to fully reverse the effects of cannabidiol. We confirmed that exogenous CGRP, similar to cannabidiol, caused a concentration-dependent inhibition of contraction to methoxamine, where the lower concentrations of CGRP (1-10 nM) dextrally shifted the contraction curves, while the higher concentration (100 nM) caused both a significant dextral shift and attenuation of $R_{max}$. This similar pattern of cannabidiol and exogenous CGRP on methoxamine curves is compelling. It is however important to note that tissues used in this study were sourced from only male rats, hence future studies should also include tissues from female rats as there may be biological differences in tissue responses between the sexes.

O-1918, a cannabidiol analogue, has been claimed to inhibit a putative endothelial cannabinoid receptor ($CB_e$), which has been suggested to mediate the vasorelaxant effects of various cannabinoids (Offertaler *et al.*, 2003). In our study, O-1918 reversed the effects of cannabidiol on contractions to 5-HT, while having no effect on methoxamine-contracted arteries. The involvement of a potential $CB_e$ receptor should be interpreted with caution as it is known today that O-1918 has several endothelium-independent off-targets at concentrations (3-10 μM), which are the concentrations normally used to verify the involvement of $CB_e$ receptors in the effects of cannabinoids (Bondarenko, 2014). In our study, we observed that the incubation of small mesenteric arteries with the higher concentration of O-1918 (10 μM) led to spontaneous spike-like contractions of small mesenteric arteries prior to any addition of contractile agonists (Figure 4-18). Similarly to cannabidiol, O-1918 is also a ligand to the putative receptors GPR18 and GPR55. O-1918 interacts with GPR18 as an antagonist (McHugh *et al.*, 2010) or as a biased agonist at GPR18 (Console-Bram *et al.*, 2014) and has been suggested to interact with GPR55 as an antagonist (Henstridge, 2012). Hence, O-1918 may be interacting with cannabidiol at the GPR18 and GPR55 instead.

Cannabidiol (1-3 μM) caused concentration-dependent inhibition of calcium entry through voltage-operated calcium channels in arteries stimulated with both methoxamine (10 μM) and KCl (80 mM), in the absence of extracellular calcium. In addition, cannabidiol blocked the L-type voltage-operated calcium channel agonist Bay

K8644 from contracting arteries. Abnormal-cannabidiol, a synthetic cannabidiol analogue, has also been reported to mediate some of its effects by inhibiting the entry of calcium through voltage-operated calcium channels (Ho & Hiley, 2003). While CGRP potently inhibited calcium contractions of arteries in the absence of extracellular calcium, it is unlikely that CGRP is involved in the calcium inhibitory effects of cannabidiol, as olcegepant did not reverse the effects of cannabidiol on calcium contractions (Figure 4-12).

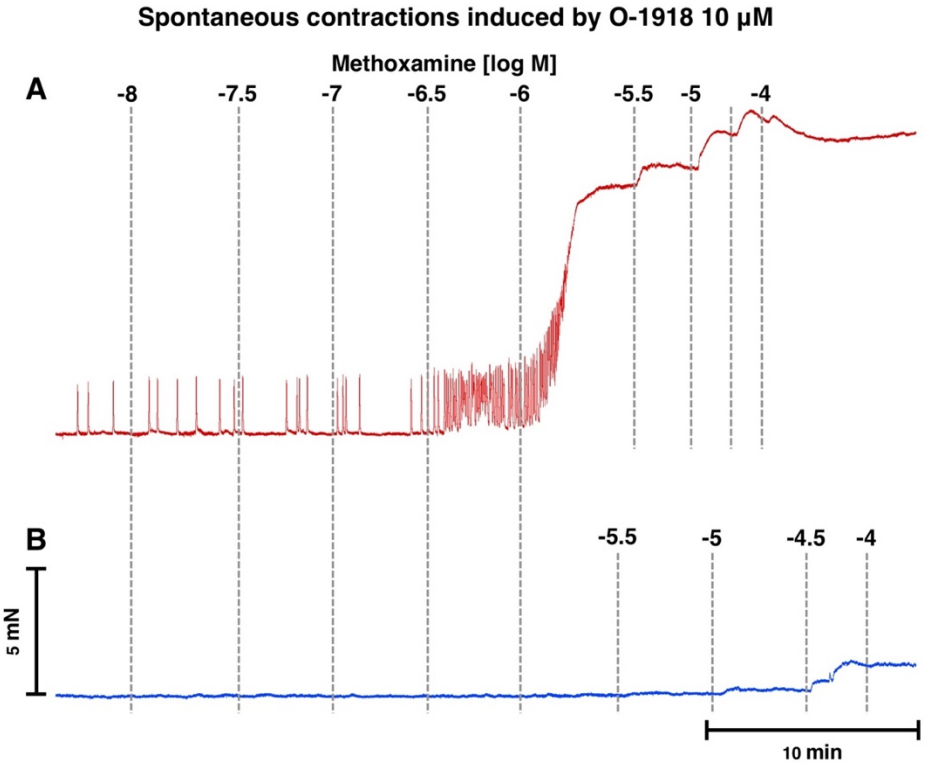


**Figure 4-18.** A representative LabChart® trace displaying the effects of O-1918 (10 µM) pretreatment on methoxamine concentration-contraction curves in rat isolated mesenteric arteries (endothelium intact) in the presence of A. vehicle (DMSO 0.1%) or B. cannabidiol (3 µM), each added 30 min before beginning the curve.
O-1918 was added 60 min before adding the first methoxamine concentration and spontaneous spike-like contractions began after about 30 min; these were no longer observed when tissues were treated with cannabidiol. The additions of methoxamine (in half-log M units) are indicated by dashed lines.

### 4.4.2 Large arteries and non-vascular tissues

Our data show that cannabidiol and exogenous CGRP inhibit the contraction of small arteries to methoxamine. In contrast, in the large saphenous artery, the weak inhibitory action of cannabidiol was matched by the weak action of exogenous CGRP (100 nM). The failure of therapeutic concentrations (1-3 μM) of cannabidiol to alter the effects of contractile agents in large arteries is in stark contrast to the resistance arteries. Moreover, the 10-100 times higher concentrations of cannabidiol that were almost without effect on non-vascular tissues highlight a very targeted action of the drug in small arteries.

### 4.4.3 Conclusions

Our study has quantified the potent effects of cannabidiol, at therapeutic concentrations (1-3 μM), in inhibiting the contraction by multiple agents of small resistance arteries, but not large conduit arteries. The sensitivity of the small resistance arteries to cannabidiol involves CGRP and voltage-operated calcium channels. We also show that non-vascular smooth muscles are generally unaffected by cannabidiol even at 10-100 times the therapeutic plasma level. This high sensitivity of the resistance arterial circulation to cannabidiol may offer a therapeutic opportunity in peripheral vascular disease that excludes off-target sites of the heart and non-vascular smooth muscle.

# Chapter 5

## The haemodynamic effects of cannabidiol in anaesthetised rats

## 5.1 Introduction

Phyto-, endo- and synthetic cannabinoids induce cardiovascular changes in humans and animals by interacting with the endocannabinoidome in cardiovascular tissues and associated nervous system (section 1.7). The potential therapeutic benefits of cannabidiol are many, including in the cardiovascular system. The assumptions of the cardiovascular benefits of cannabidiol stem from various preclinical cardiovascular findings (Chapter 4; Booz, 2011; Stanley *et al.*, 2013a; Sultan *et al.*, 2017). However, the haemodynamic effects of cannabidiol *in vivo* remain unclear.

### 5.1.1 The principles of haemodynamics

The term haemodynamics deals with the physical factors that govern blood flow, and is defined as "the physical study of flowing blood and of all the solid structures through which it flows" (reviewed in Secomb, 2016). The basic principle of haemodynamics is often explained through the electronic-hydraulic analogy (Figure 5-1; Secomb, 2016; Smith & Madigan, 2018). In a simple electrical circuit, a source of voltage drives current through a conductive path. Similarly, in blood circulation, the heart supplies a force for blood to flow through the intricate vascular network. In the electrical circuit analogy, the pressure in the circulation (blood pressure; BP) corresponds to voltage (V), the systemic blood flow (cardiac output; CO) corresponds to the current and the resistance to blood flow through blood vessels (total peripheral resistance; TPR) corresponds to electrical resistance (R; Figure 5-1). However, the electrical circuit analogy is an oversimplification of haemodynamics since it assumes that if blood pressure and cardiac output are known, the total peripheral resistance could be solved through a simple arithmetic equation, as the analogy ignores the influence of heart rate by assuming that systemic blood flow is constant over time (Figure 5-1; Smith & Madigan, 2018). In reality, the systemic blood flow alters according to stroke volume (SV) and heart rate (section 5.1.1.4).

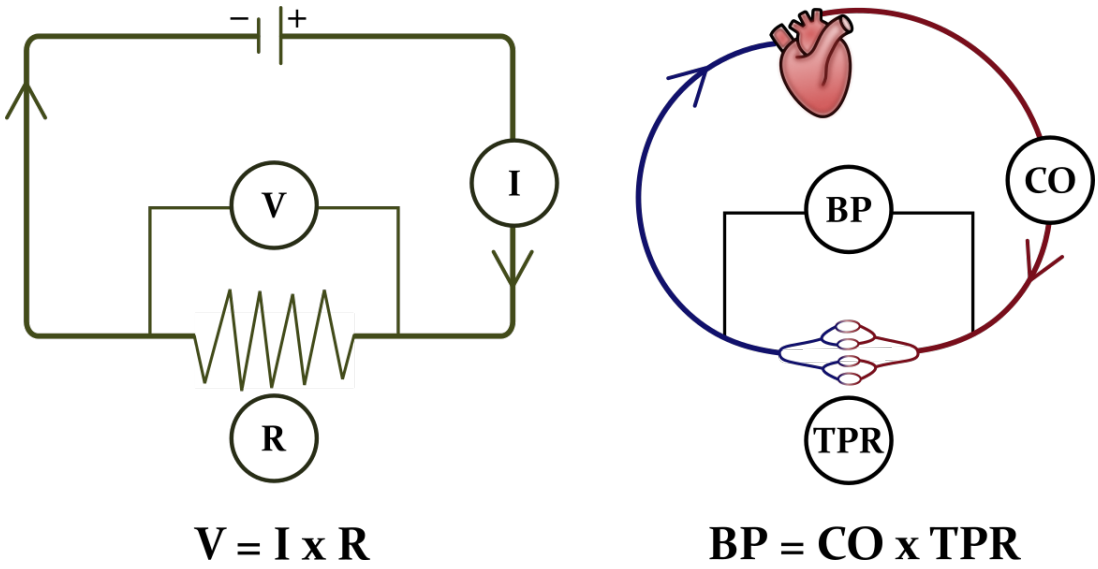


**Figure 5-1.** Electronic-hydraulic analogy of the cardiovascular circulation where blood pressure (BP) is analogous to voltage (V), cardiac output to current flow (I) and total peripheral resistance (TPR) to electrical resistance.
The figure was adapted from Smith and Madigan (2018).

#### 5.1.1.1 Blood pressure

Blood pressure in animals can be measured with indirect and direct techniques (reviewed in Kurtz *et al.*, 2005). Indirect blood pressure measurements may be performed with tail or limb cuffs. Cuff techniques are non-invasive as blood measurements can be performed without surgery. As indirect techniques can only measure blood pressure over a limited number of cardiac cycles, they are unable to assess the average blood pressure over an extended period. Furthermore, the accuracy of the cuff technique has been questioned as there is poor agreement between simultaneous direct and indirect blood pressure measurements (reviewed in Kurtz *et al.*, 2005). Indirect measurements, particularly with tail cuffs, also have the disadvantage of being poorly suited to measuring diastolic blood pressure and therefore could skew average blood pressure estimations. In contrast, direct techniques are accurate while being invasive, as they require surgery. Radiotelemetry and externally connected fluid-filled catheters are the two main direct techniques. Radiotelemetry devices are biocompatible radio transmitters that are surgically implanted in the peritoneal cavity of rats or under the flank skin in mice (Huetteman & Bogie, 2009). Remote and continuous blood pressure monitoring can be performed by inserting a

flexible catheter in a major artery and connecting the end of the catheter to a radio transmitter. The oldest method of measuring blood pressure in animals involves externally connected fluid-filled catheters. Under surgical anaesthesia, heparin solution-filled catheters are inserted into a major artery and coupled to an external pressure transducer connected to an amplifier and recording device. Both direct techniques have several advantages over indirect techniques. Firstly, they produce more accurate blood pressure readings that can be collected over an extended study period. In turn, this decreases the variation in mean blood pressure estimations and allows for the detection of small blood pressure changes over time which may have an important physiological or pathophysiological role. While radiotelemetry and fluid-filled catheterisation mostly share the same advantages, they have differences that would affect a researcher's preference for one technique over the other. Fluid-filled catheterisation has the advantage of allowing more accurate blood pressure readings, as the transducer can be calibrated regularly to correct for any potential baseline shifts that may happen during an experiment. In contrast, radiotelemetry cannot be calibrated during an experiment and therefore any possible baseline shifts need to be evaluated after the end of the experiment. Fluid-filled catheterisation is also advantageous from a cost perspective, as it is relatively inexpensive. The main expense associated with this technique is the high one-time cost of attaining a recording device and amplifier, which are usually already available in a laboratory that performs cardiovascular research. The high expense associated with radiotelemetry is attributed to the initial purchase of the equipment and the maintenance, including battery changes and refurbishment. Radiotelemetry is a preferred method of measuring blood pressure in conscious animals, as it allows animals to move without restraint. In contrast, externally connected fluid-filled catheters can restrict animals from freely moving in all directions and therefore may cause the animal stress (stress itself will affect blood pressure and heart rate).

In this study, fluid-filled catheterisation was the chosen method of measuring blood pressure, as the animals were undergoing invasive non-recovery surgery to enable the measurements of various other haemodynamic parameters.

#### 5.1.1.2 Blood flow

Understanding the physical factors that determine blood flow is key when dealing with haemodynamics. Blood flowing through a blood vessel is analogous to the movement of a fluid through a pipe (Mohrman & Heller, 2018; Pappano & Wier, 2019; Pollock *et al.*, 2020). The fluid will only flow through the pipe if there is a pressure difference between the fluid coming in and out of the pipe. Blood flow is generally laminar meaning that fluid in the middle of the pipe has the highest velocity, with a subsequent gradient decrease of velocity the closer the fluid gets to the vessel walls. Blood closest to the vessel wall will experience friction which creates resistance to the blood flow. Hence, the blood flow is dependent on the pressure difference and resistance in a vessel according to the following equation:

$$\text{blood flow} = \frac{\text{pressure difference}}{\text{resistance}} \qquad (4)$$

The blood flow of a particular vessel can be measured using an ultrasound Transonic flow probe that is placed around the artery of interest without constricting the natural blood flow (ADInstruments, 2020). The Transonic flow probe uses ultrasound to measure the velocity of a passing fluid which is then converted to a volume blood flow measured in ml/min (ADInstruments, 2020). Heart rate (section 5.1.1.4) and vascular conductance (section 5.1.1.3) measurement can be derived from blood flow recordings.

#### 5.1.1.3 Vascular conductance and resistance

Vascular conductance and resistance are used reciprocally to describe vascular tone (Chapter 4). Vascular conductance is defined as "the ease with which blood flows through a circulation (or vascular bed) at a given pressure difference". Hence, vascular resistance is defined as: "the hindrance to blood flow in the circulation (or a vascular bed) at a given pressure difference" (Chapter 4; Joyce *et al.*, 2019). Mathematically, conductance is the inverse of resistance:

$$\text{conductance} = \frac{\text{blood flow}}{\text{mean arterial pressure}} \qquad (5)$$

$$\text{resistance} = \frac{\text{mean arterial pressure}}{\text{blood flow}} \qquad (6)$$

The choice between conductance or resistance may alter the conclusion of a study (Joyce *et al.*, 2019). This is especially apparent when a strong vasoconstrictor drug is used causing blood flow in a particular vascular bed to almost cease. Consequently, the conductance in that vascular bed would approach 0 (Equation 1) while the corresponding measurement of resistance would near infinity (Equation 2) as illustrated in Figure 5-2. Hence, in this study, the effects of cannabidiol on vascular tone were described in terms of vascular conductance as a wider range of drug-induced changes of vascular tone are generally better portrayed by conductance (Joyce *et al.*, 2019; Lautt, 1989; O'Leary, 1991; Wright *et al.*, 1987).

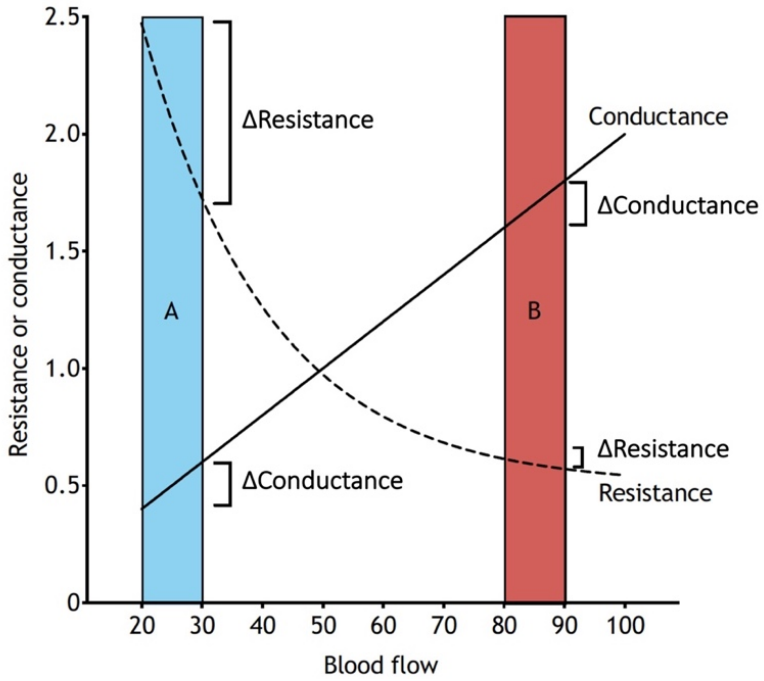


**Figure 5-2.** The hypothetical relationship between conductance, resistance and blood flow under constant blood pressure.
In case A (blue bar) and case B (red bar) the blood flow increases by an equal amount (10 arbitrary units). The change in resistance is 12 times greater in case A compared to case B which had a greater starting blood flow. The change in conductance is directly proportional to the change in blood flow irrespective of the starting blood flow. The figure was reproduced from Joyce *et al.* (2019).

#### 5.1.1.4 Heart rate

The cyclic contraction and relaxation of cardiac muscle create the forces necessary to pump blood throughout the body. The number of contractions per time unit is defined as heart rate. The heart rate and stroke volume are the physiological determinants of cardiac output:

$$\text{cardiac output} = \text{heart rate} \times \text{stroke volume} \quad (7)$$

Heart rate measurements are derived from haemodynamic pulsatile measurements such as blood pressure (section 5.1.1.1) and blood flow (section 5.1.1.2).

#### 5.1.1.5 Cutaneous blood flow

Cutaneous blood flow has an important thermoregulatory role (Mohrman & Heller, 2018). Cutaneous blood flow can increase and decrease during dilation and constriction of vessels as heat is being lost and retained, respectively.

Laser Doppler flowmetry is a non-invasive technique for measuring cutaneous blood flow. Laser Doppler flowmetry relies on the Doppler effect (Choi & Bennett, 2003; Tamura, 2014). To measure cutaneous blood flow, a laser Doppler surface probe is attached to shaved skin such as on a hindpaw. As the laser is emitted, a monochromatic and coherent beam will strike the surface under the laser Doppler probe. The beam can be reflected in two ways depending on its target. If the beam strikes a stationary surface, the light will be reflected with the same frequency as the transmitted light. However, if the beam strikes a moving surface (e.g. a red blood cell), the reflected light will undergo a frequency shift that corresponds to the movement of the object (Choi & Bennett, 2003). It is difficult to obtain reproducible cutaneous blood flow data with laser Doppler flowmetry because of the heterogeneity in tissue perfusion and vascular geometry in skin regions within and between animals (Tamura, 2014). It is also difficult to ensure that the laser probe is placed in the same proximate area in different animals. Because of these limitations, it is advisable to normalise the changes in cutaneous blood flow to baseline values within each experiment.

### 5.1.2 The appropriate anaesthesia for invasive haemodynamic studies

During invasive surgery, general anaesthesia is essential to alleviate the discomfort of the animal. The choice of anaesthetic agent should be carefully considered to ensure the appropriate depth of anaesthesia is achieved while maintaining the animal's normal physiological and pharmacological functions. The depth of anaesthesia may be evaluated through toe, tail and abdominal pinches, where the lack of withdrawal or movement indicates the loss of nociception. Field *et al.* (1993) evaluated and compared the depth of anaesthesia of three animal anaesthetic agents including urethane, pentobarbital and chloral hydrate. They concluded that intraperitoneal administration of an anaesthetic drug to rats first led to the loss of muscle tone, palpebral reflex and abdominal pinch response, followed by the disappearance of tail pinch response and loss of corneal reflex. Field *et al.* (1993) concluded that the lack of response to tail and toe pinches is an adequate indicator of the appropriate depth of anaesthesia for moderate to markedly painful procedures.

Most anaesthetic agents induce cardiovascular changes as demonstrated in rats administered with pentobarbital (60 mg/kg i.p.), isoflurane (2% in air vaporizer), ketamine-xylazine (75 and 5 mg/kg, respectively, i.m.) and chloralose-urethane (100 and 500 mg/kg i.p.; Bencze *et al.*, 2013). With the exception of pentobarbital, all anaesthetic agents decreased blood pressure by blunting the sympathetic nervous system. Blood pressure effects of isoflurane and chloralose-urethane are likely mediated by an enhanced contribution of the renin-angiotensin system and/or decreased contribution of the sympathetic nervous system and nitric oxide. Ketamine-xylazine was the only anaesthetic agent that lowered the heart rate of rats. Pentobarbital is a useful anaesthetic for rats as it preserves the resting blood pressure close to conscious animal levels. However, it is known to blunt the parasympathetic nervous system, so its use depends on the experimental question. Further, pentobarbital has become difficult to obtain for laboratory use because of import bans due to illegal use of the drug in human euthanasia.

#### 5.1.2.1 Urethane

Urethane is a widely used animal anaesthetic agent due to its long-lasting duration (6-10 h) and limited effects on cardiorespiratory and spinal reflexes (Bauquier & Golder, 2010; Flecknell, 2015; Hara & Harris, 2002; Teppema & Baby, 2011). It is inappropriate to use urethane for long-term chronic studies as it is carcinogenic. The mechanisms of action behind urethane's anaesthetic effects likely involve the enhancement of synaptic inhibitory neurotransmission or inhibition of excitatory neurotransmission (Hara & Harris, 2002). More specifically, urethane modestly potentiates the effects of neuronal $GABA_A$, nicotinic acetylcholine and glycine receptors, and inhibits NMDA and AMPA receptors.

There is controversy regarding urethane's anaesthetic effectiveness as electroencephalograms after urethane administration are similar to those recorded in conscious animals (reviewed in Bauquier & Golder, 2010). Adding to the controversy, urethane's ability to block gross purposeful movement to pain stimuli is not a sole indicator of its anaesthetic efficiency since effective anaesthesia also involves blocking sensory and perceptive components (Bauquier & Golder, 2010). The controversy surrounding urethane prompted Bauquier and Golder (2010) to study its anaesthetic properties. They concluded that intravenous urethane provided appropriate anaesthesia at a high dose (1.5 mg/kg) by preventing gross movement in response to the clamping of tail tips with a haemostat. Similarly, intraperitoneal administration of high urethane doses (1.2 and 1.5 mg/kg) abolished motor responses to toe, tail and abdominal pinch with an alligator clip for at least 2 h after urethane administration (Field *et al.*, 1993). They also noted that while urethane removed rats' motor response to pain stimuli, they retained occasional limb twitches, whisker movements and breathing over the ventilator, indicating that urethane is unlikely to induce pain relief by solely blocking motor functions (Bauquier & Golder, 2010). While studies generally claim that urethane has limited cardiovascular effects, a recent study on cannabidiol's haemodynamic effects in rats observed that urethane-anaesthetised rats had 25 and 10% lower systolic blood pressure and heart rate, respectively, compared to conscious rats (Kossakowski *et al.*, 2019).

### 5.1.3 The haemodynamic effects of acute cannabidiol administration under physiological cardiovascular conditions

Recent publications have reviewed the haemodynamic effects (heart rate, blood pressure and blood flow) of cannabidiol in humans, dogs, piglets, rabbits, rats and mice (Kicman & Toczek, 2020; Sultan *et al.*, 2017). The publications noted extensive heterogeneity between study protocols regarding species, dosage, route of administration, the time between cannabidiol administration and measurements of cardiovascular effects. Cannabidiol generally had little to no effect on haemodynamic parameters under physiological conditions.

#### 5.1.3.1 In humans

To date, nineteen studies have assessed the haemodynamic effects of cannabidiol in humans under normal cardiovascular conditions (Table 5-1). While most studies report that acute cannabidiol administration does not alter cardiovascular function, there are some exceptions. For instance, one study reported that participants who received a single oral dose of cannabidiol (600 mg) had a resulting lower heart rate (-10 beats/min; Jadoon *et al.*, 2017). Three studies reported a lower mean arterial pressure (-2 to -6 mmHg) in participants who were treated with oral cannabidiol (600 mg) or enhanced cannabidiol delivery capsules (TurboCBDTM; 90 mg; Jadoon *et al.*, 2017; Patrician *et al.*, 2019; Sultan *et al.*, 2020). Two of the studies also reported that cannabidiol decreased diastolic blood pressure (DBP; Jadoon *et al.*, 2017; Patrician *et al.*, 2019). While few studies have assessed the effects of cannabidiol on blood flow, two studies reported that cannabidiol (400 mg p.o.) and TurboCBD$^{TM}$ (90 mg p.o.) increased regional cerebral blood flow (Crippa *et al.*, 2004; Patrician *et al.*, 2019). In contrast, one study reported that cannabidiol (600 mg p.o.) decreased forearm skin blood flow (Jadoon *et al.*, 2017).

While the cardiovascular effects of cannabidiol under physiological cardiovascular conditions appear to be small, cannabidiol has been shown to blunt the haemodynamic effects of stress in humans (Sultan *et al.*, 2017).

Studies of the cardiovascular effects of cannabidiol in humans have several limitations. Firstly, there is a lack of diversity among participants as studies were mainly performed on young white men (Table 5-1). As it is well-established that a patient's response to a drug may be heavily governed by the patient's sex, race and ethnicity (Ramamoorthy *et al.*, 2015), it is important that future studies are performed in a more diverse population. Another limitation is associated with the small sample size of participants.

**Table 5-1.** Literature-reported haemodynamic effects of acute cannabidiol administration in human under physiological conditions

| Participants (age) | Dose[1] | RoA | HR | MAP | SBP | DBP | BF | Other | Reference |
|---|---|---|---|---|---|---|---|---|---|
| 11♂, 4♀ (18-24, x̃: 20.9) | 320 µg/kg (17.5-30 mg) | p.o. | ↔ | – | – | – | – | – | Belgrave *et al.* (1979) |
| 6♂, 2♀ (20-38, x̄: 27) | 1 mg/kg (67 mg)[2] | p.o. | ↔ | – | – | – | – | – | Zuardi *et al.* (1982) |
| 12♂ (x̄: 24) | 45, 90 mg | p.o. | ↔ | ↔ | ↔ | ↔ | ↔CBF | – | Patrician *et al.* (2019) |
| | TurboCBD™ 3 45, 90 mg | | ↔ | ↓[4] | ↔ | ↓[4] | ↑CBF | – | |
| 18♂, 22♀ (20-30, x̄: 22.8) | 300 mg | p.o. | ↔ | – | ↔ | – | – | – | Zuardi *et al.* (1993) |
| 10♂ (25-42, x̄: 29.8) | 400 mg | p.o. | – | – | – | – | ↑CBF | – | Crippa *et al.* (2004) |
| 14♂; White (20-42, x̄: 26.) | 600 mg | p.o. | ↔ | – | ↔ | ↔ | | – | Borgwardt *et al.* (2008) |
| 15♂ (x̄: 26) | 600 mg | p.o. | ↔ | ↔ | – | – | – | – | Bhattacharyya *et al.* (2009) |
| 15♂; White (18-35, x̄: 26.7) | 600 mg | p.o. | ↔ | ↔ | – | – | – | – | Fusar-Poli *et al.* (2009) |
| 15♂; White (20-42, x̄: 26.7) | 600 mg | p.o. | ↔ | ↔ | – | – | – | – | Bhattacharyya *et al.* (2010) |
| 10♂; White, mixed (7:3) (20-36) | 600 mg | p.o. | ↔ | – | ↔ | ↔ | – | – | Hallak *et al.* (2011) |
| 14♂; White (20-42, x̄: 26.7) | 600 mg | p.o. | ↔ | ↔ | – | – | – | – | Winton-Brown *et al.* (2011) |
| 16♂ (20-42, x̄: 26.4) | 600 mg | p.o. | ↔ | – | ↔ | ↔ | – | – | Martin-Santos *et al.* (2012) |
| 9♂ (19-29, x̄: 23.7) | 600 mg | p.o. | ↑ | ↓ | ↓ | ↓ | ↓Forearm SBF | ↓SV, ↔CO, ↔EJT, ↓TPR | Jadoon *et al.* (2017) |
| 13♂ (x̄: 26.3) | 600 mg | p.o. | ↔ | ↓ | ↔ | ↔ | – | ↔SV, ↔CO, ↔EJT, ↔TPR | Sultan *et al.* (2020) |
| 31 ♂ & ♀; Black, White, mixed (15:12:4) (18-50, x̄: 29.1) | 200, 400, 800 mg | p.o. | ↔ | – | ↔ | ↔ | – | – | Haney *et al.* (2016) |
| 10♂ | 100, 600, 1200 mg | p.o. | ↔ | – | ↔ | ↔ | – | – | Gong *et al.* (1984) |

| | | | | | | | | | |
|---|---|---|---|---|---|---|---|---|---|
| (21-32) | | | | | | | | | |
| 12 | 20, 40 mg | s.l. | ↔ | — | ↑ | ↔ | — | — | Tomida *et al.* (2006) |
| 8♂ & 4♀; Black, White, Asian (2:9:1) (21-48, $\bar{x}$: 26.) | 83 mg[5] | inhalation (smoking) | ↔ | — | ↔ | ↔ | — | — | Kayser *et al.* (2020) |
| 31♂ & 5♀ (18-51) | 400 mg | inhalation (vapour) | ↔ | ↔ | ↔ | — | — | — | Solowij *et al.* (2019) |

**CBF**, cerebral blood flow; **CO**, cardiac output; **EJT**, ejection time; **p.o.**, peroral; **SBF**, skin blood flow; **s.l.**, sublingual; **SV**, stroke volume; **TPR**, total peripheral resistance; **↑**, increase; **↓**, decrease; **↔**, no change; **—**, not reported; **$\tilde{x}$**, median; **$\bar{x}$**, mean; **♂**, male; **♀**, female [1]Cannabidiol dose ∝ blue shade intensity. [2]Dose estimation based on average participant weight (67 kg). [3]Enhanced cannabidiol delivery capsules which increase the bioavailability of cannabidiol. [4]A trend towards decreased values at $c_{max}$ of TurboCBD™ 90 mg. [5]Contained: 800 mg *Cannabis* 0.4% THC and 10.4% cannabidiol. This table was reproduced from Kicman and Toczek (2020).

#### 5.1.3.2 In rats

There is a notable heterogeneity in study protocols of cannabidiol's haemodynamic effects in rats which may explain the mixed reports of cannabidiol's cardiovascular effects (Table 5-2). Cannabidiol (10 µg/kg to 20 mg/kg) administered locally to the bed nucleus of the stria terminalis and cisterna magna, and via the intravenous and intraperitoneal route, generally did not affect heart rate (Table 5-2). However, in pithed and vagotomised rats, cannabidiol 1, 3 and 10 mg/kg (i.v.) increased heart rate and systolic blood pressure by 50-100 beats/min and 20 mmHg, respectively, in both SHR and WKY rats (Kossakowski *et al.*, 2019). In contrast, diastolic blood pressure was dose-dependently decreased by 5-10 mmHg. In the same study, rats were also rapidly injected with cannabidiol (3, 10 and 30 mg/kg i.v.) which caused a dose-dependent decrease in heart rate, systolic and diastolic blood pressure in SHR by 65, 20 and 65%, respectively. All cardiovascular responses to cannabidiol were 30-40% smaller in WKY. Maximum cardiovascular responses occurred within the first 30 s after cannabidiol administration. In conscious rats, cannabidiol 10 mg/kg (i.p.) had no effect on cardiovascular parameters measured via telemetry (section 5.1.1.1), however, one study reported that cannabidiol (50 µg/kg i.v.) decreased mean arterial pressure (-16 mmHg) without affecting heart rate in pentobarbital-anaesthetised Sprague-Dawley rats (Walsh *et al.*, 2015). No studies to date have investigated the effects of cannabidiol on blood flow *in vivo*.

**Table 5-2.** Literature-reported haemodynamic effects of acute cannabidiol administration in rats

| Animals | Anaesthesia | Dose[1] | RoA | HR | MAP | SBP | DBP | Reference |
|---|---|---|---|---|---|---|---|---|
| ♀SD 200-300 g | Pentobarbital | 50 µg/kg | i.v. | ↔ | ↓ | — | — | Walsh *et al.* (2015) |
| ♂Wistar albino 280-380 g | Thiopental | 50 µg/kg | i.v. | ↔ | ↔ | — | — | Gonca and Darıcı (2015) |
| ♀SD 180-220 g | Urethane | 1 mg/kg | i.v. | ↔ | ↔ | — | — | Graham and Li (1973) |
| ♂Wistar 214-455 g ($\bar{x}$: 350 g) | Pentobarbital | 0.003-5.7 mg/kg | i.a., i.v | — | ↔ | — | — | McQueen *et al.* (2004) |
| ♂SHR & WKY 270-320 g & 290-390 g | Urethane (pithed[2]) | 1, 3, 10 mg/kg | i.v. | ↑ | — | ↑ | ↓ | Kossakowski *et al.* (2019) |
| ♂SHR & WKY 270-320 g & 290-390 g | Urethane | 3, 10, 30 mg/kg | i.v. (rapid) | ↓ | — | ↓ | ↓ | Kossakowski *et al.* (2019) |
| ♂Wistar 250 g | — | 10 mg/kg | i.p. | ↔ | ↔ | — | — | Resstel *et al.* (2006) |
| ♂SHR & WKY 270-320 g & 290-390 g | — | 10 mg/kg | i.p. | ↔ | — | ↔ | ↔ | Kossakowski *et al.* (2019) |
| ♂Wistar | — | 1, 10, 20 mg/kg | i.p. | ↔ | ↔ | — | — | Resstel *et al.* (2009) |
| ♂Wistar 250-270 g | — | 15, 30, 60 nmol (19-76 µg/kg[3]) | i.c. | ↔ | ↔ | — | — | Granjeiro *et al.* (2011) |
| ♂Wistar 230-270 g | — | 15, 30, 60 nmol (21-82 µg/kg[3]) | Into BNST | ↔ | ↔ | — | — | Gomes *et al.* (2012) |
| ♂Wistar 230-270 g | — | 15, 30, 60 nmol (21-82 µg/kg[3]) | Into BNST | ↔ | ↔ | — | — | Gomes *et al.* (2013a) |
| ♂Wistar 230-270 g | — | 60 nmol (82 µg/kg[3]) | Into BNST | ↔ | ↔ | — | — | Alves *et al.* (2010) |

**BNST**, bed nucleus of the stria terminalis; **i.a.**, intra-arterially; **i.c.**, intracisternally; **i.p.**, intraperitoneal; **i.v.**, intravenous; **SD**, Sprague Dawley; **SHR**, Spontaneously Hypertensive Rats; **WKY**, Wistar Kyoto Rat; ↑, increase; ↓, decrease; ↔, no change; —, not reported; $\bar{x}$, mean; ♂, male; ♀, female
[1]Cannabidiol dose ∝ blue shade intensity. [2]The central nervous system has been destroyed. [3]Dose estimation based on the lowest rat weight. The table was reproduced from Kicman and Toczek (2020).

#### 5.1.3.3 Allometric dose scaling

Interspecies dose extrapolation is important in biomedical research as it ensures safe and effective drug treatment of both humans and animals. Drug dose scaling is not simply based on dose per body weight since there are greater physiological differences between species that need to be considered (reviewed in Nair & Jacob, 2016). To more accurately predict the interspecies pharmacokinetic differences of a drug, the interspecies surface area difference is used. The surface area of an animal is a strong indicator of an animal's metabolic rate. Allometric scaling has proven to be appropriate for drugs with lesser hepatic metabolism, low volume of distribution, and are excreted via the renal route, all characteristics that poorly fit the pharmacokinetic profile of cannabidiol (section 1.5.3). Allometric scaling has been able to successfully predict the renal clearance of drugs (Chaturvedi *et al.*, 2001). In contrast, hepatic clearance has proved difficult to predict with allometric scaling.

To convert doses between species, a species-specific correction factor ($K_m$) is used. $K_m$ is calculated by dividing an estimation of the average body weight of a species (kg) by its body surface area ($m^2$). A human equivalent dose is calculated by multiplying the animal dose with the $K_m$ ratio of the two different species:

$$\text{Human equivalent dose (mg/kg)} = \text{Animal dose (mg/kg)} \times \frac{\text{Animal } K_m}{\text{Human } K_m} \qquad (8)$$

In this study, the human equivalent dose for the rat cannabidiol doses of 10 and 30 mg/kg (i.v.) would be 1.9 and 5.7 mg/kg, respectively. The corresponding absolute dose in a person that weighs 60 kg would be 114 and 341 mg, respectively (Table 5-3). However, as cannabidiol is a poor candidate for allometric calculation, there is a great risk of inaccuracy in this calculation.

**Table 5-3.** Human equivalent cannabidiol dose calculations based on rat doses

| Species | Body weight (kg) | $K_m$ | Dose 1 | Dose 2 |
|---|---|---|---|---|
| Rat | 0.25 | 7 | 10 mg/kg | 30 mg/kg |
| Human | 60 | 37 | 1.9 mg/kg | 5.7 mg/kg |

$K_m$: species-specific correction factor

### 5.1.4 Study aims

This study aimed to investigate the acute haemodynamic effects of intravenously administered cannabidiol in urethane-anaesthetised rats. We measured the influence of single and cumulative i.v. bolus cannabidiol (10-30 mg/kg) administration on heart rate and mean arterial pressure, and importantly, on vascular conductance in two vascular beds and on hindpaw cutaneous blood flow. We further investigated the haemodynamic mechanisms of action of cannabidiol with administration of inhibitors of various potential targets.

## 5.2 Methods

### 5.2.1 Animals

The Animal Ethics Committee of the University of Melbourne approved experiments (approval #1814705) in accordance with *The Australian Code for the care and use of animals for scientific purposes* (8th edition, 2013, National Health and Medical Research Council, Canberra). Male Sprague-Dawley rats (270-300 g, Biomedical Animal Facility, Melbourne, Australia) were used in this study and housed in groups of 3–4 in standard cages under constant climatic conditions (21°C, 12 h light/dark cycle), with food and water *ad libitum*.

### 5.2.2 Experimental procedures

#### 5.2.2.1 Anaesthesia

Rats were placed in an induction container and briefly anaesthetised with 5% isoflurane (Baxter Healthcare, Old Toongabbie, NSW, Australia) in room air/$O_2$ using an isoflurane anaesthetic vaporiser (Penlon Sigma Delta; Penlon Limited, Abingdon, UK) before being deeply anaesthetised with urethane (2 g/kg i.p.). Surgical procedures were initiated once the rat stopped responding to toe pinches, demonstrating an appropriate depth of anaesthesia (section 5.1.2.1).

#### 5.2.2.2 Surgical procedures

The anaesthetised rat was placed in a supine position on a heating pad (Physiosuite, Kent Scientific Corp., Torrington, CT, USA) connected to a rectal probe to monitor that an appropriate body temperature was maintained (37.5-38.0°C). The local anaesthetic lignocaine was administered (1% s.c.) to the shaved neck and abdomen, prior to incisions.

##### 5.2.2.2.1 Tracheotomy

Rats were tracheotomised to enable airway access for mechanical ventilation. A horizontal incision between tracheal cartilages was made where a plastic Y-connector attached to a tracheotomy tube was inserted. The tube was connected to a rodent

respiratory pump (#7025 Rodent Ventilator, Ugo Basile, Comerio, VA, Italy) which utilised room air supplemented with 100% oxygen to ventilate the animal. The stroke volume was initially set at 6 ml/kg body weight and stroke rate at ~76 breaths/min and were adjusted to maintain arterial pH at 7.4 ± 0.2 as determined by regular measurements of blood pH, $O_2$ and $CO_2$ (ABL5, Radiometer Medical A/S, Copenhagen, Denmark).

#### 5.2.2.2.2 Measurement of haemodynamic parameters

The right jugular vein was isolated and catheterised with a saline-filled polyvinyl chloride catheter (i.d. 0.50 mm and o.d. 0.80 mm) for intravenous drug administration. To enable blood pressure measurement, a heparinised (10 U/ml) saline-filled catheter was inserted in the right carotid artery. The catheter was connected to a blood pressure transducer (Argon Medical Devices, Athens, Greece) that continuously measured phasic arterial blood pressure via a PowerLab data acquisition system (ADInstruments Pty. Ltd., Bella Vista, NSW, Australia). The left carotid artery was exposed and carefully isolated from the vagus nerve and surrounding tissues. An incision was made in the midline abdomen and the superior mesenteric artery was isolated. Perivascular Transonic flow probes (2.5 mm i.d., ADInstruments) were placed around the left carotid and superior mesenteric arteries to measure volume blood flow. To measure hindpaw cutaneous blood flow, a laser Doppler surface probe (MSP300XP, ADInstruments) was attached to the shaved skin of one hindpaw using an adhesive ring for surface probes (MSP140AR, ADInstruments). To ensure minimal interference of the ambient room conditions, rats were covered with bubble wrap and the rat's body temperature was maintained with a heating pad. The blood pressure transducer and the flow probes were calibrated, and stable haemodynamic parameters were measured for 20 min prior to starting the experiment (section 5.2.2.3).

#### 5.2.2.3 Experimental protocol

##### 5.2.2.3.1 Haemodynamic effects of cumulative or single cannabidiol administration

For cumulative cannabidiol treatment, rats were either administered with cumulative cannabidiol bolus doses (10 and 30 mg/kg i.v.) or corresponding vehicle (ethanol:cremophor:saline 2:2:6, 1 and 3 ml/kg i.v.) at 30 min intervals. For single cannabidiol treatment, rats were administered with the antagonist vehicle (ethanol:cremophor:saline 1:1:18, 1 ml/kg i.v.) prior to a single cannabidiol bolus dose, 30 mg/kg i.v., 30 min later. Bolus doses were administered slowly over 3-4 min.

##### 5.2.2.3.2 Mechanisms of action of cannabidiol

To investigate the possible involvement of $CB_1$, $CB_2$, TRPV1, CGRP or 5-$HT_{1A}$ receptors in the effects of cannabidiol, rats were administered either i.v. rimonabant 3 mg/kg, SR144528 1 mg/kg, capsazepine 1 mg/kg, rimegepant 2.5 mg/kg or WAY-100635 1 mg/kg, respectively, prior to a single bolus i.v. administration of cannabidiol 30 mg/kg 20 min later

#### 5.2.2.4 Euthanasia

At the completion of the experimental protocol, each rat was euthanised with an overdose of pentobarbitone (Lethobarb, >100 mg/kg i.v.) and a cut through the spinal cord.

### 5.2.3 Data and statistical analyses

The haemodynamic variables assessed included heart rate (HR), mean arterial pressure (MAP), carotid vascular conductance (CVC, carotid blood flow/MAP), mesenteric vascular conductance (MVC, mesenteric blood flow/MAP) and hindpaw cutaneous laser Doppler flux (LDF). All data are expressed as the mean ± S.E.M. from *n* experiments. *n* is the number of separate rats. Heart rate, mean arterial pressure, carotid and mesenteric vascular conductance were expressed as absolute values while LDF was

expressed as % from individual baseline values. Data plotting and statistical analyses were performed with Prism 9 (Graphpad Software, La Jolla, CA, USA).

Baseline values prior to drug administration were compared between 2 different groups with Student's unpaired *t*-test (Figure 5-3). The effects of drug treatment compared to baseline values within a treatment group were analysed using repeated measures one-way ANOVA with Greenhouse-Geisser correction for lack of sphericity and Dunnett's *post hoc* test for multiple comparisons. The effects between drug treatments over time were analysed using repeated measures two-way ANOVA with Greenhouse-Geisser correction for lack of sphericity and Šidàk's *post hoc* test for multiple comparisons. *P* values ≤ 0.05 were considered significant.

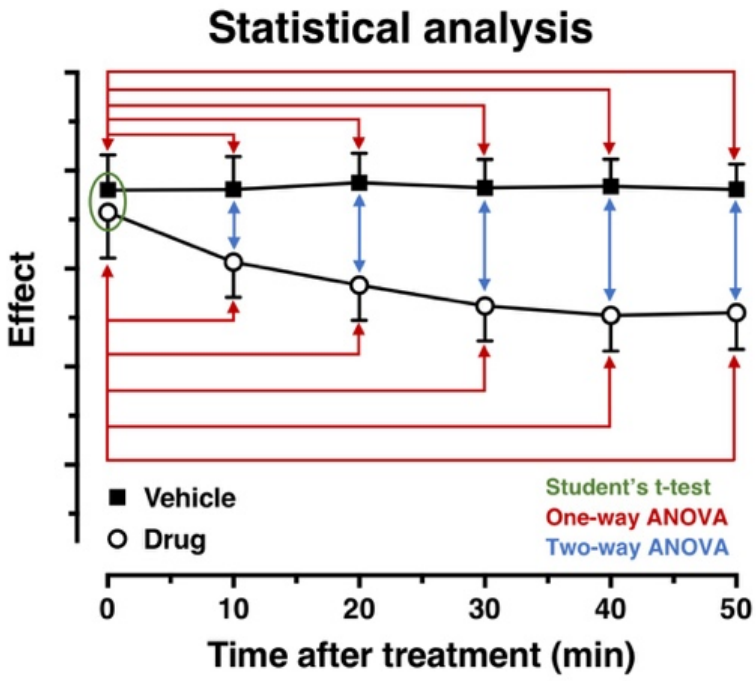


**Figure 5-3.** Schematic presentation of the repeated and multiple comparisons statistical tests performed in this study according to Ludbrook (1994) recommendations to minimise the risk of type 1 errors (false positives).
Student's unpaired *t*-test was performed to compare baseline levels between two different groups prior to drug treatments. Repeated measures one-way ANOVA with Greenhouse-Geisser correction for lack of sphericity and Dunnett's *post hoc* test for multiple comparisons was performed to compare the effects with baseline within a group over time. Repeated measures two-way ANOVA with Greenhouse-Geisser correction for lack of sphericity and Šidàk *post hoc* test for multiple comparisons was performed to compare the effects of two different treatment groups at different time points (Ludbrook, 1994).

### 5.2.4 Drugs

Drugs used were: (-)-cannabidiol; rimegepant; rimonabant; SR144528 (all from Cayman Chemical, Ann Arbor, MI, USA); capsazepine (Biomol, Hamburg, Germany); WAY-100635 (AdooQ, Irvine, CA, USA). All drugs solution were prepared on the day of the experiment except for WAY-100635 (1 mg/ml) which was dissolved in saline and single-use aliquots were stored at -20°C. Cannabidiol (10 mg/ml) was dissolved in ethanol, cremophor and saline (2:2:6). Capsazepine (1 mg/ml), rimonabant (3 mg/ml) and SR144528 (1 mg/ml) were dissolved in ethanol, cremophor and saline (1:1:18). Rimegepant (1 mg/ml) was dissolved in ethanol and PEG300 (1:9).

## 5.3 Results

### 5.3.1 Haemodynamic effects of cumulative or single cannabidiol administration

There were no differences in baseline haemodynamic measurements prior to single or cumulative bolus i.v. cannabidiol (10-30 mg/kg) or corresponding vehicle administration ($P$>0.05; Figure 5-4 and Figure 5-5), except for baseline heart rate values (prior to cumulative vehicle or cannabidiol administration) where rats in the vehicle group had higher baseline heart rates (+66 ± 23 beats/min) compared with rats in the cannabidiol group ($P$=0.014; Figure 5-4A).

The initial acute effects (at 1-3 min) of cumulative cannabidiol administration of 10 and 30 mg/kg included dose-dependent falls in heart rate of -50 ± 10 and -70 ± 15 beats/min, respectively ($P$≤0.01; Table 5-4 and Figure 5-4A). In comparison, a single cannabidiol dose of 30 mg/kg acutely (at 2 min) decreased heart rate by 122 ± 15 beats/min (Table 5-4; $P$=0.0002). Heart rate recovered to baseline levels after 30 min for single cannabidiol 30 mg/kg administration (Figure 5-5A; $P$>0.05, compared with time 0 min). The cumulative doses of cannabidiol 10 and 30 mg/kg also acutely decreased mean arterial pressure by 17 ± 4 mmHg and 17 ± 5, respectively ($P$≤0.05; Table 5-4). The decrease in mean arterial pressure was transient and not apparent 5 min after each cumulative cannabidiol administration (Figure 5-4B; $P$=0.10). The single cannabidiol 30 mg/kg dose acutely decreased mean arterial pressure by 16 ± 5 mmHg ($P$=0.019; Table 5-4), before returning to baseline at 10 min (Figure 5-5B; $P$=0.11).

Cumulative cannabidiol 10 and 30 mg/kg doses acutely increased carotid vascular conductance by 0.021 ± 0.004 and 0.026 ± 0.006 ml/min/mmHg, respectively ($P$≤0.01; Table 5-4). Single cannabidiol 30 mg/kg administration also caused an acute increase in carotid vascular conductance (+0.016 ± 0.003 ml/min/mmHg; $P$=0.0013; Table 5-4). The increase in carotid vascular conductance was transient and only maintained for single cannabidiol 30 mg/kg i.v administration (5 min; $P$=0.018; Figure 5-5C). The carotid vascular conductance in response to single cannabidiol 30 mg/kg administration is likely underestimated as the corresponding vehicle dose caused a significant and maintained (25 min) decrease in carotid vascular conductance ($P$≤0.05)

before returning to baseline ($P$>0.05; Figure 5-5C). Neither cumulative nor single doses of cannabidiol 30 mg/kg changed mesenteric vascular conductance acutely or over time ($P$>0.05; Table 5-4; Figure 5-4D, Figure 5-5D). However, the vehicle corresponding to the single cannabidiol 30 mg/kg dose acutely decreased mesenteric vascular conductance by 0.029 ± 0.009, which recovered to baseline levels after 15 min ($P$>0.05; Figure 5-5D). On the other hand, the lower cumulative dose of cannabidiol (10 mg/kg) acutely increased mesenteric vascular conductance by 0.012 ± 0.003 ($P$=0.0086; Table 5-4) which was maintained for 25 min ($P$≤0.05; Figure 5-4D). Cannabidiol did not change hindpaw laser Doppler flux compared to baseline ($P$>0.05; Table 5-4, Figure 5-4E, Figure 5-5E). In contrast, vehicle corresponding to the single cannabidiol 30 mg/kg dose significantly decreased hindpaw laser Doppler flux by 16 ± 4 ($P$=0.016) and 18 ± 5% ($P$=0.043) at 10 and 15 min, respectively ($P$<0.05; Figure 5-5E).

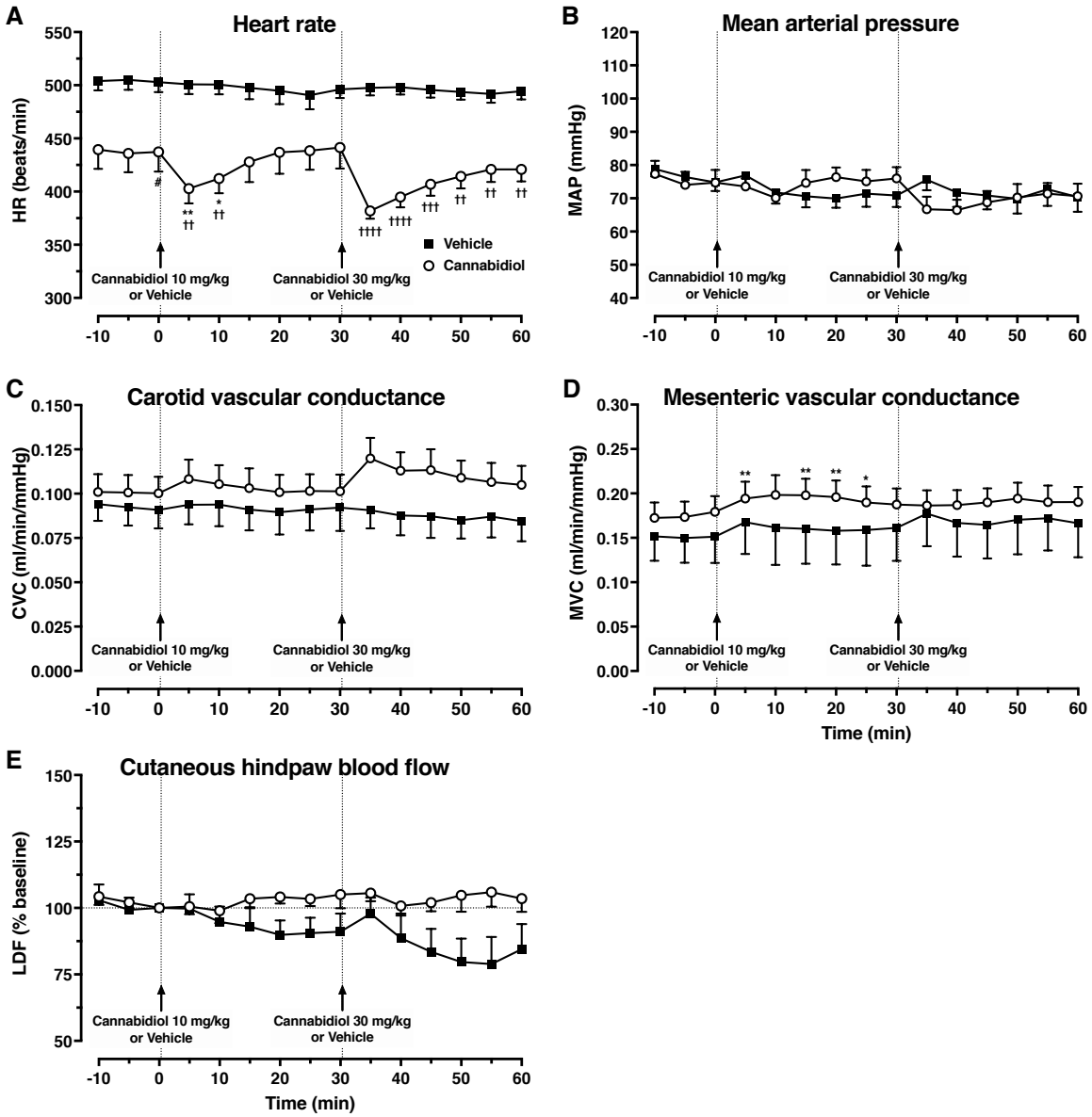


**Figure 5-4.** Effects of cumulative i.v. bolus administration of cannabidiol 10 and 30 mg/kg (*n*=6-8) and corresponding vehicle (ethanol, cremophor and saline; 2:2:6; 1 and 3 ml/kg; *n*=6) on rat haemodynamic parameters including heart rate (HR; A), mean arterial pressure (MAP; B), carotid vascular conductance (CVC; C), mesenteric vascular conductance (MVC; D) and hindpaw laser Doppler flux (LDF, values are expressed as a % of the within rat baseline at time 0 min; E).

Baseline recordings were taken at -10 to 0 min, followed by cannabidiol 10 mg/kg administration just after 0 min and cumulative administration of cannabidiol 30 mg/kg after 30 min. Data are mean ± S.E.M. $^{\#}P\leq0.05$ compared with vehicle baseline responses at 0 min; Student's unpaired *t*-test. $^{*}P\leq0.05$ or $^{**}P\leq0.01$ compared with baseline (at 0 min); repeated measures one-way ANOVA with Greenhouse-Geisser and Dunnett's *post hoc* test for multiple comparisons. $^{\dagger\dagger}P\leq0.01$, $^{\dagger\dagger\dagger}P\leq0.001$ or $^{\dagger\dagger\dagger\dagger}P\leq0.0001$ compared with vehicle treatment at each time point; repeated measures two-way ANOVA with Greenhouse-Geisser and Šidàk's *post hoc* test for multiple comparisons. *n*, number of rats.

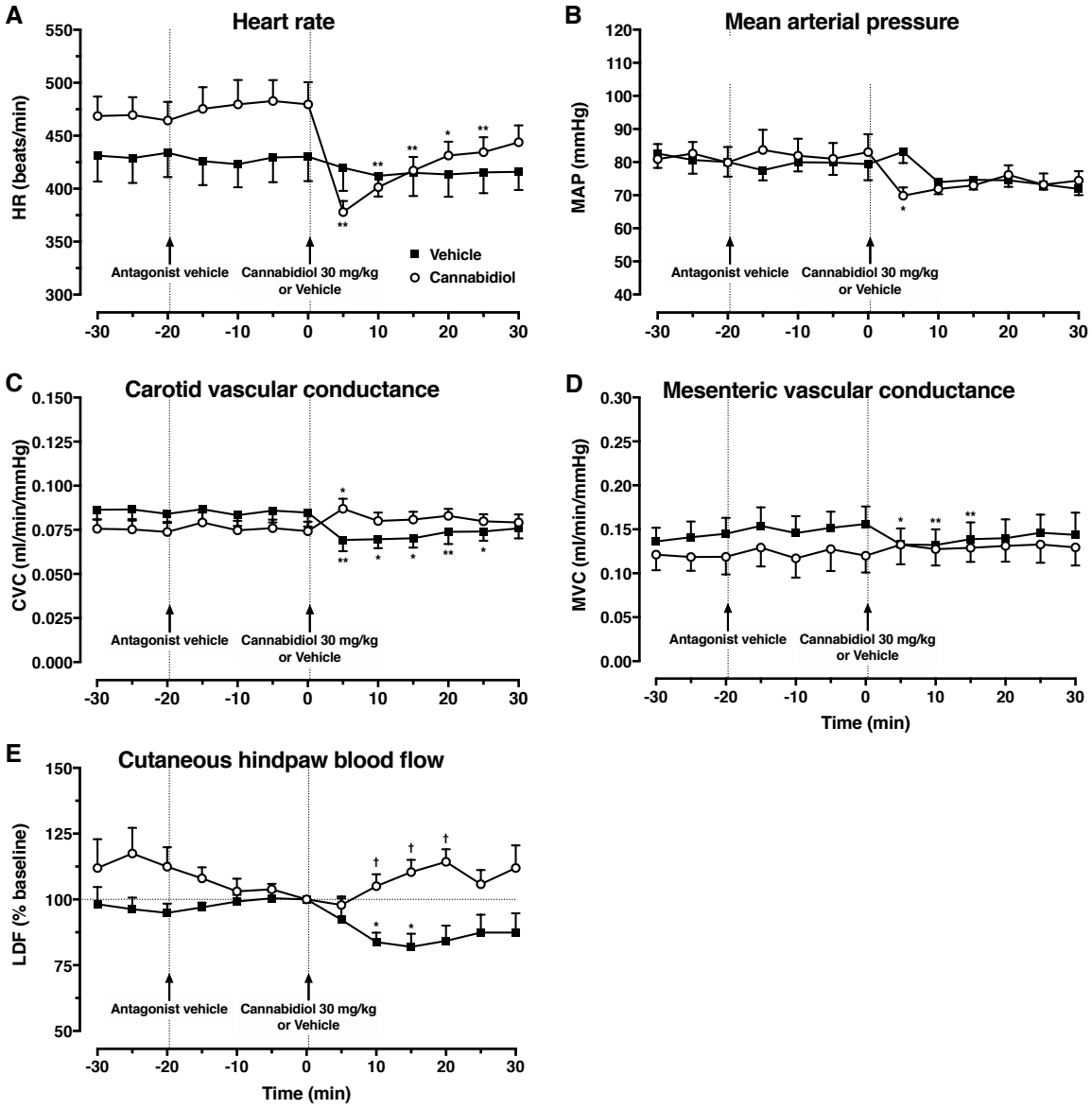


**Figure 5-5.** Effects of single i.v. bolus administration of cannabidiol 30 mg/kg (*n*=7) or corresponding vehicle (ethanol, cremophor and saline 2:2:6; 3 ml/kg; *n*=7) on rat haemodynamic parameters including heart rate (HR; A), mean arterial pressure (MAP; B), carotid vascular conductance (CVC; C), mesenteric vascular conductance (MVC; D) and hindpaw laser Doppler flux (LDF, values are expressed as a % of the within rat baseline at time 0 min; E).

Baseline recordings were taken at -30 to -20 min, followed by antagonist vehicle administration (ethanol, cremophor and saline 1:1:18; 1 ml/kg) after -20 min and a single cannabidiol 30 mg/kg administration after 0 min. Data are mean ± S.E.M. **P*≤0.05 or ***P*≤ 0.01 compared with pre-antagonist vehicle (at -20 min) or cannabidiol 30 mg/kg (at 0 min) administration; repeated measures one-way ANOVA with Greenhouse-Geisser and Dunnett's *post hoc* test for multiple comparisons. †*P*≤0.05 compared with vehicle treatment at each time point; repeated measures two-way ANOVA with Greenhouse-Geisser and Šidàk's *post hoc* test for multiple comparisons. *n*, number of rats.

**Table 5-4.** Peak haemodynamic changes to single or cumulative i.v. bolus cannabidiol administration

| Haemodynamic parameters | Cumulative i.v. cannabidiol | | Single i.v. cannabidiol |
|---|---|---|---|
| | **10 mg/kg** | **30 mg/kg** | **30 mg/kg** |
| **HR** (beats/min) | -50 ± 10** | -70 ± 15** | -122 ± 15*** |
| Time (min) | 1.2 ± 0.2 | 1.6 ± 0.2 | 1.7 ± 0.2 |
| *n* | 8 | 8 | 7 |
| **MAP** (mmHg) | -17 ± 4** | -17 ± 5* | -16 ± 5* |
| Time (min) | 0.8 ± 0.4 | 1.0 ± 0.3. | 2.4 ± 0.4 |
| *n* | 8 | 8 | 7 |
| **CVC** (ml/min/mmHg) | 0.021 ± 0.004** | 0.026 ± 0.006** | 0.016 ± 0.003** |
| Time (min) | 1.1 ± 0.3 | 1.4 ± 0.4 | 2.4 ± 0.4 |
| *n* | 8 | 8 | 7 |
| **MVC** (ml/min/mmHg) | 0.012 ± 0.003* | 0.001 ± 0.017 | 0.019 ± 0.011 |
| Time (min) | 2.0 ± 0.3 | 1.7 ± 0.3 | 3.0 ± 0.5 |
| *n* | 8 | 8 | 7 |
| **LDF** (%) | 20 ± 8 | 13 ± 8 | 3 ± 5 |
| Time (min) | 1.3 ± 0.4 | 0.8 ± 0.3 | 2.4 ± 0.7 |
| *n* | 6 | 6 | 7 |

HR, heart rate; MAP, mean arterial pressure; CVC, carotid vascular conductance; MVC, mesenteric vascular conductance; LDF, laser Doppler flux. Peak haemodynamic changes from respective pre-dose baseline values to single cannabidiol (30 mg/kg i.v.) or cumulative cannabidiol (10-30 mg/kg i.v.) treatment and the time from the end of cannabidiol administration (Figure 5-6) to peak changes are expressed as mean ± S.E.M. *$P \leq 0.05$, **$P \leq 0.01$ or ***$P \leq 0.001$ compared with the respective baseline measurement (0 min). Cumulative cannabidiol 10-30 mg/kg compared to baseline measurements (0 min); repeated measures one-way ANOVA with Greenhouse-Geisser correction and Dunnett's *post hoc* test for multiple comparisons. Single cannabidiol 30 mg/kg administration compared to baseline measurements (0 min); Student's paired *t*-test. *n*, number of rats.

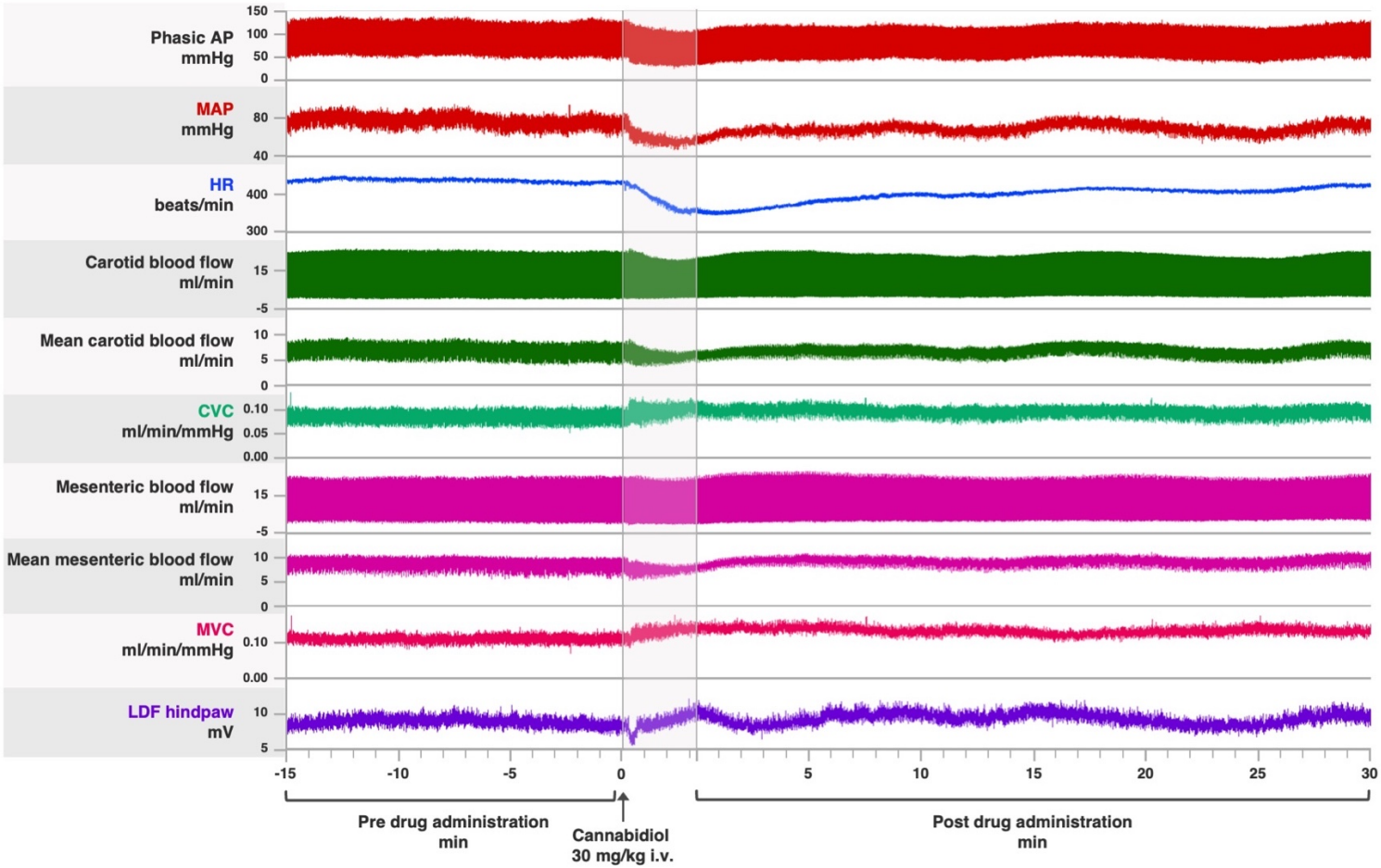


**Figure 5-6.** Representative recording of the acute effects of a single i.v. bolus of cannabidiol 30 mg/kg on rat haemodynamic parameters including: phasic arterial pressure (AP; mmHg), mean arterial pressure (MAP; mmHg), heart rate (HR; beats/min), carotid blood flow (ml/min), mean carotid blood flow (ml/min), carotid vascular conductance (CVC; ml/min/mmHg), mesenteric blood flow (ml/min), mean mesenteric blood flow (ml/min), mesenteric vascular conductance (MVC; ml/min/mmHg) and hindpaw laser Doppler flux (LDF; mV).
The carotid and mesenteric conductance (ml/min/mmHg) were calculated by dividing the respective vascular blood flow (ml/min) by MAP (mmHg).

### 5.3.2 The potential haemodynamic mechanisms of action of cannabidiol

To test the potential haemodynamic mechanisms of action of cannabidiol, rats were pre-administered with the $CB_1$ receptor antagonist rimonabant (3 mg/kg i.v.), $CB_2$ antagonist SR144528 (1 mg/kg i.v.), TRPV1 antagonist capsazepine (1 mg/kg i.v.), CGRP antagonist rimegepant (2.5 mg/kg i.v.) or 5-$HT_{1A}$ antagonist WAY-100635 (1 mg/kg i.v.) followed 20 min later by a single bolus i.v. administration of cannabidiol 30 mg/kg. There was no difference in baseline (-20 min) haemodynamic values prior to treatment with either vehicle or antagonists ($P$>0.05; Figure 5-7, Figure 5-9 and Figure 5-10).

#### 5.3.2.1 The possible involvement of cannabinoid receptors

Rimonabant increased resting heart rate and mean arterial pressure by 30 ± 9 beats/min and 26 ± 4 mmHg, respectively ($P$<0.05; Figure 5-7A, B). Neither the effects of rimonabant on heart rate nor mean arterial pressure recovered to baseline levels prior to the administration of cannabidiol 20 min later. SR144528 alone did not have an effect on heart rate or mean arterial pressure ($P$>0.05). Furthermore, neither rimonabant nor SR144528 attenuated the effects of cannabidiol on heart rate and mean arterial pressure ($P$>0.05; Figure 5-7A, B). Rimonabant and SR144528 alone had opposite effects on carotid vascular conductance. More specifically, rimonabant decreased carotid vascular conductance (-0.011 ± 0.003; $P$=0.021) while SR144528 slightly increased carotid vascular conductance (+0.0059 ± 0.001; $P$=0.025) at 10 and 5 min after administration, respectively (Figure 5-7C). Interestingly, rimonabant caused a 3.2-fold potentiation of the cannabidiol-induced increase in carotid vascular conductance (Figure 5-7C; Figure 5-8C; $P$=0.020). Rimonabant also maintained the cannabidiol-induced carotid vascular conductance increase throughout the experiment (30 min; $P$<0.05). In contrast, SR144528 inhibited the cannabidiol-induced increase in carotid vascular conductance at the 5 min time point (Figure 5-7C; Figure 5-8C; $P$=0.60). Rimonabant and SR1441528 generally had no effect on mesenteric vascular conductance and hindpaw laser Doppler flux, neither prior nor after the administration of cannabidiol ($P$>0.05; Figure 5-7D, E), with the exception of SR144528 which caused a transient increase in mesenteric vascular conductance (+0.015 ± 0.001; $P$=0.0003) 5 min after drug administration (Figure 5-7D).

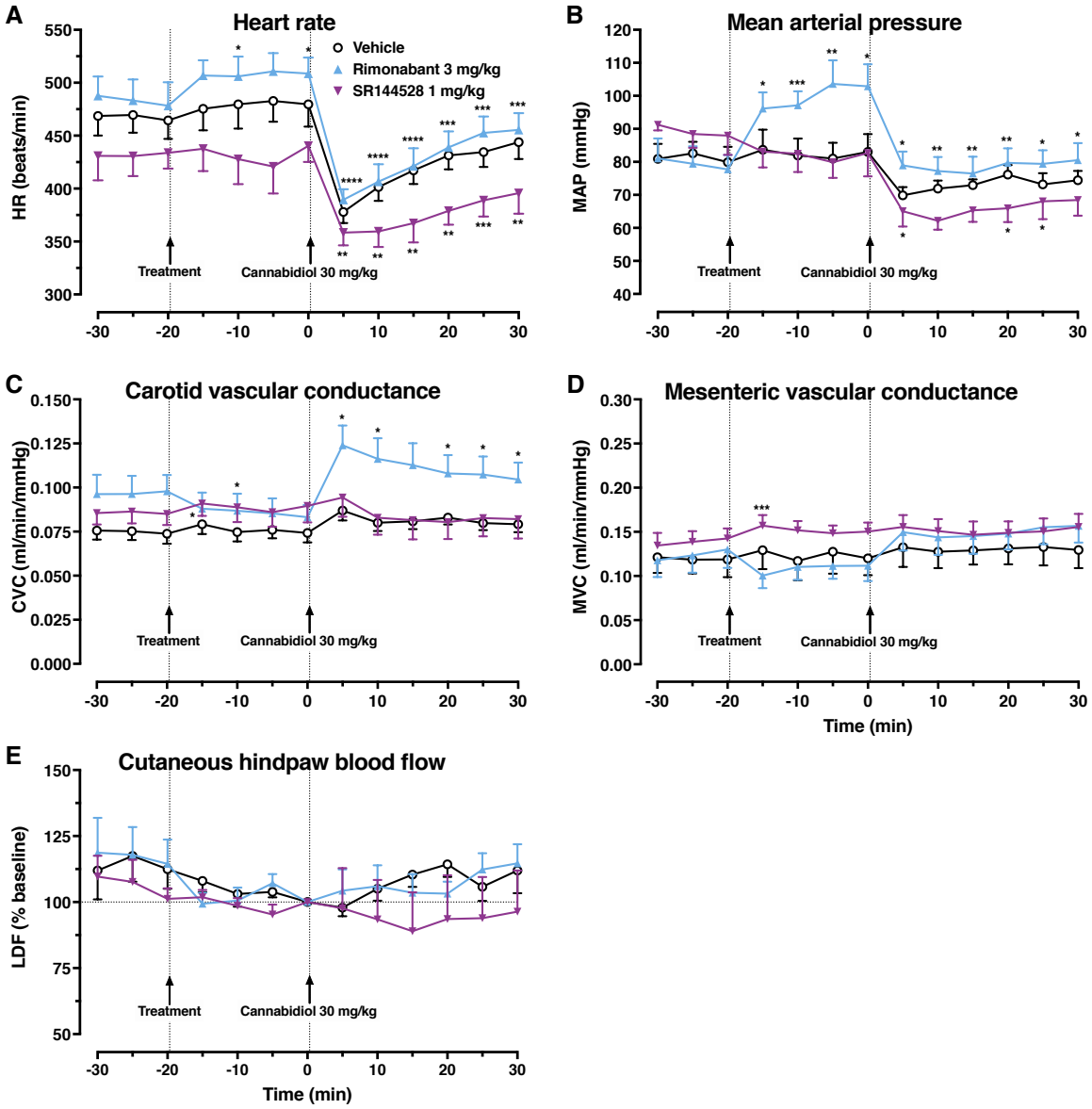


**Figure 5-7.** Effect of single i.v. bolus administration of cannabidiol 30 mg/kg in rats pretreated with the $CB_1$ antagonist rimonabant (3 mg/kg i.v.; *n*=6) and $CB_2$ antagonist SR144528 (1 mg/kg i.v.; *n*=5) on rat haemodynamic parameters including heart rate (HR; A), mean arterial pressure (MAP; B), carotid vascular conductance (CVC; C), mesenteric vascular conductance (MVC; D) and hindpaw laser Doppler flux (LDF, values are expressed as a % of the within rat baseline at time 0 min; E).

Baseline recordings were taken at -30 to -20 min, followed by administration of antagonists after -20 min and a single cannabidiol (30 mg/kg i.v.) administration after 0 min. As a reference, the cannabidiol 30 mg/kg responses in the absence of antagonists (*n*=7) are reproduced from Figure 5-5. Data are mean ± S.E.M. **P*≤0.05, ***P*≤0.01, ****P*≤0.001 or *****P*≤0.0001 compared with pre-antagonist (at -20 min) or cannabidiol 30 mg/kg (at 0 min) administration; repeated measures one-way ANOVA with Greenhouse-Geisser and Dunnett's *post hoc* test for multiple comparisons. *n*, number of rats.

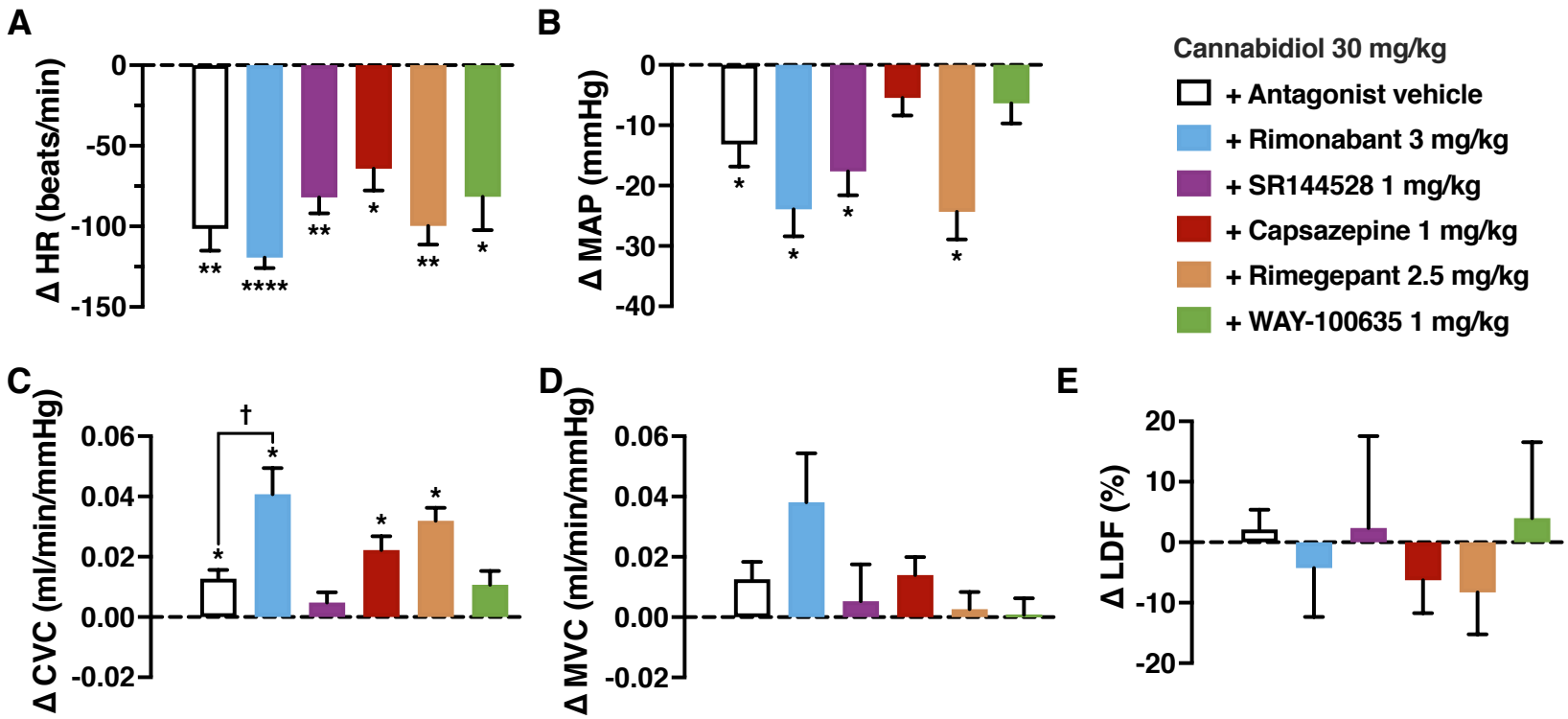


**Figure 5-8.** The haemodynamic effects of cannabidiol 30 mg/kg (single i.v. bolus) 5 min after administration in rats pretreated with antagonist vehicle (ethanol, cremophor and saline 1:1:18; 1 ml/kg; *n*=7), $CB_1$ antagonist rimonabant (3 mg/kg i.v.; *n*=6), $CB_2$ antagonist SR144528 (1 mg/kg i.v.; *n*=5), TRPV1 antagonist capsazepine (1 mg/kg; *n*=5), CGRP antagonist rimegepant (2.5 mg/kg; *n*=4-5) or 5-$HT_{1A}$ antagonist WAY-100635 (1 mg/kg; *n*=6-7).

Haemodynamic parameters measured include heart rate (HR; A), mean arterial pressure (MAP; B), carotid vascular conductance (CVC; C), mesenteric vascular conductance (MVC; D) and hindpaw laser Doppler flux (LDF; E). Data are Δ (change) mean ± S.E.M at 5 min after cannabidiol 30 mg/kg administration from baseline (0 min; Figure 5-7 to Figure 5-10). **P*≤0.05, ***P*≤0.01 or **** *P*≤0.0001, compared with pre-cannabidiol 30 mg/kg (at 0 min) administration; repeated measures one-way ANOVA with Greenhouse-Geisser and Dunnett's *post hoc* test for multiple comparisons. $^{\dagger\dagger}P$≤0.01 compared with cannabidiol 30 mg/kg only treatment (white bar); one-way ANOVA with Dunnett's *post hoc* test. *n*, number of rats.

#### 5.3.2.2 The possible involvement of TRPV1 and CGRP

Rimegepant (2.5 mg/kg) treatment had various haemodynamic effects on its own which included decreasing heart rate and carotid vascular conductance while also transiently increasing mean arterial pressure ($P$<0.05; Figure 5-9A-C). However, data from a pilot experiment suggest that it is the rimegepant vehicle (ethanol and PEG300 1:9; 2.5 ml/kg) that causes these haemodynamic changes rather than the interaction of rimegepant with CGRP receptors (data not shown).

Capsazepine (1 mg/kg) on its own did not affect heart rate ($P$>0.05) but did cause a transient increase in mean arterial pressure of 11 ± 3 mmHg at 5 min ($P$=0.037; Figure 5-8A). Rimegepant potentiated the cannabidiol-induced decrease in mean arterial pressure by prolonging the blood pressure-lowering effects for 25 min (Figure 5-8B). Neither capsazepine nor rimegepant affected cannabidiol-induced changes in heart rate ($P$>0.05; Figure 5-8A). While not significant, rats treated with capsazepine had lower mean arterial blood pressure (Figure 5-8B; -11 mmHg; $P$=0.082) and cannabidiol did not decrease mean arterial pressure from this lower starting pressure (Figure 5-9B; $P$=0.39). Capsazepine alone did not affect carotid vascular conductance but extended the cannabidiol-induced increase in conductance over a 25 min period ($P$<0.05). Neither rimegepant nor capsazepine affected mesenteric vascular conductance or hindpaw laser Doppler flux (Figure 5-9D, E; $P$>0.05).

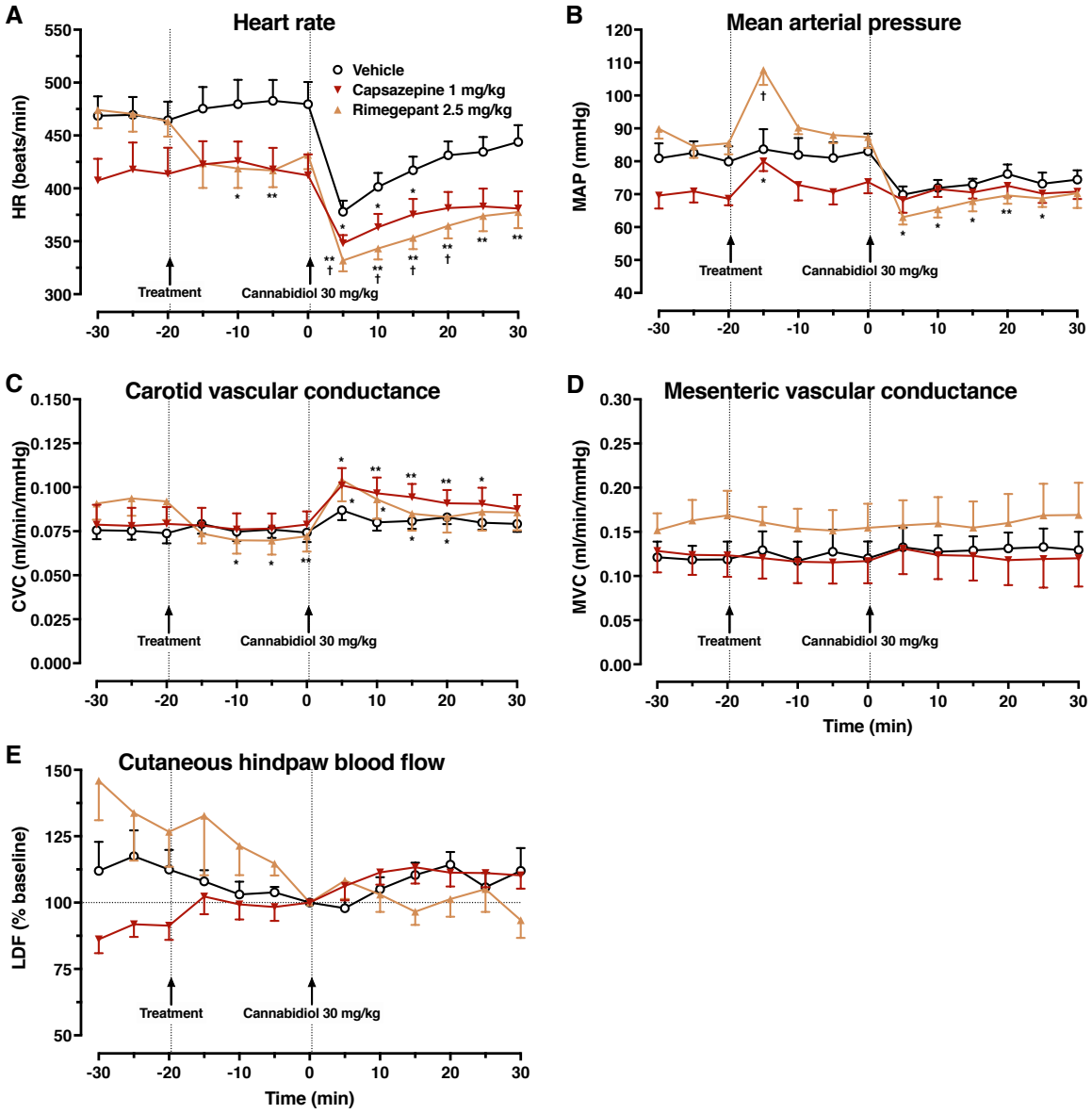


**Figure 5-9.** Effect of single i.v. bolus administration of cannabidiol 30 mg/kg in rats pretreated with TRPV1 antagonist capsazepine (1 mg/kg; *n*=5) or CGRP antagonist rimegepant (2.5 mg/kg; *n*=4-5) on rat haemodynamic parameters including heart rate (HR; A), mean arterial pressure (MAP; B), carotid vascular conductance (CVC; C), mesenteric vascular conductance (MVC; D) and hindpaw laser Doppler flux (LDF, values are expressed as a % of the within rat baseline at time 0 min; E).

Baseline recordings were taken at -30 to -20 min, followed by administration of antagonists after -20 min and a single cannabidiol 30 mg/kg administration after 0 min. As a reference, antagonist vehicle (ethanol, cremophor and saline 1:1:18; 1 ml/kg rat) and cannabidiol 30 mg/kg responses in the absence of antagonists (*n*=7) are reproduced from Figure 5-5. Data are mean ± S.E.M. **P*≤0.05 or ***P*≤0.01, compared with pre-antagonist (at -20 min) or cannabidiol 30 mg/kg (at 0 min) administration; repeated measures one-way ANOVA with Greenhouse-Geisser and Dunnett's *post hoc* test for multiple comparisons. †*P*≤0.05 compared with reference antagonist vehicle and cannabidiol 30 mg/kg responses at each time point.; repeated measures two-way ANOVA with Greenhouse-Geisser and Šidàk's *post hoc* test for multiple comparisons. *n*, number of rats.

#### 5.3.2.3 The involvement of 5-HT1A receptors

WAY-100635 1 mg/kg did not affect basal heart rate or cannabidiol-induced decreases in heart rate ($P$>0.05; Figure 5-10A). However, WAY-100635 decreased mean arterial pressure by 19 ± 3 at 5 min after administration which did not recover to baseline levels prior to cannabidiol administration ($P$>0.05; Figure 5-10B). WAY-100635 attenuated the cannabidiol-mediated decrease in mean arterial pressure (Figure 5-10B; Figure 5-8B; $P$>0.05). WAY-100635 alone did not affect hindpaw laser Doppler flux, carotid or mesenteric vascular conductance (Figure 5-10C-E). However, WAY-100635 inhibited the cannabidiol-induced increase in carotid vascular conductance (Figure 5-8C; Figure 5-10C; $P$=0.21).

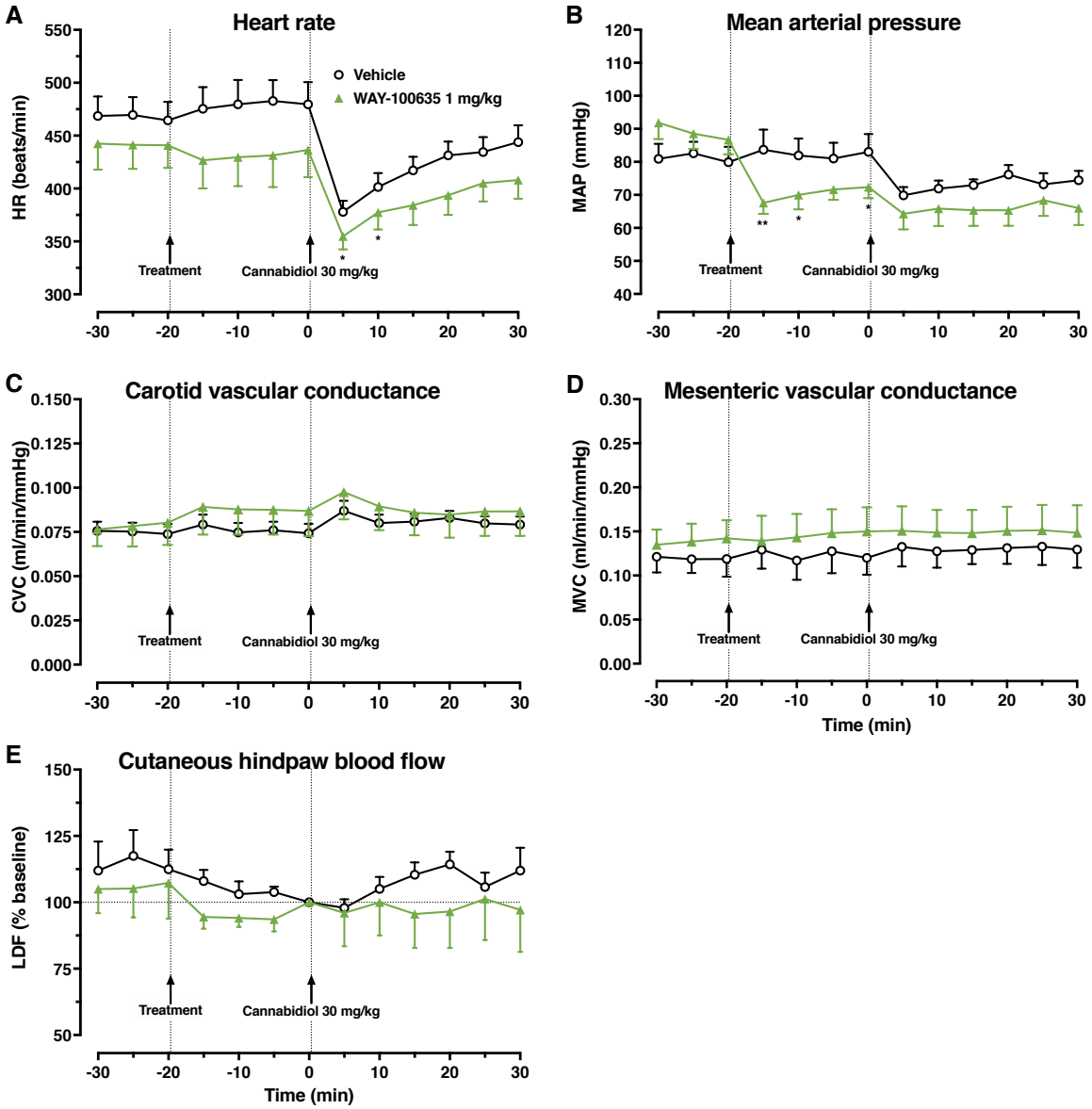


**Figure 5-10.** Effect of single i.v. bolus administration of cannabidiol 30 mg/kg in rats pretreated with the 5-$HT_{1A}$ antagonist WAY-100635 (1 mg/kg; *n*=6-7) on rat haemodynamic parameters including heart rate (HR; A), mean arterial pressure (MAP; B), carotid vascular conductance (CVC; C), mesenteric vascular conductance (MVC; D) and hindpaw laser Doppler flux (LDF, values are expressed as a % of the within rat baseline at time 0 min; E).

Baseline recordings were taken at -30 to -20 min, followed by administration of antagonist after -20 min and a single cannabidiol 30 mg/kg administration after 0 min. As a reference, antagonist vehicle (ethanol, cremophor and saline; 1:1:18; 1 ml/kg) and cannabidiol 30 mg/kg responses in the absence of antagonists (*n*=7) are reproduced from Figure 5-5. Data are mean ± S.E.M. **P*≤0.05 or ***P*≤0.01, compared with pre-antagonist (at -20 min) or cannabidiol 30 mg/kg (at 0 min) administration; repeated measures one-way ANOVA with Greenhouse-Geisser and Dunnett's *post hoc* test for multiple comparisons. *n*, number of rats.

## 5.4 Discussion

The *in vivo* haemodynamic effects of cannabidiol are not well-characterised. Extensive study heterogeneity may contribute to the reported disparity in cannabidiol's effects (Table 5-1, Table 5-2). Studies to date indicate that cannabidiol has little to no haemodynamic effects in animals and humans under resting physiological conditions (Kicman & Toczek, 2020; Sultan *et al.*, 2017). The influence of cannabidiol is mainly apparent during stress-induced cardiovascular changes.

This study aimed to characterise the haemodynamic effects and mechanisms of action of cannabidiol in anaesthetised rats. We also wanted to investigate whether the previously reported *ex vivo* vascular effects were apparent in the vasculature *in vivo*.

### 5.4.1 Haemodynamic effects of cannabidiol in urethane-anaesthetised rats

The cardiovascular responses to acute cannabidiol administration were generally transient. Therefore, the haemodynamic values returned to baseline levels within 30 min after cannabidiol administration (Figure 5-4 and Figure 5-5). All doses of cannabidiol (10-30 mg/kg i.v.) dose-dependently decreased heart rate. Single cannabidiol 30 mg/kg administration decreased heart rate by 122 ± 15 beats/min which recovered to baseline levels 25 min after cannabidiol administration. Bradycardia in response to cannabidiol has also recently been reported in urethane-anaesthetised SHR and WKY rats which were rapidly intravenously injected with cannabidiol 30 mg/kg (Kossakowski *et al.*, 2019). In the study, cannabidiol decreased the heart rate of SHR and WKY by 225 and 150 beats/min, respectively. It is important to note that they reported the maximum effect was achieved within 10 to 30 s after cannabidiol administration (Kossakowski *et al.*, 2019), while in the current study, we characterised the haemodynamic effects of cannabidiol over a 30 min period with peak recorded values at 1.7 ± 0.2 min (Table 5-4) after the end of i.v. (slow) bolus administration. We also showed that cannabidiol 30 mg/kg (i.v.) administered as a cumulative or single dose decreased mean arterial pressure by 17 ± 5 or 16 ± 5 mmHg, respectively ($P$<0.05; Table 5-4). The effects were transient as they only lasted for 5-10 min. In comparison, in urethane-anaesthetised SHR and WKY rats, rapid cannabidiol 30 mg/kg (i.v.)

injections decreased systolic blood pressure by 25 and 20 mmHg and diastolic blood pressure by 45 and 30 mmHg, respectively (achieved within 10 to 30 s after administration) (Kossakowski *et al.*, 2019).

This is the first study to investigate the *in vivo* haemodynamic effects of cannabidiol. We have previously reported that cannabidiol has prominent vascular effects *ex vivo* by both potently inhibiting the contraction and inducing potent relaxation of small mesenteric and saphenous arteries (Chapter 4; Mazeh *et al.*, 2021). In this study, we showed single cannabidiol 30 mg/kg i.v. or cumulative cannabidiol 10-30 mg/kg i.v. administration induced transient increases in carotid vascular conductance without changing mesenteric vascular conductance with the exception of the lower cannabidiol 10 mg/kg dose which caused a prolonged increase in mesenteric vascular conductance (25 min). We also showed for the first time that cannabidiol (30 mg/kg), compared to vehicle, increased hindpaw cutaneous blood flow in rats.

#### 5.4.1.1 The challenge with the hydrophobicity of cannabidiol

Our findings of the vascular effects of cannabidiol are likely underestimated as corresponding vehicle controls (ethanol, cremophor and saline 2:2:6) induced opposite effects by decreasing carotid and mesenteric vascular conductance while also decreasing hindpaw cutaneous blood flow (Figure 5-4 and Figure 5-5). As cannabidiol is highly hydrophobic (log P 6.3; section 1.5.3.6) (Odi *et al.*, 2020), there are great difficulties associated with dissolving the drug in a hydrophilic and inert vehicle. We were unsuccessful in dissolving cannabidiol in one part ethanol, one part cremophor and eighteen parts saline, which has previously been used by our laboratory to dissolve hydrophobic cannabinoid compounds as this vehicle combination does not have any apparent influence on haemodynamic parameters (Angus & Wright, 2019), as also apparent in this study (Figure 5-5). Increasing the ratio of ethanol and cremophor created a homogenous dissolved cannabidiol solution.

### 5.4.2 The potential mechanisms of action of cannabidiol

We attempted to investigate the haemodynamic mechanisms of action of cannabidiol by intravenously pretreating rats with various inhibitors of targets of interest followed by single bolus cannabidiol (30 mg/kg i.v.) administration 20 min later. None of the inhibitors attenuated cannabidiol's heart rate effects (Figure 5-8A). However, both capsazepine and WAY-100635 attenuated cannabidiol's effects on mean arterial pressure (Figure 5-8B). These results may have been confounded by the lower baseline mean arterial pressure in capsazepine and WAY-100635 animal groups (at 0 min) of 74 ± 3 and 72 ± 3 mmHg (Figure 5-9B, Figure 5-10B), respectively, compared to the basal mean arterial pressure of 83 ± 5 mmHg in the absence of inhibitors (Figure 5-5B). Furthermore, treatment with WAY-100635 or SR144528 attenuated the cannabidiol-induced increase in carotid vascular conductance (Figure 5-8C). The possible involvement of 5-$HT_{1A}$ and $CB_2$ receptors in the vascular effects of cannabidiol should only be carefully considered at this stage. Interestingly, while rimonabant did not have any effect on carotid vascular conductance on its own, pretreatment with rimonabant potentiated the cannabidiol 30 mg/kg-induced increase in carotid vascular conductance. Due to the inhibitory interaction of cannabidiol and rimonabant with $CB_1$ receptors (Chapter 3), it would be interesting to investigate the interaction of a selective $CB_1$ agonist and cannabidiol in the vasculature. There was a big variation in hindpaw cutaneous blood flow between animals and over time, complicating the study of the effects of cannabidiol in this vascular bed.

### 5.4.3 Limitations

The clinical relevance of pharmacological findings is highly dependent on the doses/concentrations used in an experiment. Following an intravenous administration of a drug, the bioavailability should be 100%. Considering rats in this study weighed 270-300 g they would have an approximate blood volume of 17-19 ml (Equation 6; Lee & Blaufox, 1985). Hence a cannabidiol 30 mg/kg dose would approximately correspond to a blood concentration of 1.5 mM, which is 500 times higher than what is considered clinically plausible in blood plasma (Chapter 4; Devinsky *et al.*, 2018; Geffrey *et al.*, 2015).

$$\text{Blood volume (ml)} = 0.06 \times \text{body weight (g)} + 0.77 \qquad (9)$$

We collected blood plasma samples from rats treated with cannabidiol which will allow us to confirm the actual blood plasma concentrations of cannabidiol in our study in the future. We did not have access to these measurements in time for this thesis.

Further, to obviate the haemodynamic effects of the vehicle used to dissolve cannabidiol, we need to explore other vehicle options that would allow a cannabidiol solution with minimal haemodynamic effects.

### 5.4.4 Conclusions

This work has confirmed previous observations that intravenously administered cannabidiol 10-30 mg/kg causes acute bradycardia and hypotension. We have also demonstrated that cannabidiol modulates vascular tone by increasing vascular conductance and cutaneous blood flow. As this study is preliminary and has not been able to elucidate the *in vivo* mechanisms of action of cannabidiol, future experiments will investigate the involvement of various suggested cardiovascular targets. Furthermore, future experiments should also investigate the haemodynamic effects of cannabidiol in female rats.

# Chapter 6

General summary

## 6.1 Main study findings

Greater access to cannabidiol products and decades of *Cannabis* prohibition have hampered medicinal research. We sought to contribute to the limited knowledge of the cardiovascular effects of cannabidiol and its potential cardiovascular (section 6.1.2) and non-cardiovascular (section 6.1.1) pharmacological targets.

### 6.1.1 Pharmacological characterisation of the $CB_1$ receptor activity of cannabidiol

Over 65 different pharmacological targets have been reported for cannabidiol. These targets are part of the endocannabinoid system, the expanded endocannabinoid system (endocannabinoidome), and targets beyond the endocannabinoidome. The nature of cannabidiol-target interactions remains elusive. One of the targets of cannabidiol, the $CB_1$ receptor, is highly expressed in neurons in the central nervous system as well as in the periphery, including in neurons of the urogenital smooth muscle, the vas deferens. The subsequent activation of $CB_1$ receptors in these neurons suppresses neurotransmitter release.

Cannabidiol is reported to modulate $CB_1$ receptor agonist activity at concentrations well below its reported affinity. This has been attributed to the ability of cannabidiol to behave as a non-competitive allosteric modulator. $CB_1$ receptor efficacy studies in tissue bioassays are limited to two published studies performed in mouse vas deferens. We expanded the efficacy study to a non-mouse assay, namely the rat vas deferens, given the intra- and interspecies differences in $CB_1$ receptor density and location. Before studying the $CB_1$ receptor activity of cannabidiol in the vas deferens bioassay, we standardised the bioassay by evaluating the effects of varying $Mg^{2+}$ concentrations on neurotransmitter-induced contractions, as most previous studies in the isolated vas deferens have been performed in modified physiological salt solution (PSS) without $Mg^{2+}$. Nerve stimulation of the vas deferens induces the release of the cotransmitter agents ATP and noradrenaline from postganglionic sympathetic nerves, causing biphasic contractions. Our results showed that the exclusion of $Mg^{2+}$ in PSS enhanced ATP-mediated contractions compared to normal PSS ($Mg^{2+}$ 1.2 mM), while not affecting

noradrenaline-induced contractions. Considering that non-physiological conditions of the bioassay may affect tissue responses to nerve stimulation, the $CB_1$ receptor activity of cannabidiol was studied here in the vas deferens using PSS with normal $Mg^{2+}$ (1.2 mM). In our study, cannabidiol antagonised $CB_1$ receptor-mediated inhibition of rat isolated electrically stimulated vas deferens in a manner consistent with simple competitive antagonism where the potency of cannabidiol matched its reported affinity, in contrast to previous literature accounts. The resulting $pK_B$ values were 5.90 or 5.29 when ATP or noradrenaline was the effector neurotransmitter agent, respectively. This suggests that cannabidiol at clinical concentrations (1-3 μM) may modulate prejunctional $CB_1$ receptors and hence alter endocannabinoid function.

### 6.1.2 Cardiovascular effects of cannabidiol

Preclinical studies have demonstrated beneficial cardiovascular effects of cannabidiol in animal models with myocarditis, cardiomyopathy, stroke and myocardial infarction. Due to the ability of cannabidiol to relax isolated arteries, it has also been suggested that cannabidiol may be beneficial in treating vascular diseases. The majority of studies on the vascular effects of cannabidiol have been performed in rat and human large conduit arteries. We aimed to examine the vascular effects of cannabidiol in rat small resistance arteries as they, unlike larger arteries, are the main contributors to peripheral vascular resistance and subsequent blood pressure regulation. We demonstrated that cannabidiol, at clinically relevant concentrations (1-3 μM), potently inhibited the contraction of small resistance arteries to multiple agents while being devoid of activity in large conduit arteries. We also investigated the involvement of various suggested cardiovascular targets and demonstrated for the first time that cannabidiol is likely inhibiting vascular contraction by potentiating the effects of CGRP, a potent endogenous vasodilator peptide. We also showed that cannabidiol is likely inhibiting L-type voltage-operated calcium channels and subsequent vascular smooth muscle contraction. The vascular effects of cannabidiol were compared with the contraction of various non-vascular tissues including bronchial, urogenital, cardiac and skeletal muscles. The contraction of non-vascular tissues was generally unaffected by cannabidiol even at 10-100 times therapeutic plasma levels, highlighting that

cannabidiol has effects that appear to be selective for the vasculature. Given the potent vascular effects of cannabidiol, we also investigated the *in vivo* haemodynamic effects in anaesthetised rats. Cannabidiol at a high bolus dose (10-30 mg/kg i.v.) caused acute transient bradycardia and hypotension. Cannabidiol also modulated vascular tone by increasing vascular conductance and cutaneous blood flow. We were unable to elucidate the haemodynamic mechanisms of action of cannabidiol. However, we found that in rats pretreated with rimonabant, a $CB_1$ antagonist, cannabidiol induced a marked 3.2-fold greater increase in carotid vascular conductance, compared to cannabidiol only-treated rats. The possible involvement of $CB_1$ receptors in this finding remains to be further investigated.

## 6.2 Concluding remarks

This project has attempted to fill the research gap on the cardiovascular effects and potential of cannabidiol. It would be untrue to state that the findings of this study completely filled that gap. We have however been able to thoroughly quantify the vascular effects of cannabidiol at clinically relevant concentrations. This study was limited in the number of vascular beds examined, hence we have expanded the study by also assessing other vascular beds, as there is a discrepancy in receptor expression, perivascular innervation and the subsequent responses.

Considering the *in vivo* haemodynamic effects of cannabidiol in rats were only observed at high intravenous bolus doses (30 mg/kg), the clinical relevance of these findings remains to be assessed. Furthermore, acute administration of cannabidiol *in vivo* does not account for the complex pharmacokinetic profile of cannabidiol which can usually only be revealed during chronic treatment.

# Appendix 1

Pharmacological characterisation of the $CB_2$ receptor activity of *Cannabis* phytochemicals in the Rat Basophilic Leukemia 2H3 cell line

## A.1 Introduction

Ligand interactions with $CB_2$ receptors have been associated with therapeutic benefits in pain management and diseases with neuroinflammatory and neurodegenerative components (reviewed in Dhopeshwarkar & Mackie, 2014). $CB_2$ receptors were discovered and isolated shortly after $CB_1$ receptors in a human promyelocytic leukemia cell line (HL60; Munro *et al.*, 1993). Since then, $CB_2$ receptors have also been isolated from mouse, rat, dog, pufferfish and zebrafish (Howlett & Abood, 2017). Unlike $CB_1$ receptors, there is less $CB_2$ receptor homology between different species. While $CB_2$ receptors are mainly expressed in immune cells, they are also expressed to a small degree in neurons in the central and peripheral nervous system, whereas $CB_1$ receptors are mainly expressed in neuron terminals in the central and peripheral nervous system (Chapter 3) and to a very small degree in other cells including immune cells (Pertwee *et al.*, 2010).

*Cannabis* phytochemicals including cannabinoids (section 1.3.2) like cannabidiol (section 1.3.2) and terpenes (section 1.3.3) like *β*-caryophyllene (section A.1.3.1) can mediate anti-inflammatory effects by interaction with $CB_2$ receptors (reviewed in Turcotte *et al.*, 2016).

### A.1.1 Rat basophilic leukemia 2H3 cell line

The immortalised rat basophilic leukemia (RBL) cell line was accidentally discovered in 1973 when a rat was injected with the potent carcinogen *β*-chlorethylamine (Eccleston *et al.*, 1973). As a result, rats developed a rare form of granulocytic leukaemia which is characterised by abnormally high levels of basophils in the blood termed peripheral blood basophilia. The rat ended up dying from basophilic leukaemia which had infiltrated various tissues including the lungs, liver, spleen, lymph nodes and bone marrow. Cytochemical analysis of these granulocytes revealed that they had the same features as basophils. The basophilic leukemia was serially transplanted (i.p. heparinised whole blood) in rats for 20 generations without changing the phenotype of leukemia (Leonard *et al.*, 1971). The cells were consequently cultured by subcutaneously transplanting newborn mice with tumour cells that were removed once the basophil-

rich tumour was appropriately sized when the rats were at the age of 2-3 weeks (Kulczycki *et al.*, 1974). This new cell line was named Rat Basophilic Leukemia (RBL-1). Due to exocytosis problems with RBL-1 cells, various sublines were eventually cloned with different degranulation characteristics, which eventually resulted in the most commonly used subline: RBL-2H3 – a hybrid basophil and mast cell line (section A.1.1.1).

RBL-2H3 cells have mainly been purposed to study the antiallergy properties of drugs by testing their ability to modulate mediator release (Passante & Frankish, 2009). *In vivo*, the exposure of B-cells or other antigen-presenting cells to allergens results in the production of antigen-specific antibodies (IgE; Elieh Ali Komi *et al.*, 2020). The IgE bind to high-affinity IgE receptors (FcεRI) expressed on the surface of mast cells and basophils, which sensitise the cells to release mediators that can promote or downregulate inflammation (Galli & Tsai, 2012). In a monotypic basophil/mast cell line, the cells are primed with antigen-specific antibodies which upon the exposure to antigen (e.g. trinitrophenyl hapten conjugated to Bovine Serum Albumin; TNP-BSA) bind to FcεRI on the cell surface to induce the release of mediators (Figure A-1). Mast cells and basophils release various mediators including biogenic amines like histamine and serotonin, proteases, lysosomal enzymes like *β*-hexosaminidase and *β*-glucuronidase, and some cytokines like TNF and IL-4 (Moon *et al.*, 2014; Passante & Frankish, 2009). *β*-Hexosaminidase is the mediator commonly used to monitor the degranulation of mast cells and is usually released in parallel with histamine (Passante & Frankish, 2009). The biological role of *β*-hexosaminidase in mast cells remains unknown.

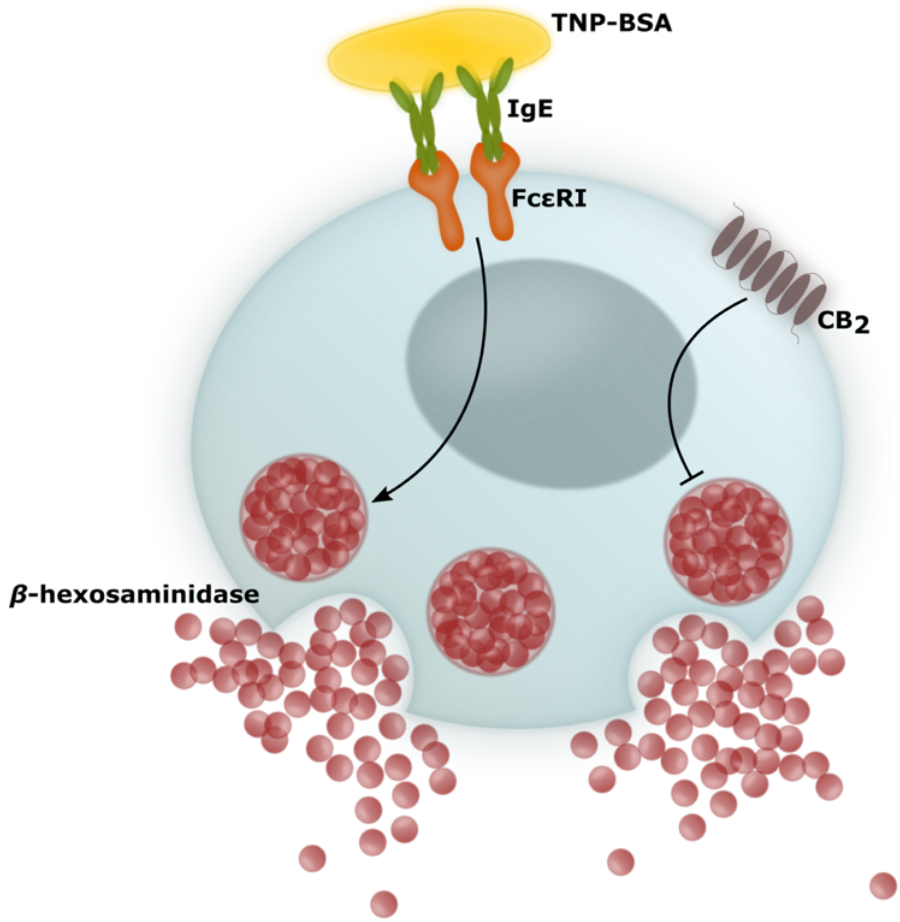


**Figure A-1.** A simplified schema of RBL-2H3 mast cell degranulation in response to the exposure of an exogenous antigen (trinitrophenyl hapten conjugated to Bovine Serum Albumin; TNP-BSA) which will crosslink the antibodies (IgE) and the high-affinity IgE receptor (FcεRI) triggering the degranulation of various mediators, including *β*-hexosaminidase.
*β*-Hexosaminidase is a mediator used in this cell assay to monitor the degranulation of RBL-2H3. $CB_2$ receptor activation in RBL-2H3 cells negatively modulates mast cell activation and hence degranulation (Facci *et al.*, 1995).

### A.1.1.1 Controversy: RBL-2H3 cell line: a basophil or mast cell model?

RBL-2H3 cells are often mistakenly referred to as a mast cell line when they in reality are better described as sharing characteristics of both mast cells and basophils without completely representing either (Passante & Frankish, 2009). This misconception is a result of inaccurate reports about the development of a new mastocytoma cell line (MCT-1) which was later proven to originate from the RBL cell line (Siraganian & Metzger, 1978; Taurog *et al.*, 1977). This was also evident as i.p. inoculation of rats with MCT-1 cells caused the development of basophilic tumours rather than mastocytoma. The RBL-2H3 cell line has proven to share characteristics common to both mast cell

and basophils while also diverging from both immune cell types. Mast cells and basophils have several biochemical and functional similarities (Galli *et al.*, 2020; Passante & Frankish, 2009). Both immune cells are involved in provoking immune allergic responses where degranulation is carried out as a result of FcεRI activation through IgE crosslinking of allergens which results in the release of various granular mediators including histamine, serotonin and *β*-hexosaminidase (Figure A-1). Further, both mast cells and basophils stain metachromatically to alcian blue. However, in contrast to mast cells which reside in tissues, basophils are circulating cells and are recruited into tissues in response to inflammation (Galli *et al.*, 2020; Passante & Frankish, 2009). Furthermore, unlike long-lived mast cells, basophils appear to undergo apoptosis after responding to tissue inflammation. The hematopoietic lineage relationship of mast cells and basophils is not fully established. Galli *et al.* (2020) suggest that mast cells and basophils should be considered as distinct hematopoietic lineages with many similar functional characteristics.

### A.1.2 RBL-2H3—a potential $CB_2$ receptor cell assay?

The anti-inflammatory effects of cannabinoids have partly been ascribed to $CB_2$ receptor activation in mast cells as they play a key role in inflammation. Facci *et al.* (1995) were first to present evidence of the existence of both $CB_2$ mRNA and a functional receptor that negatively modulated degranulation in RBL-2H3 cells when activated (Figure A-1). Later studies have also confirmed the low expression of both mRNA and a functional protein for the $CB_1$ receptor in RBL-2H3 cells (Giudice *et al.*, 2007; Samson *et al.*, 2003). Furthermore, RBL-2H3 cells do not appear to express mRNA for TRPV1, PPARα and GPR55, which are other common targets for cannabinoids.

The RBL-2H3 cell line has been utilised to study the effects of various phyto-, endo- and synthetic cannabinoids on "mast cell" degranulation (Giudice *et al.*, 2007; Granberg *et al.*, 2001; Petrosino *et al.*, 2019; Yoo *et al.*, 2013). Endocannabinoids anandamide, 2-AG and endogenous endocannabinoid-like compound palmitoylethanolamide generally only affected degranulation of RBL-2H3 cells at high concentrations (Granberg *et al.*, 2001; Yoo *et al.*, 2013). More specifically, 2-AG (10-100 μM) increased the release of both

5-HT and β-hexosaminidase (Granberg *et al.*, 2001; Yoo *et al.*, 2013), while anandamide up to 100 µM did not affect cell degranulation (Granberg *et al.*, 2001). In contrast, palmitoylethanolamide (100 µM) decreased degranulation release of both 5-HT and β-hexosaminidase, while 10 µM decreased release of only 5-HT (Granberg *et al.*, 2001). Facci *et al.* (1995) further showed that the ability of palmitoylethanolamide to suppress degranulation of antigen-activated RBL-2H3 cells is highly dependent on the solvent (DMSO) concentration, where palmitoylethanolamide dissolved in 1% DMSO decreased serotonin release with an $EC_{50}$ value of 0.27 µM, while palmitoylethanolamide dissolved in 0.2% of DMSO had no effect on degranulation.

### A.1.3 $CB_2$ receptor-mediated anti-inflammatory properties of phytochemicals

The *Cannabis* phytochemicals β-caryophyllene (section A.1.3.1) and cannabidiol (section A.1.3.2) have demonstrated anti-inflammatory effects *in vivo* by interacting with $CB_2$ receptors.

#### A.1.3.1 β-caryophyllene — a $CB_2$ active dietary terpene

(*E*)-β-caryophyllene is a bicyclic sesquiterpene (section 1.3.3) found in large amounts in essential oils of food and spices such as cinnamon, rosemary, black pepper, clove, thyme and oregano and is generally just referred to as β-caryophyllene (Gertsch *et al.*, 2008). *Cannabis* essential oils contain high amounts of β-caryophyllene (up to 35%). In essential oils with (*E*)-β-caryophyllene there is usually also smaller quantities of the isomers (*Z*)-β-caryophyllene and α-humulene, but also β-caryophyllene oxide, a β-caryophyllene oxidation product (Figure A-2; Gertsch *et al.*, 2008). As β-caryophyllene is classified as a terpene, the Therapeutic Goods Administration has not applied the same strict scheduling criteria as for cannabinoids (section 1.4.2; Therapeutic Goods Administration, 2017).

β-Caryophyllene mediates anti-inflammatory and analgesic effects by activating $CB_2$ receptors ($K_i$ 155 nM) (Gertsch *et al.*, 2008; Klauke *et al.*, 2014). In a study on the potential anti-inflammatory effects of β-caryophyllene, an oral dose of 5 and 10 mg/kg inhibited the formation of carrageenan-stimulated oedema in wild-type mice by 70 and

50%, respectively. These effects were not observed in $CB_2$ receptor-deficient mice (Cnr2-/--mice; Gertsch *et al.*, 2008). In another study on the potential analgesic effects of *β*-caryophyllene, oral administration of *β*-caryophyllene (0.1-10 mg/kg) decreased both inflammatory and neuropathic pain in mice (Klauke *et al.*, 2014). In both studies, *β*-caryophyllene was more effective than the synthetic $CB_2$ receptor agonist JWH-133 (Klauke *et al.*, 2014). *β*-Caryophyllene has also been suggested to attenuate inflammation and metabolic dysregulation in mice models of alcoholic steatohepatitis (Varga *et al.*, 2018).

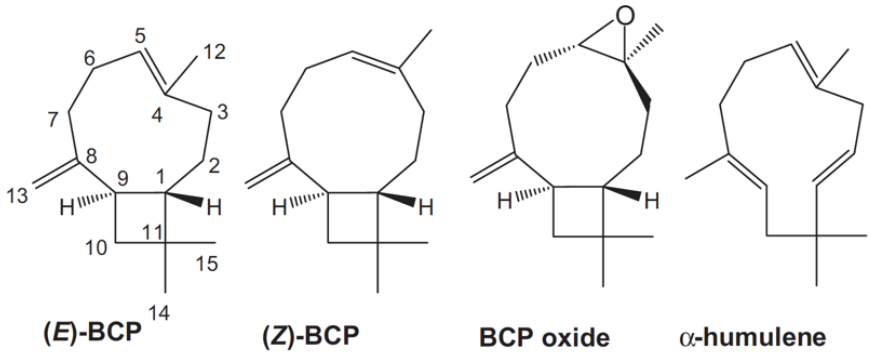


**Figure A-2.** The chemical structure of different bicyclic BCP (*β*-caryophyllene) compounds found in dietary essential oils including the *Cannabis* plant (Gertsch *et al.*, 2008).

### A.1.3.2 Cannabidiol

While cannabidiol has poor affinity at the $CB_2$ receptor (pooled Ki 3.6 μM, n=6; reviewed in McPartland *et al.*, 2015), similar to its $CB_1$ activity (Chapter 3), cannabidiol antagonises the effects of the $CB_2$ agonist CP55,940 with higher potency ($K_B$) than its affinity ($K_i$) at $CB_2$ orthosteric sites in human CHO ($K_B$ 65 nM) and HEK293A ($K_B$ 641 nM) cells (Tham *et al.*, 2018). Cannabidiol likely displays $CB_2$ receptor antagonism by acting as an inverse agonist (section 1.6.1.2; Thomas *et al.*, 2007). The inverse agonist activity of cannabidiol at $CB_2$ receptors may contribute to its anti-inflammatory actions since inverse $CB_2$ inverse agonism can inhibit immune cell migration (Lunn *et al.*, 2006). For example, Sch.336, a synthetic human $CB_2$ inverse agonist, prevented the migration of immune cells in membrane assays expressing $CB_2$ receptors (Lunn *et al.*,

2006). Sch.336 also inhibited leukocyte trafficking *in vivo* as apparent in a mouse model of allergic asthma where oral administration of Sch.336 (2-5 mg/kg) blocked ovalbumin-induced lung eosinophilia (Lunn *et al.*, 2006). Another synthetic $CB_2$ inverse agonist JTE-907 inhibited carrageenin-induced mouse paw oedema when orally administered (0.001-1 mg/kg; Iwamura *et al.*, 2001). As immune cell migration is important in ensuring that immune cells can make it to the site of infection, inhibition of this migration would cause anti-inflammatory effects (Moreau *et al.*, 2018). The immune-cell leukocytes are particularly important in providing tissues with the initial rapid immune defence through direct migration to the site of infection (Moreau *et al.*, 2018).

Cannabidiol's anti-inflammatory activity can be antagonised by selective $CB_2$ antagonists (reviewed in Atalay *et al.*, 2019). In polyinosinic-polycytidylic acid [poly-(I:C)]–stimulated human keratinocytes (HaCaT) cells, cannabidiol concentration-dependently elevated anandamide levels resulting in a decrease in the release of inflammatory chemokines and cytokines (e.g. IL-6, IL-8 and TNF-α) (Petrosino *et al.*, 2018). The effects of cannabidiol were reversed by AM630, a selective $CB_2$ receptor antagonist, indicating that cannabidiol induces anti-inflammation through the indirect activation of $CB_2$ receptors.

### A.1.4 Study aims

We aimed to assess the appropriateness of the RBL-2H3 cell assay in pharmacologically characterising the $CB_2$ receptor activity of *Cannabis* phytochemicals including the cannabinoid cannabidiol and terpene *β*-caryophyllene. The effects of these phytochemicals were compared to known $CB_2$-active synthetic cannabinoids.

## A.2 Methods

### A.2.1 Culture of RBL-2H3 cells

RBL-2H3 cells (American Type Culture Collection, USA) were cultured in 75 $cm^2$ flasks in medium consisting of Minimum Essential Media (MEM), 5% Fetal Calf Serum (FCS), GlutMAX™ (1%), penicillin (5000 U/ml)/streptomycin (5000 µg/ml). Flasks were kept at 37°C in humidified incubators (5% $CO_2$). When cultures reached 90% confluence, cells were detached by trypsin-EDTA (0.05%) and sub-cultured into fresh media.

### A.2.2 Immune activation of RBL-2H3 cells

The day before an experiment, the cells were plated into 96-well flat-bottomed plates at a density of $10^5$ cells/well in 200 µl medium (with 2% FCS) and TIB-142 IgE (mouse IgE; 2%). The plates were incubated overnight at 37°C in a humidified incubator (5% $CO_2$). On the day of an experiment, the cells were washed out twice with warm (37°C) pH-adjusted Hanks' release buffer with the following composition: $NaHCO_3$ 0.14%, HEPES 10 mM, glucose 5.5 mM, BSA 0.05%, $MgSO_4$ 0.7 mM and $CaCl_2$ 1.8 mM (pH 7.4 ± 0.03).

#### A.2.2.1 Experimental protocol

RBL-2H3 cells were incubated with different concentrations of the following compounds: WIN 55,212-2, CP 55,940, HU-210, HU-308, *β*-caryophyllene (0.1, 0.3, 1, 3 and 10 µM) or cannabidiol (1, 2.5, 5, 7.5 and 10 µM) and corresponding vehicle (DMSO 0.1%) for 10 min. In some experiments, cells were also treated with $CB_1$ and $CB_2$ inhibitors rimonabant (0.3 µM) or AM630 (1 µM), respectively, 10 min prior to cannabinoid agonist additions or the corresponding vehicle (DMSO 0.2%). Each cell plate included cell wells treated with the surfactant Triton X-100 (0.1%) which permeates cell membranes and causes a complete release of granules. During the incubation of drugs, the plates were kept covered at 37°C in an oscillator incubator (Ratek Instruments®) before cells were stimulated with a trinitrophenyl hapten conjugated to Bovine Serum Albumin (TNP-BSA; 3 ng/ml) or vehicle (MilliQ) for 45 min at 37°C.

### A.2.2.2 Measurements of *β*-hexosaminidase release

*β*-Hexosaminidase enzyme activity was measured by carefully transferring 25 µl of supernatant to a flat-bottomed 96-well plate containing 75 µl of *p*-nitrophenyl N-acetyl-*β*-D-glucosaminide (pNAG 2 mM; pH 4.5; Figure A-3) in phosphate-citrate buffer (0.2 M). The plate was incubated for 2 h at 37°C in an oscillator incubator (Ratek Instruments®; 70 rpm). The reaction between pNAG and *β*-hexosaminidase was stopped by the addition of glycine (100 µl; 0.4 M; pH 10.7; Figure A-3). The plate was read at an absorbance of 405 nm in a multi-plate reader (Multiskan Ascent; ThermoFisher Scientific).

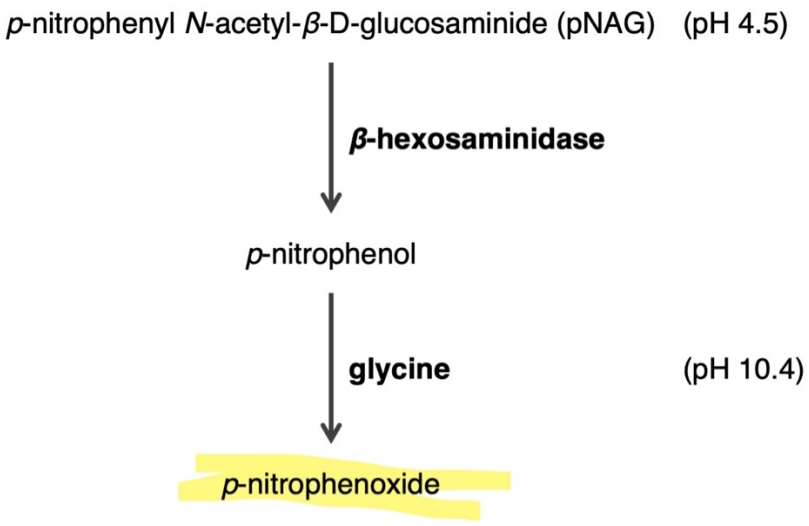


**Figure A-3.** *β*-Hexosaminidase release from RBL-2H3 cell experiments is quantified by mixing supernatant with *p*-nitrophenyl N-acetyl-*β*-D-glucosaminide (pNAG) in a phosphate-citrate buffer which is converted to *p*-nitrophenyl by the *β*-hexosaminidase in the supernatant.
The reaction is stopped by adding glycine which allows for an absorbance reading to be made at 405 nm.

### A.2.3 Data and statistical analysis

Three replicates of each cell treatment were analysed in each cell plate experiment. Experiments were excluded if the spread between replicates was more than 10%. All data are expressed as mean % of maximum $\beta$-hexosaminidase release induced by Triton-X-100 ± S.E.M. of *n* experiments (cells from separate cell passages). Repeated measures one-way ANOVA with Dunnett *post hoc* test was performed comparing the effects of various cannabinoid concentrations with the corresponding vehicle (at concentration 0 µM in graphs). Data were plotted and analysed using Prism 8 (GraphPad Software, La Jolla, CA, USA). Statistical significance was taken as $P \leq 0.05$.

### A.2.4 Drugs

Drugs used were: $CaCl_2$; glycine; Hank's buffered salts; HEPES; $MgSO_4$; $NaHCO_3$; pNAG; Triton-X-100 (all from Sigma-Aldrich, St Louis, MO, USA); 2,4,6-trinitrophenyl hapten conjugated to Bovine Serum Albumin (BioSearch Technology, USA); Trypsin–EDTA (Invitrogen, USA); GlutMAX™ (100X) supplement; phosphate-buffered saline (PBS); penicillin 5000 U/ml/streptomycin 5000 µg/ml (all from ThermoFisher Scientific, Waltham, USA) AM630; (-)-cannabidiol; rimonabant (all from Cayman Chemical, Ann Arbor, MI, USA); HU-210; HU-308; WIN 55,212-2 mesylate (all from Tocris Bioscience, Bristol, UK); $\beta$-caryophyllene (Tokyo Chemical Industry, Chuo-ku, Tokyo). All drugs were prepared as 10x stock solutions by initially being dissolved in DMSO and then dissolved in Hank's buffer. All cannabinoid aliquots were stored at -20°C as single-use $10^{-2}$ M aliquots.

## A.3 Results

### A.3.1 The effects of synthetic cannabinoids on *β*-hexosaminidase release in RBL-2H3 cells

The synthetic $CB_1$ and $CB_2$ agonists WIN 55,212-2 (0.1-10 μM) and CP 55,940 (0.1-10 μM did not modulate *β*-hexosaminidase release in either FcεRI-activated cells (+ TNP-BSA) or on their own (Figure A-4A; $P>0.05$). The $CB_1$ and $CB_2$ agonist HU-210 (0.1-10 μM) and $CB_2$ agonist HU-308 (0.1-10 μM) did not modulate *β*-hexosaminidase release and neither did the lower concentrations (0.1-3 μM) in the presence of TNP-BSA ($P>0.05$; Figure A-4B). However, the higher concentrations of HU-210 (10 μM) and HU-308 (10 μM) increased FcεRI-mediated *β*-hexosaminidase release by 11.2 ± 2.0 ($P<0.0001$) and 5.9 ± 0.8% ($P=0.040$), respectively (Table A-1).

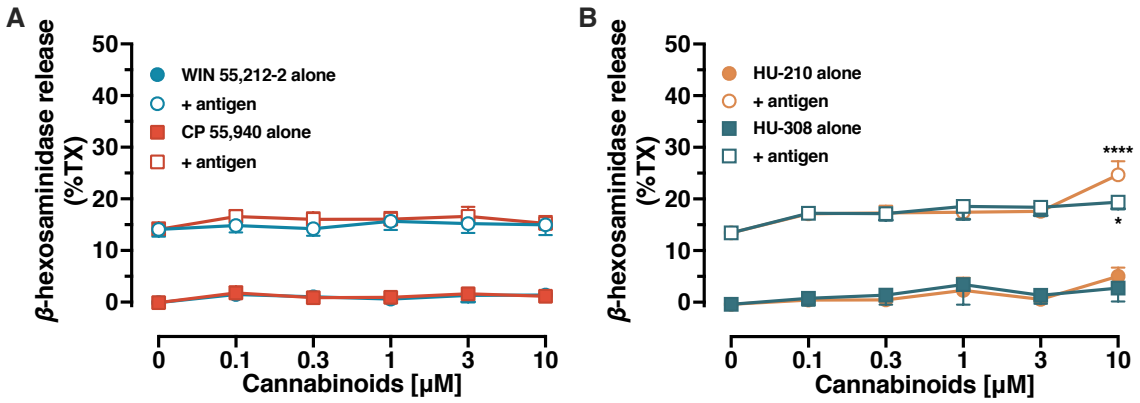


**Figure A-4.** The effects of synthetic cannabinoids on *β*-hexosaminidase release of antigen sensitised (empty symbols) and unsensitised (filled symbols) RBL-2H3 cells in response to the synthetic cannabinoids A. WIN 55,212-20 (0.1-10 μM; $n$=5-7), CP 55.940 (0.1-10 μM; $n$=5-7) and B. HU-210 (0.1-10 μM; $n$=6), HU-308 (0.1-10 μM; $n$=6).
*β*-Hexosaminidase release is expressed as % maximum release in response to cell lysis with Triton X-100 (0.1%). $n$ is from separate cell passages. Error bars are ± S.E.M. *$P\leq0.05$ or ****$P\leq0.0001$ compared with vehicle control (DMSO 0.1%; 0 μM on graph). Repeated measures one-way ANOVA with Dunnett *post hoc* test was performed.

**Table A-1.** Synthetic- and C*annabis* phytochemical-induced % *β*-hexosaminidase release in RBL-2H3 cells

| **Phytochemicals [10 μM]** | **-antigen** | ***n*** | **+antigen** | ***n*** |
|---|---|---|---|---|
| WIN 55,212-2 | 1.5 ± 1.2 | 5 | 0.9 ± 1.2 | 7 |
| CP 55,940 | 1.2 ± 1.2 | 5 | 1.2 ± 1.1 | 7 |
| HU-210 | 5.4 ± 1.4 | 6 | 11.2 ± 2.0**** | 6 |
| HU-308 | 3.1 ± 2.4 | 6 | 5.9 ± 0.8* | 6 |
| Cannabidiol | 19.8 ± 5.0* | 8 | 26.0 ± 3.2* | 10 |
| *β*-Caryophyllene | 2.9 ± 0.7* | 8 | 11.0 ± 1.4* | 10 |
| *β*-Caryophyllene + rimonabant 0.3 μM | — | — | 10.0 ± 1.1** | 4 |
| *β*-Caryophyllene + AM630 1 μM | — | — | 4.2 ± 1.0 | 4 |

Data are expressed as mean ± S.E.M. from vehicle responses (at 0 μM; Figure A-4-Figure A-6). *$P \leq 0.05$ or **$P \leq 0.01$ compared to vehicle responses; repeated measures one-way ANOVA with Dunnett's *post hoc* test. *n* is from separate cell passages.

### A.3.2 The effects of *Cannabis* phytochemicals on *β*-hexosaminidase release in RBL-2H3 cells

Cannabidiol increased *β*-hexosaminidase release of both antigen-stimulated and unstimulated cells (Figure A-5A). In the absence of antigen, cannabidiol 7.5 and 10 μM increased *β*-hexosaminidase release by 10.9 ± 2.6 and 19.8 ± 5.0%, respectively (Figure A-5A). In antigen-stimulated cells, cannabidiol (2.5-10 μM) concentration-dependently increased *β*-hexosaminidase release by 10.8 ± 1.7 to 26.0 ± 3.2% ($P<0.05$).

Similar to cannabidiol, *β*-caryophyllene (3-10 μM) increased *β*-hexosaminidase release in antigen-stimulated cells by 5.7 ± 1.3 to 11.0 ± 1.4% ($P<0.05$; Figure A-5B). In unstimulated cells, only *β*-caryophyllene 10 μM modulated *β*-hexosaminidase release by slightly increasing it by 2.9 ± 0.7% ($P=0.011$; Figure A-5B).

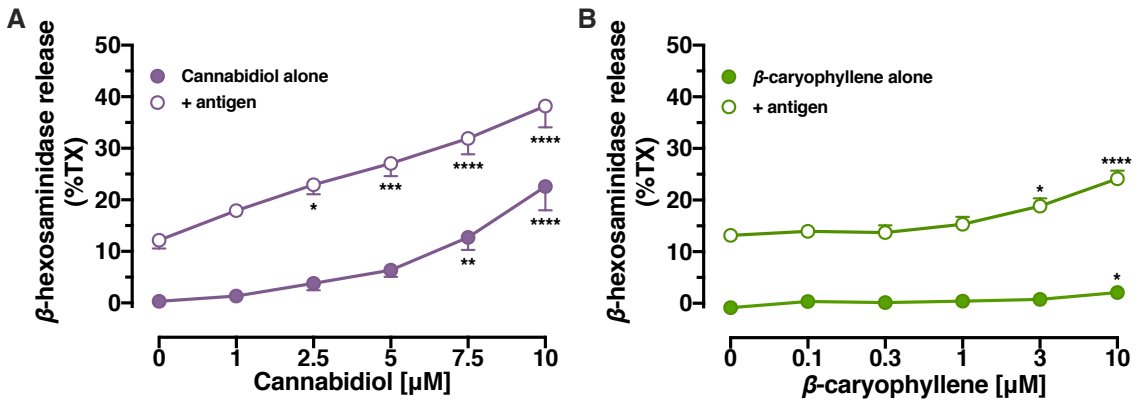


**Figure A-5.** The effects of *Cannabis* phytochemicals on β-hexosaminidase release of antigen sensitised (empty symbols) and unsensitised (filled symbols) RBL-2H3 cells in response to the phytochemicals A. cannabidiol (1-10 μM; *n*=8-10) and B. β-caryophyllene (0.1-10 μM; *n*=8-10). β-Hexosaminidase release is expressed as % maximum release in response to cell lysis with Triton X-100 (0.1%). *n* is from separate cell passages. Error bars are ± S.E.M. **P*≤0.05, ***P*≤0.01, ****P*≤0.001 or *****P*≤0.0001 compared with vehicle control (DMSO 0.1%; 0 μM on graph). Repeated measures one-way ANOVA with Dunnett *post hoc* test was performed.

### A.3.2.1 The involvement of $CB_1$ and $CB_2$ receptors

To study the involvement of $CB_1$ and $CB_2$ receptors in the effects of cannabidiol and β-caryophyllene, antigen-stimulated and unstimulated cells were incubated with the respective inhibitors rimonabant (0.3 μM) and AM630 (1 μM) prior to treatment with the *Cannabis* phytochemicals (Figure A-6). Due to the low replicate numbers (*n*=2), no statistical analysis was performed on the influence of cannabinoid receptor antagonist on the effects of cannabidiol (Figure A-6A). However, the inhibitors do not appear to have attenuated the effects of cannabidiol (2.5-10 μM) in either antigen-stimulated or unstimulated cells. While not apparent, both $CB_1$ and $CB_2$ receptor inhibitors may have slightly attenuated the β-hexosaminidase release induced by cannabidiol 10 μM (Figure A-6A). The $CB_2$ receptor antagonist AM630 attenuated the β-caryophyllene-induced increase of β-hexosaminidase release in antigen-stimulated cells to the same level as vehicle treatment (*P*=0.32), while inhibition of $CB_1$ receptors with rimonabant did not change the β-hexosaminidase modulatory effects of cannabidiol (10 μM; *P*=0.0014; Figure A-6B).

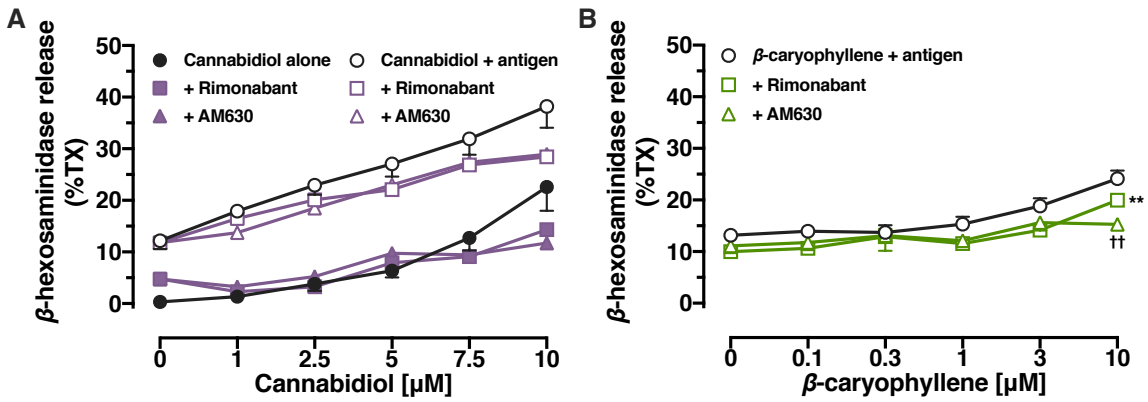


**Figure A-6.** The effect of rimonabant (0.3 μM; square symbol) and AM630 (1 μM; triangle symbol) on A. cannabidiol (1-10 μM; *n*=2) and B. *β*-caryophyllene (0.1-10 μM; *n*=4) on *β*-hexosaminidase release of antigen sensitised (empty symbols) and unsensitised (filled symbols) RBL-2H3 cells.

As a reference, the effects of cannabidiol and *β*-caryophyllene in the absence of antagonists from Figure A-5 are plotted in black symbols. *β*-Hexosaminidase release is expressed as % maximum release in response to cell lysis with Triton X-100 (0.1%). *n* is from separate cell passages. Error bars are ± S.E.M. $^{**}P \leq 0.01$ compared with vehicle control (DMSO 0.1%; 0 μM on graph). $^{††}P \leq 0.01$ compared to *β*-caryophyllene + antigen. Repeated measures one-way ANOVA with Dunnett *post hoc* test was performed.

## A.4 Discussion and preliminary conclusions

This study has not fulfilled the aim of evaluating the appropriateness of the RBL-2H3 cell line in pharmacologically characterising the $CB_2$ receptor activity of *Cannabis* phytochemical. Many questions remain unanswered. Firstly, the expression of functional $CB_2$ receptors in our cell line has not been confirmed. Secondly, we have not investigated how well the interaction with $CB_2$ receptors correlates with the modulation of degranulation, which is necessary for the examination of the $CB_2$ receptor activity of compounds. Thirdly, the possible involvement of endogenous cannabinoids in phytochemical-mediated RBL-2H3 cells degranulation has not been examined.

In this study, cannabidiol and *β*-caryophyllene potentiated degranulation of *β*-hexosaminidase in both antigen-simulated and unstimulated RBL-2H3 cells at high concentrations (>2.5 μM). Neither $CB_1$ nor $CB_2$ receptors were majorly involved in the effects of cannabidiol. $CB_2$ receptors may however be involved in the effects of *β*-caryophyllene. The possible cannabinoid receptor-independent effects remain to be evaluated.

# References


Abood M, Alexander SP, Barth F, Bonner TI, Bradshaw H, Cabral G, *et al.* (2019). Cannabinoid receptors (version 2019.4) in the IUPHAR/BPS Guide to Pharmacology Database. IUPHAR/BPS Guide to Pharmacology CITE 2019.

Abuhasira R, Shbiro L, & Landschaft Y (2018). Medical use of cannabis and cannabinoids containing products - Regulations in Europe and North America. Eur J Intern Med 49**:** 2-6.

Adams R, Hunt M, & Clark JH (1940). Structure of cannabidiol, a product isolated from the marihuana extract of Minnesota wild hemp. Journal of the American Chemical Society 62**:** 196-200.

ADInstruments (2020). *Perivascular and Tubing Flow Systems.* [Online] Available from https://www.adinstruments.com/products/perivascular-and-tubing-flow-systems#product-PL3508B13. [Accessed: 25 Jan 2020].

Ahrens J, Demir R, Leuwer M, de la Roche J, Krampfl K, Foadi N, *et al.* (2009). The nonpsychotropic cannabinoid cannabidiol modulates and directly activates alpha-1 and alpha-1-Beta glycine receptor function. Pharmacology 83**:** 217-222.

Alves FH, Crestani CC, Gomes FV, Guimarães FS, Correa FM, & Resstel LB (2010). Cannabidiol injected into the bed nucleus of the stria terminalis modulates baroreflex activity through 5-HT1A receptors. Pharmacol Res 62**:** 228-236.

Anderson LC (1980). Leaf variation among Cannabis species from a controlled garden. Botanical Museum Leaflets, Harvard University 28**:** 61-69.

Anderson LL, Low IK, McGregor IS, & Arnold JC (2020). Interactions between cannabidiol and Δ(9) -tetrahydrocannabinol in modulating seizure susceptibility and survival in a mouse model of Dravet syndrome. Br J Pharmacol 177**:** 4261-4274.

Andre CM, Hausman JF, & Guerriero G (2016). Cannabis sativa: The Plant of the Thousand and One Molecules. Front Plant Sci 7**:** 19.

Andre CM, Larondelle Y, & Evers D (2010). Dietary antioxidants and oxidative stress from a human and plant perspective: a review. Current Nutrition & Food Science 6**:** 2-12.

Angus JA, & Wright CE (2000). Techniques to study the pharmacodynamics of isolated large and small blood vessels. J Pharmacol Toxicol Methods 44**:** 395-407.

Angus JA, & Wright CE (2015). ATP is not involved in alpha1-adrenoceptor-mediated vasoconstriction in resistance arteries. Eur J Pharmacol 769**:** 162-166.

Angus JA, & Wright CE (2019). Role of endothelin-1 clearance in the haemodynamic responses to endothelin-1 in the pulmonary and hindquarter vasculature of anaesthetised rats. Eur J Pharmacol 855**:** 124-136.

Arkell TR, Lintzeris N, Kevin RC, Ramaekers JG, Vandrey R, Irwin C*, et al.* (2019). Cannabidiol (CBD) content in vaporized cannabis does not prevent tetrahydrocannabinol (THC)-induced impairment of driving and cognition. Psychopharmacology (Berl) 236**:** 2713-2724.

Arunlakshana O, & Schild HO (1959). Some quantitative uses of drug antagonists. Br J Pharmacol Chemother 14**:** 48-58.

Atalay S, Jarocka-Karpowicz I, & Skrzydlewska E (2019). Antioxidative and Anti-Inflammatory Properties of Cannabidiol. Antioxidants (Basel) 9**:** 21.

Australian Federal Police (2020). *Drugs and the law*. [Online] Available from https://www.police.act.gov.au/safety-and-security/alcohol-and-drugs/drugs-and-law. [Accessed: 10 Nov 2020].

Bakas T, van Nieuwenhuijzen PS, Devenish SO, McGregor IS, Arnold JC, & Chebib M (2017). The direct actions of cannabidiol and 2-arachidonoyl glycerol at GABA(A) receptors. Pharmacol Res 119**:** 358-370.

Baker D, Jackson SJ, & Pryce G (2007). Cannabinoid control of neuroinflammation related to multiple sclerosis. Br J Pharmacol 152**:** 649-654.

Baranowska-Kuczko M, Kozłowska H, Kloza M, Sadowska O, Kozłowski M, Kusaczuk M*, et al.* (2020). Vasodilatory effects of cannabidiol in human pulmonary and rat small mesenteric arteries: modification by hypertension and the potential pharmacological opportunities. J Hypertens 38**:** 896-911.

Barnes MP (2006). Sativex: clinical efficacy and tolerability in the treatment of symptoms of multiple sclerosis and neuropathic pain. Expert Opin Pharmacother 7**:** 607-615.

Bauquier SH, & Golder FJ (2010). The effects of urethane on the isoflurane minimum alveolar concentration in rats. Lab Anim 44**:** 323-328.

Belgrave BE, Bird KD, Chesher GB, Jackson DM, Lubbe KE, Starmer GA*, et al.* (1979). The effect of cannabidiol, alone and in combination with ethanol, on human performance. Psychopharmacology (Berl) 64**:** 243-246.

Belz GG (1995). Elastic properties and Windkessel function of the human aorta. Cardiovasc Drugs Ther 9**:** 73-83.

Bencze M, Behuliak M, & Zicha J (2013). The impact of four different classes of anesthetics on the mechanisms of blood pressure regulation in normotensive and spontaneously hypertensive rats. Physiol Res 62**:** 471-478.

Berzetei-Gurske IP, Schwartz RW, & Toll L (1996). Determination of activity for nociceptin in the mouse vas deferens. Eur J Pharmacol 302**:** R1-2.

Bhattacharyya S, Fusar-Poli P, Borgwardt S, Martin-Santos R, Nosarti C, O'Carroll C*, et al.* (2009). Modulation of mediotemporal and ventrostriatal function in humans by Delta9-tetrahydrocannabinol: a neural basis for the effects of Cannabis sativa on learning and psychosis. Arch Gen Psychiatry 66**:** 442-451.

Bhattacharyya S, Morrison PD, Fusar-Poli P, Martin-Santos R, Borgwardt S, Winton-Brown T*, et al.* (2010). Opposite effects of delta-9-tetrahydrocannabinol and cannabidiol on human brain function and psychopathology. Neuropsychopharmacology 35**:** 764-774.

Bisogno T, Hanus L, De Petrocellis L, Tchilibon S, Ponde DE, Brandi I*, et al.* (2001). Molecular targets for cannabidiol and its synthetic analogues: effect on vanilloid VR1 receptors and on the cellular uptake and enzymatic hydrolysis of anandamide. Br J Pharmacol 134**:** 845-852.

Bitencourt RM, Pamplona FA, & Takahashi RN (2008). Facilitation of contextual fear memory extinction and anti-anxiogenic effects of AM404 and cannabidiol in conditioned rats. Eur Neuropsychopharmacol 18**:** 849-859.

Bonaccorso S, Ricciardi A, Zangani C, Chiappini S, & Schifano F (2019). Cannabidiol (CBD) use in psychiatric disorders: A systematic review. Neurotoxicology 74**:** 282-298.

Bondarenko AI (2014). Endothelial atypical cannabinoid receptor: do we have enough evidence? Br J Pharmacol 171**:** 5573-5588.

Booth JK, & Bohlmann J (2019). Terpenes in Cannabis sativa - From plant genome to humans. Plant Sci 284**:** 67-72.

Booz GW (2011). Cannabidiol as an emergent therapeutic strategy for lessening the impact of inflammation on oxidative stress. Free Radic Biol Med 51**:** 1054-1061.

Borgwardt SJ, Allen P, Bhattacharyya S, Fusar-Poli P, Crippa JA, Seal ML*, et al.* (2008). Neural basis of Delta-9-tetrahydrocannabinol and cannabidiol: effects during response inhibition. Biol Psychiatry 64**:** 966-973.

Breivogel CS, Griffin G, Di Marzo V, & Martin BR (2001). Evidence for a new G protein-coupled cannabinoid receptor in mouse brain. Mol Pharmacol 60**:** 155-163.

Brown KJ, Laun AS, & Song ZH (2017). Cannabidiol, a novel inverse agonist for GPR12. Biochem Biophys Res Commun 493**:** 451-454.

Brunklaus A, & Zuberi SM (2014). Dravet syndrome--from epileptic encephalopathy to channelopathy. Epilepsia 55**:** 979-984.

Burnstock G (1972). Purinergic nerves. Pharmacol Rev 24**:** 509-581.

Burnstock G (1990). Noradrenaline and ATP as cotransmitters in sympathetic nerves. Neurochem Int 17**:** 357-368.

Burnstock G, & Holman ME (1961). The transmission of excitation from autonomic nerve to smooth muscle. J Physiol 155**:** 115-133.

Burnstock G, & Verkhratsky A (2010). Vas deferens--a model used to establish sympathetic cotransmission. Trends Pharmacol Sci 31**:** 131-139.

Burstein S (2015). Cannabidiol (CBD) and its analogs: a review of their effects on inflammation. Bioorg Med Chem 23**:** 1377-1385.

Burstein S, & Hunter SA (1978). Prostaglandins and cannabis--VI. Release of arachidonic acid from HeLa cells by delta1-tetrahydrocannabinol and other cannabinoids. Biochem Pharmacol 27**:** 1275-1280.

Campos AC, & Guimarães FS (2008). Involvement of 5HT1A receptors in the anxiolytic-like effects of cannabidiol injected into the dorsolateral periaqueductal gray of rats. Psychopharmacology (Berl) 199**:** 223-230.

Carrier EJ, Auchampach JA, & Hillard CJ (2006). Inhibition of an equilibrative nucleoside transporter by cannabidiol: a mechanism of cannabinoid immunosuppression. Proc Natl Acad Sci U S A 103**:** 7895-7900.

Casarotto PC, Gomes FV, Resstel LB, & Guimarães FS (2010). Cannabidiol inhibitory effect on marble-burying behaviour: involvement of CB1 receptors. Behav Pharmacol 21**:** 353-358.

Castillo A, Tolón MR, Fernández-Ruiz J, Romero J, & Martinez-Orgado J (2010). The neuroprotective effect of cannabidiol in an in vitro model of newborn hypoxic-ischemic brain damage in mice is mediated by CB(2) and adenosine receptors. Neurobiol Dis 37**:** 434-440.

Chakrabarti A, Onaivi ES, & Chaudhuri G (1995). Cloning and sequencing of a cDNA encoding the mouse brain-type cannabinoid receptor protein. DNA Seq 5**:** 385-388.

Chandra S, Lata H, Khan IA, & ElSohly MA (2017). Cannabis sativa L.: botany and horticulture. In Cannabis sativa L-Botany and Biotechnology. Springer, pp 79-100.

Chaturvedi PR, Decker CJ, & Odinecs A (2001). Prediction of pharmacokinetic properties using experimental approaches during early drug discovery. Curr Opin Chem Biol 5**:** 452-463.

Chen JW, Borgelt LM, & Blackmer AB (2019). Cannabidiol: A New Hope for Patients With Dravet or Lennox-Gastaut Syndromes. Ann Pharmacother 53**:** 603-611.

Chen Z, Brodie MJ, Liew D, & Kwan P (2018). Treatment outcomes in patients with newly diagnosed epilepsy treated with established and new antiepileptic drugs: a 30-year longitudinal cohort study. JAMA neurology 75**:** 279-286.

Chiang N, Dalli J, Colas RA, & Serhan CN (2015). Identification of resolvin D2 receptor mediating resolution of infections and organ protection. J Exp Med 212**:** 1203-1217.

Chiurchiù V, Lanuti M, De Bardi M, Battistini L, & Maccarrone M (2015). The differential characterization of GPR55 receptor in human peripheral blood reveals a distinctive expression in monocytes and NK cells and a proinflammatory role in these innate cells. Int Immunol 27**:** 153-160.

Choi CM, & Bennett RG (2003). Laser Dopplers to determine cutaneous blood flow. Dermatol Surg 29**:** 272-280.

Christopoulos A, Coles P, Lay L, Lew MJ, & Angus JA (2001). Pharmacological analysis of cannabinoid receptor activity in the rat vas deferens. Br J Pharmacol 132**:** 1281-1291.

Chung H, Fierro A, & Pessoa-Mahana CD (2019). Cannabidiol binding and negative allosteric modulation at the cannabinoid type 1 receptor in the presence of delta-9-tetrahydrocannabinol: An In Silico study. PLoS One 14**:** e0220025.

Clapper JR, Moreno-Sanz G, Russo R, Guijarro A, Vacondio F, Duranti A*, et al.* (2010). Anandamide suppresses pain initiation through a peripheral endocannabinoid mechanism. Nat Neurosci 13**:** 1265-1270.

Clark A (1926). The antagonism of acetyl choline by atropine. The Journal of Physiology 61**:** 547-556.

Cohen K, Weizman A, & Weinstein A (2019). Positive and Negative Effects of Cannabis and Cannabinoids on Health. Clin Pharmacol Ther 105**:** 1139-1147.

Comelli F, Giagnoni G, Bettoni I, Colleoni M, & Costa B (2008). Antihyperalgesic effect of a Cannabis sativa extract in a rat model of neuropathic pain: mechanisms involved. Phytother Res 22**:** 1017-1024.

Console-Bram L, Brailoiu E, Brailoiu GC, Sharir H, & Abood ME (2014). Activation of GPR18 by cannabinoid compounds: a tale of biased agonism. Br J Pharmacol 171**:** 3908-3917.

Corbett AD, Gillan MG, Kosterlitz HW, McKnight AT, Paterson SJ, & Robson LE (1984). Selectivities of opioid peptide analogues as agonists and antagonists at the delta-receptor. Br J Pharmacol 83**:** 271-279.

Costa B, Giagnoni G, Franke C, Trovato AE, & Colleoni M (2004). Vanilloid TRPV1 receptor mediates the antihyperalgesic effect of the nonpsychoactive cannabinoid, cannabidiol, in a rat model of acute inflammation. Br J Pharmacol 143**:** 247-250.

Coutts AA, & Pertwee RG (1997). Inhibition by cannabinoid receptor agonists of acetylcholine release from the guinea-pig myenteric plexus. Br J Pharmacol 121**:** 1557-1566.

Crippa JA, Guimarães FS, Campos AC, & Zuardi AW (2018). Translational Investigation of the Therapeutic Potential of Cannabidiol (CBD): Toward a New Age. Front Immunol 9**:** 2009.

Crippa JA, Zuardi AW, Garrido GE, Wichert-Ana L, Guarnieri R, Ferrari L*, et al.* (2004). Effects of cannabidiol (CBD) on regional cerebral blood flow. Neuropsychopharmacology 29**:** 417-426.

Cristino L, Bisogno T, & Di Marzo V (2020). Cannabinoids and the expanded endocannabinoid system in neurological disorders. Nat Rev Neurol 16**:** 9-29.

Danish Myo Technology A/S (2020). *DMT NORMALIZATION GUIDE*. [Online] Available from https://www.dmt.dk/uploads/6/5/6/8/65689239/dmt_normalization_guide.pdf. [Accessed: 14 Feb 2020].

Davies C, & Bhattacharyya S (2019). Cannabidiol as a potential treatment for psychosis. Ther Adv Psychopharmacol 9**:** 2045125319881916.

De Filippis D, D'Amico A, & Iuvone T (2008). Cannabinomimetic control of mast cell mediator release: new perspective in chronic inflammation. J Neuroendocrinol 20 Suppl 1**:** 20-25.

de la Monte SM, & Wands JR (2006). Molecular indices of oxidative stress and mitochondrial dysfunction occur early and often progress with severity of Alzheimer's disease. J Alzheimers Dis 9**:** 167-181.

De Petrocellis L, Ligresti A, Moriello AS, Allarà M, Bisogno T, Petrosino S*, et al.* (2011). Effects of cannabinoids and cannabinoid-enriched Cannabis extracts on TRP channels and endocannabinoid metabolic enzymes. Br J Pharmacol 163**:** 1479-1494.

Deutsch DG, & Chin SA (1993). Enzymatic synthesis and degradation of anandamide, a cannabinoid receptor agonist. Biochem Pharmacol 46**:** 791-796.

Devane WA, Dysarz FA, 3rd, Johnson MR, Melvin LS, & Howlett AC (1988). Determination and characterization of a cannabinoid receptor in rat brain. Mol Pharmacol 34**:** 605-613.

Devane WA, Hanus L, Breuer A, Pertwee RG, Stevenson LA, Griffin G, *et al.* (1992). Isolation and structure of a brain constituent that binds to the cannabinoid receptor. Science 258**:** 1946-1949.

Devinsky O, Cilio MR, Cross H, Fernandez-Ruiz J, French J, Hill C, *et al.* (2014). Cannabidiol: pharmacology and potential therapeutic role in epilepsy and other neuropsychiatric disorders. Epilepsia 55**:** 791-802.

Devinsky O, Cross JH, Laux L, Marsh E, Miller I, Nabbout R, *et al.* (2017). Trial of Cannabidiol for Drug-Resistant Seizures in the Dravet Syndrome. N Engl J Med 376**:** 2011-2020.

Devinsky O, Patel AD, Thiele EA, Wong MH, Appleton R, Harden CL, *et al.* (2018). Randomized, dose-ranging safety trial of cannabidiol in Dravet syndrome. Neurology 90**:** e1204-e1211.

Dhopeshwarkar A, & Mackie K (2014). CB2 Cannabinoid receptors as a therapeutic target-what does the future hold? Mol Pharmacol 86**:** 430-437.

Di Marzo V (2014) *Cannabinoids*. John Wiley & Sons, Incorporated: Hoboken, UNITED KINGDOM.

Di Marzo V (2018). New approaches and challenges to targeting the endocannabinoid system. Nat Rev Drug Discov 17**:** 623-639.

Di Marzo V, & Petrocellis LD (2006). Plant, synthetic, and endogenous cannabinoids in medicine. Annu Rev Med 57**:** 553-574.

Driessen B, von Kugelgen I, & Starke K (1994). P1-purinoceptor-mediated modulation of neural noradrenaline and ATP release in guinea-pig vas deferens. Naunyn Schmiedebergs Arch Pharmacol 350**:** 42-48.

Eccleston E, Leonard BJ, Lowe JS, & Welford HJ (1973). Basophilic leukaemia in the albino rat and a demonstration of the basopoietin. Nat New Biol 244**:** 73-76.

Elieh Ali Komi D, Wöhrl S, & Bielory L (2020). Mast Cell Biology at Molecular Level: a Comprehensive Review. Clin Rev Allergy Immunol 58**:** 342-365.

Ellis JL, & Burnstock G (1990). Neuropeptide Y neuromodulation of sympathetic co-transmission in the guinea-pig vas deferens. Br J Pharmacol 100**:** 457-462.

Elsohly MA, & Slade D (2005). Chemical constituents of marijuana: the complex mixture of natural cannabinoids. Life Sci 78**:** 539-548.

Esposito G, Scuderi C, Valenza M, Togna GI, Latina V, De Filippis D, *et al.* (2011). Cannabidiol reduces Aβ-induced neuroinflammation and promotes hippocampal neurogenesis through PPARγ involvement. PLoS One 6**:** e28668.

European Medicines Agency (2007). Acomplia, European Public Assessment Report 2007.

European Monitoring Centre for Drugs and Drug Addiction (2018). Cannabis legislation in Europe: an overview, Publications Office of the European UnionLuxembourg.

Evans AT, Formukong E, & Evans FJ (1987). Activation of phospholipase A2 by cannabinoids. Lack of correlation with CNS effects. FEBS Lett 211**:** 119-122.

Facci L, Dal Toso R, Romanello S, Buriani A, Skaper SD, & Leon A (1995). Mast cells express a peripheral cannabinoid receptor with differential sensitivity to anandamide and palmitoylethanolamide. Proc Natl Acad Sci U S A 92**:** 3376-3380.

Felson J, Adamczyk A, & Thomas C (2019). How and why have attitudes about cannabis legalization changed so much? Soc Sci Res 78**:** 12-27.

Field KJ, White WJ, & Lang CM (1993). Anaesthetic effects of chloral hydrate, pentobarbitone and urethane in adult male rats. Lab Anim 27**:** 258-269.

Flecknell P (2015) *Laboratory animal anaesthesia*. Academic press.

Flores-Sanchez IJ, & Verpoorte R (2008). Secondary metabolism in cannabis. Phytochemistry reviews 7**:** 615-639.

Fogaça MV, Reis FM, Campos AC, & Guimarães FS (2014). Effects of intra-prelimbic prefrontal cortex injection of cannabidiol on anxiety-like behavior: involvement of 5HT1A receptors and previous stressful experience. Eur Neuropsychopharmacol 24**:** 410-419.

Fowler CJ, Doherty P, & Alexander SPH (2017). Endocannabinoid Turnover. Adv Pharmacol 80**:** 31-66.

French AM, & Scott NC (1983). Feedback inhibition of responses of rat vas deferens to twin pulse stimulation. Eur J Pharmacol 86**:** 379-383.

Fusar-Poli P, Crippa JA, Bhattacharyya S, Borgwardt SJ, Allen P, Martin-Santos R, *et al.* (2009). Distinct effects of {delta}9-tetrahydrocannabinol and cannabidiol on neural activation during emotional processing. Arch Gen Psychiatry 66**:** 95-105.

Galiegue S, Mary S, Marchand J, Dussossoy D, Carriere D, Carayon P, *et al.* (1995). Expression of central and peripheral cannabinoid receptors in human immune tissues and leukocyte subpopulations. Eur J Biochem 232**:** 54-61.

Galli SJ, Gaudenzio N, & Tsai M (2020). Mast Cells in Inflammation and Disease: Recent Progress and Ongoing Concerns. Annu Rev Immunol 38**:** 49-77.

Galli SJ, & Tsai M (2012). IgE and mast cells in allergic disease. Nat Med 18**:** 693-704.

Gao Y (2017) *Biology of vascular smooth muscle: vasoconstriction and dilatation*. vol. 8. Springer.

Gaoni Y, & Mechoulam R (1964). [Isolation, structure, and partial synthesis of an active constituent of hashish]. J Am Chem Soc 86**:** 1646-1647.

Geffrey AL, Pollack SF, Bruno PL, & Thiele EA (2015). Drug-drug interaction between clobazam and cannabidiol in children with refractory epilepsy. Epilepsia 56**:** 1246-1251.

Gerard C, Mollereau C, Vassart G, & Parmentier M (1990). Nucleotide sequence of a human cannabinoid receptor cDNA. Nucleic Acids Res 18**:** 7142.

Gerard CM, Mollereau C, Vassart G, & Parmentier M (1991). Molecular cloning of a human cannabinoid receptor which is also expressed in testis. Biochem J 279 ( Pt 1)**:** 129-134.

Gertsch J, Leonti M, Raduner S, Racz I, Chen JZ, Xie XQ*, et al.* (2008). Beta-caryophyllene is a dietary cannabinoid. Proc Natl Acad Sci U S A 105**:** 9099-9104.

Giacoppo S, Bramanti P, & Mazzon E (2017). Sativex in the management of multiple sclerosis-related spasticity: An overview of the last decade of clinical evaluation. Mult Scler Relat Disord 17**:** 22-31.

Giudice ED, Rinaldi L, Passarotto M, Facchinetti F, D'Arrigo A, Guiotto A*, et al.* (2007). Cannabidiol, unlike synthetic cannabinoids, triggers activation of RBL-2H3 mast cells. J Leukoc Biol 81**:** 1512-1522.

Gomes FV, Alves FH, Guimaraes FS, Correa FM, Resstel LB, & Crestani CC (2013a). Cannabidiol administration into the bed nucleus of the stria terminalis alters cardiovascular responses induced by acute restraint stress through 5-HT(1)A receptor. Eur Neuropsychopharmacol 23**:** 1096-1104.

Gomes FV, Del Bel EA, & Guimarães FS (2013b). Cannabidiol attenuates catalepsy induced by distinct pharmacological mechanisms via 5-HT1A receptor activation in mice. Prog Neuropsychopharmacol Biol Psychiatry 46**:** 43-47.

Gomes FV, Reis DG, Alves FH, Corrêa FM, Guimarães FS, & Resstel LB (2012). Cannabidiol injected into the bed nucleus of the stria terminalis reduces the expression of contextual fear conditioning via 5-HT1A receptors. J Psychopharmacol 26**:** 104-113.

Gonca E, & Darıcı F (2015). The effect of cannabidiol on ischemia/reperfusion-induced ventricular arrhythmias: the role of adenosine A1 receptors. J Cardiovasc Pharmacol Ther 20**:** 76-83.

Gong H, Jr., Tashkin DP, Simmons MS, Calvarese B, & Shapiro BJ (1984). Acute and subacute bronchial effects of oral cannabinoids. Clin Pharmacol Ther 35**:** 26-32.

Graham JD, & Li DM (1973). Cardiovascular and respiratory effects of cannabis in cat and rat. Br J Pharmacol 49**:** 1-10.

Granberg M, Fowler CJ, & Jacobsson SO (2001). Effects of the cannabimimetic fatty acid derivatives 2-arachidonoylglycerol, anandamide, palmitoylethanolamide and methanandamide upon IgE-dependent antigen-induced beta-hexosaminidase, serotonin and TNF alpha release from rat RBL-2H3 basophilic leukaemic cells. Naunyn Schmiedebergs Arch Pharmacol 364**:** 66-73.

Granja AG, Carrillo-Salinas F, Pagani A, Gómez-Cañas M, Negri R, Navarrete C, *et al.* (2012). A cannabigerol quinone alleviates neuroinflammation in a chronic model of multiple sclerosis. J Neuroimmune Pharmacol 7**:** 1002-1016.

Granjeiro EM, Gomes FV, Guimaraes FS, Correa FM, & Resstel LB (2011). Effects of intracisternal administration of cannabidiol on the cardiovascular and behavioral responses to acute restraint stress. Pharmacol Biochem Behav 99**:** 743-748.

GW Pharmaceuticals (2019a). *GW's Epilepsy Clinical Program.* [Online] Available from https://www.gwpharm.com/healthcare-professionals/epidiolex. [Accessed: 7 Sep 2019].

GW Pharmaceuticals (2019b). *Sativex®.* [Online] Available from https://www.gwpharm.com/healthcare-professionals/sativex. [Accessed: 7 Sep 2019].

Hallak JE, Dursun SM, Bosi DC, de Macedo LR, Machado-de-Sousa JP, Abrão J, *et al.* (2011). The interplay of cannabinoid and NMDA glutamate receptor systems in humans: preliminary evidence of interactive effects of cannabidiol and ketamine in healthy human subjects. Prog Neuropsychopharmacol Biol Psychiatry 35**:** 198-202.

Haney M, Malcolm RJ, Babalonis S, Nuzzo PA, Cooper ZD, Bedi G, *et al.* (2016). Oral cannabidiol does not alter the subjective, reinforcing or cardiovascular effects of smoked cannabis. Neuropsychopharmacology 41**:** 1974-1982.

Hanus LO, Meyer SM, Munoz E, Taglialatela-Scafati O, & Appendino G (2016). Phytocannabinoids: a unified critical inventory. Nat Prod Rep 33**:** 1357-1392.

Hara K, & Harris RA (2002). The anesthetic mechanism of urethane: the effects on neurotransmitter-gated ion channels. Anesth Analg 94**:** 313-318, table of contents.

Hartmann A, Lisboa SF, Sonego AB, Coutinho D, Gomes FV, & Guimarães FS (2019). Cannabidiol attenuates aggressive behavior induced by social isolation in mice:

Involvement of 5-HT1A and CB1 receptors. Prog Neuropsychopharmacol Biol Psychiatry 94**:** 109637.

Hegde VL, Nagarkatti PS, & Nagarkatti M (2011). Role of myeloid-derived suppressor cells in amelioration of experimental autoimmune hepatitis following activation of TRPV1 receptors by cannabidiol. PLoS One 6**:** e18281.

Henstridge CM (2012). Off-target cannabinoid effects mediated by GPR55. Pharmacology 89**:** 179-187.

Ho WS, & Hiley CR (2003). Vasodilator actions of abnormal-cannabidiol in rat isolated small mesenteric artery. Br J Pharmacol 138**:** 1320-1332.

Honner V, & Docherty JR (1999). Investigation of the subtypes of alpha1-adrenoceptor mediating contractions of rat vas deferens. Br J Pharmacol 128**:** 1323-1331.

Hourani SM, Nicholls J, Lee BS, Halfhide EJ, & Kitchen I (1993). Characterization and ontogeny of P1-purinoceptors on rat vas deferens. Br J Pharmacol 108**:** 754-758.

Howlett AC (2005). Cannabinoid receptor signaling. Handb Exp Pharmacol**:** 53-79.

Howlett AC, & Abood ME (2017). CB(1) and CB(2) Receptor Pharmacology. Adv Pharmacol 80**:** 169-206.

Howlett AC, Barth F, Bonner TI, Cabral G, Casellas P, Devane WA*, et al.* (2002). International Union of Pharmacology. XXVII. Classification of cannabinoid receptors. Pharmacol Rev 54**:** 161-202.

Huetteman DA, & Bogie H (2009). Direct blood pressure monitoring in laboratory rodents via implantable radio telemetry. Methods Mol Biol 573**:** 57-73.

Hughes J, Kosterlitz HW, & Leslie FM (1975). Effect of morphine on adrenergic transmission in the mouse vas deferens. Assessment of agonist and antogonist potencies of narcotic analgesics. Br J Pharmacol 53**:** 371-381.

Huković S (1997). Responses of the isolated sympathetic nerve-ductus deferens preparation of the guinea-pig. 1961. Br J Pharmacol 120**:** 195-201; discussion 192-194.

Iannotti FA, Hill CL, Leo A, Alhusaini A, Soubrane C, Mazzarella E*, et al.* (2014). Nonpsychotropic plant cannabinoids, cannabidivarin (CBDV) and cannabidiol (CBD), activate and desensitize transient receptor potential vanilloid 1 (TRPV1) channels in vitro: potential for the treatment of neuronal hyperexcitability. ACS Chem Neurosci 5**:** 1131-1141.

Ibeas Bih C, Chen T, Nunn AV, Bazelot M, Dallas M, & Whalley BJ (2015). Molecular Targets of Cannabidiol in Neurological Disorders. Neurotherapeutics 12**:** 699-730.

Ishac EJ, Jiang L, Lake KD, Varga K, Abood ME, & Kunos G (1996). Inhibition of exocytotic noradrenaline release by presynaptic cannabinoid CB1 receptors on peripheral sympathetic nerves. Br J Pharmacol 118**:** 2023-2028.

Iwamura H, Suzuki H, Ueda Y, Kaya T, & Inaba T (2001). In vitro and in vivo pharmacological characterization of JTE-907, a novel selective ligand for cannabinoid CB2 receptor. J Pharmacol Exp Ther 296**:** 420-425.

Jadoon KA, Tan GD, & O'Sullivan SE (2017). A single dose of cannabidiol reduces blood pressure in healthy volunteers in a randomized crossover study. JCI Insight 2**:** e93760.

Jahnen-Dechent W, & Ketteler M (2012). Magnesium basics. Clin Kidney J 5**:** i3-i14.

Jakowiecki J, Abel R, Orzeł U, Pasznik P, Preissner R, & Filipek S (2021). Allosteric Modulation of the CB1 Cannabinoid Receptor by Cannabidiol-A Molecular Modeling Study of the N-Terminal Domain and the Allosteric-Orthosteric Coupling. Molecules 26.

James GT (1978). Inactivation of the protease inhibitor phenylmethylsulfonyl fluoride in buffers. Anal Biochem 86**:** 574-579.

Jarai Z, Wagner JA, Varga K, Lake KD, Compton DR, Martin BR*, et al.* (1999). Cannabinoid-induced mesenteric vasodilation through an endothelial site distinct from CB1 or CB2 receptors. Proc Natl Acad Sci U S A 96**:** 14136-14141.

Jiang R, Yamaori S, Okamoto Y, Yamamoto I, & Watanabe K (2013). Cannabidiol is a potent inhibitor of the catalytic activity of cytochrome P450 2C19. Drug Metab Pharmacokinet 28**:** 332-338.

Jones CA, Watson DJ, & Fone KC (2011). Animal models of schizophrenia. Br J Pharmacol 164**:** 1162-1194.

Jouanjus E, Leymarie F, Tubery M, & Lapeyre-Mestre M (2011). Cannabis-related hospitalizations: unexpected serious events identified through hospital databases. Br J Clin Pharmacol 71**:** 758-765.

Joyce W, White DW, Raven PB, & Wang T (2019). Weighing the evidence for using vascular conductance, not resistance, in comparative cardiovascular physiology. J Exp Biol 222.

Karl T, Cheng D, Garner B, & Arnold JC (2012). The therapeutic potential of the endocannabinoid system for Alzheimer's disease. Expert Opin Ther Targets 16**:** 407-420.

Kasakov L, Ellis J, Kirkpatrick K, Milner P, & Burnstock G (1988). Direct evidence for concomitant release of noradrenaline, adenosine 5'-triphosphate and neuropeptide Y

from sympathetic nerve supplying the guinea-pig vas deferens. J Auton Nerv Syst 22**:** 75-82.

Kathmann M, Flau K, Redmer A, Tränkle C, & Schlicker E (2006). Cannabidiol is an allosteric modulator at mu- and delta-opioid receptors. Naunyn Schmiedebergs Arch Pharmacol 372**:** 354-361.

Kayser RR, Haney M, Raskin M, Arout C, & Simpson HB (2020). Acute effects of cannabinoids on symptoms of obsessive-compulsive disorder: A human laboratory study. Depress Anxiety 37**:** 801-811.

Kenakin T (2014) *A Pharmacology Primer, Techniques for More Effective and Strategic Drug Discovery, 4th Edition*.

Kendall DA, & Alexander SP (2017) *Cannabinoid pharmacology*. Cambridge, MA : Academic Press, 2017

Khakh BS, & North RA (2006). P2X receptors as cell-surface ATP sensors in health and disease. Nature 442**:** 527-532.

Kicman A, & Toczek M (2020). The Effects of Cannabidiol, a Non-Intoxicating Compound of Cannabis, on the Cardiovascular System in Health and Disease. Int J Mol Sci 21**:** 6740.

Klauke AL, Racz I, Pradier B, Markert A, Zimmer AM, Gertsch J*, et al.* (2014). The cannabinoid CB(2) receptor-selective phytocannabinoid beta-caryophyllene exerts analgesic effects in mouse models of inflammatory and neuropathic pain. Eur Neuropsychopharmacol 24**:** 608-620.

Koch N, Jennotte O, Gasparrini Y, Vandenbroucke F, Lechanteur A, & Evrard B (2020). Cannabidiol aqueous solubility enhancement: Comparison of three amorphous formulations strategies using different type of polymers. Int J Pharm 589**:** 119812.

Koslov DS, & Andersson KE (2013). Physiological and pharmacological aspects of the vas deferens-an update. Front Pharmacol 4**:** 101.

Kossakowski R, Schlicker E, Toczek M, Weresa J, & Malinowska B (2019). Cannabidiol Affects the Bezold-Jarisch Reflex via TRPV1 and 5-HT3 Receptors and Has Peripheral Sympathomimetic Effects in Spontaneously Hypertensive and Normotensive Rats. Front Pharmacol 10**:** 500.

Kulczycki A, Jr., Isersky C, & Metzger H (1974). The interaction of IgE with rat basophilic leukemia cells. I. Evidence for specific binding of IgE. J Exp Med 139**:** 600-616.

Kumar A, Potts JD, & DiPette DJ (2019). Protective Role of α-Calcitonin Gene-Related Peptide in Cardiovascular Diseases. Frontiers in Physiology 10**:** 821.

Kurtz TW, Griffin KA, Bidani AK, Davisson RL, & Hall JE (2005). Recommendations for blood pressure measurement in humans and experimental animals: part 2: blood pressure measurement in experimental animals: a statement for professionals from the Subcommittee of Professional and Public Education of the American Heart Association Council on High Blood Pressure Research. Arterioscler Thromb Vasc Biol 25**:** e22-33.

Laires MJ, Monteiro CP, & Bicho M (2004). Role of cellular magnesium in health and human disease. Front Biosci 9**:** 262-276.

Laprairie RB, Bagher AM, Kelly ME, & Denovan-Wright EM (2015). Cannabidiol is a negative allosteric modulator of the cannabinoid CB1 receptor. Br J Pharmacol 172**:** 4790-4805.

Laun AS, Shrader SH, Brown KJ, & Song ZH (2019). GPR3, GPR6, and GPR12 as novel molecular targets: their biological functions and interaction with cannabidiol. Acta Pharmacol Sin 40**:** 300-308.

Laun AS, & Song ZH (2017). GPR3 and GPR6, novel molecular targets for cannabidiol. Biochem Biophys Res Commun 490**:** 17-21.

Lautt WW (1989). Resistance or conductance for expression of arterial vascular tone. Microvasc Res 37**:** 230-236.

Lay L, Angus JA, & Wright CE (2000). Pharmacological characterisation of cannabinoid CB(1) receptors in the rat and mouse. Eur J Pharmacol 391**:** 151-161.

Lee H, & Blaufox M (1985). Blood volume in the rat. Journal of Nuclear Medicine 26**:** 72-76.

Leonard BJ, Eccleston E, Jones D, Lowe J, & Turner E (1971). Basophilic leukemia in the rat induced by a -chlorethylamine--ICI 42464. J Pathol 103**:** Pxv.

Lew MJ, & Angus JA (1995). Analysis of competitive agonist-antagonist interactions by nonlinear regression. Trends Pharmacol Sci 16**:** 328-337.

Leweke FM, Piomelli D, Pahlisch F, Muhl D, Gerth CW, Hoyer C, *et al.* (2012). Cannabidiol enhances anandamide signaling and alleviates psychotic symptoms of schizophrenia. Transl Psychiatry 2**:** e94.

Li H-L (1974). An archaeological and historical account of cannabis in China. Economic Botany 28**:** 437-448.

Ligresti A, Moriello AS, Starowicz K, Matias I, Pisanti S, De Petrocellis L, *et al.* (2006). Antitumor activity of plant cannabinoids with emphasis on the effect of cannabidiol on human breast carcinoma. J Pharmacol Exp Ther 318**:** 1375-1387.

Lin XH, Yuece B, Li YY, Feng YJ, Feng JY, Yu LY, *et al.* (2011). A novel CB receptor GPR55 and its ligands are involved in regulation of gut movement in rodents. Neurogastroenterol Motil 23**:** 862-e342.

Linares IM, Zuardi AW, Pereira LC, Queiroz RH, Mechoulam R, Guimarães FS, *et al.* (2019). Cannabidiol presents an inverted U-shaped dose-response curve in a simulated public speaking test. Braz J Psychiatry 41**:** 9-14.

Liu B, Song S, Jones PM, & Persaud SJ (2015). GPR55: from orphan to metabolic regulator? Pharmacol Ther 145**:** 35-42.

Liu SQ (2020) *Cardiovascular Engineering: A Protective Approach*. McGraw-Hill Education.

Loewe S (1946). Studies on the pharmacology and acute toxicity of compounds with marihuana activity. J Pharmacol Exp Ther 88**:** 154-161.

Long LE, Chesworth R, Huang XF, McGregor IS, Arnold JC, & Karl T (2010). A behavioural comparison of acute and chronic Delta9-tetrahydrocannabinol and cannabidiol in C57BL/6JArc mice. Int J Neuropsychopharmacol 13**:** 861-876.

Lucas CJ, Galettis P, & Schneider J (2018). The pharmacokinetics and the pharmacodynamics of cannabinoids. Br J Clin Pharmacol 84**:** 2477-2482.

Ludbrook J (1994). Repeated measurements and multiple comparisons in cardiovascular research. Cardiovasc Res 28**:** 303-311.

Lunn CA, Fine JS, Rojas-Triana A, Jackson JV, Fan X, Kung TT, *et al.* (2006). A novel cannabinoid peripheral cannabinoid receptor-selective inverse agonist blocks leukocyte recruitment in vivo. J Pharmacol Exp Ther 316**:** 780-788.

Lynch JW (2004). Molecular structure and function of the glycine receptor chloride channel. Physiol Rev 84**:** 1051-1095.

MacGillivray N (2017). Sir William Brooke O'Shaughnessy (1808-1889), MD, FRS, LRCS Ed: Chemical pathologist, pharmacologist and pioneer in electric telegraphy. J Med Biogr 25**:** 186-196.

Madden K, Tanco K, & Bruera E (2020). Clinically Significant Drug-Drug Interaction Between Methadone and Cannabidiol. Pediatrics 145**:** e20193256.

Magen I, Avraham Y, Ackerman Z, Vorobiev L, Mechoulam R, & Berry EM (2010). Cannabidiol ameliorates cognitive and motor impairments in bile-duct ligated mice via 5-HT1A receptor activation. Br J Pharmacol 159**:** 950-957.

Maione S, Piscitelli F, Gatta L, Vita D, De Petrocellis L, Palazzo E, *et al.* (2011). Non-psychoactive cannabinoids modulate the descending pathway of antinociception in anaesthetized rats through several mechanisms of action. Br J Pharmacol 162**:** 584-596.

Mallard N, Marshall R, Sithers A, & Spriggs B (1992). Suramin: a selective inhibitor of purinergic neurotransmission in the rat isolated vas deferens. Eur J Pharmacol 220**:** 1-10.

Martin-Santos R, Crippa JA, Batalla A, Bhattacharyya S, Atakan Z, Borgwardt S, *et al.* (2012). Acute effects of a single, oral dose of d9-tetrahydrocannabinol (THC) and cannabidiol (CBD) administration in healthy volunteers. Curr Pharm Des 18**:** 4966-4979.

Matsuda LA, Lolait SJ, Brownstein MJ, Young AC, & Bonner TI (1990). Structure of a cannabinoid receptor and functional expression of the cloned cDNA. Nature 346**:** 561-564.

Mazeh AC, Angus JA, & Wright CE (2019). The effects of varying Mg(2+) ion concentrations on contractions to the cotransmitters ATP and noradrenaline in the rat vas deferens. Auton Neurosci 222**:** 102588.

Mazeh AC, Angus JA, & Wright CE (2021). Cannabidiol selectively inhibits the contraction of rat small resistance arteries: possible role for CGRP and voltage-gated calcium channels. Eur J Pharmacol 891**:** 173767.

McGrath JC (1978). Adrenergic and 'non-adrenergic' components in the contractile response of the vas deferens to a single indirect stimulus. J Physiol 283**:** 23-39.

McGuire P, Robson P, Cubala WJ, Vasile D, Morrison PD, Barron R, *et al.* (2018). Cannabidiol (CBD) as an Adjunctive Therapy in Schizophrenia: A Multicenter Randomized Controlled Trial. Am J Psychiatry 175**:** 225-231.

McHugh D, Hu SS, Rimmerman N, Juknat A, Vogel Z, Walker JM, *et al.* (2010). N-arachidonoyl glycine, an abundant endogenous lipid, potently drives directed cellular migration through GPR18, the putative abnormal cannabidiol receptor. BMC Neurosci 11**:** 44.

McHugh D, Page J, Dunn E, & Bradshaw HB (2012). Δ(9) -Tetrahydrocannabinol and N-arachidonyl glycine are full agonists at GPR18 receptors and induce migration in human endometrial HEC-1B cells. Br J Pharmacol 165**:** 2414-2424.

McNeish A, Roux B, Aylett S-B, Van Den Brink A, & Cottrell G (2012). Endosomal proteolysis regulates calcitonin gene-related peptide responses in mesenteric arteries. British Journal of Pharmacology 167**:** 1679-1690.

McPartland JM (2018). Cannabis Systematics at the Levels of Family, Genus, and Species. Cannabis Cannabinoid Res 3**:** 203-212.

McPartland JM, Duncan M, Di Marzo V, & Pertwee RG (2015). Are cannabidiol and Delta(9) -tetrahydrocannabivarin negative modulators of the endocannabinoid system? A systematic review. Br J Pharmacol 172**:** 737-753.

McPartland JM, Matias I, Di Marzo V, & Glass M (2006). Evolutionary origins of the endocannabinoid system. Gene 370**:** 64-74.

McPartland JM, & Russo EB (2001). Cannabis and cannabis extracts: greater than the sum of their parts? Journal of Cannabis Therapeutics 1**:** 103-132.

McQueen DS, Bond SM, Smith PJ, Balali-Mood K, & Smart D (2004). Cannabidiol lacks the vanilloid VR1-mediated vasorespiratory effects of capsaicin and anandamide in anaesthetised rats. Eur J Pharmacol 491**:** 181-189.

Mecha M, Feliú A, Iñigo PM, Mestre L, Carrillo-Salinas FJ, & Guaza C (2013). Cannabidiol provides long-lasting protection against the deleterious effects of inflammation in a viral model of multiple sclerosis: a role for A2A receptors. Neurobiol Dis 59**:** 141-150.

Mechoulam R (2005) *Cannabinoids as Therapeutics* Birkhauser Verlag AG: Basel, Switzerland

Mechoulam R, Ben-Shabat S, Hanus L, Ligumsky M, Kaminski NE, Schatz AR*, et al.* (1995). Identification of an endogenous 2-monoglyceride, present in canine gut, that binds to cannabinoid receptors. Biochem Pharmacol 50**:** 83-90.

Mechoulam R, & Shvo Y (1963). Hashish. I. The structure of cannabidiol. Tetrahedron 19**:** 2073-2078.

Millar SA, Maguire RF, Yates AS, & O'Sullivan SE (2020). Towards Better Delivery of Cannabidiol (CBD). Pharmaceuticals (Basel) 13**:** 219.

Millar SA, Stone NL, Yates AS, & O'Sullivan SE (2018). A Systematic Review on the Pharmacokinetics of Cannabidiol in Humans. Front Pharmacol 9**:** 1365.

Mittleman MA, Lewis RA, Maclure M, Sherwood JB, & Muller JE (2001). Triggering myocardial infarction by marijuana. Circulation 103**:** 2805-2809.

Mohrman DE, & Heller LJ (2018) *Cardiovascular physiology*. McGraw-Hill.

Moon TC, Befus AD, & Kulka M (2014). Mast cell mediators: their differential release and the secretory pathways involved. Front Immunol 5**:** 569.

Moreau HD, Piel M, Voituriez R, & Lennon-Duménil AM (2018). Integrating Physical and Molecular Insights on Immune Cell Migration. Trends Immunol 39**:** 632-643.

Moreira FA, & Guimarães FS (2005). Cannabidiol inhibits the hyperlocomotion induced by psychotomimetic drugs in mice. Eur J Pharmacol 512**:** 199-205.

Morrison G, Crockett J, Blakey G, & Sommerville K (2019). A Phase 1, Open-Label, Pharmacokinetic Trial to Investigate Possible Drug-Drug Interactions Between Clobazam, Stiripentol, or Valproate and Cannabidiol in Healthy Subjects. Clin Pharmacol Drug Dev 8**:** 1009-1031.

Moss DE, & Fahrney D (1978). Kinetic analysis of differences in brain acetylcholinesterase from fish or mammalian sources. Biochem Pharmacol 27**:** 2693-2698.

Mukamal KJ, Maclure M, Muller JE, & Mittleman MA (2008). An exploratory prospective study of marijuana use and mortality following acute myocardial infarction. Am Heart J 155**:** 465-470.

Mulryan K, Gitterman DP, Lewis CJ, Vial C, Leckie BJ, Cobb AL, *et al.* (2000). Reduced vas deferens contraction and male infertility in mice lacking P2X1 receptors. Nature 403**:** 86-89.

Mulvany MJ, & Aalkjaer C (1990). Structure and function of small arteries. Physiol Rev 70**:** 921-961.

Mulvany MJ, & Halpern W (1977). Contractile properties of small arterial resistance vessels in spontaneously hypertensive and normotensive rats. Circ Res 41**:** 19-26.

Munro S, Thomas KL, & Abu-Shaar M (1993). Molecular characterization of a peripheral receptor for cannabinoids. Nature 365**:** 61-65.

Nair AB, & Jacob S (2016). A simple practice guide for dose conversion between animals and human. J Basic Clin Pharm 7**:** 27-31.

Nazıroğlu M (2015). TRPV1 Channel: A Potential Drug Target for Treating Epilepsy. Curr Neuropharmacol 13**:** 239-247.

North RA, & Surprenant A (2000). Pharmacology of cloned P2X receptors. Annu Rev Pharmacol Toxicol 40**:** 563-580.

NPS MedicineWise (2020). *Consumer medicine information-Frisium-clobazam.* [Online] Available from https://www.nps.org.au/medicine-finder/frisium-tablets. [Accessed: 11 Jun 2020].

O'Leary DS (1991). Regional vascular resistance vs. conductance: which index for baroreflex responses? Am J Physiol 260**:** H632-637.

O'Sullivan SE, Sun Y, Bennett AJ, Randall MD, & Kendall DA (2009). Time-dependent vascular actions of cannabidiol in the rat aorta. Eur J Pharmacol 612**:** 61-68.

Odi R, Bibi D, Wager T, & Bialer M (2020). A perspective on the physicochemical and biopharmaceutic properties of marketed antiseizure drugs-From phenobarbital to cenobamate and beyond. Epilepsia 61**:** 1543-1552.

Offertaler L, Mo FM, Batkai S, Liu J, Begg M, Razdan RK*, et al.* (2003). Selective ligands and cellular effectors of a G protein-coupled endothelial cannabinoid receptor. Mol Pharmacol 63**:** 699-705.

Ohlsson A, Lindgren JE, Andersson S, Agurell S, Gillespie H, & Hollister LE (1986). Single-dose kinetics of deuterium-labelled cannabidiol in man after smoking and intravenous administration. Biomed Environ Mass Spectrom 13**:** 77-83.

Pacher P, Steffens S, Hasko G, Schindler TH, & Kunos G (2018). Cardiovascular effects of marijuana and synthetic cannabinoids: the good, the bad, and the ugly. Nat Rev Cardiol 15**:** 151-166.

Pappano AJ, & Wier WG (2019) *Cardiovascular physiology*. Eleventh edition. edn. Elsevier.

Parker LA, Kwiatkowska M, Burton P, & Mechoulam R (2004). Effect of cannabinoids on lithium-induced vomiting in the Suncus murinus (house musk shrew). Psychopharmacology (Berl) 171**:** 156-161.

Parker LA, Kwiatkowska M, & Mechoulam R (2006). Delta-9-tetrahydrocannabinol and cannabidiol, but not ondansetron, interfere with conditioned retching reactions elicited by a lithium-paired context in Suncus murinus: An animal model of anticipatory nausea and vomiting. Physiol Behav 87**:** 66-71.

Passante E, & Frankish N (2009). The RBL-2H3 cell line: its provenance and suitability as a model for the mast cell. Inflamm Res 58**:** 737-745.

Patrician A, Versic-Bratincevic M, Mijacika T, Banic I, Marendic M, Sutlović D*, et al.* (2019). Examination of a New Delivery Approach for Oral Cannabidiol in Healthy Subjects: A Randomized, Double-Blinded, Placebo-Controlled Pharmacokinetics Study. Adv Ther 36**:** 3196-3210.

Pazos MR, Mohammed N, Lafuente H, Santos M, Martínez-Pinilla E, Moreno E*, et al.* (2013). Mechanisms of cannabidiol neuroprotection in hypoxic-ischemic newborn pigs: role of 5HT(1A) and CB2 receptors. Neuropharmacology 71**:** 282-291.

Pertwee RG (1997). Pharmacology of cannabinoid CB1 and CB2 receptors. Pharmacol Ther 74**:** 129-180.

Pertwee RG (2006). Cannabinoid pharmacology: the first 66 years. Br J Pharmacol 147 Suppl 1**:** S163-171.

Pertwee RG (2008a). The diverse CB1 and CB2 receptor pharmacology of three plant cannabinoids: delta9-tetrahydrocannabinol, cannabidiol and delta9-tetrahydrocannabivarin. Br J Pharmacol 153**:** 199-215.

Pertwee RG (2008b). Ligands that target cannabinoid receptors in the brain: from THC to anandamide and beyond. Addict Biol 13**:** 147-159.

Pertwee RG (2014) *Handbook of cannabis*. Oxford University Press, USA.

Pertwee RG, & Fernando SR (1996). Evidence for the presence of cannabinoid CB1 receptors in mouse urinary bladder. Br J Pharmacol 118**:** 2053-2058.

Pertwee RG, Fernando SR, Griffin G, Abadji V, & Makriyannis A (1995a). Effect of phenylmethylsulphonyl fluoride on the potency of anandamide as an inhibitor of electrically evoked contractions in two isolated tissue preparations. Eur J Pharmacol 272**:** 73-78.

Pertwee RG, Fernando SR, Nash JE, & Coutts AA (1996a). Further evidence for the presence of cannabinoid CB1 receptors in guinea-pig small intestine. Br J Pharmacol 118**:** 2199-2205.

Pertwee RG, & Griffin G (1995). A preliminary investigation of the mechanisms underlying cannabinoid tolerance in the mouse vas deferens. Eur J Pharmacol 272**:** 67-72.

Pertwee RG, Griffin G, Lainton JA, & Huffman JW (1995b). Pharmacological characterization of three novel cannabinoid receptor agonists in the mouse isolated vas deferens. Eur J Pharmacol 284**:** 241-247.

Pertwee RG, Howlett AC, Abood ME, Alexander SP, Di Marzo V, Elphick MR*, et al.* (2010). International Union of Basic and Clinical Pharmacology. LXXIX. Cannabinoid receptors and their ligands: beyond CB(1) and CB(2). Pharmacol Rev 62**:** 588-631.

Pertwee RG, Joe-Adigwe G, & Hawksworth GM (1996b). Further evidence for the presence of cannabinoid CB1 receptors in mouse vas deferens. Eur J Pharmacol 296**:** 169-172.

Pertwee RG, Ross RA, Craib SJ, & Thomas A (2002). (-)-Cannabidiol antagonizes cannabinoid receptor agonists and noradrenaline in the mouse vas deferens. Eur J Pharmacol 456**:** 99-106.

Pertwee RG, Stevenson LA, Elrick DB, Mechoulam R, & Corbett AD (1992). Inhibitory effects of certain enantiomeric cannabinoids in the mouse vas deferens and the myenteric plexus preparation of guinea-pig small intestine. Br J Pharmacol 105**:** 980-984.

Petrosino S, Schiano Moriello A, Verde R, Allarà M, Imperatore R, Ligresti A, *et al.* (2019). Palmitoylethanolamide counteracts substance P-induced mast cell activation in vitro by stimulating diacylglycerol lipase activity. J Neuroinflammation 16**:** 274.

Petrosino S, Vaia M, Verde R, Iuvone T, & Di Marzo V (2018). Anti-inflammatory properties of cannabidiol, a non-psychotropic cannabinoid, in experimental allergic contact dermatitis. J Pharmacol Exp Ther 365**:** 652-663.

Pisanti S, & Bifulco M (2017). Modern History of Medical Cannabis: From Widespread Use to Prohibitionism and Back. Trends Pharmacol Sci 38**:** 195-198.

Pisanti S, & Bifulco M (2019). Medical Cannabis: A plurimillennial history of an evergreen. J Cell Physiol 234**:** 8342-8351.

Pollastro F, De Petrocellis L, Schiano-Moriello A, Chianese G, Heyman H, Appendino G, *et al.* (2017). Amorfrutin-type phytocannabinoids from Helichrysum umbraculigerum. Fitoterapia 123**:** 13-17.

Pollock JD, Murray I, Bordes S, & Makaryus AN (2020). Physiology, Cardiovascular Hemodynamics. In StatPearls. StatPearls Publishing LLC.: Treasure Island (FL).

Porter BE, & Jacobson C (2013). Report of a parent survey of cannabidiol-enriched cannabis use in pediatric treatment-resistant epilepsy. Epilepsy Behav 29**:** 574-577.

Pruneau D, & Angus JA (1990). Omega-conotoxin GVIA is a potent inhibitor of sympathetic neurogenic responses in rat small mesenteric arteries. Br J Pharmacol 100**:** 180-184.

Pryce G, & Baker D (2007). Control of spasticity in a multiple sclerosis model is mediated by CB1, not CB2, cannabinoid receptors. Br J Pharmacol 150**:** 519-525.

Pusiak RJ, Cox C, & Harris CS (2021). Growing pains: An overview of cannabis quality control and quality assurance in Canada. Int J Drug Policy 93**:** 103111.

Qin Y, Verdegaal EM, Siderius M, Bebelman JP, Smit MJ, Leurs R, *et al.* (2011). Quantitative expression profiling of G-protein-coupled receptors (GPCRs) in metastatic melanoma: the constitutively active orphan GPCR GPR18 as novel drug target. Pigment Cell Melanoma Res 24**:** 207-218.

Ramamoorthy A, Pacanowski MA, Bull J, & Zhang L (2015). Racial/ethnic differences in drug disposition and response: review of recently approved drugs. Clin Pharmacol Ther 97**:** 263-273.

Ramer R, Heinemann K, Merkord J, Rohde H, Salamon A, Linnebacher M, *et al.* (2013). COX-2 and PPAR-γ confer cannabidiol-induced apoptosis of human lung cancer cells. Mol Cancer Ther 12**:** 69-82.

Randall MD, Kendall DA, & O'Sullivan S (2004). The complexities of the cardiovascular actions of cannabinoids. Br J Pharmacol 142**:** 20-26.

Regard JB, Sato IT, & Coughlin SR (2008). Anatomical profiling of G protein-coupled receptor expression. Cell 135**:** 561-571.

Resstel LB, Joca SR, Moreira FA, Correa FM, & Guimaraes FS (2006). Effects of cannabidiol and diazepam on behavioral and cardiovascular responses induced by contextual conditioned fear in rats. Behav Brain Res 172**:** 294-298.

Resstel LB, Tavares RF, Lisboa SF, Joca SR, Correa FM, & Guimaraes FS (2009). 5-HT1A receptors are involved in the cannabidiol-induced attenuation of behavioural and cardiovascular responses to acute restraint stress in rats. Br J Pharmacol 156**:** 181-188.

Ribeiro A, Ferraz-de-Paula V, Pinheiro ML, Vitoretti LB, Mariano-Souza DP, Quinteiro-Filho WM*, et al.* (2012). Cannabidiol, a non-psychotropic plant-derived cannabinoid, decreases inflammation in a murine model of acute lung injury: role for the adenosine A(2A) receptor. Eur J Pharmacol 678**:** 78-85.

Ribeiro LI, & Ind PW (2016). Effect of cannabis smoking on lung function and respiratory symptoms: a structured literature review. NPJ Prim Care Respir Med 26**:** 16071.

Rice S, & Koziel JA (2015). Characterizing the Smell of Marijuana by Odor Impact of Volatile Compounds: An Application of Simultaneous Chemical and Sensory Analysis. PLoS One 10**:** e0144160.

Rinaldi-Carmona M, Barth F, Heaulme M, Alonso R, Shire D, Congy C*, et al.* (1995). Biochemical and pharmacological characterisation of SR141716A, the first potent and selective brain cannabinoid receptor antagonist. Life Sci 56**:** 1941-1947.

Rinaldi-Carmona M, Barth F, Heaulme M, Shire D, Calandra B, Congy C*, et al.* (1994). SR141716A, a potent and selective antagonist of the brain cannabinoid receptor. FEBS Lett 350**:** 240-244.

Robson P (2005). Human studies of cannabinoids and medicinal cannabis. Handb Exp Pharmacol**:** 719-756.

Rock EM, Bolognini D, Limebeer CL, Cascio MG, Anavi-Goffer S, Fletcher PJ*, et al.* (2012). Cannabidiol, a non-psychotropic component of cannabis, attenuates vomiting and nausea-like behaviour via indirect agonism of 5-HT(1A) somatodendritic autoreceptors in the dorsal raphe nucleus. Br J Pharmacol 165**:** 2620-2634.

Rosenthaler S, Pöhn B, Kolmanz C, Huu CN, Krewenka C, Huber A*, et al.* (2014). Differences in receptor binding affinity of several phytocannabinoids do not explain their effects on neural cell cultures. Neurotoxicol Teratol 46**:** 49-56.

Russell GR, Phelps SJ, Shelton CM, & Wheless JW (2018). Impact of Drug Interactions on Clobazam and N-Desmethylclobazam Concentrations in Pediatric Patients With Epilepsy. Ther Drug Monit 40**:** 452-462.

Russo E (2013). *Cannabis Strains: Do Cannabis Strains Differ?* [Online] Available from http://www.cannabis-med.org/index.php?tpl=faq&red=faqlist&id=278&lng=en. [Accessed: 2 Jun 2020].

Russo E, & Guy GW (2006). A tale of two cannabinoids: the therapeutic rationale for combining tetrahydrocannabinol and cannabidiol. Medical hypotheses 66**:** 234-246.

Russo EB (2007). History of cannabis and its preparations in saga, science, and sobriquet. Chem Biodivers 4**:** 1614-1648.

Russo EB, & Marcu J (2017). Cannabis Pharmacology: The Usual Suspects and a Few Promising Leads. Adv Pharmacol 80**:** 67-134.

Ryberg E, Larsson N, Sjögren S, Hjorth S, Hermansson NO, Leonova J, *et al.* (2007). The orphan receptor GPR55 is a novel cannabinoid receptor. Br J Pharmacol 152**:** 1092-1101.

Sam AH, Salem V, & Ghatei MA (2011). Rimonabant: From RIO to Ban. J Obes 2011**:** 432607.

Samanta D (2019). Cannabidiol: A Review of Clinical Efficacy and Safety in Epilepsy. Pediatr Neurol 96**:** 24-29.

Samson MT, Small-Howard A, Shimoda LM, Koblan-Huberson M, Stokes AJ, & Turner H (2003). Differential roles of CB1 and CB2 cannabinoid receptors in mast cells. J Immunol 170**:** 4953-4962.

Schlicker E, & Kathmann M (2001). Modulation of transmitter release via presynaptic cannabinoid receptors. Trends Pharmacol Sci 22**:** 565-572.

Schlicker E, Redmer A, Werner A, & Kathmann M (2003). Lack of CB1 receptors increases noradrenaline release in vas deferens without affecting atrial noradrenaline release or cortical acetylcholine release. Br J Pharmacol 140**:** 323-328.

Secomb TW (2016). Hemodynamics. Compr Physiol 6**:** 975-1003.

Seeman P (2016). Cannabidiol is a partial agonist at dopamine D2High receptors, predicting its antipsychotic clinical dose. Transl Psychiatry 6**:** e920.

Sekar K, & Pack A (2019). Epidiolex as adjunct therapy for treatment of refractory epilepsy: a comprehensive review with a focus on adverse effects. Faculty Rev 8**:** F1000.

Shen Yun Performing Arts (2020). *Mythistory's Divine Farmer.* [Online] Available from https://www.shenyunperformingarts.org/explore/view/article/e/gE85hnlKY-c/shennong-divine-farmer.html. [Accessed: 5 Mar 2020].

Shire D, Calandra B, Delpech M, Dumont X, Kaghad M, Le Fur G, *et al.* (1996). Structural features of the central cannabinoid CB1 receptor involved in the binding of the specific CB1 antagonist SR 141716A. J Biol Chem 271**:** 6941-6946.

Silver RJ (2019). The Endocannabinoid System of Animals. Animals (Basel) 9**:** 686.

Siraganian RP, & Metzger H (1978). Evidence that the "mouse mastocytoma" cell line (MCT-1) is of rat origin. J Immunol 121**:** 2584-2585.

Smith BE, & Madigan VM (2018). Understanding the Haemodynamics of Hypertension. Curr Hypertens Rep 20**:** 29.

Sneddon P, & Westfall DP (1984). Pharmacological evidence that adenosine triphosphate and noradrenaline are co-transmitters in the guinea-pig vas deferens. J Physiol 347**:** 561-580.

Solowij N, Broyd S, Greenwood LM, van Hell H, Martelozzo D, Rueb K, *et al.* (2019). A randomised controlled trial of vaporised Δ(9)-tetrahydrocannabinol and cannabidiol alone and in combination in frequent and infrequent cannabis users: acute intoxication effects. Eur Arch Psychiatry Clin Neurosci 269**:** 17-35.

Sotudeh N, Morales P, Hurst DP, Lynch DL, & Reggio PH (2019). Towards A Molecular Understanding of The Cannabinoid Related Orphan Receptor GPR18: A Focus on Its Constitutive Activity. Int J Mol Sci 20**:** 2300.

Spindle TR, Cone EJ, Goffi E, Weerts EM, Mitchell JM, Winecker RE, *et al.* (2020). Pharmacodynamic effects of vaporized and oral cannabidiol (CBD) and vaporized CBD-dominant cannabis in infrequent cannabis users. Drug Alcohol Depend 211**:** 107937.

Stanley CP, Hind WH, & O'Sullivan SE (2013a). Is the cardiovascular system a therapeutic target for cannabidiol? Br J Clin Pharmacol 75**:** 313-322.

Stanley CP, Hind WH, Tufarelli C, & O'Sullivan SE (2015). Cannabidiol causes endothelium-dependent vasorelaxation of human mesenteric arteries via CB1 activation. Cardiovasc Res 107**:** 568-578.

Stanley CP, Wheal AJ, Randall MD, & O'Sullivan SE (2013b). Cannabinoids alter endothelial function in the Zucker rat model of type 2 diabetes. Eur J Pharmacol 720**:** 376-382.

Steel D, Symonds JD, Zuberi SM, & Brunklaus A (2017). Dravet syndrome and its mimics: Beyond SCN1A. Epilepsia 58**:** 1807-1816.

Stone M, & Angus JA (1978). Developments of computer-based estimation of pA2 values and associated analysis. J Pharmacol Exp Ther 207**:** 705-718.

Stott C, White L, Wright S, Wilbraham D, & Guy G (2013). A Phase I, open-label, randomized, crossover study in three parallel groups to evaluate the effect of Rifampicin, Ketoconazole, and Omeprazole on the pharmacokinetics of THC/CBD oromucosal spray in healthy volunteers. Springerplus 2**:** 236.

Sultan SR, Millar SA, England TJ, & O'Sullivan SE (2017). A Systematic Review and Meta-Analysis of the Haemodynamic Effects of Cannabidiol. Front Pharmacol 8**:** 81.

Sultan SR, O'Sullivan SE, & England TJ (2020). The effects of acute and sustained cannabidiol dosing for seven days on the haemodynamics in healthy men: A randomised controlled trial. Br J Clin Pharmacol 86**:** 1125-1138.

Swedin G (1971). Studies on neurotransmission mechanisms in the rat and guinea-pig vas deferens. Acta Physiol Scand Suppl 369**:** 1-34.

Tamura T (2014). 5.05 - Blood Flow Measurement. In Comprehensive Biomedical Physics. ed Brahme A. Elsevier: Oxford, pp 91-105.

Taurog JD, Mendoza GR, Hook WA, Siraganian RP, & Metzger H (1977). Noncytotoxic IgE-mediated release of histamine and serotonin from murine mastocytoma cells. J Immunol 119**:** 1757-1761.

Teppema LJ, & Baby S (2011). Anesthetics and control of breathing. Respir Physiol Neurobiol 177**:** 80-92.

Tham M, Yilmaz O, Alaverdashvili M, Kelly MEM, Denovan-Wright EM, & Laprairie RB (2018). Allosteric and orthosteric pharmacology of cannabidiol and cannabidiol-dimethylheptyl at the type 1 and type 2 cannabinoid receptors. Br J Pharmacol 176**:** 1455-1469.

The Office of Drug Control (2019). *Review of the Narcotic Drugs Act 1967 - Final Report.* [Online] Available from https://www.odc.gov.au/news-media/news/tabling-report-review-2016-medicinal-cannabis-amendments-narcotic-drugs-act-1967. [Accessed: 21 Feb 2020].

Therapeutic Goods Administration (2013). *Australian Public Assessment Report for Nabiximols.* [Online] Available from https://www.tga.gov.au/sites/default/files/auspar-nabiximols-130927.pdf. [Accessed: 9 Jun 2020].

Therapeutic Goods Administration (2017). *Scheduling delegate's final decisions: Cannabis, May 2017.* [Online] Available from https://www.tga.gov.au/book-page/11-cannabis. [Accessed: 17 Mar 2018].

Therapeutic Goods Administration (2018). *Access to medicinal cannabis products.* [Online] Available from https://www.tga.gov.au/access-medicinal-cannabis-products. [Accessed: 20 Feb 2018].

Therapeutic Goods Administration (2020). *Notice of interim decisions on proposed amendments to the Poisons Standard - ACMS and Joint ACMS-ACCS meetings, June 2020.* . [Online] Available from https://www.tga.gov.au/book-page/41-cannabidiol-private-application-and-cannabidiol-delegate-initiated. [Accessed: 10 Nov 2020].

Thomas A, Baillie GL, Phillips AM, Razdan RK, Ross RA, & Pertwee RG (2007). Cannabidiol displays unexpectedly high potency as an antagonist of CB1 and CB2 receptor agonists in vitro. Br J Pharmacol 150**:** 613-623.

Thomas A, Ross RA, Saha B, Mahadevan A, Razdan RK, & Pertwee RG (2004). 6"-Azidohex-2"-yne-cannabidiol: a potential neutral, competitive cannabinoid CB1 receptor antagonist. Eur J Pharmacol 487**:** 213-221.

Tomida I, Azuara-Blanco A, House H, Flint M, Pertwee RG, & Robson PJ (2006). Effect of sublingual application of cannabinoids on intraocular pressure: a pilot study. J Glaucoma 15**:** 349-353.

Tominaga M, Caterina MJ, Malmberg AB, Rosen TA, Gilbert H, Skinner K, *et al.* (1998). The cloned capsaicin receptor integrates multiple pain-producing stimuli. Neuron 21**:** 531-543.

Turcotte C, Blanchet MR, Laviolette M, & Flamand N (2016). The CB(2) receptor and its role as a regulator of inflammation. Cell Mol Life Sci 73**:** 4449-4470.

U.S. Food and Drug Administration (2020). *Warning letters and test results for cannabidiol-related products.* [Online] Available from https://www.fda.gov/news-events/public-health-focus/warning-letters-and-test-results-cannabidiol-related-products. [Accessed: 8 Jun 2020].

U.S. National Library of Medicine (2020). *ClinicalTrials.gov.* [Online] Available from https://clinicaltrials.gov. [Accessed: 3 Jun].

United Nations (2020). *UN commission reclassifies cannabis, yet still considered harmful.* [Online] Available from https://news.un.org/en/story/2020/12/1079132. [Accessed: 10 Sep 2021].

United Nations Office on Drugs and Crime (1961). The International Drug Control ConventionsUnited Nations: Vienna.

United Nations Office on Drugs and Crime (2015). World Drug Report 2015: Vienna

Vallée A, Lecarpentier Y, Guillevin R, & Vallée JN (2017). Effects of cannabidiol interactions with Wnt/β-catenin pathway and PPARγ on oxidative stress and

neuroinflammation in Alzheimer's disease. Acta Biochim Biophys Sin (Shanghai) 49**:** 853-866.

Varga ZV, Matyas C, Erdelyi K, Cinar R, Nieri D, Chicca A, *et al.* (2018). beta-Caryophyllene protects against alcoholic steatohepatitis by attenuating inflammation and metabolic dysregulation in mice. Br J Pharmacol 175**:** 320-334.

Vilela LR, Lima IV, Kunsch É B, Pinto HPP, de Miranda AS, Vieira É LM, *et al.* (2017). Anticonvulsant effect of cannabidiol in the pentylenetetrazole model: Pharmacological mechanisms, electroencephalographic profile, and brain cytokine levels. Epilepsy Behav 75**:** 29-35.

Walsh SK, Hepburn CY, Keown O, Åstrand A, Lindblom A, Ryberg E, *et al.* (2015). Pharmacological profiling of the hemodynamic effects of cannabinoid ligands: a combined in vitro and in vivo approach. Pharmacol Res Perspect 3**:** e00143.

Ware MA, Adams H, & Guy GW (2005). The medicinal use of cannabis in the UK: results of a nationwide survey. Int J Clin Pract 59**:** 291-295.

Westfall DP, Stitzel RE, & Rowe JN (1978). The postjunctional effects and neural release of purine compounds in the guinea-pig vas deferens. Eur J Pharmacol 50**:** 27-38.

Wheal AJ, Cipriano M, Fowler CJ, Randall MD, & O'Sullivan SE (2014). Cannabidiol improves vasorelaxation in Zucker diabetic fatty rats through cyclooxygenase activation. J Pharmacol Exp Ther 351**:** 457-466.

Wheal AJ, Jadoon K, Randall MD, & O'Sullivan SE (2017). In Vivo Cannabidiol Treatment Improves Endothelium-Dependent Vasorelaxation in Mesenteric Arteries of Zucker Diabetic Fatty Rats. Front Pharmacol 8**:** 248.

White CW, Choong YT, Short JL, Exintaris B, Malone DT, Allen AM, *et al.* (2013). Male contraception via simultaneous knockout of alpha1A-adrenoceptors and P2X1-purinoceptors in mice. Proc Natl Acad Sci U S A 110**:** 20825-20830.

White HL, & Tansik RL (1980). Effects of delta 9-tetrahydrocannabinol and cannabidiol on phospholipase and other enzymes regulating arachidonate metabolism. Prostaglandins Med 4**:** 409-417.

Whorlow SL, Angus JA, & Wright CE (1996). Selectivity of omega-conotoxin GVIA for n-type calcium channels in rat isolated small mesenteric arteries. Clin Exp Pharmacol Physiol 23**:** 16-21.

Whyte LS, Ryberg E, Sims NA, Ridge SA, Mackie K, Greasley PJ, *et al.* (2009). The putative cannabinoid receptor GPR55 affects osteoclast function in vitro and bone mass in vivo. Proc Natl Acad Sci U S A 106**:** 16511-16516.

Wiley JL, Breivogel CS, Mahadevan A, Pertwee RG, Cascio MG, Bolognini D, *et al.* (2011). Structural and pharmacological analysis of O-2050, a putative neutral cannabinoid CB(1) receptor antagonist. Eur J Pharmacol 651**:** 96-105.

Winton-Brown TT, Allen P, Bhattacharyya S, Borgwardt SJ, Fusar-Poli P, Crippa JA, *et al.* (2011). Modulation of auditory and visual processing by delta-9-tetrahydrocannabinol and cannabidiol: an FMRI study. Neuropsychopharmacology 36**:** 1340-1348.

Witkamp R (2016). Fatty acids, endocannabinoids and inflammation. Eur J Pharmacol 785**:** 96-107.

Wolf SA, Bick-Sander A, Fabel K, Leal-Galicia P, Tauber S, Ramirez-Rodriguez G, *et al.* (2010). Cannabinoid receptor CB1 mediates baseline and activity-induced survival of new neurons in adult hippocampal neurogenesis. Cell Commun Signal 8**:** 12.

World Health Organization (2016). *The health and social effects of nonmedical cannabis use* [Online] Available from https://www.who.int/substance_abuse/publications/msbcannabis.pdf. [Accessed: 14 Jan 2019].

Wright CE, & Angus JA (2000). Techniques to measure pharmacodynamics in the intact vasculature. J Pharmacol Toxicol Methods 44**:** 385-394.

Wright CE, Angus JA, & Korner PI (1987). Vascular amplifier properties in renovascular hypertension in conscious rabbits. Hindquarter responses to constrictor and dilator stimuli. Hypertension 9**:** 122-131.

Xie S, Furjanic MA, Ferrara JJ, McAndrew NR, Ardino EL, Ngondara A, *et al.* (2007). The endocannabinoid system and rimonabant: a new drug with a novel mechanism of action involving cannabinoid CB1 receptor antagonism--or inverse agonism--as potential obesity treatment and other therapeutic use. J Clin Pharm Ther 32**:** 209-231.

Xiong W, Cheng K, Cui T, Godlewski G, Rice KC, Xu Y, *et al.* (2011). Cannabinoid potentiation of glycine receptors contributes to cannabis-induced analgesia. Nat Chem Biol 7**:** 296-303.

Yoo JM, Sok DE, & Kim MR (2013). Effect of endocannabinoids on IgE-mediated allergic response in RBL-2H3 cells. Int Immunopharmacol 17**:** 123-131.

Zanelati TV, Biojone C, Moreira FA, Guimarães FS, & Joca SR (2010). Antidepressant-like effects of cannabidiol in mice: possible involvement of 5-HT1A receptors. Br J Pharmacol 159**:** 122-128.

Zendulka O, Dovrtělová G, Nosková K, Turjap M, Šulcová A, Hanuš L, *et al.* (2016). Cannabinoids and Cytochrome P450 Interactions. Curr Drug Metab 17**:** 206-226.

Zhu HJ, Wang JS, Markowitz JS, Donovan JL, Gibson BB, Gefroh HA*, et al.* (2006). Characterization of P-glycoprotein inhibition by major cannabinoids from marijuana. J Pharmacol Exp Ther 317**:** 850-857.

Zuardi AW, Cosme RA, Graeff FG, & Guimarães FS (1993). Effects of ipsapirone and cannabidiol on human experimental anxiety. J Psychopharmacol 7**:** 82-88.

Zuardi AW, Rodrigues NP, Silva AL, Bernardo SA, Hallak JEC, Guimarães FS*, et al.* (2017). Inverted U-Shaped Dose-Response Curve of the Anxiolytic Effect of Cannabidiol during Public Speaking in Real Life. Front Pharmacol 8**:** 259.

Zuardi AW, Shirakawa I, Finkelfarb E, & Karniol IG (1982). Action of cannabidiol on the anxiety and other effects produced by delta 9-THC in normal subjects. Psychopharmacology (Berl) 76**:** 245-250.